INFORMATION TO USERS

This manuscript has been reproduced from the microfilm master. UMI films the text directly from the original or copy submitted. Thus, some thesis and dissertation copies are in typewriter face, while others may be from any type of computer printer.

The quality of this reproduction is dependent upon the quality of the copy submitted. Broken or indistinct print, colored or poor quality illustrations and photographs, print bleedthrough, substandard margins, and improper alignment can adversely affect reproduction.

In the unlikely event that the author did not send UMI a complete manuscript and there are missing pages, these will be noted. Also, if unauthorized copyright material had to be removed, a note will indicate the deletion.

Oversize materials (e.g., maps, drawings, charts) are reproduced by sectioning the original, beginning at the upper left-hand corner and continuing from left to right in equal sections with small overlaps. Each original is also photographed in one exposure and is included in reduced form at the back of the book.

Photographs included in the original manuscript have been reproduced xerographically in this copy. Higher quality 6" x 9" black and white photographic prints are available for any photographs or illustrations appearing in this copy for an additional charge. Contact UMI directly to order.

UMI

A Bell & Howell Information Company
300 North Zeeb Road, Ann Arbor MI 48106-1346 USA
313/761-4700 800/521-0600

Reproduced with permission of the copyright owner. Further reproduction prohibited without permission.

Reproduced with permission of the copyright owner. Further reproduction prohibited without permission.

The Kinetics of Bromate Decomposition During UV Irradiation of Aqueous Solutions

By

Neal Hudson Phillip

A dissertation submitted to the Graduate Faculty in Engineering in partial fulfillment of the requirements for the degree of Doctor of Philosophy, The City University of New York.

1998

Reproduced with permission of the copyright owner. Further reproduction prohibited without permission.

UMI Number: 9908348

UMI Microform 9908348
Copyright 1998, by UMI Company. All rights reserved.

This microform edition is protected against unauthorized copying under Title 17, United States Code.

UMI
300 North Zeeb Road
Ann Arbor, MI 48103

Reproduced with permission of the copyright owner. Further reproduction prohibited without permission.

This manuscript has been read and has been accepted by the Graduate Faculty in Engineering in satisfaction of the dissertation requirement for the degree of Doctor of Philosophy.

[signature]

9/14/98
Date

Chair of Examining Committee

9/14/98
Date

Executive Officer

Vasil Diyamandoglu, Ph.D., AssistantProfessor
Civil Engineering Department, CCNY
(Mentor & Chair of Examining Committee)

John Fillos, Ph.D., Professor
Civil Engineering Department, CCNY

Lin Ferrand, Ph.D., Associate Professor
Civil Engineering Department, CCNY

Richard Birchwood, Ph.D., Assistant Professor
Civil Engineering Department, CCNY

Stanley Gedzelman,Ph.D., Professor
Earth and Atmospheric Sciences Department, CCNY

Supervisory Committee

THE CITY UNIVERSITY OF NEW YORK

Reproduced with permission of the copyright owner. Further reproduction prohibited without permission.

ABSTRACT

The Kinetics of Bromate Decomposition During UV Irradiation of Aqueous Solutions

by

Neal Hudson Phillip

Advisor: Vasil Diyamandoglu, Ph.D., Assistant Professor

The kinetics of bromate decomposition during UV irradiation at 254 nm was studied in pure aqueous solutions, as well as in the presence of nitrite and acetate.

UV irradiation of bromate solution produced bromide as a final product and free bromine as reaction intermediate. A bromine balance during the experiments eliminated the possibility of formation of other bromine species in significant quantities. Experiments conducted at initial pH<9.0, had pH decreases by as much as 1.5 pH units.

Bromate decay kinetics has been shown to be first order with respect to initial bromate molar concentration. Kinetic analysis of the data showed the observed bromate decay rate constant, k_{obs}, to be independent of initial bromate, initial pH, and bicarbonate alkalinity.

During UV irradiation of bromate/nitrite solution, bromate decomposition to bromide and free bromine proceeded faster than in bromate alone solutions. Nitrite was oxidized stoichiometrically to nitrate. The increased free bromine formation during UV irradiation of bromate/nitrite solution suggested that bromine intermediate species other

Reproduced with permission of the copyright owner. Further reproduction prohibited without permission.

species other than free bromine was principally responsible for nitrite oxidation. A marked decrease in the bromate decay was observed when nitrite became limiting, though the reduced rate was still about 50% higher than in corresponding bromate alone experiments. Bromate decay was shown to be pseudo-first order for bromate/nitrite ratios <1, ~1, and >1 and to be independent of initial bromate, initial nitrite and initial pH.

In the presence of acetate, bromate was reduced to bromide while acetate was converted to unidentified product(s). Free bromine remained at trace levels throughout the experiments. A bromine balance for the experiments suggested the formation of organic by-products from the reaction of free bromine and acetate. Kinetic analysis showed bromate decay to be pseudo-first order and to be markedly increased by acetate.

A kinetic model to describe UV catalyzed bromate decomposition in bromate solution and bromate/nitrite solution was developed. For bromate alone, the model was in good qualitative agreement with the experimental data, except for bromate levels below 0.5 mg/L, while the predictions for the bromate/nitrite system were in good agreement until nitrite became limiting. The bromate/acetate system was not modeled.

Reproduced with permission of the copyright owner. Further reproduction prohibited without permission.

ACKNOWLEDGEMENT

I would like to acknowledge the undying support of my family in completing this dissertation. My mother, ***Ruby Phillip***, was always a rock in a vast ocean and nothing would have been possible without her. My wife, ***Shelly Phillip***,and son, ***Dijon Phillip***, were a constant source of love and support and without them this long journey would have been more arduous. My brothers ***Don Phillip*** and ***Wayne Phillip***, my sisters, ***Debbie Phillip*** and ***Zilla Morris***, and my father ***Kelvin Phillip*** all share in my accomplishments. The support of my uncle, ***Ulric "Buggy" Haynes***, my aunt, ***Mavis Bailey***, my grandfather, ***Denzil Haynes*** and my late grandmother, ***Constance Haynes***, were instrumental in the formative years of my early education. I also owe a great deal to my late grandparents, **Agnes Morris**, and **Evans Morris** from whom I learned so much about life. My uncle, ***Oswald Haynes*** and my aunt, ***Elma Josiah***, assisted greatly during my primary and secondary education. My aunts, ***Wilma Phillip***, ***Joyce Phillip***, and ***Audrey Grant***, were always very supportive of me.

I would like to express my sincere and deepest gratitude to my mentor, ***Professor Vasil Diyamandoglu***, for his patience, guidance and encouraging words of support throughout my graduate education.

I am eternally grateful to ***Professor John Fillos*** of the Department of Civil Engineering, and ***Dean Gerard Lowen*** for both the financial and moral support they provided during my graduate education. It is truly an honor to be associated with them.

I am also beholden to ***Dr Daniel Akins*** and the ***Center for the Analysis of Structures and Interfaces*** (C.A.S.I.) for the financial support they provided during my graduate studies. ***Dean Ramona Brown*** was also a *lifeline* during both my graduate and undergraduate studies.

Last, and by no means least, I would like to thank ***Anna Kaplan***, ***Reggie Blake***, ***Michael Lewis***, ***Laurence Noel***, ***Noel Blackburn*** and the rest of the long list of friends and colleagues who encouraged me to push on when the road ahead seemed especially narrow and hilly.

Reproduced with permission of the copyright owner. Further reproduction prohibited without permission.

TABLE OF CONTENTS

Reproduced with permission of the copyright owner. Further reproduction prohibited without permission.

Reproduced with permission of the copyright owner. Further reproduction prohibited without permission.

Reproduced with permission of the copyright owner. Further reproduction prohibited without permission.

LIST OF TABLES

Reproduced with permission of the copyright owner. Further reproduction prohibited without permission.

LIST OF TABLES (cont'd)

Reproduced with permission of the copyright owner. Further reproduction prohibited without permission.

LIST OF TABLES (cont'd)

Reproduced with permission of the copyright owner. Further reproduction prohibited without permission.

LIST OF TABLES (cont'd)

Reproduced with permission of the copyright owner. Further reproduction prohibited without permission.

LIST OF TABLES (cont'd)

Reproduced with permission of the copyright owner. Further reproduction prohibited without permission.

LIST OF FIGURES

Reproduced with permission of the copyright owner. Further reproduction prohibited without permission.

LIST OF FIGURES (cont'd)

Reproduced with permission of the copyright owner. Further reproduction prohibited without permission.

LIST OF FIGURES (cont'd)

Reproduced with permission of the copyright owner. Further reproduction prohibited without permission.

LIST OF FIGURES (cont'd)

Reproduced with permission of the copyright owner. Further reproduction prohibited without permission.

CHAPTER 1

INTRODUCTION

Disinfection by-products (DBPs) are organic and inorganic compounds formed as a result of reactions between disinfectants and natural constituents of water. Bromate is an inorganic DBP formed that has attracted considerable attention over the last 10 years because of its potential adverse health effects on humans. Sodium and potassium salts of bromate are used in a number of commercial applications such as maturing agents in malted beverages, as a dough conditioner, in confectionary products, boilers and in the oxidation of sulfur and vat dyes (Borum, 1991). Since only a limited amount of food products are expected to contain bromate and no significant bromate levels are expected in ambient or indoor air, it is believed that drinking water is the predominant source of intake for bromate (USEPA, 1994). It has been shown to form during ozonation (Haag and Hoigné, 1983; Richardson et al., 1981) or chlorination of bromide containing waters (Macalady et al., 1977; Haag, 1981).

1.1 Health Effects of Bromate

The health effects of bromate have been the cause for much concern. It is rapidly absorbed, in part, unchanged from the gastrointestinal tract following ingestion and is distributed throughout the body, appearing in blood plasma and in urine as bromate and in other tissues as bromide (USEPA, 1993a). Following exposure to bromate,

Reproduced with permission of the copyright owner. Further reproduction prohibited without permission.

bromide concentrations are significantly increased in the kidney, pancreas, stomach, small intestine, and red blood cells. It becomes poisonous when the hydrochloric acid in the stomach turns the potassium bromate into bromic acid (Turkington, 1994). Accute symptoms of bromate toxicity include decreased locomotion, hypothermia, kidney damage, and lung congestion. In subchronic drinking water studies, decreased body weight gain and marked kidney damage were observed in treated rodents. These effects were observed at the lowest doses tested (30 mg/Kg/d) (USEPA, 1993a).

In a cancer bioassay, Kurowaka et al. (1986) supplied F344 rats with water containing $KBrO_3$ at 0, 15, 30 60, 125, 250 or 500 mg/L for 104 weeks with incidence of renal cell tumors observed at 0, 0, 4, 21, 50, 95 and 95%, respectively. The authors concluded that $KBrO_3$ was carcinogenic to rats. Using the linearized multistage model and combining incidences of renal tumors in rats and a daily water consumption for an adult, a lifetime risk of 10^{-4} was associated with bromate concentrations in water at 5µg/L.

Limited data are available on the health effects of bromate in humans. Deafness and renal failure has been reported as a possible consequences of high bromate consumption (Quick et al., 1975). Bromate has been included in the drinking water guidelines of the World Health Organization (WHO, 1993) with a proposed maximum level of 25 µg/L which corresponds to a 7×10^{-5} excess cancer risk level based on a 10^{-5} cancer risk level of 3µg/L.

Reproduced with permission of the copyright owner. Further reproduction prohibited without permission.

The International Agency for Research on Cancer (IARC) placed bromate in Group 2B for agents that are probably carcinogenic to humans (IARC Monograph, 1987). EPA has performed a cancer weight of evidence evaluation and has placed bromate in Group B2: probable human carcinogen. In addition, positive mutagenicity studies have reported on DNA interactions with bromate at doses of 30 mg/L over 12 hours (Ono et al., 1994).

Stage 1 of the USEPA's proposed disinfectants/disinfection by-products rule (D/DBPR) of July 1994 has set a maximum contaminant level (MCL) of 10 µg/L and a maximum contaminant level goal (MCLG) of 0 µg/L for bromate in drinking water based on a 10^{-5} risk level of 0.5 µg/L. The proposed MCL is based on the priority of safe disinfection and current analytical methods with ion chromatography for bromate ion, which has a detection limit of 2 µg/L (Koudjonou et al., 1995). The timetable for implementation of this rule is July 1998 (USEPA, 1993b).

1.2 Bromide Occurrence in Water

Bromide occurs in freshwater and groundwater supplies. Bowen (1979) reported values of 0.2 mg/L and 0.014 mg/L as mean Br^- concentrations in freshwater. Wegman et al. (1983) found bromide concentrations in the range of 41 - 71 mg/L in sea-water while Flury and Papritz (1993) report on mean concentrations of 2.26 mg/L of bromide in groundwater in coastal locations in southeast England. Thus, sea-water intrusion can be a major source of bromide ion in surface water and groundwater.

Reproduced with permission of the copyright owner. Further reproduction prohibited without permission.

Another major source of bromide in water is pesticides such as methyl bromide (CH_3Br) which is used extensively as a fumigant to control insects, nematodes, rodents and bacteria, and to sterilize soils. Even though a large fraction (70-80%) of CH_3Br evaporates into the atmosphere, the fraction remaining in the soil is degraded by methylation of organic matter or hydrolysis which releases Br^- into the soil (Wegman et al., 1981). Soils must sometimes be leached after methyl bromide application to prevent large Br^- residues in crops. Wegman et al. (1981, 1983) reported Br^- concentrations up to 45 mg/L in water draining from an intensive horticultural area in the Netherlands, due to soil leaching.

1.3 Bromate Formation During Water Treatment

The mechanism of bromate ion formation by the reaction of molecular ozone with bromide is shown below (Haag and Hoigne, 1983).

$$O_3 + Br^- \rightarrow O_2 + OBr^- \qquad k = 160\pm20 M^{-1}s^{-1} \qquad (1\text{-}1)$$

$$O_3 + OBr^- \rightarrow 2O_2 + Br^- \qquad k = 330\pm60 M^{-1}s^{-1} \qquad (1\text{-}2)$$

$$2O_3 + OBr^- \rightarrow 2O_2 + BrO_3^- \qquad k = 100\pm20 M^{-1}s^{-1} \qquad (1\text{-}3)$$

Ozone oxidizes bromide to form hypobromite (EQN 1-1) which is in association with hypobromous acid ($pK_a = 8.69$). Hypobromite reacts with ozone to form bromate

Reproduced with permission of the copyright owner. Further reproduction prohibited without permission.

(EQN 1-3), and also to regenerate bromide (EQN 1-2). Though hydroxyl radicals (OH•) are produced as a result of the decomposition of molecular ozone at pH>8 (von Gunten and Elovitz, 1997) the mechanism of bromate formation by the radical pathway is not well understood. It is reported to involve reactions with secondaty oxidants such as Br_2^- and CO_3^- (von Gunten et al., 1996).

The fact that hypobromite is considered the only pre-cursor to bromate formation in the molecular ozone pathway, suggests that pH reduction which would result in higher fractions of free bromine available as hypobromous acid (and lower the hypobromite fraction) may reduce bromate formation. Figure 1.1 is a fractional composition diagram of the HOBr-OBr^- system. Lowering the pH from 8.7 to 6.0, results in an increase in hypobromous acid fraction from 50% to approximately 100%. However, hypobromous acid reacts with natural organic matter (NOM) in water, to form brominated organic by-products such as bromoform, bromoacetonitriles, bromoacetone, bromoacetic acid and a group of labile compounds referred to as bromohydrins after the ozonation of natural waters containing bromide (Krasner et al., 1993; Glaze et al., 1993).

Reproduced with permission of the copyright owner. Further reproduction prohibited without permission.

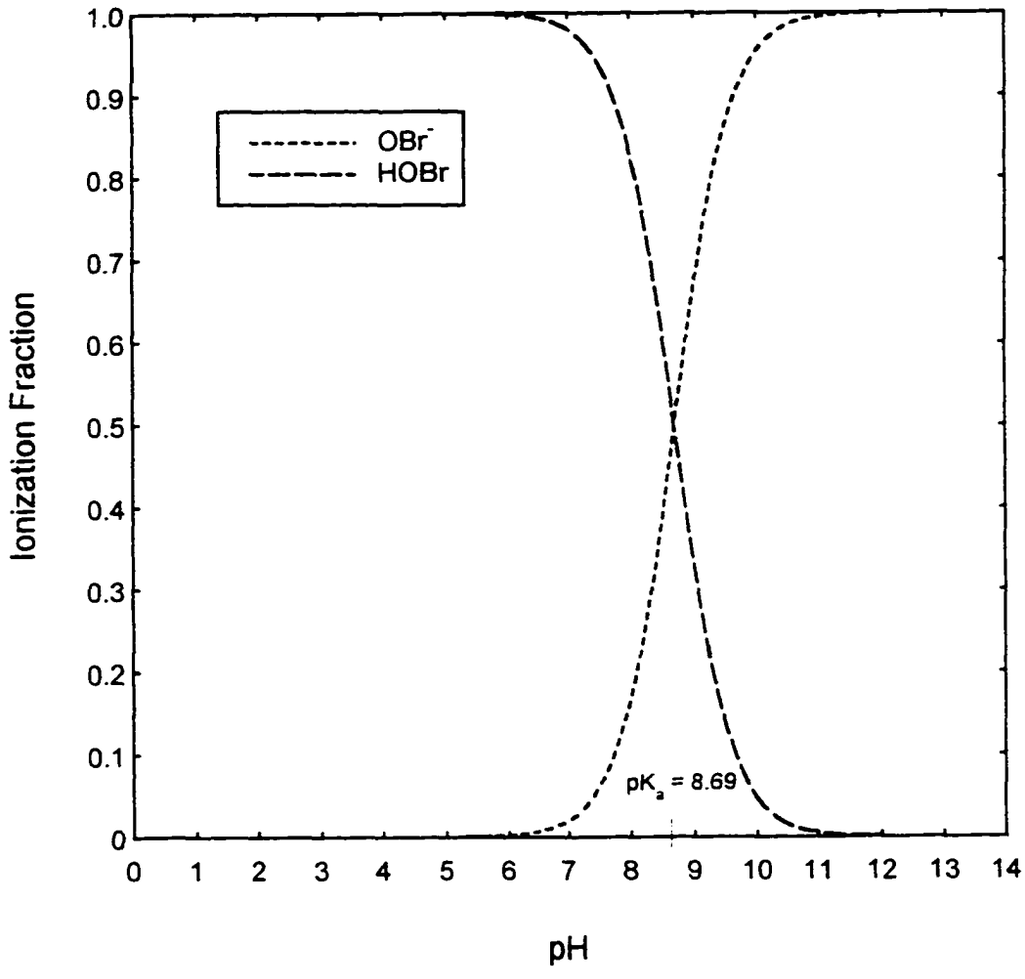

Figure 1.1. Fractional Composition Diagram of HOBr - OBr^- System at 25°C (Pourbaix, 1966).

Reproduced with permission of the copyright owner. Further reproduction prohibited without permission.

Richardson et al. (1981) also report on the formation of bromate upon the ozonation of estuarine waters and of artificial sea-water. Experiments carried out in the dark and under sunlamps revealed that the majority of total bromate was formed during the actual ozone bubbling period, with an additional smaller amount formed later through photolysis of the ozonated sample. Bromate levels in the non-photolyzed samples were found to be extremely stable for the entire 24hr exposure period.

The presence of bromide in water can also lead to bromate formation during chlorination. Farkas et al. (1949) used EQN (1-4) to describe the formation of hypobromite ion under alkaline pH conditions:

$$OCl^- + Br^- \rightarrow OBr^- + Cl^- \qquad (1\text{-}4)$$

Chapin (1934) and Engel et al. (1953) showed that hypobromite can disproportionate to form bromate:

$$3OBr^- \rightarrow BrO_3^- + 2Br^- \qquad (1\text{-}5)$$

Macalady et al. (1977) reported considerable production of bromate from solutions of chlorinated sea-water exposed to full natural sunlight. Approximately 50% of residual oxidant was converted into bromate in as little as 3 hours. Less intense sunlight conditions produced less bromate. The authors did not observe bromate formation in the dark which was in agreement with Lewin and Avrahami (1955) who

Reproduced with permission of the copyright owner. Further reproduction prohibited without permission.

reported substantial bromate formation in their 0.05M hypobromite solutions, almost 1000 times stronger than that used by Macalady et al. (1977).

Haag (1981) also reported formation of chlorate and bromate during chlorination of seawater. Chlorinated seawater samples containing mixtures of hypochlorite and hypobromite disproportionated much faster to form the halates than separate solutions of hypohalites. Bromate and chlorate formation was shown to involve cross-oxidation reactions as shown below:

$$HOCl + HOBr \rightarrow HBrO_2 + H^+ + 2Cl^- \qquad (1\text{-}6)$$

$$HOCl + HBrO_2 \rightarrow BrO_3^- + 2H^+ + Cl^- \qquad (1\text{-}7)$$

Furthermore, no enhancement of bromate formation rate was observed for the mixed hypohalite system when exposed to sunlight. The rate was merely that observed in pure hypohalite solution.

A report by the British Department of the Environment (DoE, 1993) showed that commercial sodium hypochlorite contains low ug/L levels of bromate as a contaminant. It was speculated that bromate occurrence was a result of bromide present in the brine used in hypochlorite production. Reactions such as EQN (1-6) and EQN (1-7) could result in the formation of bromate.

Reproduced with permission of the copyright owner. Further reproduction prohibited without permission.

1.4 Bromate Removal Strategies

The technologies currently in place to control bromate formation are limited, still in their infancy, and provide mixed results. While pH reduction significantly reduces the fraction of free bromine available to react with ozone and thus restricts bromate formation (Kruithof et al., 1993; Krasner et al., 1993), the formation of hydroxyl radicals, the first step in the advanced oxidation process, will be retarded. Therefore, degradation of micropollutants such as pesticides will be significantly slower. Also, circumstances are more favorable for formation of brominated organic compounds under acidic pH conditions. Addition of hydrogen peroxide increases the formation of hydroxyl radicals because of the reaction with ozone and peroxide. However it has not been established unequivocally in what way hydroxyl radicals affect bromate formation. Krasner et al. (1993) reported that the addition of hydrogen peroxide may increase the formation of bromate, particularly if it is added in the first stage of ozonation. However, Symons and Zheng (1997) showed that in exposing bromide ion laden water to hydrogen peroxide and H_2O_2-UV/Visible irradiation did not result in the formation of bromate ion. The addition of ammonia to react with free bromine and restrict bromate formation, depends on many water quality parameters and may provide mixed results (Siddiqui et al., 1994; Song et al., 1997).

UV radiation at 254 nm can be used for disinfection though it is not considered to be cost effective (Siddiqui et al., 1994). However it may be a viable option if it can

Reproduced with permission of the copyright owner. Further reproduction prohibited without permission.

also achieve bromate removal. The work of Farkas and Klein (1948) showed that it is capable of converting bromate into less harmful compounds. The concentration of bromate used in their study was four orders of magnitude higher than that commonly encountered in drinking water and the pH levels were at the extreme end of the acidic and alkaline pH scales.

The study presented herein focuses on the kinetics of bromate removal by UV radiation in the absence and in the presence of nitrite(or acetate) in aqueous solution. Ammonia addition is mentioned as a possible bromate control strategy. However, ammonia may be oxidized by ozone to form nitrite/nitrate, with the result that the solution may contain both bromate and nitrite.

Nitrite may also be a principal nitrogen component under reducing conditions such as in groundwater. A United States Geological Survey study of the South Platte River Basin in Colorado, Nebraska and Wyoming (USGS,1993), examined the available nutrients in surface water and in groundwater over a 12 year period. The data showed the concentration of nitrite plus nitrate comprised most of the nitrogen load in the downstream agricultural areas. Only two surface waters were found to exceed the maximum contaminant level (MCL) of 10 mg/L as nitrogen. However forty-six percent of the dissolved nitrite plus nitrate analyses from wells completed in the alluvium underlying agricultural areas equaled or exceeded the MCL. A previous study has shown that the presence of nitrite in solution with bromate caused a marked increase

Reproduced with permission of the copyright owner. Further reproduction prohibited without permission.

in the rate of bromate decay during gamma irradiation (Arnikar et al., 1975).

Surface waters and groundwater also include diverse types of natural organic matter (NOM) produced in various environmental systems (Thurman, 1985). NOM can be leached from soils or peat bogs or released by plankton or bacteria. The NOM can be roughly divided into two parts. The larger fraction which is labile, is quickly reused for the growth of organisms. A small part which is not easily degraded but is recycled, is accumulated in aquatic systems. Thus, most of the NOM in surface waters is composed of rather stable compounds of various origins. Krasner et al. (1996) found that one of the major components of NOM in water is acetate/acetic acid (CH_3COO^- /CH_3COOH). Also, Miltner et al (1992) found that ozonation of natural waters results in the production of aldehydes, ketones and carboxylic acid such as acetic acid.

1.5 Research Objectives

(i) To determine the stoichiometry and kinetics of bromate decomposition by UV radiation at 254 nm and product formation in aqueous bromate solution using distilled-deionized water under varying light intensity, pH and initial reactant concentrations.

(ii) To determine the effect of nitrite on the kinetics of UV catalyzed decomposition of bromate at 254nm for various UV light intensities, pH and initial reactant

Reproduced with permission of the copyright owner. Further reproduction prohibited without permission.

concentrations.

(iii) To study the effects of acetate on bromate decomposition during UV irradiation at 254 nm.

(iv) To develop a kinetic model that describes the concentration of major reactants and products in solution during UV irradiation of aqueous bromate solution or aqueous bromate solution containing nitrite.

Reproduced with permission of the copyright owner. Further reproduction prohibited without permission.

CHAPTER 2

BACKGROUND OF BROMATE PHOTODECOMPOSITION IN BROMATE AND BROMATE/NITRITE SOLUTIONS

2.1 Bromate Physical Data

Bromate is the conjugate base of bromic acid, $HBrO_3$ with an acid dissociation constant, pK_a, value of 0.7 at 25°C (Pourbaix, 1966). Figure 2.1 is a fractional composition diagram of the $HBrO_3$-BrO_3^- system at 25°C. At the levels normally encountered in water treatment, the ionized form is predominant.

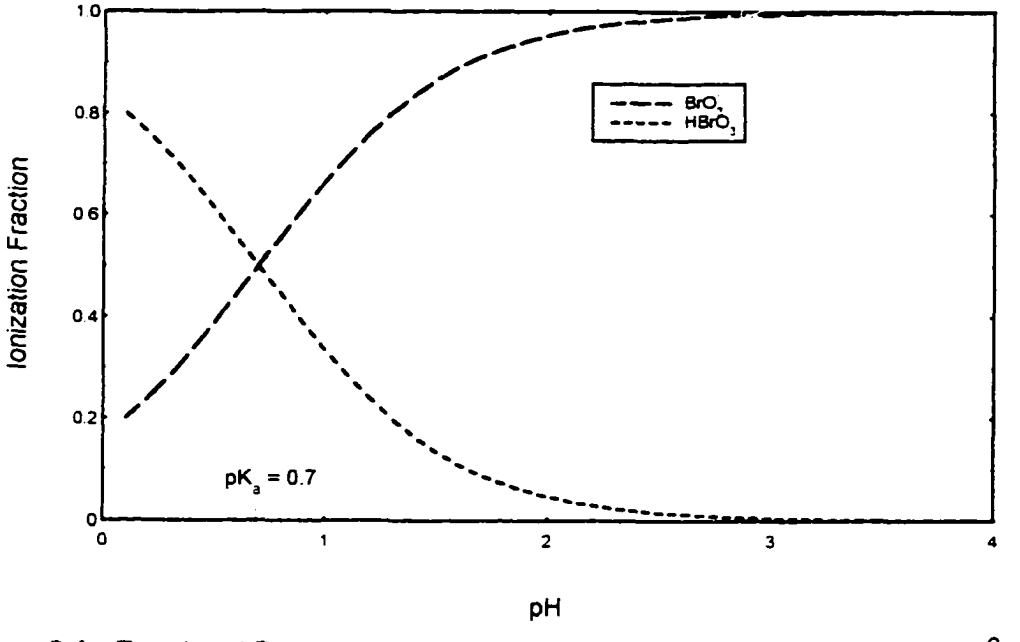

Figure 2.1. Fractional Decomposition Diagram of $HBrO_3$ - BrO_3^- System at 25°C (Pourbaix, 1966).

Reproduced with permission of the copyright owner. Further reproduction prohibited without permission.

The light absorption properties of bromate are weaker than other aqueous bromine species of interest, as shown in Table 2.1.

Table 2.1. Light Absorption Properties of Some Aqueous Bromine Compounds (Bridge and Matheson, 1960).

Species	λ_{max} (nm)	ϵ_{254} (M^{-1} cm^{-1})
BrO_3^-	195	9.77
Br^-	200	-
HOBr	266	79.4
OBr^-	330	42.2

λ_{max} ≡ wavelength of maximum absorption; ϵ_{254} ≡ molar absorptivity at 254 nm

Table 2.2 shows the thermodynamic values for bromate at various temperatures (Barner and Scheuerman, 1978).

Table 2.2. Bromate Thermodynamic Data (Barner and Scheuerman, 1978)

T (°C)	ΔH°_f (kcal/mol)	ΔG°_f (kcal/mol)	S (cal/°K mol)
25	-20	0.4	44.0
50	-21	2.2	40.8
58	-24.8	2.7	39.8
75	-25.3	4.1	37.4
100	-26.0	6.3	33.9
150	-27.6	10.7	27.8
200	-29.2	15.4	21.9
250	-30.8	20.1	15.6
300	-32.7	25.1	9.2

Reproduced with permission of the copyright owner. Further reproduction prohibited without permission.

Relevant standard electrode half-cell reduction reactions for bromate are shown below (Milazzo and Caroli, 1978):

$$BrO_3^- + 6H^+ + 5e^- \rightarrow \frac{1}{2}Br_2 + 3H_2O \qquad E^o = 1.52V \qquad (2\text{-}1)$$

$$BrO_3^- + 5H^+ + 4e^- \rightarrow HOBr + 2H_2O \qquad E^0 = 1.49V \qquad (2\text{-}2)$$

$$BrO_3^- + 3H_2O + 6e^- \leftrightarrow Br^- + 6OH^- \qquad E^o = 0.61V \qquad (2\text{-}3)$$

The reduction potential, E°, is positive for all three reactions. The Gibbs free energy, ΔG, is related to E° by EQN (*2-4*):

$$\Delta G = - n F E^o \qquad (2\text{-}4)$$

where n is the number of moles of electrons transferred in the redox reaction, and F, Faraday's constant (9.65×10^4 C). The more negative ΔG, the more spontaneous is the half reaction. Therefore, from thermodynamic considerations alone, the reduction of bromate is favored in all three half-reactions.

2.2 Fundamental Principles of Light

Light can be described in terms of both particles and waves. Two characteristic properties describing the wave nature of light is wavelength(λ) and frequency (ν). The relationship between frequency and wavelength is

Reproduced with permission of the copyright owner. Further reproduction prohibited without permission.

$$\nu = \frac{c}{\lambda} \tag{2-5}$$

where c is the speed of light (2.998 x 10^8 m/s in vacuum). UV light has wavelengths in the range of 100 - 350 nm.

With regard to its energy, it is more convenient to think of light as particles called photons. Each photon has an energy, E, defined by

$$E = h\nu = h\frac{c}{\lambda} \tag{2-6}$$

where h is Planck's constant (Note: 1 Einstein ≡ mole of photons).

The amount of light absorbed is an essential factor in photocemical transformations. The light that penetrates an absorbing medium does not have the same intensity due to partial reflection that takes place at the interface between the media. The relation between the amount of light absorbed and concentation, C, of the absorbing media is given by Beer-Lambert's law:

$$I = I_o e^{-\epsilon_\lambda C d} \tag{2-7}$$

where, d is the depth of the absorbing medium, and ϵ_λ it's molar absorptivity, which is determined by the nature of the absorbing substance and the wavelength of the light under consideration. This law is valid for dilute solutions and for monochromatic light.

Upon absorption of a quanta of radiant energy a molecule may rotate about its

Reproduced with permission of the copyright owner. Further reproduction prohibited without permission.

center of gravity and the two atomic nuclei may vibrate with respect to each other along the lines joining their centers (Ellis and Wells, 1941). Each of these motions is quantized, only discrete rotational and vibrational energy levels being possible.

Upon light absorption, electrons may be promoted from the ground state to other excited states. The successive energy increments between such electronic states vary in different molecules from about electron volt 23-230 kcal (Ferraudi, 1988). For a given electronic shift, there may be a diversity of simultaneous changes in the vibrational and rotational levels.

Excitation of a molecule by long wavelengths such as infrared leads only to an increase in the population of the higher vibrational-rotational levels of the ground electronic configuration (Hampley and Rawley, 1973). For radiation with wavelengths in the UV-Visible region, electrons in a molecule are promoted to higher electronic energy levels. Vibrational and rotational transitions occur as well. The quanta of these wavelengths are also sufficiently energetic to rupture bonds and produce chemical changes in molecules which absorb them (Rollefson and Burton, 1939).

2.3 The Photochemical Primary Process of Ions in Solution

The halogens are relatively simple ions and their primary photochemical process has been investigated by a number of authors. Inferences to the primary process for more complex ions are based on these findings.

Reproduced with permission of the copyright owner. Further reproduction prohibited without permission.

The absorption spectra of the halogens ions in the ultraviolet were stated by Franck and Scheibe (1928) to be electron affinity spectra. They suggested the splitting of the electron from the ion as the primary process and that the energy of the absorbed radiation is given by

$$h\nu = E + H + P - S - S^{*} \qquad (2\text{-}8)$$

E being the electron affinity of the halogen atoms, H the energy of hydration of the halogen ion, P the residual polarization of the water dipoles, and S and S^{*} the heat of solution of the halogen atom and of the electron, respectively. The chemical change involved in the absorption process is the formation of free halogen atoms and the evolution of the equivalent amount of hydrogen, the latter being produced by the attachment of the free electron to a hydrogen ion.

Subsequently this mechanism was modified by Franck and Haber (1931) according to whom the electron was not set free as such in the absorption process, but decomposes a water molecule in the hydration layer in the same elementary act. For iodine, the scheme was formulated as

$$I^{-} + H_2O + h\nu \rightarrow I + H + OH^{-} \qquad (2\text{-}9)$$

and the absorbed energy is given by

$$h\nu = D_{H_2O} + E_I - E_{OH} + X \qquad (2\text{-}10)$$

Reproduced with permission of the copyright owner. Further reproduction prohibited without permission.

where D_{H2O} is the energy necessary to dissociate the water molecule, E_I and E_{OH} are the electron affinities of the I atom and the OH• radical respectively, and X is the energy which the dissociation products retain owing to their charge and position. This view assumes that the dissociation energy of the dissociation energy of the hydrating water molecule is identical with that of a water molecule in the gaseous state and that there is only one water molecule in the hydration layer around the negative ion. According to Farkas and Farkas (1938), the latter assumption is probably valid for univalent ions such as I or Br, but that it is more difficult to justify the first assumption since the heat of dissociation of a water molecule in the hydration layer is D_{H2O} plus the energy of hydration, H, of the ion.

Farkas and Farkas (1938) suggested that the primary process of light absorption consists of the transfer of an electron from the absorbing ion to the one of the water molecules in the hydration layer. The photochemical change takes place when the electron jumps to a positive ion from the water molecule. This concept differs from the Franck and Scheibe primary process in that no formation of free electrons was postulated, and that water is not decomposed directly. The transfer of the electron to the positive ion was possible, since according to the Debye Huckel theory (Atkins, 1978) for strong electrolytes, there are positive ions in the vicinity of negative ions and vice versa, even at relatively low concentration, because of the electrostatic attraction between unlike ions.

Reproduced with permission of the copyright owner. Further reproduction prohibited without permission.

Three states were involved in the proposed mechanism: (1) the initial state in which the electron is bound to the negative ion with the energy, $-E_- - H_-$ (E_- = is the electron affinity of the anion in the gaseous state and , H_- = its hydration energy), (2) the intermediate state in which the electron is attached to the water molecule and has the energy $-E_{H2O}$ (E_{H2O} = electron affinity of water), and (3) the final state in which the electron has been transferred to a positive ion with the energy $I_- - H_-$ (I_- = ionization potential of the positive ion and H_- = energy of hydration for the positive ion). The energy of the absorbed radiation is then given by

$$h\nu = E_- + H_- - E_{H_2O} \qquad (2\text{-}11)$$

2.4 Bromate Decomposition by UV Radiation

Farkas and Klein (1948) using conventional techniques of photochemistry, studied the ultraviolet decomposition of halates ions (BrO_3^-,ClO_3^-,IO_3^-) in air saturated aqueous solution and found that the main reaction was formation of hypohalite (OBr^-, OCl^-, IO^-) and molecular oxygen. Furthermore, the irradiation of the hypohalite caused the formation of halide (Br^-,Cl^-, I^-) and halate ions and the evolution of oxygen. For bromate ion, the detailed reactions postulated for neutral solution were

$$(BrO_3^- H_2O) + h\nu \rightarrow (BrO_3 \bullet H_2O \bullet)^- \qquad \textit{electron transfer} \qquad (2\text{-}12)$$

Reproduced with permission of the copyright owner. Further reproduction prohibited without permission.

$$(BrO_3 \bullet H_2O\bullet)^- \rightarrow (BrO_3^- H_2O)^* \quad (2\text{-}13)$$

This excited complex because of the known exothermicity of the thermal decomposition of bromate (10 kcal/mol) to oxygen and hypobromite (Farkas and Klein, 1948), is then presumed to decompose as

$$(BrO_3^- H_2O)^* \rightarrow OBr^- + O_2 + H_2O \quad (2\text{-}14)$$

This explained the observed relatively high OBr^- quantum yield. In more acid solutions (pH < 6), some hydrogen (H_2) was also evolved and this was attributed to an increased probability of the photoexcited electron moving from the solvating water molecule to a neighboring proton as shown in EQN (2-15).

$$(BrO_3 \bullet H_2O\bullet)^- + H^+ \rightarrow BrO_3\bullet + H\bullet + H_2O* \quad (2\text{-}15)$$

Recombination of hydrogen atoms results in the evolution of hydrogen gas

$$H\bullet + H\bullet \rightarrow H_2 \quad (2\text{-}16)$$

For the hypobromite ion, a similar self-decomposition was postulated

$$(OBr^- H_2O) + h\nu \rightarrow (OBr\bullet H_2O\bullet)^- \rightarrow (OBr^- H_2O)^* \quad (2\text{-}17)$$

$$(OBr^- H_2O)^* \rightarrow Br^- + H_2O + O \quad (2\text{-}18)$$

with the oxygen atom responsible for the reformation of bromate. These results were

Reproduced with permission of the copyright owner. Further reproduction prohibited without permission.

obtained mainly for the bromate ion, but experimental evidence showed that chlorate and iodate behaved similarly. However chlorate, because of its low ultraviolet absorption, gave a low yield, and iodate being unstable, liberated iodine which absorbed the active light and led to a lower rate of decomposition.

Bridge and Matheson (1960) studied the flash photolysis of aqueous bromate solution by UV-Visible spectrophotometry. They observed an increase in absorption around 340 nm attributed to the known OBr^- formation accompanied by a reduction in absorption at wavelengths below 200 nm due to bromate decay. Two transients were observed and were tentatively identified. A short-lived transient (~1 μsec) absorbing at 350-390 nm was assigned to $BrO_3\bullet$ or $(BrO_3\bullet\ H_2O\bullet)^-$ and a longer lived transient (~10 μsec) absorbing at 460 nm to $BrO\bullet$ or $(OBr\bullet\ H_2O\bullet)^-$.

In the flash photolysis of bromate and hypobromite, Amichai and Treinin (1969) found evidence for a primary process that appears to refute the findings of Farkas and Klein (1948). The photodecomposition of oxybromine species were found to yield O^- ions:

$$BrO_3^- + h\nu \rightarrow BrO_2\bullet + O^- \qquad (2\text{-}19)$$

$$OBr^- + h\nu \rightarrow Br\bullet + O^- \qquad (2\text{-}20)$$

These were followed by secondary reactions involving O^- (or $OH\bullet$) with the parent ions to produce $BrO_3\bullet$ and $BrO_2\bullet$

Reproduced with permission of the copyright owner. Further reproduction prohibited without permission.

$$BrO_3^- + O^- + H_2O \rightarrow BrO_3\bullet + 2OH^- \quad (2\text{-}21)$$

$$BrO_3^- + OH\bullet \rightarrow BrO_3\bullet + 2OH^- \quad (2\text{-}22)$$

$$OBr^- + O^- + H_2O \rightarrow BrO\bullet + 2OH^- \quad (2\text{-}23)$$

In the presence of O_2 , the flash photolysis of BrO_3^- and OBr^- gave rise to a transient absorption peak at 430 nm consistent with that of O_3^-.

$$O^- + O_2 \rightarrow O_3^- \quad (2\text{-}24)$$

2.5 Bromate Decomposition in the Presence of Other Species

Bridge and Matheson (1960) confirmed the earlier finding of Farkas and Klein (1948) that the addition of ammonium (NH_4^+) to a bromate solution enhanced the rate of bromate decomposition. Ammonium was believed to react with OBr^- to produce the much less light absorbing Br^- (and N_2). This being the case, BrO• absorption at 460 nm should decrease with a correpsonding increase in BrO_3• absorption when ammonia is present during UV irradiation of bromate. Observance of the UV-Visible spectra showed that BrO• absorption at 460 nm decreased and BrO_3• absorption increased in the presence of NH_4^+.

Reproduced with permission of the copyright owner. Further reproduction prohibited without permission.

Radiation chemistry or radiolysis involves the application of γ- and x- rays in studying photo-sensitive substances. Radiolysis of water leads to the production of the hydrated electron (e-) , H•, OH• and hydrogen peroxide (H_2O_2). During the radiolysis of aqueous cesium bromate ($CsBrO_3$) solution with a ^{60}CO γ-ray source, Boyd and Larson (1965) reported on the disappearance of a previously observed hypobromite band at 330 nm after the addition of excess NH_4^+. The rapid and irreversible removal of this band was attributed to the reaction of hypobromite and NH_4^+ as suggested by Farkas and Klein (1948).

Species capable of reacting with OBr^- to form more weakly absorbing products are expected to produce similar results as NH_4^+ during UV irradiation of bromate solution. Nitrite is known to react favorably with aqueous free bromine. Using a stopped-flow spectrophotometric technique, Pendlebury and Smith (1972), studied this reaction which they proposed to proceed as follows:

$$NO_2^- + Br_2 + H_2O \rightarrow NO_3^- + 2Br^- + 2H^+ \qquad (2\text{-}25)$$

Since liquid bromine hydrolyzes in solution (EQN 2-26) to give free bromine (Beckwith et al., 1996) nitrite oxidation results from the reaction with both Br_2 and $HOBr/OBr^-$.

$$Br_2 + H_2O \rightleftharpoons HOBr + Br^- + H^+ \quad ; K_f = 3.5 \times 10^{-9}\ M^2 \qquad (2\text{-}26)$$

Reproduced with permission of the copyright owner. Further reproduction prohibited without permission.

Generally nitrite was held in large excess over bromine and the pseudo-first order rate constant was found to be independent of initial total bromine in the range (1.8 - 8.2) x 10^{-5} M, independent of ionic strength in the range 0.12 - 0.37 M and independent of nitrate up to 0.2M. In the pH range 4.2 - 5.8, the decay rate was found to be

$$-\frac{d[Br_2]}{dt} = k\,[Br_2][NO_2^-]^2 \qquad (2\text{-}27)$$

where $k = (4.6 \times 10^{1} + 3.3 \times 10^{4}/[Br^-])$ L/mol · s. In the pH range of 0.8 - 2.5 the rate law was described as

$$-\frac{d[Br_2]}{dt} = k\,[Br_2][HNO_2]^2 \qquad (2\text{-}28)$$

where $k = (5.9 \times 10^{4} + 3.4 \times 10^{4}/[Br])/(1 + 1.90 \times 10^{7}[H^+][Br^-])$. In the pH range of 2.8 - 3.3 a combination of these two rate laws adequately described the kinetics of the reaction.

Lengyel et al. (1989) studied the nitrous acid - bromine reaction

$$NO_3^- + 2Br^- \rightleftharpoons Br_2 + HNO_2 + H_2O \qquad (2\text{-}29)$$

The rate of the reverse reaction (r_{-1}) was found to be first order in nitrous acid in the range (5-200) x 10^{-4} M and half-order in bromine in the range (1.9 - 18) x 10^{-3} M. Upon

Reproduced with permission of the copyright owner. Further reproduction prohibited without permission.

increasing the initial proton concentration from 0.2 to 2.0M the rate of the reaction was reported to decrease. The overall rate of the reverse reaction was described by the following expression:

$$r_{-1} = k[Br_2]^{0.5}[HNO_2]h^{0.5} \quad (2\text{-}30)$$

Amikar et al. (1975) studied the radiolysis of nitrite in the presence of bromate using a ^{60}CO γ-ray source and found evidence that both bromate and nitrite decomposition increases when the two species are present in solution. During γ-irradiation of aqueous nitrite solution, nitrite was found to disappear in a linear manner reaching an equilibrium with nitrate at a NO_3^-/NO_2^- ratio of 9:1. In the presence of bromate, however, there was a complete conversion of nitrite to nitrate. It was suggested that the radiolytic products of bromate decomposition ($BrO_2\bullet$ and $BrO\bullet$) may directly attack the nitrite ion converting it to nitrate

$$BrO_2\bullet + NO_2^- \rightarrow BrO\bullet + NO_3^- \quad (2\text{-}31)$$

$$BrO\bullet + NO_2^- \rightarrow Br\bullet + NO_3^- \quad (2\text{-}32)$$

The bromine atom formed in EQN (2-32) is converted back into Br^- by the hydrated electron. Furthermore, an increase in the bromide yield during the irradiation of bromate solution in the presence of nitrite over that observed in pure bromate solution

Reproduced with permission of the copyright owner. Further reproduction prohibited without permission.

suggests that bromate decomposition increased in the presence of nitrite.

The literature did not show any research on the bromate/acetate system under UV irradiation. However, acetate is known to react favorably with free bromine to form a series of substituted haloacetic acids (Pourmoghhadas et al., 1993). Acetate (λ_{max} = 280, ϵ_{max} = 24) lacks the carbon-carbon double bond (C=C) that is characteristic of more stronly absorbing organic compounds. Its presence in a UV irradiated solution of bromate could enhance bromate decay by removing free bromine from solution.

2.5 Nitrite Decomposition During UV Irradiation

Nitrite is photosensitive and undergoes a photochemical reaction under UV irradiation. Treinin and Haynon (1970) found that the flash photolysis of nitrite ions in pure aqueous solution gives rise to three transient absorptions assigned to NO_2 (λ_{max} ~400nm), N_2O_4 (λ_{max} ~340nm) and N_2O_3 (λ_{max} ~250 nm). However, no net chemical reaction was proposed. During the UV irradiation (228 nm) of a 2.7 x 10^{-4} M NO_2^- solution, the authors reported that the quantum yield of nitrite depletion was less than 10^{-3}. Efficient back reactions were considered to be responsible for this result. The formation of the ozonide radical (O_3^-) in air saturated alkaline solutions of nitrite ions was suggested as being indicative of the production of O^- (or OH•) by the primary photolytic process:

Reproduced with permission of the copyright owner. Further reproduction prohibited without permission.

$$NO_2^- + h\nu \rightarrow (NO_2^-)^* \quad (2\text{-}33)$$

$$(NO_2^-)^* \rightarrow NO + O^- \quad (2\text{-}34)$$

$$O^- + H_2O \rightarrow OH + OH^- \quad (2\text{-}35)$$

However, Zafiriou and True (1979) and Zafiriou et al. (1980) reported on the net loss of nitrite and the formation of nitrate during the UV photolysis of natural waters. Treinin and Haynon (1970) did report on a net chemical reaction to form nitrate during the UV photolysis of HNO_2.

$$3HNO_2 \rightarrow 3NO\bullet + NO_3^- \quad (2\text{-}36)$$

Bilski et al. (1992) found that the UV excitation of nitrite anions in anaerobic solution leads to the formation of NO• and OH• radicals (EQN 2-37). The hydroxyl radical may recombine with NO• giving HNO_2 (EQN 2-38) or be scavenged by nitrite ions at a diffusion controlled rate to yield OH^- and $NO_2\bullet$ (EQN 2-39). NO• and $NO_2\bullet$ may react to give N_2O_3 (EQN 2-40) which hydrolyzes to regenerate nitrite (EQN 2-41). Thus no apparent chemical change is observed during anaerobic photolysis. However in air saturated solution, NO• may be competitively oxidized by oxygen which leads to oxygen depletion and the formation of nitrate (EQN 2-42).

Reproduced with permission of the copyright owner. Further reproduction prohibited without permission.

$$(NO_2^-)^* + H_2O \rightarrow OH\bullet + NO\bullet + OH^- \quad (2\text{-}37)$$

$$HO\bullet + NO\bullet \rightarrow HNO_2 \quad (2\text{-}38)$$

$$HO\bullet + NO_2^- \rightarrow NO_2\bullet + OH^- \quad (2\text{-}39)$$

$$NO\bullet + NO_2\bullet \rightarrow N_2O_3 \quad (2\text{-}40)$$

$$N_2O_3 + H_2O \rightarrow 2HNO_2 \quad (2\text{-}41)$$

$$NO\bullet + NO_2\bullet + O_2 + H_2O \rightarrow 2HNO_3 \quad (2\text{-}42)$$

Reproduced with permission of the copyright owner. Further reproduction prohibited without permission.

CHAPTER 3

METHODS AND MATERIALS

3.1 Experimental Methods

The experiments were carried out in a 1.6L pure fused quartz reactor (Ace Glass, Vineland, NJ) with index of refraction, $\eta = 1.506$. The quartz reactor was positioned in the center of a cylindrical photochemical reactor chamber (Rayonet RPR-200, Southern New England Ultraviolet Company, Branford, CT) equipped with sixteen removable low pressure mercury lamps (35W) aligned symmetrically opposite each other on the aluminum polished inner walls of the chamber. The lamps had a life of 3000 hours and produced *line radiation* at 254 nm. The reactor could be operated either in a horizontal or vertical position. Figure 3.1 is a schematic of photochemical reactor.

All photochemical experiments were carried out in a dark room. The entire system was placed in a fume hood. The reactor was always operated in batch mode and in a vertical position. BrO_3^- or BrO_3^-/NO_2^- (or BrO_3^-/Acetate) solutions were prepared in 2-liter volumetric flasks. The pH of the solutions were adjusted to the desired level with 5N NaOH. The UV lamps were allowed 10 minutes warm-up prior to each photochemical experiment. The reactor was filled with the BrO_3^- or BrO_3^-/NO_2^- (or BrO_3^-/Acetate) solution and the photoreaction commenced.

Reproduced with permission of the copyright owner. Further reproduction prohibited without permission.

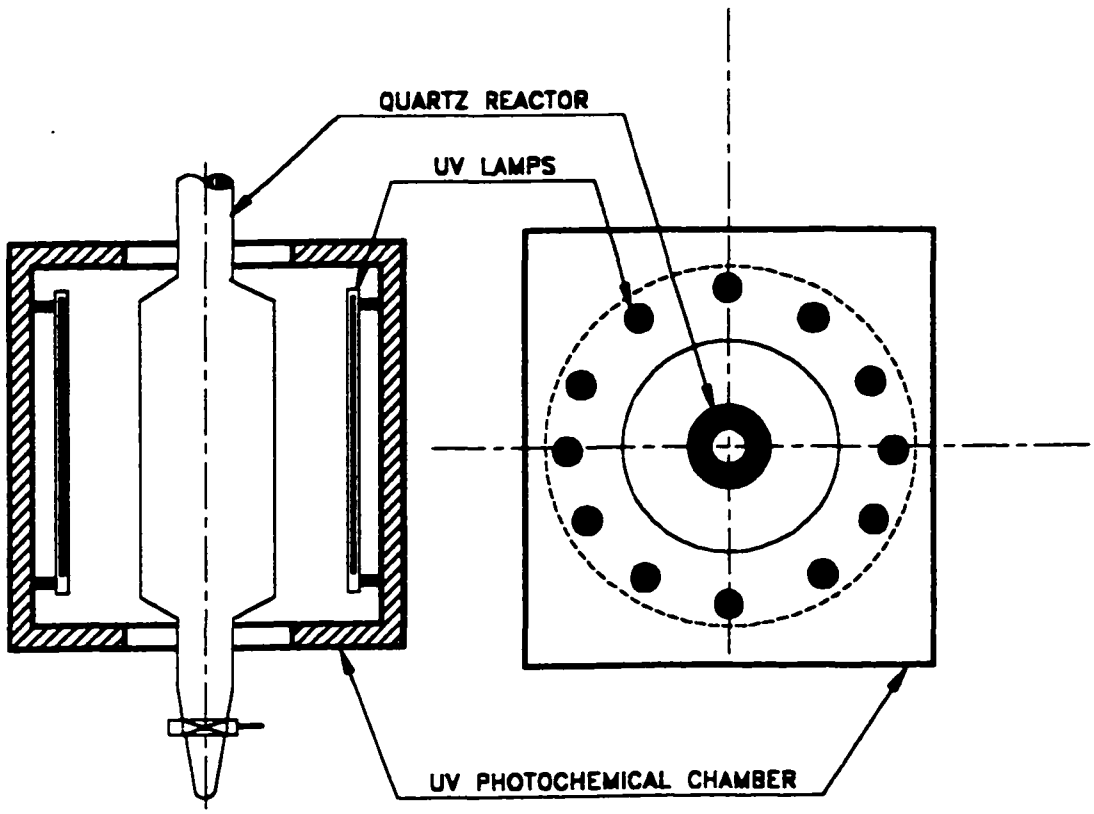

Figure 3.1. Schematic of UV Photochemical Chamber Reactor.

Reproduced with permission of the copyright owner. Further reproduction prohibited without permission.

The reaction temperature was monitored through a thermometer permanently positioned at the top port of the reactor. A fan placed underneath the photochemical chamber helped limit temperature variations in the reactor medium to within 1.5°C of the initial temperature. Approximately 15mL of sample was withdrawn periodically from the bottom port of the reactor. Eight mL were used to determine total free bromine, one mL was used in ion chromatography to determine bromate, bromide, nitrite, nitrate and acetate concentrations, and the rest for pH determination. The dependency of BrO_3^- decay rate on UV light intensity was studied by varying the number of lamps in the reaction chamber.

3.2 Analytical Methods

All chemicals were reagent ACS grade with the exception of free bromine solution which was prepared in the laboratory (section 3.2.4). Distilled-deionized water (Barnstead, Dubuque, Iowa, Model E-pure) with a specific resistance of 18.2 μmhos-cm was used in the preparation of all reagents and solutions. Analysis of the distilled-deionized water according to Method 2320B of Standard Methods for the Analysis of Water and Wastewater (APHA, AWWA, WEF, 1995) showed the alkalinity to be below the detection limit. An Orion Model 611 digital pH/millivolt meter equipped with a Corning combination electrode was used for all pH measurements.

Reproduced with permission of the copyright owner. Further reproduction prohibited without permission.

3.2.1 Determination of Ionic Species By Ion Chromatography

Bromate, bromide, nitrite, nitrate and acetate were determined using a single channel ion chromatograph equipped with gradient mixing (Model 4500i, Dionex Corporation, Sunnyvale, CA) according to Method 4110 of Standard Methods for the Examination of Water and Wastewater (APHA, AWWA, WEF, 1995). Table 3.1 lists the operating parameters of the instrument.

Table 3.1. Operating Parameters of the Ion Chromatograph.

Guard Column / Separator Columns	AG9 (4mm) / AS9-SC (4mm)
Eluent	1.8 mMNa_2CO_3/1.7 mM $NaHCO_3$
Eluent Flow	2.0 mL/min
Regenerant	0.025 N H_2SO_4
Suppressor	AMMS-II
Detector	CDM-1
Sample Loop	50 µL

The quantification of each ion was performed by comparison of the peak height to that of standard solutions. According to the manufacturer and for the operating conditions used in this study, the detection limit was 50 - 100 µg/L for bromate and 50 µg/L for bromide, nitrite, nitrate (Kaplan, 1998).

Stock bromate solution (1000 mg/L as Br) was prepared by dissolving 1.8886 g of dessicator dried $NaBrO_3$ (Fisher Scientific) in distilled-deionized water and

Reproduced with permission of the copyright owner. Further reproduction prohibited without permission.

diluting to a final volume of 1000 mL. Stock bromide solution (1000 mg/L) was prepared by dissolving 1.2879 g NaBr (Fisher Scientific), dried at 105°C, in distilled-deionized water and diluting to 1000 mL. Stock nitrite (1000 mg/L as N) was prepared by dissolving 0.9856 g $NaNO_2$ (Fisher Scientific), dried in a dessicator, in distilled-deionized water and diluting to 200 mL. Stock nitrate (1000 mg/L as N) was prepared by dissolving 1.4443 g KNO_3 (Fisher Scientific), dried at 105°C, in distilled-deionized water and diluting to 200 mL. Stock acetate solution (1000 mg/L) was prepared by dissolving 1.3898 g of sodium acetate (CH_3COONa) in approximately 700 mL of water and diluting to 1000 mL. All stock solutions were refrigerated at 4°C. Fresh stock solutions were prepared monthly.

Stock solutions of sodium carbonate (0.5M) and sodium bi-carbonate (0.5M) were used for eluent preparation. The 0.5M sodium carbonate was prepared by dissolving 26.49 g of Na_2CO_3 (Fisher Scientific) in 400 mL of distilled-deionized water and diluting to a final volume of 500 mL. The 0.5M sodium bicarbonate stock was prepared by dissolving 21.00 g of $NaHCO_3$ (Fisher Scientific) in 400 mL of distilled-deionized water and diluting to a final volume of 500 mL. The eluent solution of 1.8mMNa_2CO_3/1.7mM $NaHCO_3$ was prepared by diluting 7.2 mL of stock sodium carbonate and 6.8 mL of stock sodium bi-carbonate with distilled-deionized water to a final volume of 2000 mL. The 0.025N H_2SO_4 regenerant for ion chromatography was prepared by the addition of 2.8 mL concentrated sulfuric acid to distilled-deionized

Reproduced with permission of the copyright owner. Further reproduction prohibited without permission.

water and making a final volume of 4L.

Preparation of standard anion solutions for ion chromatographic analyis was as follows. Combined bromate and bromide standards of 0.5, 1.0, 2.0 and 4.0 mg/L as Br, respectively, were prepared by pipetting the appropriate amount of stock bromate and stock bromide solutions into each of four 100 mL volumetric flasks and diluting to volume. Combined nitrite and nitrate standards of 0.5 and 1.0 mg/L as N, respectively, were prepared by pipetting the appropriate volume of stock nitrite and stock nitrate solutions into 100 mL volumetric flasks and diluting to volume. Acetate standards in the range of 2 mg/L to 20 mg/L were prepared by pipetting the appropriate amount of stock acetate into 100 mL volumetric flasks and diluting to volume. These solutions were prepared bi-weekly.

To develop the calibration curve for the anions, the standard solutions were removed from the refrigerator and allowed to come to room temperature (22- 25°C). The ion chromatograph was turned on and allowed approximately 30 minutes for equilibration. The output range on the instrument was set to either 3μS or 10 μS to ensure high height towidth ratio. Approximately 1 mL of the combined standard was injected and the peak heights recorded on the strip-chart recorder. The detention time of each anion in the ion chromatograph varied as shown in Table 3.2.

Reproduced with permission of the copyright owner. Further reproduction prohibited without permission.

Table 3.2. Ion Chromatographic Detention Time of the Anions.

Anion	Detention Time (min)
Acetate	1.1
BrO_3^-	1.4
NO_2^-	1.9
Br^-	2.9
NO_3^-	3.4

The products of the peak height (mm) and output range (μS) were plotted versus concentration (mM) for each anion using EASYPLOT (Spiral Software, Massachussets Institute of Technology, MA). Regression lines were drawn through the data points to give the calibration equation for each anion. Figure 3.2 depicts a typical calibration curve developed prior to a UV photochemical experiment.

Reproduced with permission of the copyright owner. Further reproduction prohibited without permission.

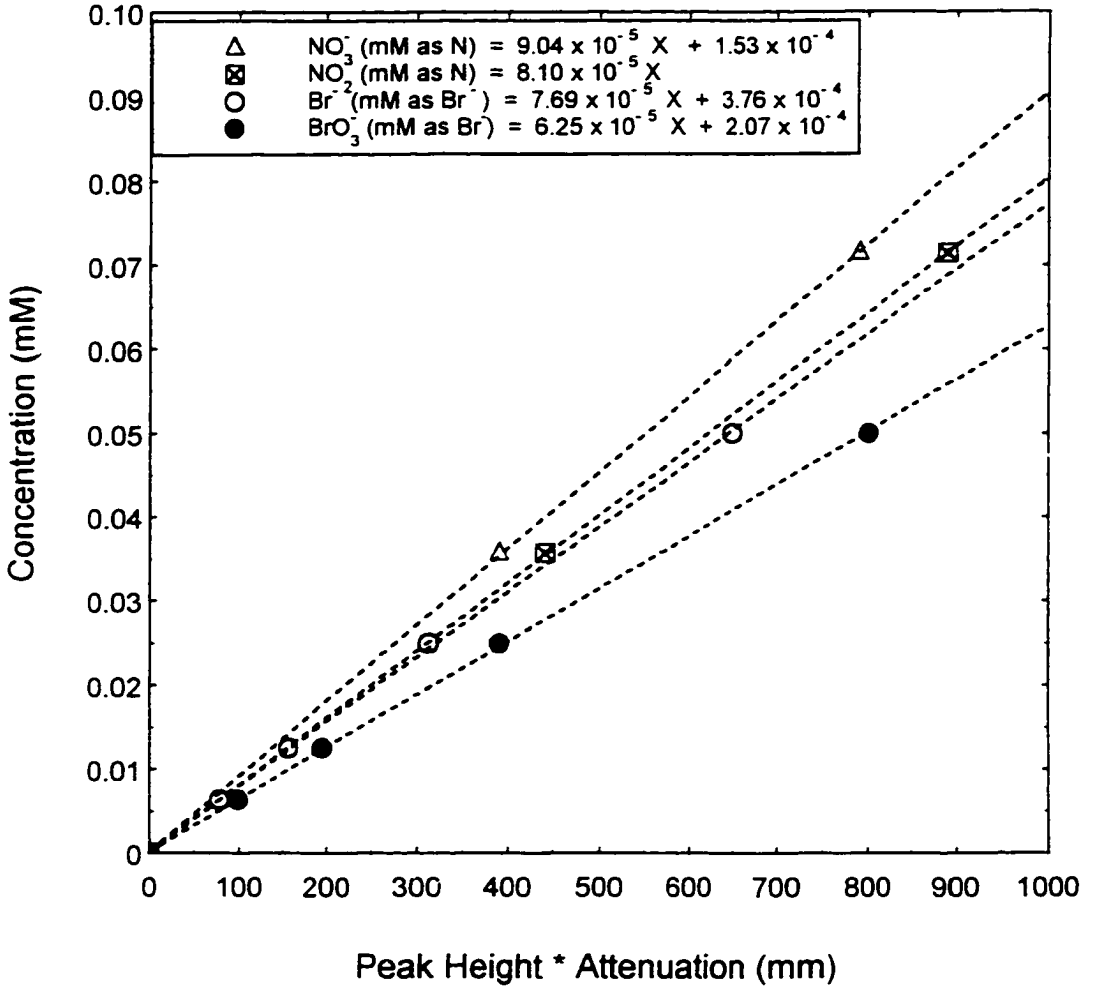

Figure 3.2. Typical Ion Chromatography Calibration Curves (Experiment No. 64).

Reproduced with permission of the copyright owner. Further reproduction prohibited without permission.

3.2.2 Free Bromine Determination By Spectrophotometric Analysis

A single beam spectrophotometer (Spectronic 20D, Milton Roy, Rochester, N.Y.) was used to determine total free bromine colorimetrically at 515 nm during bromate photodecomposition experiments. A wavelength accuracy check (Spectronic 20D Operator's Manual, Milton Roy, Rochester) of the instrument was performed with Cobalt Chloride periodically to ensure proper calibration of the instrument. The results always showed a minimum transmittance between 505 and 515 nm, which according to the manufacturer, indicates proper calibration. Figure 3.3 shows a typical wavelength calibration curve.

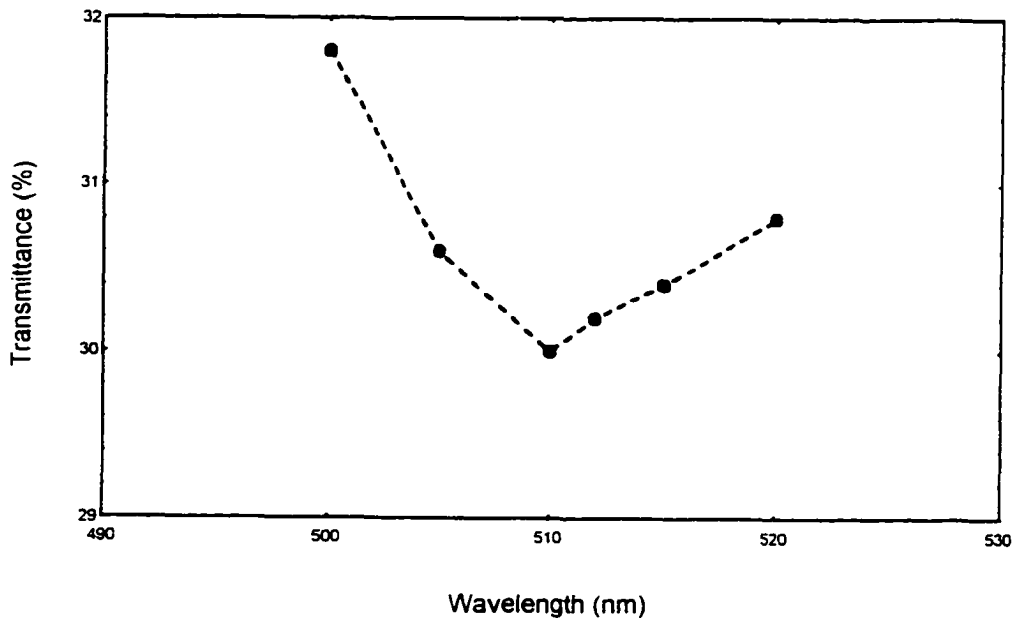

Figure 3.3. Wavelength Calibration for Spectrophotometer.

Reproduced with permission of the copyright owner. Further reproduction prohibited without permission.

Solution preparation for spectrophotometric analysis was as follows. A 1% hydrochloric acid solution was prepared by slowly adding 20 mL of concentrated HCl (Fisher Scientific) to 400 mL of distilled-deionized water and diluting to a final volume of 2000 mL. Stock Cobalt Chloride was prepared by dissolving 22 g of $CoCl_2$ (Fisher Scientific) in 1% HCl and bringing the solution to a final volume of 1000 mL with 1% HCl. Stock potassium permanganate was prepared by dissolving 891 mg $KMnO_4$ (Mallinckrodt) in 700 mL of distilled-deionized water and diluting to a final volume of 1000 mL (Stock B). This solution was placed in a brown bottle and refrigerated at 4°C. Fresh stock was prepared monthly. Phosphate buffer and DPD indicator were prepared according to Method 4500-Cl of Standard Methods for the Analysis of Water and Wastewater (APHA, AWWA, WEF, 1995).

Calibration of the Spectronic 20D with potassium permanganate was performed about 20 minutes prior to each experiment. Ten mL of stock potassium permanganate was diluted to 100 mL with distilled-deionized water in a volumetric flask (stock B). Dilution of 1mL of stock B to a final volume of 100 mL produces a bromine equivalent of 1.13 mg/L as Br (0.014 mM). Standards of 0.0014mM, 0.0028 mM, 0.0042 mM and 0.0056 mM were prepared by pipetting the appropriate amount of stock B into volumetric flasks containing distilled-deionized water and making a final volume of 100 mL. To each of four 1cm test tubes, 0.4 mL of DPD and 0.4 mL of phosphate buffer was added. Eight mL of 0.0014 mM standard was added, the cell stoppered and

Reproduced with permission of the copyright owner. Further reproduction prohibited without permission.

mixed, and the absorbance measured. The point from the addition of DPD and buffer to obtaining the absorbance reading was completed within 10 seconds. This procedure was repeated for the other three standards. A plot of concentration versus absorbance was developed and a best fit line drawn through the data points to give the calibration equation. Figure 3.4 depicts typical calibration curves.

Bromate photodecomposition experiments were begun within five minutes of calibration. Of the total sample volume of 15 mL withdrawn from the quartz reactor, 8 mL were used for free bromine determination by the procedure described above. Free bromine concentration in mM was determined by substituting the absorbance reading of the sample, into the calibration equation.

Reproduced with permission of the copyright owner. Further reproduction prohibited without permission.

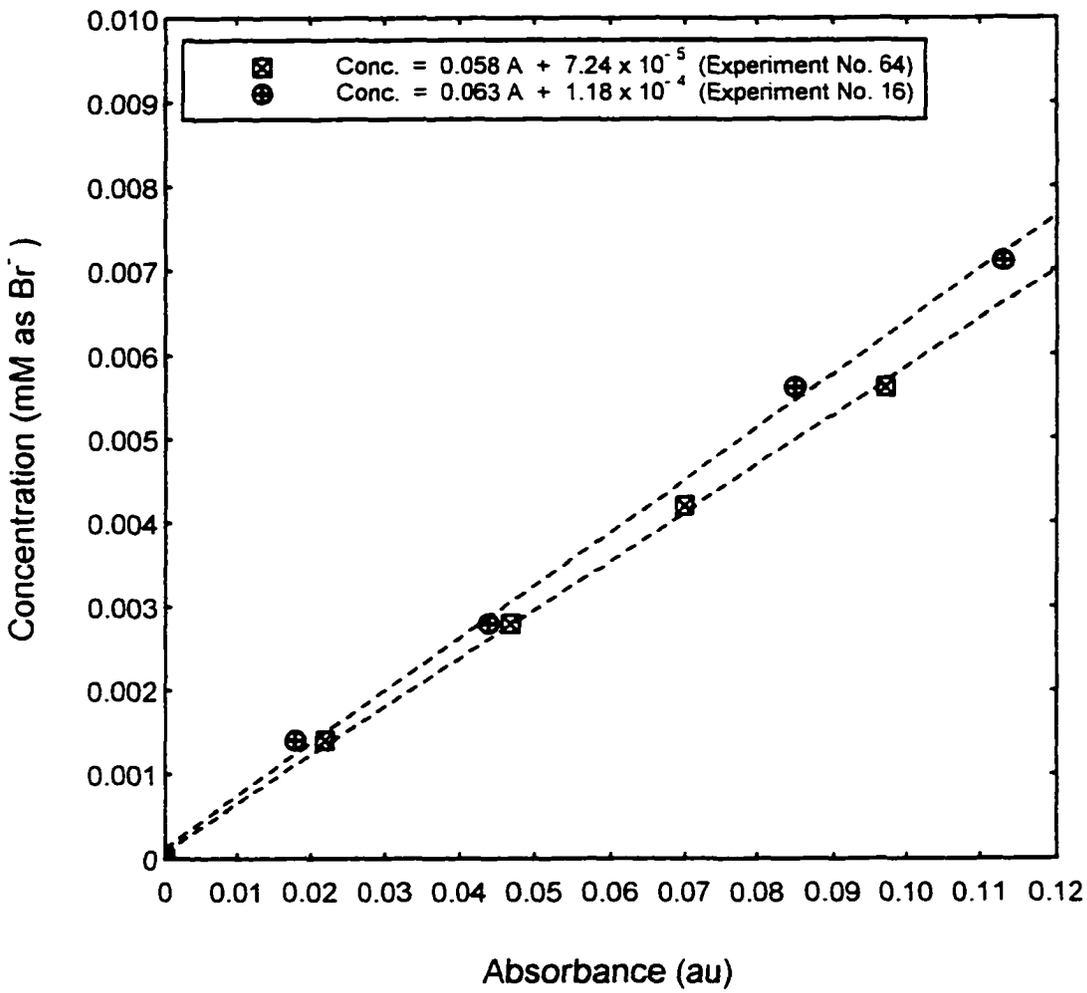

Figure 3.4. Typical $KMnO_4$ Calibration Curves for Free Bromine Determination.

Reproduced with permission of the copyright owner. Further reproduction prohibited without permission.

3.2.3 UV Absorbance of Bromate, Bromide, Nitrite, Nitrate and Acetate

A UV-Visible spectrophotometer (Model HP8453, Hewlett Packard) was used to determine the absorption characteristics of aqueous solutions of bromate, bromide, nitrite, nitrate and acetate. It was equipped with a mirror to direct the source radiation from a Deuterium and a Tungsten lamp through a quartz sample cell. A concave holographic grating dispersed the radiation unto a multielement photo-diode array detector, which enabled full spectrum capture (190 - 1100 nm) in 0.1 s.

The absorbance of a 500 mg/L solution of each anion was determined by mixing 1.5 mL of distilled-deionized water in the quartz cell with an equal volume of stock solution of each anion. Figures C-1 through C-5 of Appendix C show the wavelength scans for the respective anions. The absorbance maxima in the range of 190 - 1100 nm was also determined and is shown in Table 3.3.

Table 3.3. Wavelength of Maximum UV Absorption for Anions of Interest.

Anion	λ_{max} (nm)
BrO_3^-	197
Br^-	196
NO_2^-	354
NO_3^-	302
Acetate	363

The absorbance spectrum of a free bromine solution (pH ~ 9) prepared by

Reproduced with permission of the copyright owner. Further reproduction prohibited without permission.

mixing equimolar amounts of bromide and free chlorine had been determined earlier and showed the wavelength of maximum absorption at 326 nm. This value is in close agreement to the λ_{max} value of 329 nm for OBr^- reported by Gazda and Margerum (1994). The same authors reported a λ_{max} of 260 nm for HOBr.

3.2.4 Preparation of Free Bromine Solution

Since free bromine has a molar absorptivity greater than that of bromate at 254nm (Farkas and Klein, 1948; Bridge and Matheson, 1960) it was necessary to determine its decay characteristics under conditions similar to that of the bromate decomposition experiments.

A 2.7 mg/L bromide solution was prepared by diluting 5.4 mL of stock bromide (1000 mg/L) in a 2L volumetric flask. The total free chlorine concentration of a purified grade sodium hypochlorite (Fisher Scientific) was determined using the DPD FAS Titrimetric method (APHA, AWWA, WEF, 1995). Seventy-nine μL of NaOCl stock was diluted to 2L in a volumetric flask and the concentration determined by the DPD Titrimetric method.

Free bromine was prepared by mixing equal volumes (900 mL) of bromide and free chlorine solution in a 2L Erlenmeyer beaker. Farkas et al. (1949) found that the overall reaction could be represented by EQN (3-3).

$$OCl^- + Br^- \rightarrow OBr^- + Cl^- \qquad (3\text{-}3)$$

Reproduced with permission of the copyright owner. Further reproduction prohibited without permission.

The progress of the reaction was monitored by observing the change in bromide and chloride concentrations by ion chromatography. The end of the reaction was signaled when there was no observed change in either the bromide or chloride concentrations over time. The free bromine was then determined by the DPD titrimetric method. The overall reaction time was approximately one hour. Figure C-6 of Appendix C shows the monitoring of free chlorine removal and free bromine formation upon mixing equal volumes of a free chlorine solution and bromide solution in a quartz cell of the UV-Visible spectrophotometer.

After ion chromatography showed that the reaction was complete, the pH of the mixture was then adjusted to the desired level using 5M NaOH. Prior to UV irradiation, the initial bromide concentration was determined by ion chromatography and free bromine concentration determined by the DPD FAS Titrimetric method. Sixteen hundred mL of free bromine solution was placed in the quartz reactor. The initial temperature of the solution was recorded and the UV lamps were switched on. Samples were periodically withdrawn and analyzed for free bromine by the DPD Titrimetric method, and bromide, chloride and bromate by ion chromatography. No change in chloride concentration was observed during UV irradiation indicating that free chlorine was not initially present and that free bromine was the active species.

Reproduced with permission of the copyright owner. Further reproduction prohibited without permission.

3.2.5 Light Intensity Determination by Chemical Actinometry

Light flux was measured using chemical actinometry. It requires a solution that undergoes a chemical change of a known quantum yield (ϕ_λ) defined by the following:

$$\phi_\lambda = \frac{1}{I_a}\frac{d[P]}{dt} \qquad (3\text{-}4)$$

where I_a is the light intensity in Einstein / L s, and d[P]/dt is the change in product concentration (mol/L s) with time. (Note: 1 Einstein = the amount of light absorbed by 1 mol or 6.022×10^{23} photons). Solving the above expression for I_a gives:

$$I_a = \frac{1}{\phi_\lambda}\frac{d[P]}{dt} \qquad (3\text{-}5)$$

Potassium ferricoxalate, $K_3Fe(C_2O_4)_3 \bullet 3H_2O$, is the most commonly used chemical actinometer (Nussbaum et al., 1987). The photochemical reactions which are initially acid catalyzed are shown below:

$$Fe(C_2O_4)_3^{3-} \rightarrow Fe(C_2O_4)^{-} + 2(C_2O_4)^{2-} \quad (acidic\ solution) \qquad (3\text{-}6)$$

$$Fe(C_2O_4)^{-} + h\nu \rightarrow Fe^{2+} + (C_2O_4)^{-} \qquad (3\text{-}7)$$

$$Fe(C_2O_4)^{-} + (C_2O_4)^{-} \rightarrow Fe^{2+} + (C_2O_4)^{2} + 2CO_2 \qquad (3\text{-}8)$$

A single photon can theoretically produce two Fe^{2+} ions (EQN 3-7 and 3-8). The Fe^{2+}

Reproduced with permission of the copyright owner. Further reproduction prohibited without permission.

produced can then be determined spectrophotometrically by complexation with 1,10 phenanthroline (λ_{max} = 510 nm).

In the determination of the light intensity from a photon source it is assumed that ϕ_{Fe2+} is accurately known. For the ferricoxalate actinometer, the generally accepted quantum yields have been those obtained in the classic work of Hatchard and Parker (1956). These authors carried out an exhaustive study of interferences, spectral sensitivity, photon flux dependence, and the effect of ferricoxalate concentration on the quantum yield. The absolute value of their determinations of ϕ_{Fe2+} were based on either a calibrated thermophile traceable to the National Physics Laboratory or the quantum yields of the uranyl oxalate actinometer. They also used a thermophile as a relative standard, normalizing all of the data to the quantum yield of the 0.006M ferricoxalate actinomter at 436 nm. The absolute value of ϕ_{Fe2+} determined at 254 nm with 0.006 M ferrioxalate solution was 1.28.

In calibrating the ferricoxalate actinometer, Bowman and Demas (1976) found it to be erratic and irreproducible. The problem was traced to a previously unrecognized slow photodegradation of the 1, 10-phenanthroline solutions which could result in errors in excess of 40% when using published procedures. The errors were reduced when the 1,10-phenthroline solution was stored in the dark, and freshly prepared every three months. Under these conditions, development of the actinometer solution after addition of 1,10-phenthroline and buffer was less than two minutes.

Reproduced with permission of the copyright owner. Further reproduction prohibited without permission.

A 0.006M potassium ferricoxalate solution was prepared in the dark room in the manner described by Hatchard and Parker (1956). The K_3 Fe $(C_2O_4)_3 \cdot 3H_2O$ (Pfaltz and Bauer, Inc., Waterbury, Connecticut) was dessicated for an hour and 5.8944 g weighed and dissolved in about 1400 mL of distilled-deionized water containing 200 mL of 1N H_2SO_4. The solution was diluted to a final volume of 2000 mL with distilled-deionized water.

Twenty-five mL of potassium ferricoxalate solution was placed in each of two calibrated 25 mL square glass cells (Hach Company, Loveland, CO). To one, designated as the sample cell, the contents of one *ferrous iron reagent powder pillow* (Hach Company, Loveland, CO) containing 1,10 phenanthroline and acetate buffer was dissolved and the timer on the spectrometer set (Model DR3000, Hach Company, Loveland, CO) set. After 3 minutes, the cell designated as "blank", was placed in the spectrometer and zeroed at 510nm. The sample cell was then placed in the spectrometer, and the initial Fe^{2+} concentration read in mg/L.

Before starting the experiment, the UV lamps were allowed 10 minutes warm-up. Sixteen hundred mL of the potassium ferricoxalate solution was placed in the quartz vessel and positioned in the center of the photochemical chamber reactor. The initial temperature of the solution was recorded and the UV lamps and the fan positioned below the quartz reactor were simultaneously turned on. After 20 minutes of irradiation, the UV lamps and the fan were turned off and the final temperature

Reproduced with permission of the copyright owner. Further reproduction prohibited without permission.

recorded. Approximately 10 mL of sample was withdrawn from the reactor. One mL of the sample was diluted to 200 mL in a volumetric flask and Fe^{2+} determined as described above. The change in Fe^{2+} molar concentration was determined and the light intensity calculated according to EQN 3-5. This procedure was performed for 16, 12, 8, and 4 UV lamps. Table3.4 shows the results of the light intensity determinations. The data in Table 3.4 along with statistical data for each UV light intensity is plotted in Figure 3.5. The figure also show number of data points lying within ±n standard deviations of the mean, for each UV light intensity.

Table 3.4. UV Lamp Intensity For Various Lamp Configurations.

DATE	UV LAMP INTENSITY (Einstein L^{-1} s^{-1})			
	16 Lamps	**12 Lamps**	**8 Lamps**	**4 Lamps**
2/20/96	2.44×10^{-6}	1.08×10^{-6}	3.20×10^{-7}	2.21×10^{-7}
2/21/96	2.61×10^{-6}	-	-	2.20×10^{-7}
5/10/96	3.32×10^{-6}	1.02×10^{-6}	4.49×10^{-7}	2.36×10^{-7}
6/19/96	2.36×10^{-6}	-	4.59×10^{-7}	
6/20/96	2.55 x 10-^{6}	-	-	2.28×10^{-7}
6/26/96	-	1.17×10^{-6}	-	
2/26/97	2.50×10^{-6}	-	4.81×10^{-7}	
6/17/97	-	1.26×10^{-6}	-	2.32×10^{-7}
8/12/97	2.37×10^{-6}	1.20×10^{-6}	4.66×10^{-7}	
1/22/98	2.74×10^{-6}	-	-	2.40×10^{-7}
AVERAGE	**2.61×10^{-6} ± 4.8×10^{-8}**	**1.15×10^{-6} ± 4.2×10^{-8}**	**4.35×10^{-7} ± 2.9×10^{-8}**	**2.30×10^{-7} ± 3.0×10^{-9}**

Reproduced with permission of the copyright owner. Further reproduction prohibited without permission.

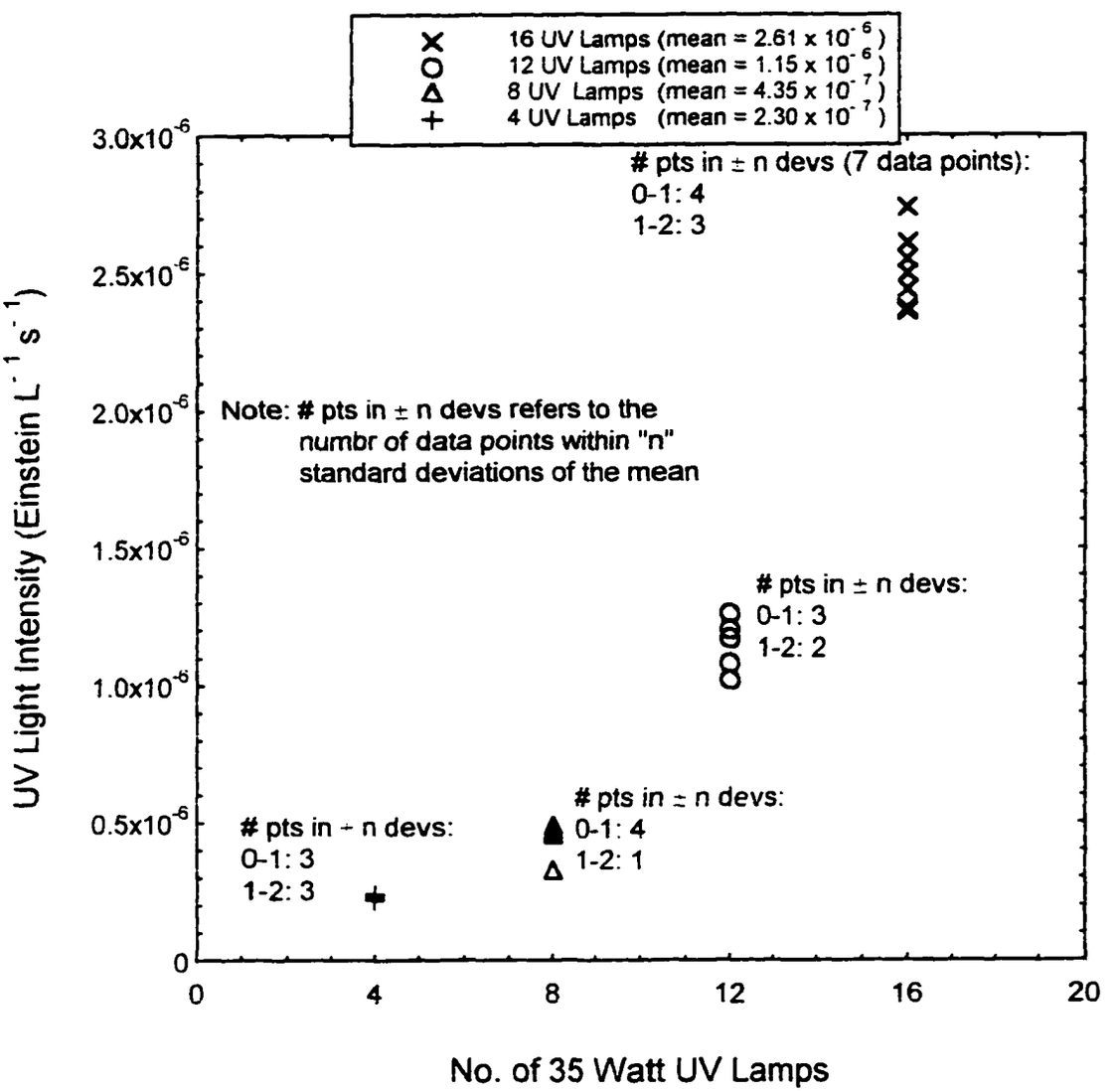

Figure 3.5. UV Lamp Intensity for Each UV Lamp Configuration Used in the Study.

Reproduced with permission of the copyright owner. Further reproduction prohibited without permission.

CHAPTER 4
RESULTS AND DISCUSSION

4.1 Bromate Decomposition During UV Irradiation of Bromate Solution

4.1.1 Experimental Observations

Typical concentration-time profiles of species during UV irradiation of aqueous solutions of bromate are shown in Figures 4.1 through 4.4 for the four UV intensities used in this study. In all experiments, bromate decay was followed by bromide formation. TFB formed in the early stages of the experiments and remained in solution in low levels throughout. The comparison of the initial total bromine (TBr_i) depicted by the dashed horizontal line and the bromine balance during the experiment (TBr_t) as calculated by EQN (4-1), virtually eliminates the possibility of formation of other bromine end products in detectable quantities.

$$[TBr]_t = [BrO_3^-]_t + [Br^-]_t + [TFB]_t \qquad (4\text{-}1)$$

A statistical analysis of TBr_t for each of the four experiments showed that the number of data points lying within one standard deviation of the mean was 87, 79, 67, and 86% for Figures 4.1 through 4.4 respectively. The low value in Figure 4.3, could be possibly explained by some error in determining low levels of free bromine since the data points lie consistently below the horizontal line when TFB is shown to disappear. In Figure 4.1, σ_s is relatively higher due to outliers between twenty and thirty minutes.

Reproduced with permission of the copyright owner. Further reproduction prohibited without permission.

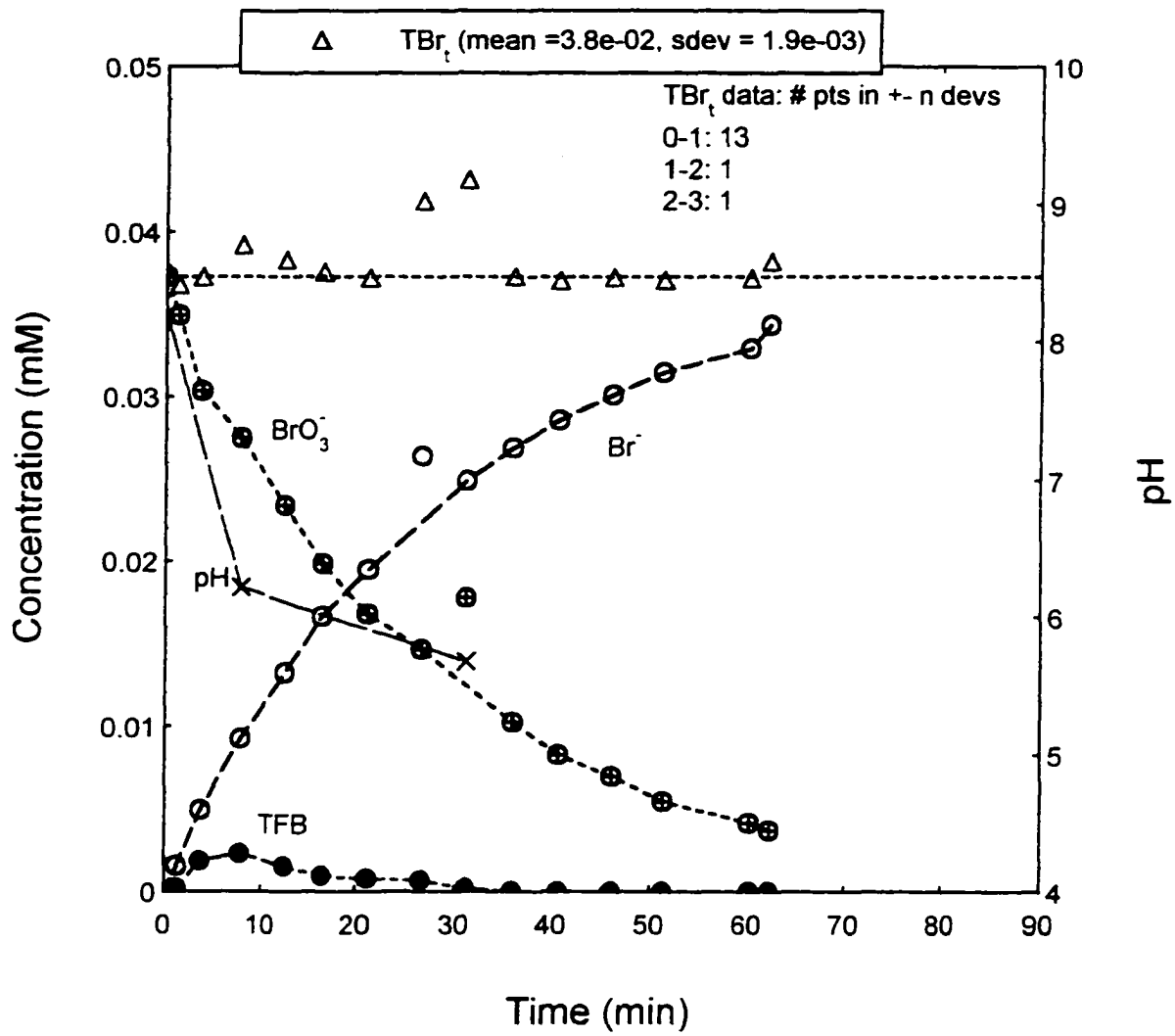

Figure 4.1. Species Profiles During UV Irradiation of Aqueous Bromate ($I = 2.61 \times 10^{-6}$ Einstein/L*s, $BrO_3^- = 0.037$ mM, $pH_i = 8.20$, $T_i = 21.8°C$; EXP 41).

Reproduced with permission of the copyright owner. Further reproduction prohibited without permission.

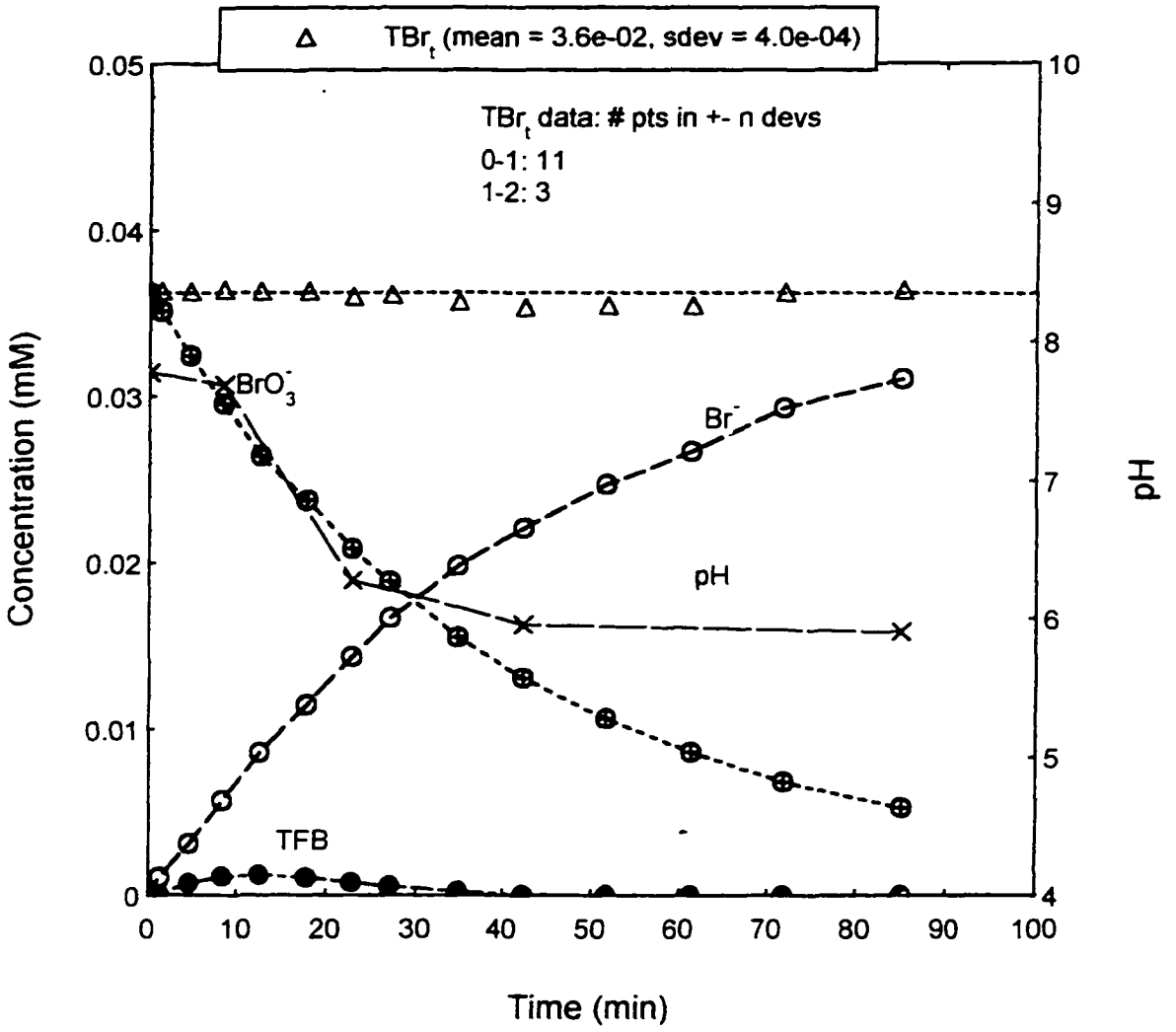

Figure 4.2. Species Profiles During UV Irradiation of Aqueous Bromate ($I = 1.15 \times 10^{-6}$ Einstein/L*s, BrO_3^- = 0.038 mM, pH_i = 7.77, T_i = 25°C; EXP 38).

Reproduced with permission of the copyright owner. Further reproduction prohibited without permission.

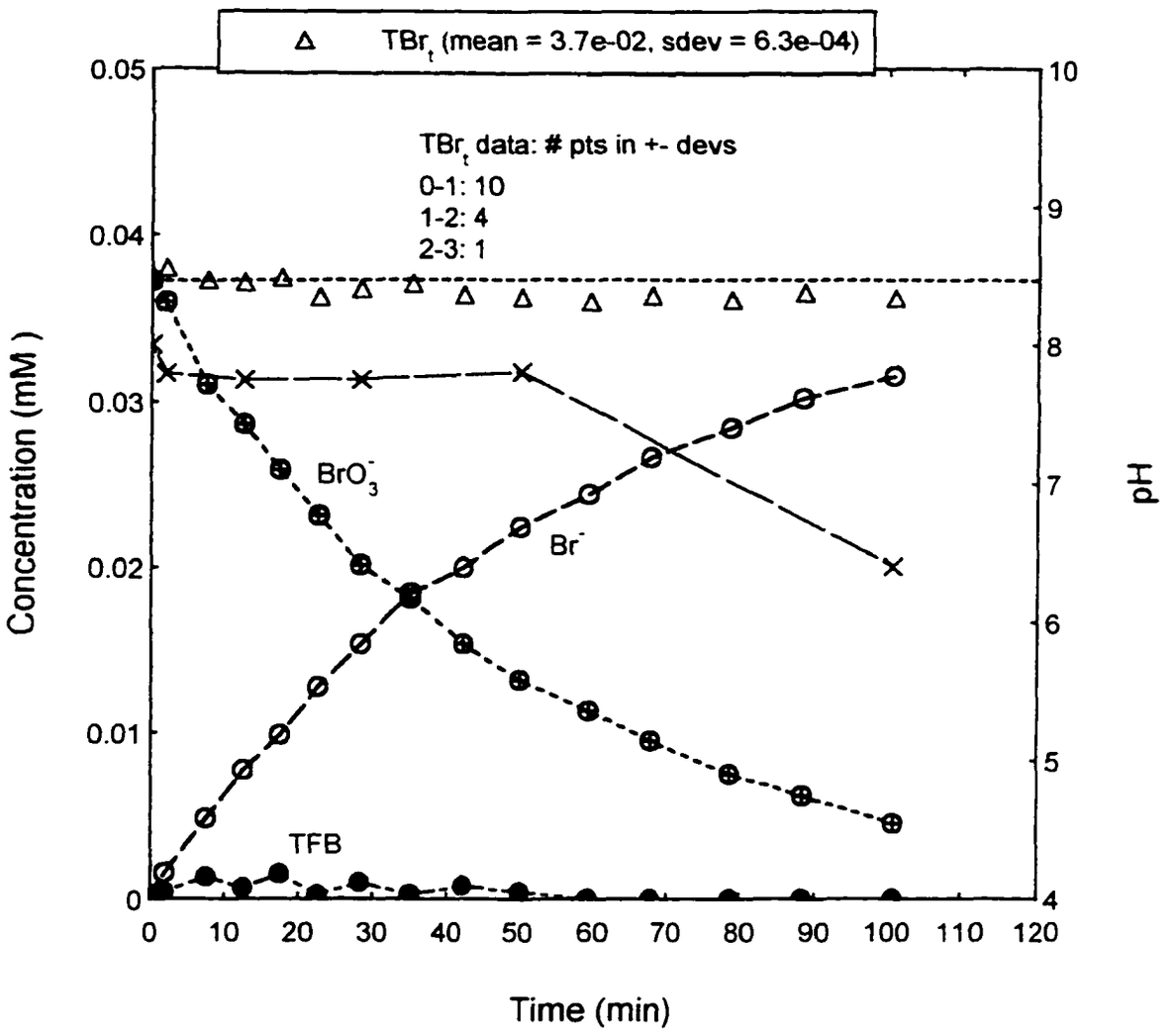

Figure 4.3. Species Profiles During UV Irradiation of Aqueous Bromate ($I = 4.35 \times 10^{-7}$ Einstein/L*s, BrO_3^- = 0.038 mM, pH_i = 8.01, T_i = 23°C; EXP 88).

Reproduced with permission of the copyright owner. Further reproduction prohibited without permission.

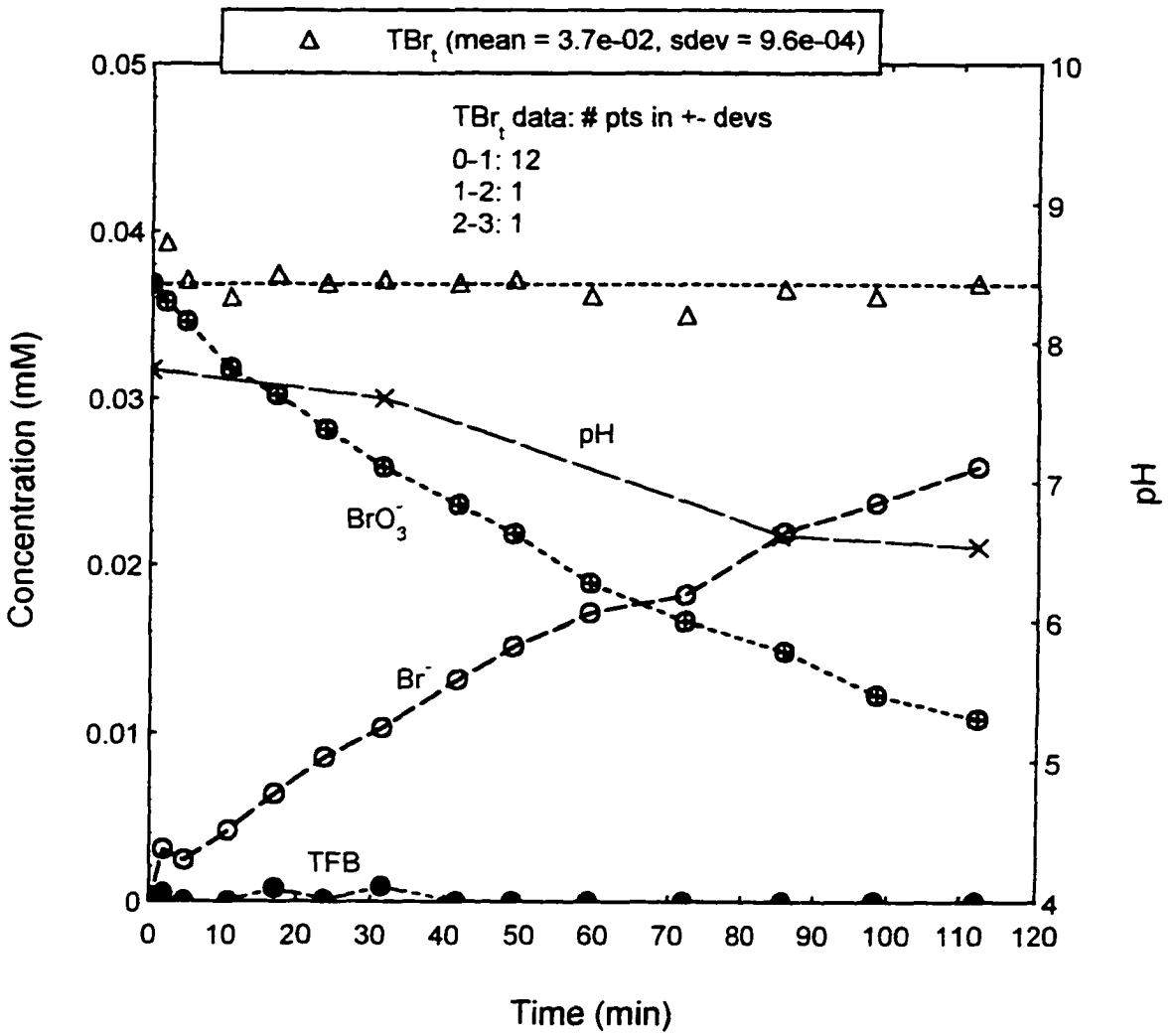

Figure 4.4. Species Profiles During UV Irradiation of Aqueous Bromate ($I = 2.30 \times 10^{-7}$ Einstein/L*s, $BrO_3^- = 0.038$ mM, $pH_i = 8.17$, $T_i = 24°C$; EXP 82).

Reproduced with permission of the copyright owner. Further reproduction prohibited without permission.

Solution pH is seen to decrease during the experiments depicted in Figures 4.1 through 4.4. This was characteristic of all photochemical experiments with pH < 9.0. For experiments with initial pH > 9.0, solution pH remained within 0.4 pH units of the initial value during UV irradiation. Figure 4.5 shows the species profile of a typical experiment conducted at initial pH > 9.0. The species profiles are similar to that in the four previous figures but the pH decrease is markedly smaller.

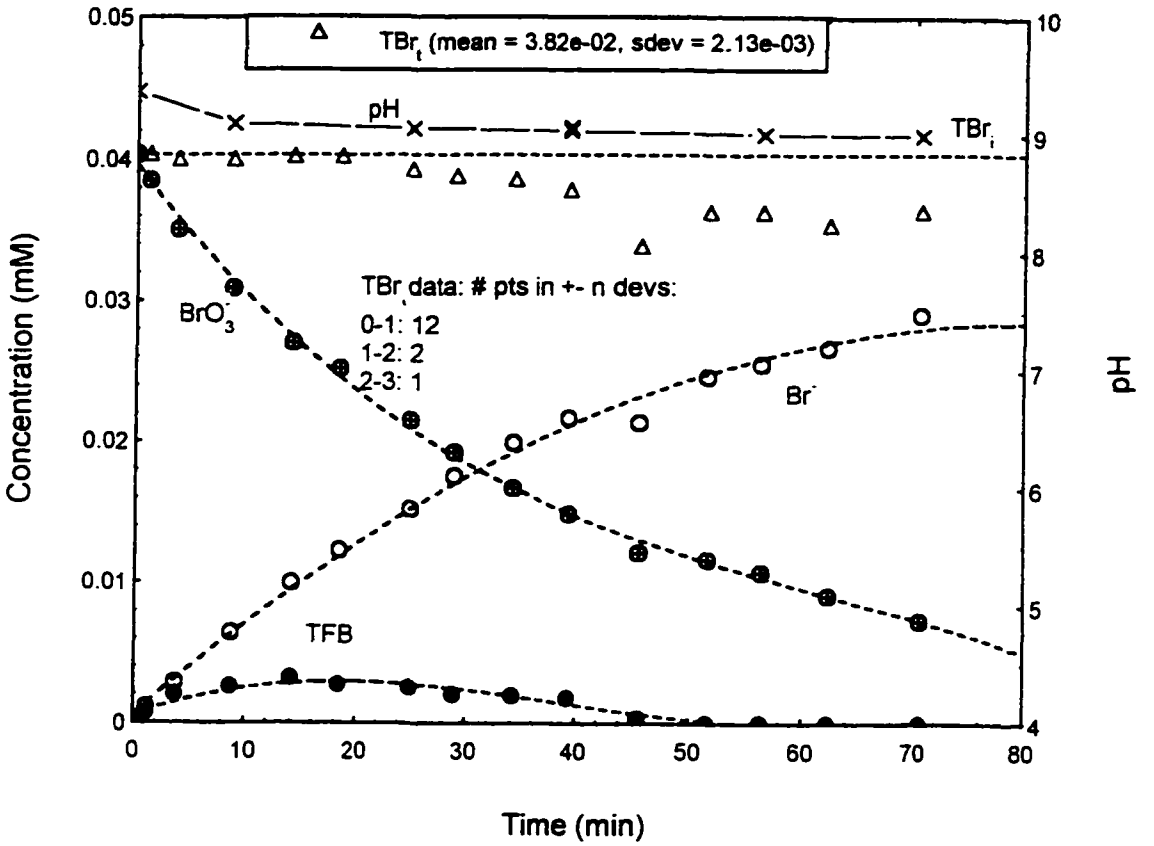

Figure 4.5. Species Profile During UV Irradiation of Aqueous Bromate ($I = 1.15 \times 10^{-6}$ Einstein $L^{-1} s^{-1}$, BrO_3^-=0.038 mM, pH_i=9.37, T_i = 21°C; EXP 47).

Reproduced with permission of the copyright owner. Further reproduction prohibited without permission.

Figure 4.6 shows the results of an experiment monitoring the pH of an aqueous bromate solution compared to that of a control (i.e. distilled-deionized water) during UV irradiation. The pH of the control solution is relatively stable throughout the experiment while the pH of the bromate solution initially drops then stabilizes after approximately 10 minutes of reaction time. The fact that initial pH of the control was less than that of the bromate solution was not significant. Experiments with bromate solutions at similar initial pH levels, routinely experienced drops in pH by as much as 1.5 units.

Siddiqui et al. (1996) reported similar pH profiles during the application of High Energy Electron Beam (HEEB) irradiation to reagent water spiked with bromate. Irradiation of water with electron beams results in the formation of reducing aqueous species such as aqueous electrons, hydrogen atoms and oxidizing species such as hydroxyl radicals (Allen, 1961). Decreases in pH by as much as 1.2 units observed in their study were attributed to the consumption of OH^- by an unexplained reaction. Thomas et al. (1964) showed the reaction of H• with OH^- to be

$$H\bullet + OH^- \rightarrow e^-_{aq} + H_2O \qquad k = 2 \times 10^7\ M^{-1}\ s^{-1} \qquad (4\text{-}2)$$

Since H• is a product of both UV irradiation of bromate (EQN 2-15) and of water (Ellis and Wells, 1941), EQN (4-2) may explain the pH decreases found in this study.

Reproduced with permission of the copyright owner. Further reproduction prohibited without permission.

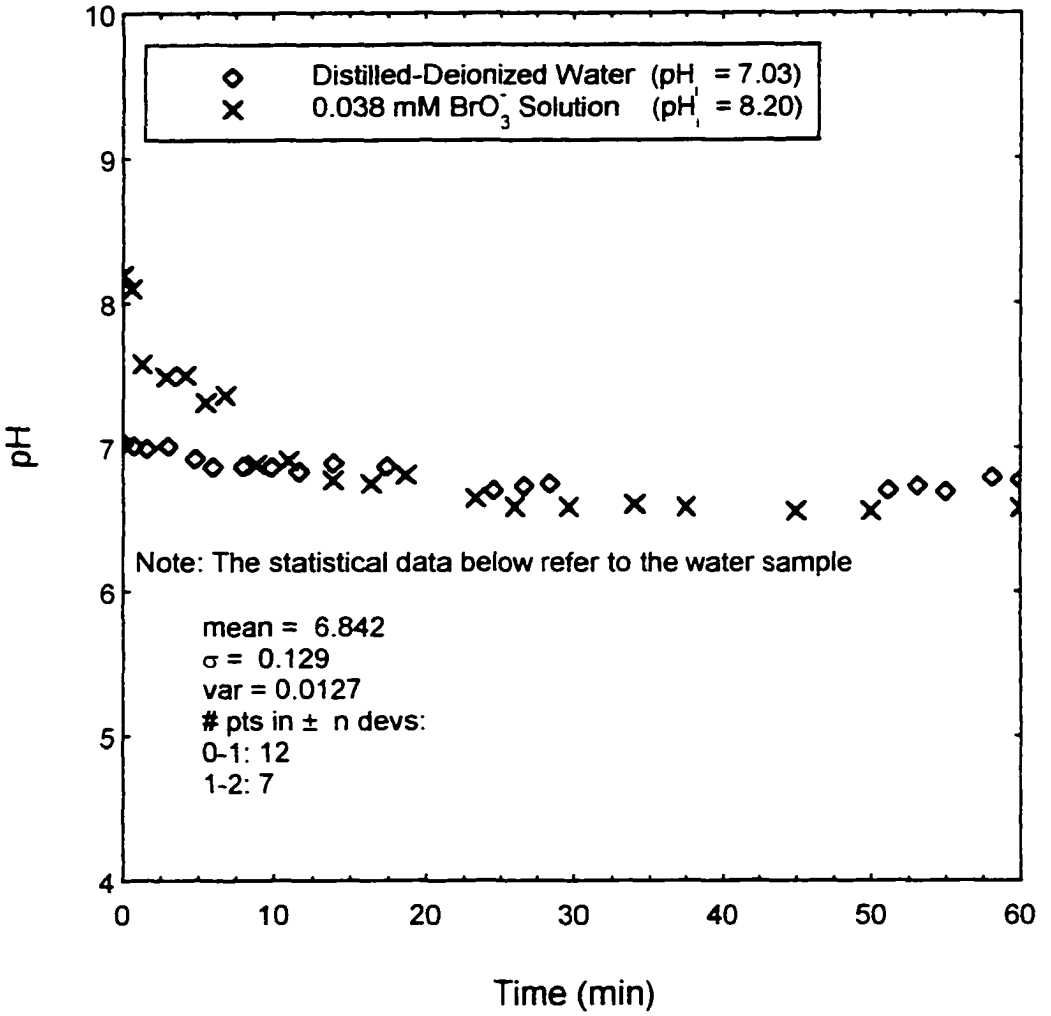

Figure 4.6. pH Profile During UV Irradiation of Aqueous Solution.
$I = 1.15 \times 10^{-6}$ Einstein $L^{-1} s^{-1}$, $T_i = 25°C$.

Reproduced with permission of the copyright owner. Further reproduction prohibited without permission.

4.1.2 Bromate Decay Kinetic Expressions Under UV Irradiation

For first order bromate decay kinetics, the change of bromate concentration with time depends only on the bromate molar concentration in solution or

$$\frac{d[BrO_3^-]}{dt} = k_{obs}\,[BrO_3^-] \qquad (4\text{-}3)$$

where k_{obs}, is the bromate decay pseudo-first order rate constant in min^{-1}. k_{obs} is a product of the true rate constant, k, in L/Einstein and, $f(I)$, the UV light intensity function in Einstein $L^{-1}\,s^{-1}$.

$$k_{obs} = k\,f(I) \qquad (4\text{-}4)$$

The integrated form of EQN (4-3) is shown in EQN (4-5):

$$\ln\frac{[BrO_3^-]_t}{[BrO_3^-]_o} = -k_{obs}\,t \qquad (4\text{-}5)$$

For pseudo-first order kinetics, a plot of the left hand side of EQN (4-5) versus time will give a straight line. The slope of the line is $-k_{obs}$. This value is determined for various initial experimental conditions for the four UV light intensities used in this study. Figure 4.7 represents a pseudo-first order plot of bromate decay for four UV light intensities at a fixed bromate concentration of 3 mg/L and initial pH in the range of 8.17-8.30. The initial temperature for the four experiments was held within a narrow

Reproduced with permission of the copyright owner. Further reproduction prohibited without permission.

range. The data indicates that bromate decay is first order with respect to the bromate molar concentration. The slope of each line represents the bromate decay pseudo-first order rate constant (k_{obs}). An almost tenfold increase in photon flux from 2.30 x 10^{-7} Einstein L^{-1} s^{-1} to 2.61 x 10^{-6} Einstein L^{-1} s^{-1} approximately quadruples the bromate decay pseudo-first order rate constant from 0.0101 min^{-1} to 0.0376 min^{-1}. The rate constant for all photon fluxes are the same order of magnitude as the that from the work of Farkas and Klein (1948), though the photon flux reported for their study was higher than used here.

Figure 4.8 is a similar plot to that in Figure 4.7 except that the initial pH is greater than 9.0. All the data points are linear indicating pseudo-first order bromate decay kinetics. Again the increase in photon flux from 2.30 x 10^{-7} Einstein L^{-1} s^{-1} to 2.61 x 10^{-6} Einstein L^{-1} s^{-1} results in more than a four fold increase in k_{obs} from 0.0102 to 0.0447 min^{-1}.

Figure 4.9 is a similar plot to figures 4.7 and 4.8 except that except that initial bromate concentration was held at 0.5 mg/L. Here three photon fluxes are represented. Again the plots indicates pseudo-first order bromate decay with an increase in k_{obs} at higher photon fluxes.

Reproduced with permission of the copyright owner. Further reproduction prohibited without permission.

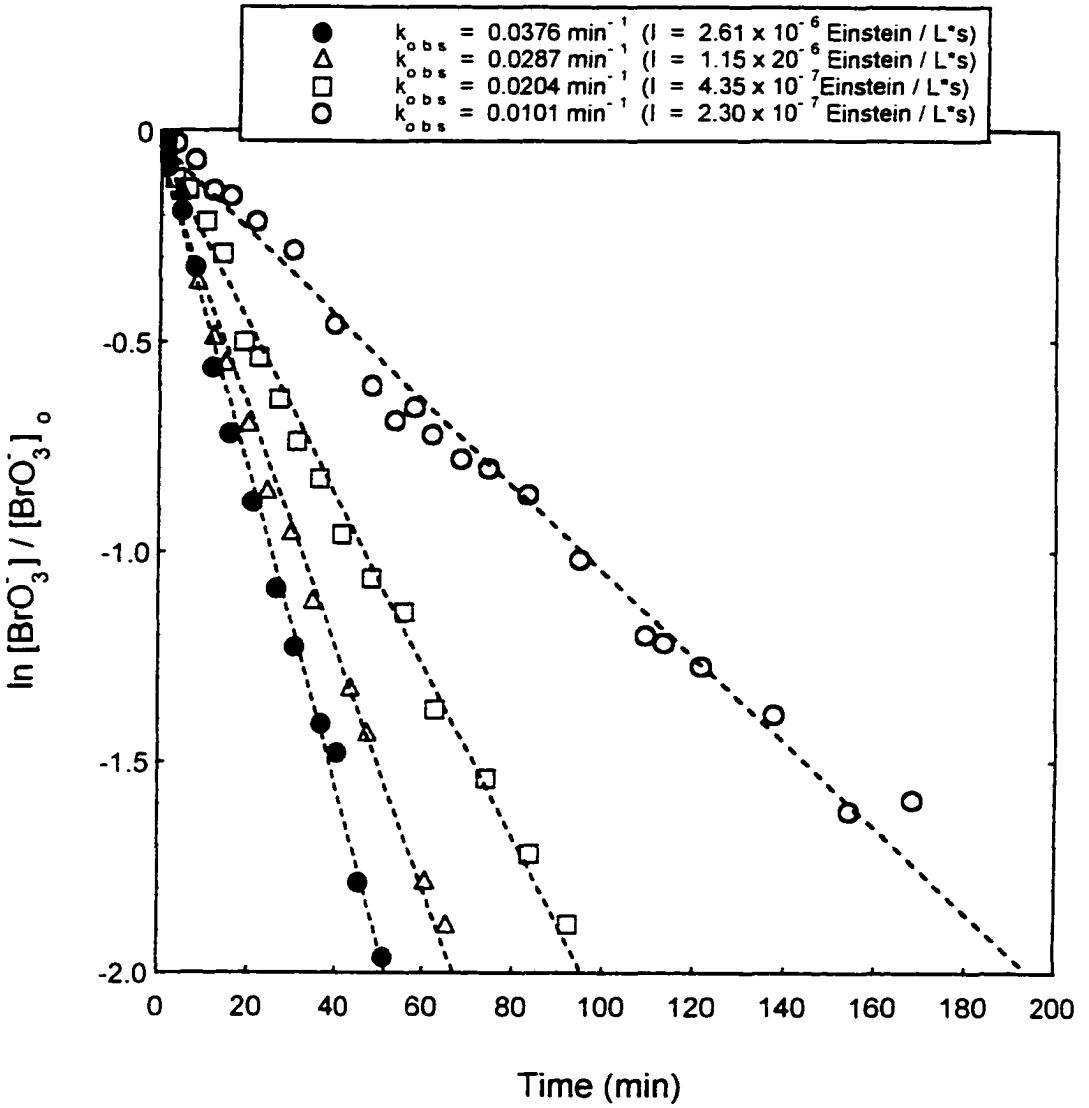

Figure 4.7. Bromate Decay Pseudo-First Order Plots for Various Light Intensity (BrO_3^- = 0.038 mM, Range pH_i = 8.17 - 8.30. Range T_i = 21.0 - 23.0 °C; EXP 10 -13).

Reproduced with permission of the copyright owner. Further reproduction prohibited without permission.

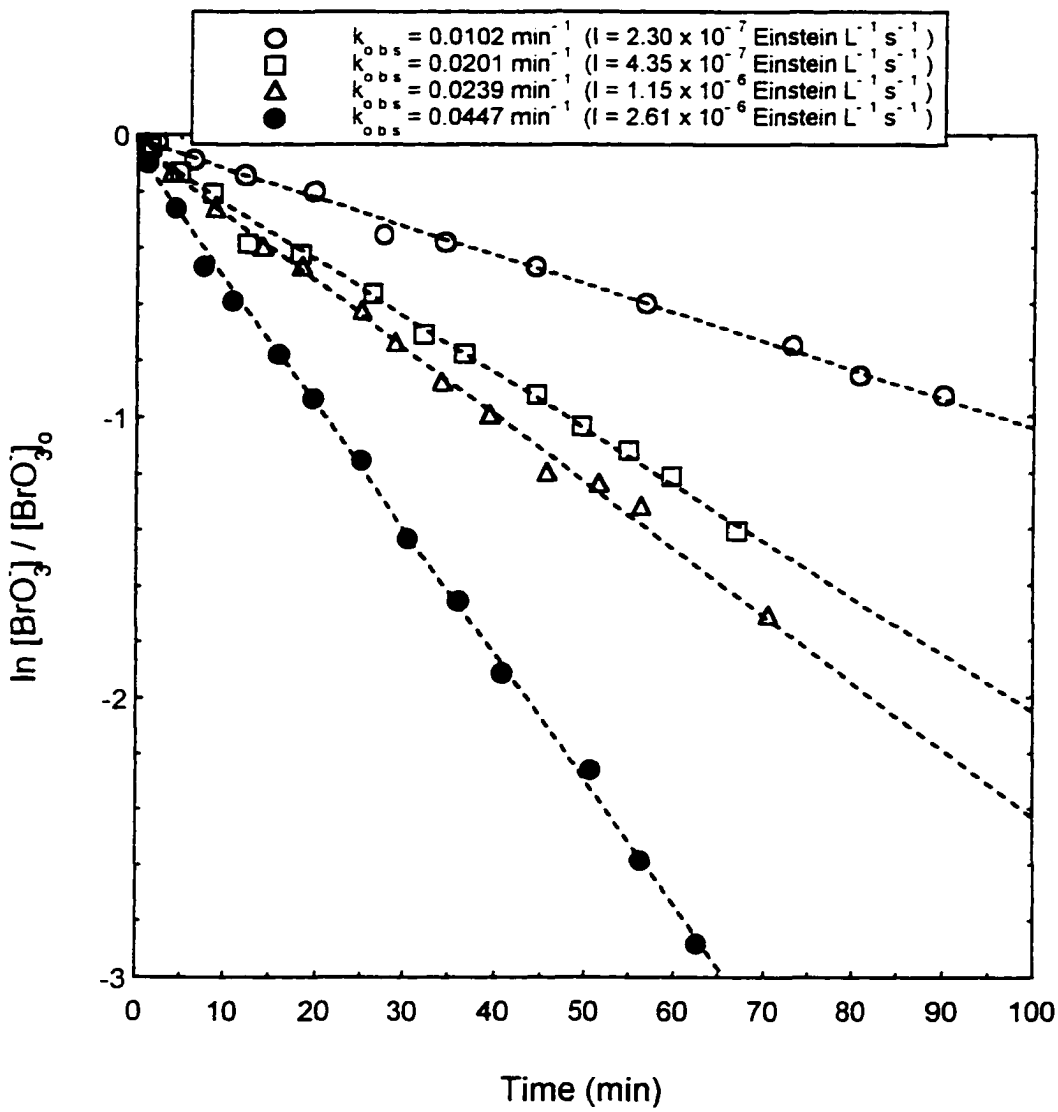

Figure 4.8. Bromate Decay Pseudo First Order Plots for Various Light Intensities BrO_3^- = 0.038 mM, Range pH_i = 9.30 - 9.47, Range T_i = 22 - 25°C; EXP 47, 60, 78, 84).

Reproduced with permission of the copyright owner. Further reproduction prohibited without permission.

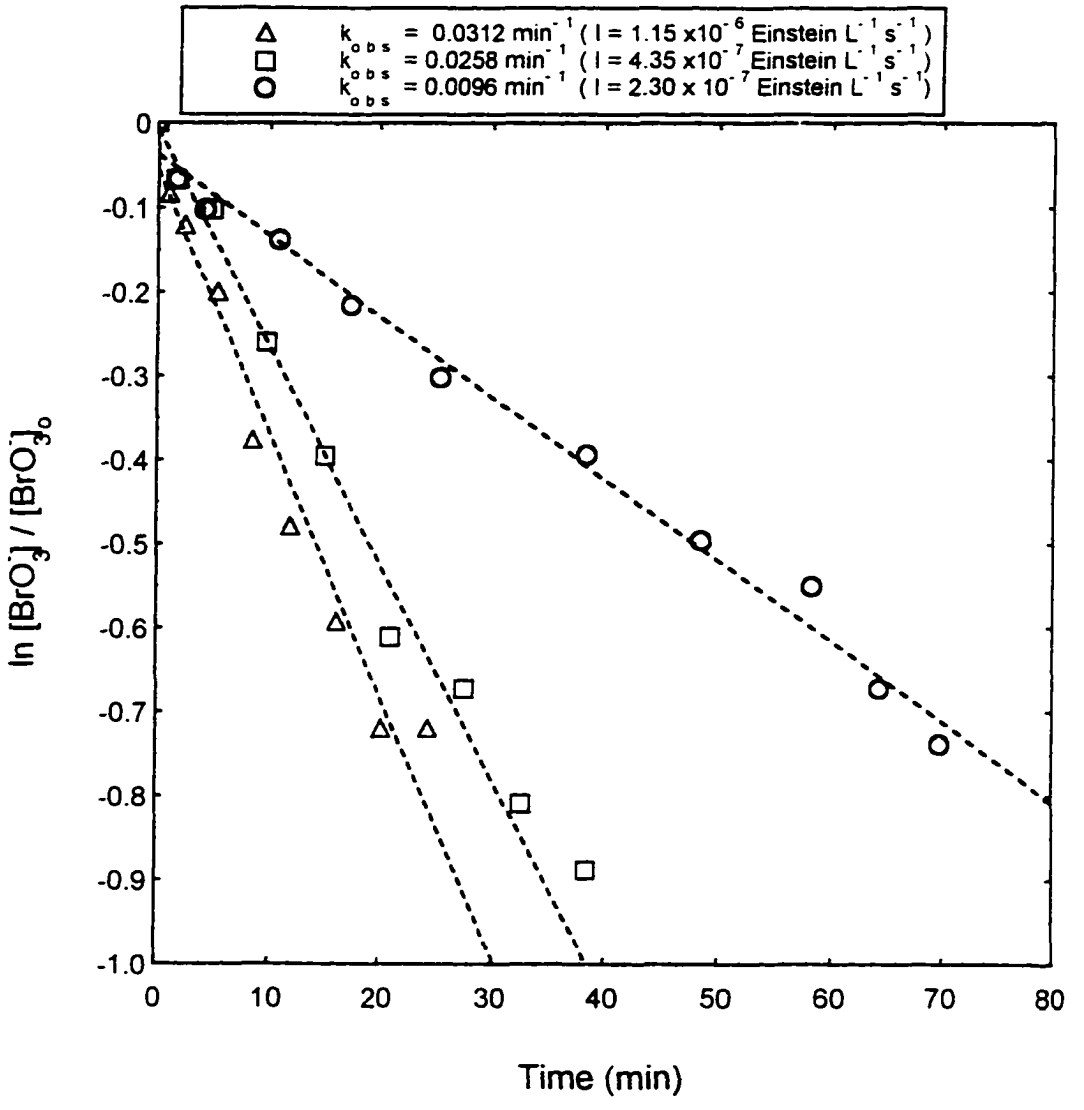

Figure 4.9. Bromate Decay Pseudo-First Order Plots for Various Light Intensities (BrO_3^-=0.007 mM,Range pH_i = 8.13 - 8.30, T_i = 25°C; EXP 98,101,104).

Reproduced with permission of the copyright owner. Further reproduction prohibited without permission.

4.1.3 Kinetic Effect of Initial pH and Alkalinity

The effect of initial pH on bromate decomposition kinetics was investigated for the four UV Lamp configurations. Initial pH ranged from 6 - 10, while initial bromate was kept constant for all the experiments reported here. Initial temperature for each experiment ranged from 24 - 25 °C.

Figure 4.10 is a plot of k_{obs} at the various initial pH values for the four UV light intensities. The horizontal lines represent the average k_{obs} value for each UV light intensity. The data points for all four UV ligh intensities show that k_{obs} is relatively independent of intial pH in the range of 6 to 10. This confirms the findings of Siddiqui et al. (1996) who worked within a similar pH range and of Farkas and Klein (1948) who worked at the extreme end of the acid and alkaline scale. A statistical analysis was performed on the data for each UV light intensity. For the highest UV intensity, 57% of the k_{obs} values lie within ±1 standard deviation (σ) of the average value and the other 50%, within ±2 σ of the average. For each of the three other UV light intensities, 80% of the k_{obs} values lie within ±1σ of the average. The other 20% of the values lie within ±2σ of the average. The average k_{obs} is more than quadrupled from 0.00996 min^{-1} to 0.04190 min^{-1} as the UV light intensity is increased from 2.30 x 10^{-7} to 2.61 x 10^{-6} Einstein L^{-1} s^{-1}.

Reproduced with permission of the copyright owner. Further reproduction prohibited without permission.

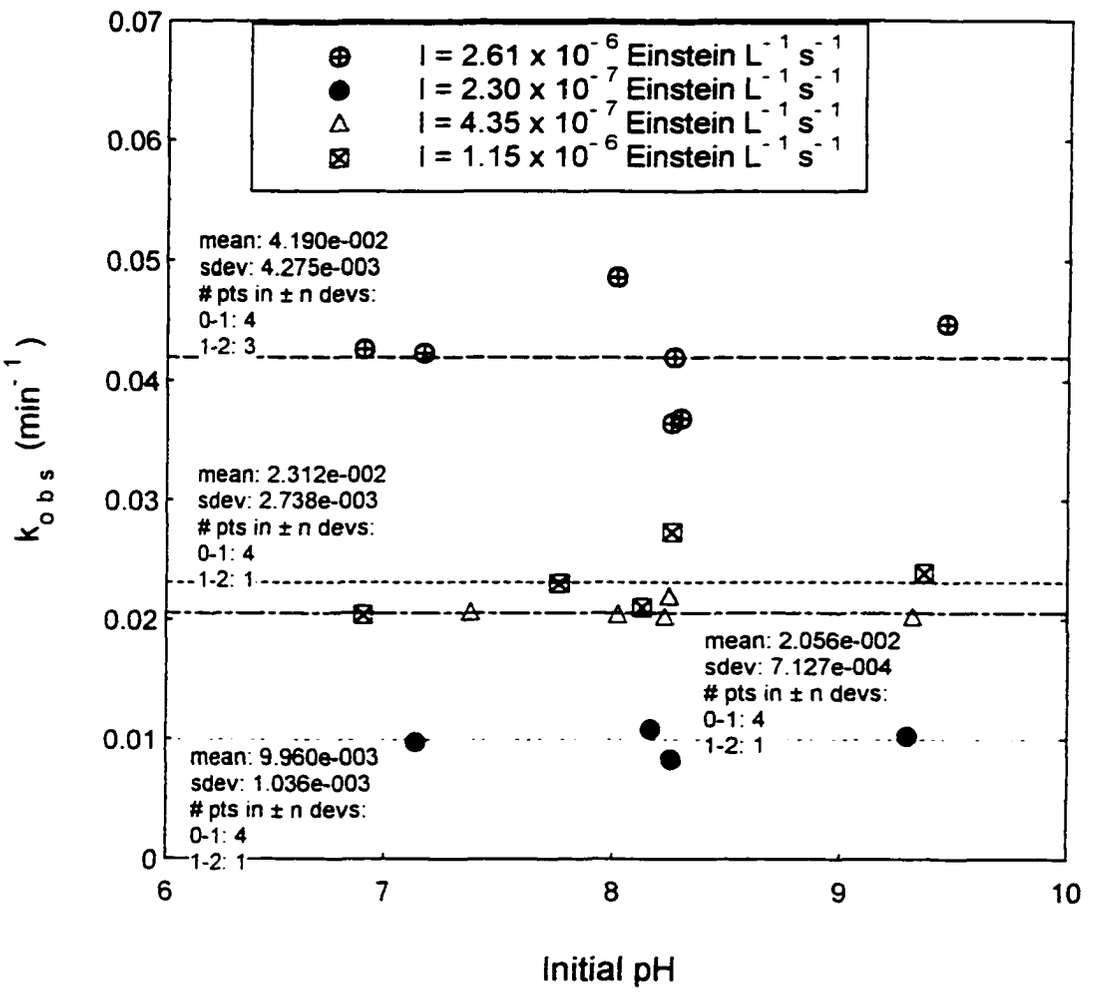

Figure 4.10. pH Dependency of Bromate Decay Observed Rate Constant (BrO_3^- = 0.038 mM, Range T_i = 24-25°C; EXP 1,7,10-13,15,29, 38,46,47,60-62,76-78,82-84,88).

Reproduced with permission of the copyright owner. Further reproduction prohibited without permission.

Siddiqui et al. (1996) reported greater bromate removal at pH 9.0 than at pH 4.5 during application of HEEB to raw drinking water spiked with bromate. The increased removal (13%) at higher pH was attributed to the scavenging effect of aqueous electrons on protons as described by Neta et al. (1988) and shown in EQN (4-6)

$$H^{+} + e_{aq}^{-} \rightarrow H\bullet \qquad k = 1.0 \times 10^{10}\ M^{-1}\ s^{-1} \qquad (4\text{-}6)$$

More aqueous electrons were therefore available to reduce bromate at higher pH levels. Hydroxide is not scavenged by aqueous electrons (Thomas et al., 1964). Matheson et al. (1963) show that like the case of electron beam and gamma irradiation, the aqueous electrons are also an important intermediate in the steady UV irradiation of many aqueous anion solutions.

Bromate and bromic acid have different light absorbing properties. However, explanation of the slight pH dependency of k_{obs} on bromate speciation is invalid. Bromate is predominant in solution at pH greater than 0.7 (see Figure 2.1) and since these experiments were conducted at much higher pH levels, bromic acid concentrations were negligible. The existence of a pH dependency suggests that aqueous electrons are produced in sufficient quantities to influence H^{+} concentration directly and bromate decay indirectly.

In the pH dependency experiments described above, pH decreased from the initial level during UV irradiation. Using bicarbonate buffer, a series of experiments

Reproduced with permission of the copyright owner. Further reproduction prohibited without permission.

were performed to investigate the effect of the bicarbonate alkalinity or buffering capacity on bromate decay. Figure 4.11 is a plot of k_{obs} versus bicarbonate concentration for the UV light intensity of 2.61 x 10 Einstein L^{-1} s^{-1}. The horizontal line depicts the average k_{obs} value for the three experiments. The figure clearly shows that bromate decay is independent of bicarbonate concentration in the range 0.05 - 1.0 mM. For the bicarbonate concentration of 0.05 mM the pH dropped from an initial value of 7.37 to 6.54 during UV irradiation. For the other two bicarbonate concentrations, initial pH was > 9.0 and remained within 0.04 pH units of the initial value during UV irradiation.

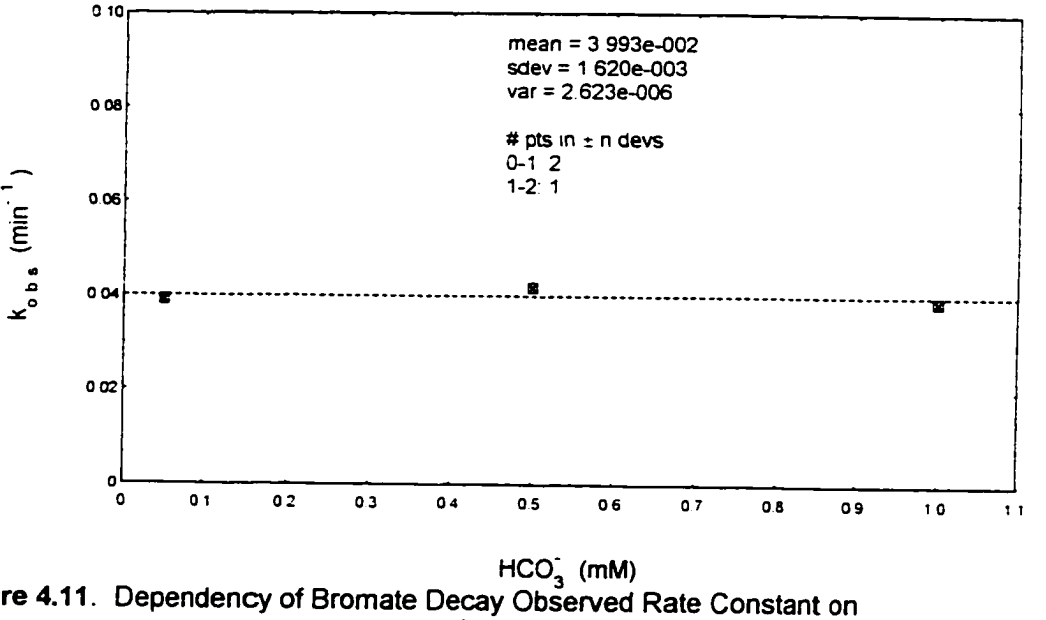

Figure 4.11. Dependency of Bromate Decay Observed Rate Constant on Bicarbonate (I = 2.61 x 10^{-6} Einstein / L*s, BrO_3^- = 0.038 mM, Range pH_i = 7.37 - 9.31; EXP 105 - 107).

Reproduced with permission of the copyright owner. Further reproduction prohibited without permission.

4.1.4 Effect of Initial Bromate Concentration

The effect of initial bromate concentration on k_{obs} was investigated with initial pH and temperature within a narrow range. Figure 4.12 shows the the effect on k_{obs} for varying initial bromate concentrations for the four UV light intensities used in this study. The dashed horizontal lines represents the average k_{obs} for each UV light intensity. The figure shows that bromate is relatively independent of initial bromate concentration in the range studied.

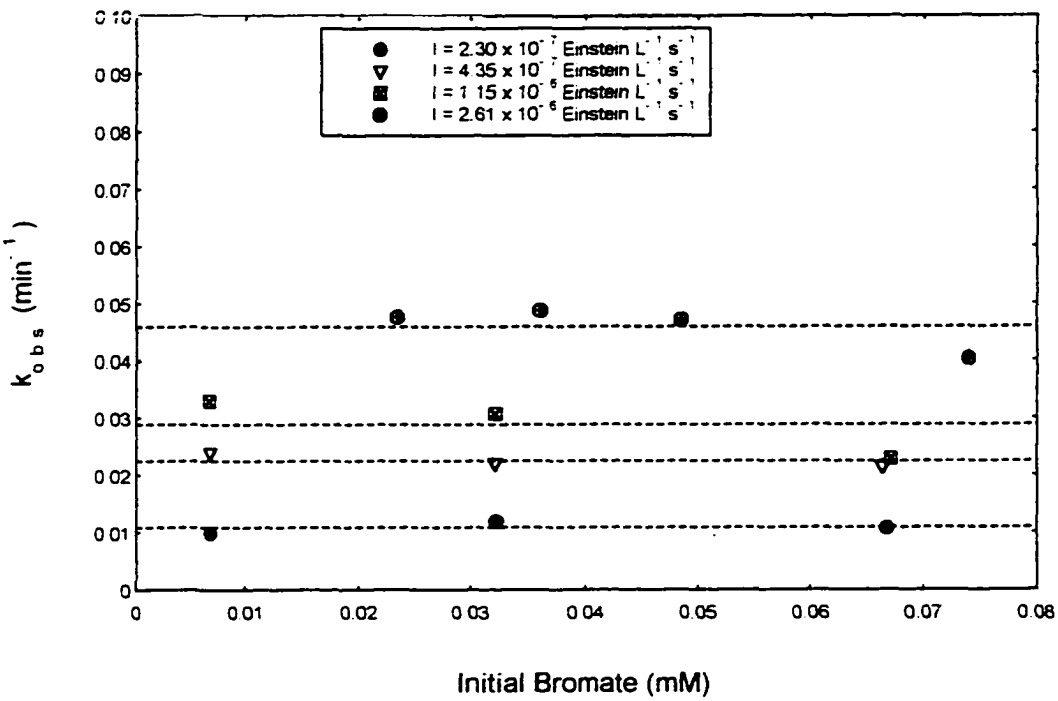

Figure 4.12. Dependency of Bromate Decay Rate Pseudo-First Order Constant on Initial Bromate (BrO_3^- = 0.0375 mM, Range of pH_i = 8.01- 8.43, T_i = 25°C; EXP 1-4, 96-98, 99-101, 102-104).

Reproduced with permission of the copyright owner. Further reproduction prohibited without permission.

4.1.5 Light Intensity Effect

The fact that the dependency of bromate decay on initial pH and on initial bromate is insignificant, a plot of k_{obs} versus UV light intensity for bromate alone experiments with a bromate concentration of 3 mg/L (0.038 mM) was developed and is shown in figure 4.13. Bromate decay increases for higher UV light intensities, however the relationship appears to be non-linear. Siddiqui et al. (1996) reported a linear intensity at lower UV doses and a curvilinear relationship at higher UV doses.

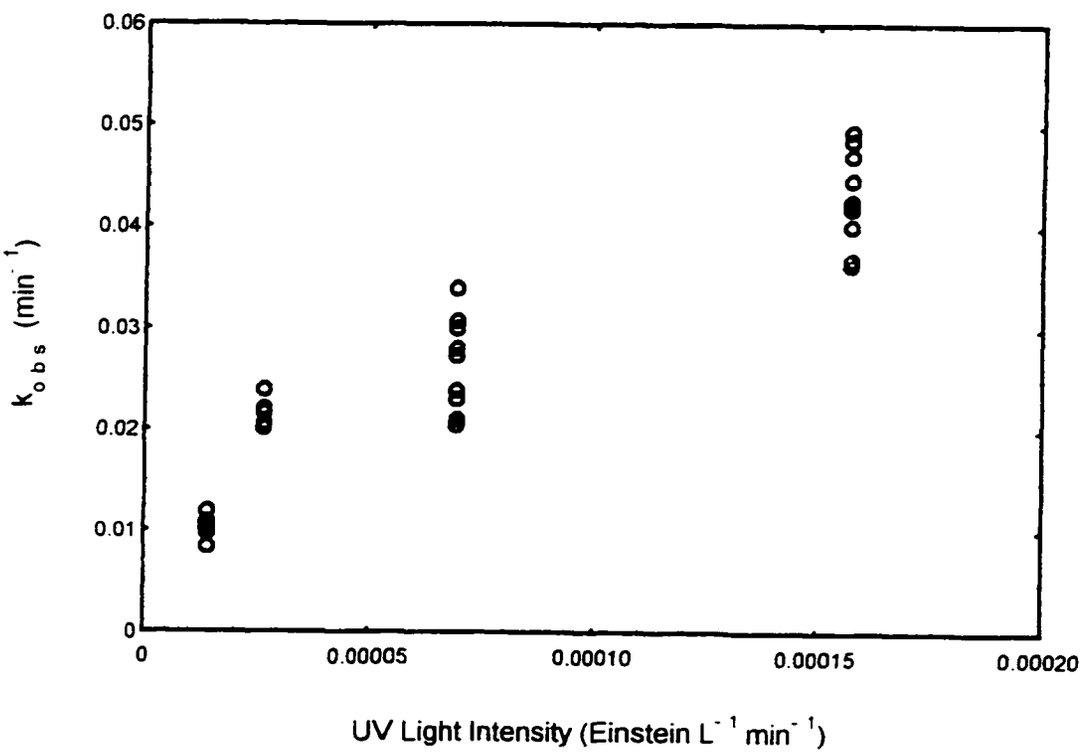

Figure 4.13. Bromate Decay Pseudo-First Order Rate Constant for Bromate Experiments (Range Initial BrO_3^-=0.007 mM - 0.074 mM, Range pH_i = 6.90 - 9.47, Range T_i = 20 - 25°C).

Reproduced with permission of the copyright owner. Further reproduction prohibited without permission.

4.2 Free Bromine Decay Under UV Irradiation

Free bromine is an intermediate product of bromate decay and has substantial UV light absorbing properties. Thus, a study of its decay kinetics under experimental conditions similar to the bromate and bromate-nitrite experiments was essential.

Figure 4.14 is a typical profile of reactants and products during the UV irradiation of a 0.015 mM free bromine solution prepared as described in section 3.2.4. Free bromine decays to form bromide and some bromate at a much lower rate. During the course of the experiment pH drops by only 0.07 pH unit, from 8.35 to 8.28. This is to be expected since the free bromine system ($HOBr/OBr^-$) is a buffer with pK_a of 8.69. Buffers are most effective within ±1 pH unit of pK_a (Harris, 1987).

A first order plot of free bromine decay as a function of UV light intensity suggested first order decay kinetics (Figure 4.15). A comparison of the rates of decomposition with that of bromate under similar experimental conditions, shows that free bromine decay is at least an order of magnitude greater for each UV light intensity. Removing free bromine from solution will make more UV radiation available for bromate and enhance decay rate.

The effect of pH on free bromine decay is shown in Figure 4.16 where the observed rate constant increases with decreasing pH. The molar absorptivity of HOBr is greater than that of OBr^- at 254 nm. Since HOBr predominates at lower pH values, an increase decay of free bromine is expected.

Reproduced with permission of the copyright owner. Further reproduction prohibited without permission.

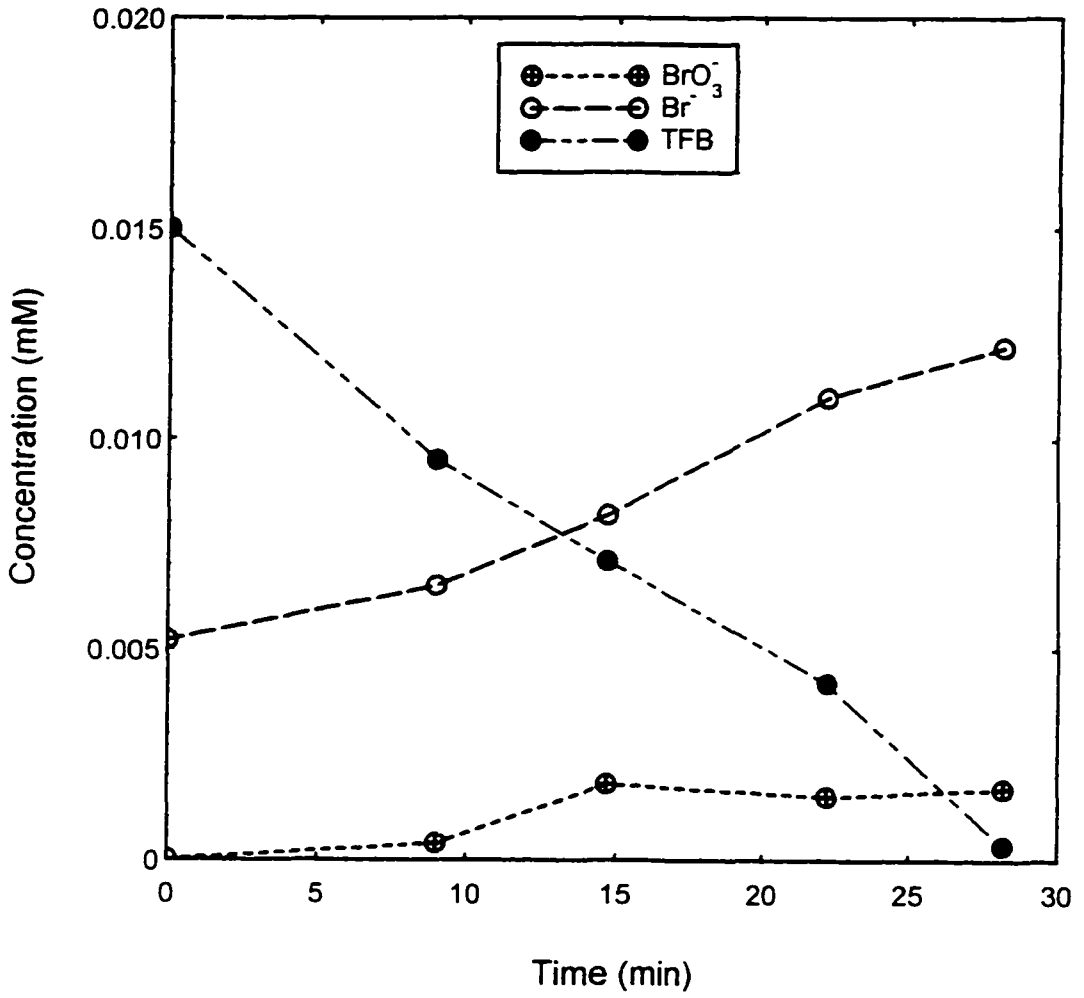

Figure 4.14. Species Profiles During UV Irradiation of Free Bromine Solution ($I = 2.30 \times 10^{-7}$ Einstein /L*s, TFB = 0.015, $pH_i = 8.35$, $T_i = 21°C$; EXP 59).

Reproduced with permission of the copyright owner. Further reproduction prohibited without permission.

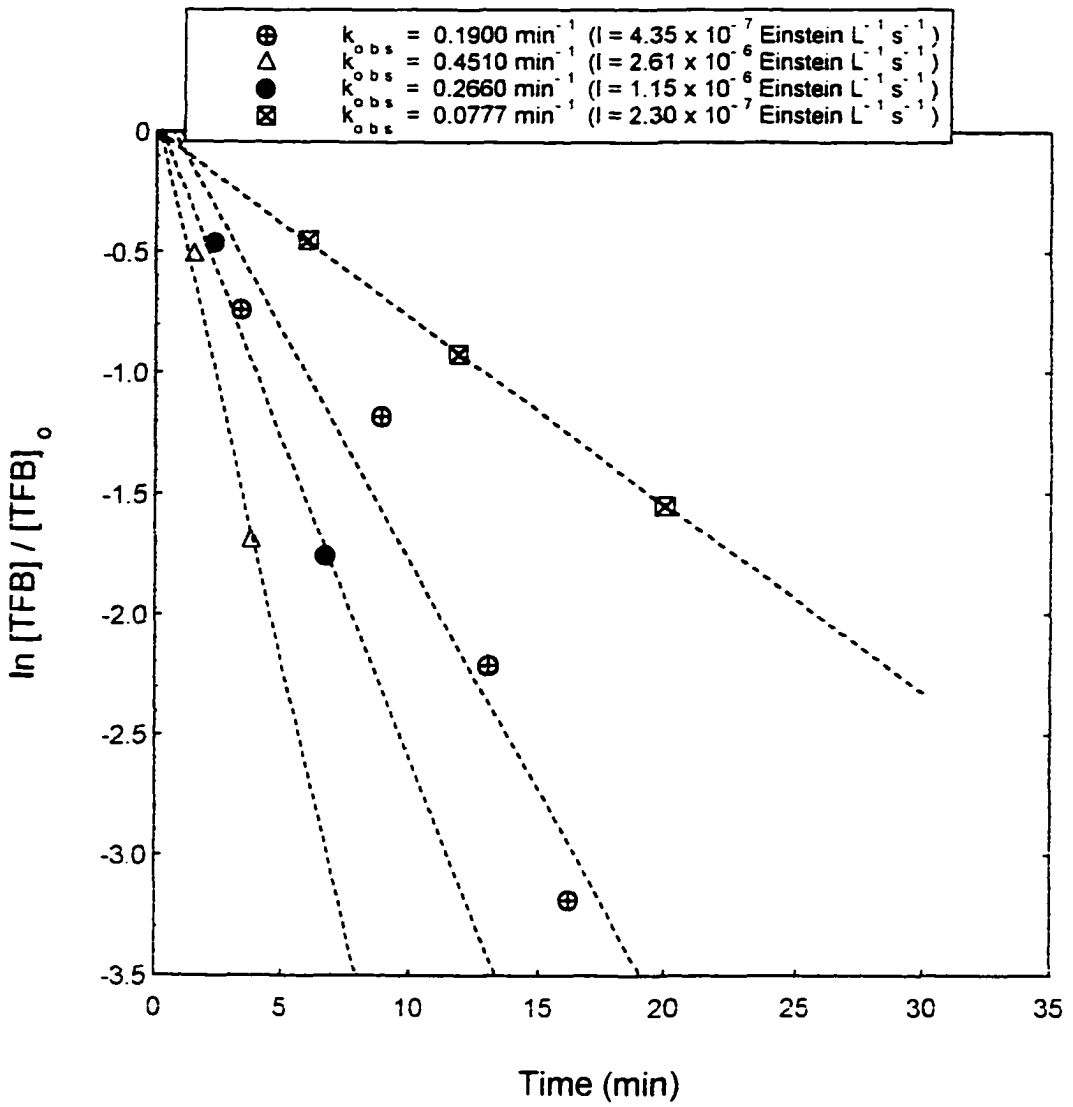

Figure 4.15. Free Bromine Decay Pseudo-First Order Plots (TFB = 0.0146 mM, pH_i = 8.15, T_i = 25.0°C (EXP 52-55)

Reproduced with permission of the copyright owner. Further reproduction prohibited without permission.

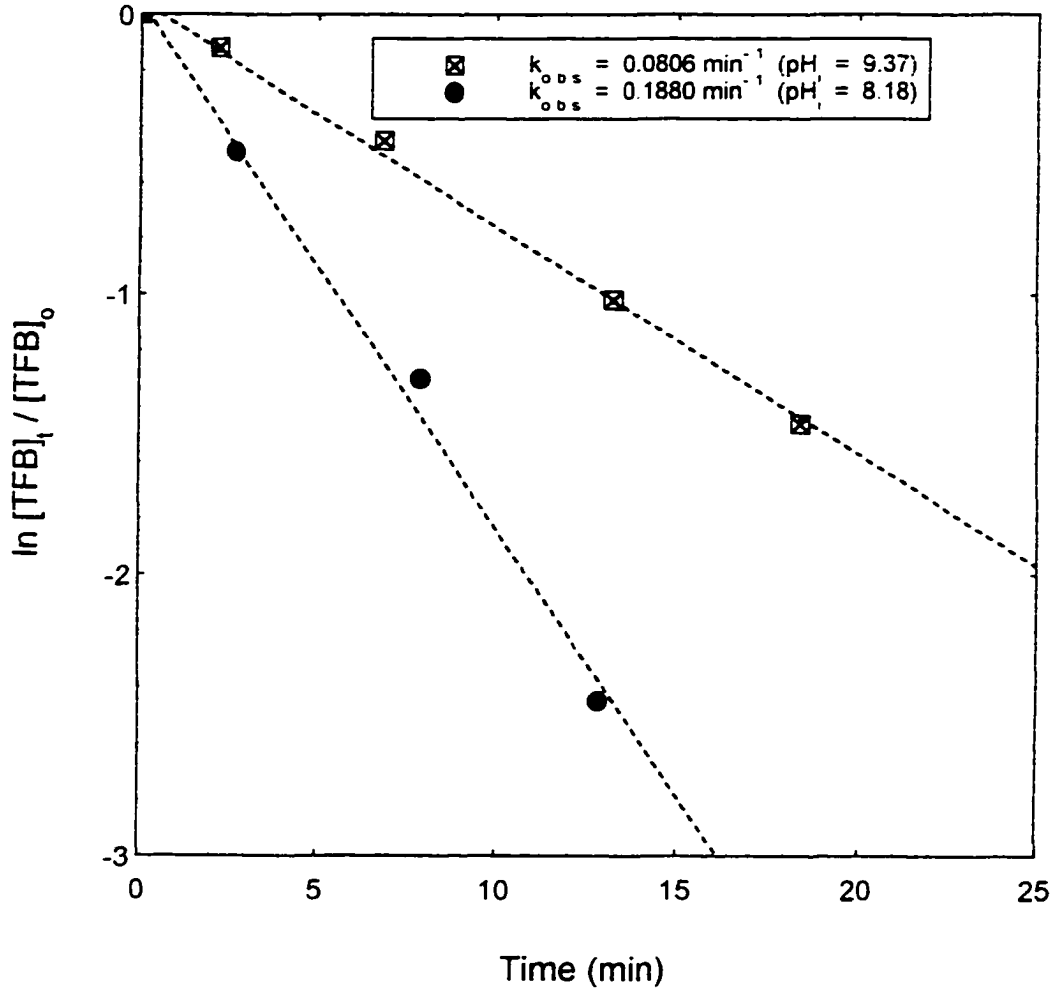

Figure 4.16. pH Dependency of Free Bromine Decay ($I = 1.15 \times 10^{-6}$ Einstein /L*s, TFB = 0.0144 - 0.0151 mM, $T_i = 21^{\circ}C$; EXP 56-57).

Reproduced with permission of the copyright owner. Further reproduction prohibited without permission.

4.3 Nitrite Decomposition Under UV Irradiation

In the nitrite-bromate system, it is important to quantify all photochemical reactions occuring in solution. As described above, nitrite decomposition under UV irradiation to form nitrate as the major product. Preliminary experiments performed at 185 nm showed that nitrite was quantitatively oxidized to nitrate (Figure 4.17). A series of experiments were performed to determine the rates of nitrite decomposition under UV irradiation at 254 nm and under conditions similar to those performed for the mixed nitrite-bromate system.

Figures 4.18 through 4.21 show the nitrite and nitrate profiles during UV irradiation of a 0.0357 mM nitrite solution at 254 nm. pH remained within 0.3 units of the initial value during each experiment. Nitrite is converted stoichiometrically to nitrate in all the experiments. Nitrite decomposition slows at lower UV light intensities.

A first order plot of nitrite decay is shown in Figure 4.22 for all four experiments. The data points are linear indicating that nitrite decay is first order with respect to initial nitrite concentration. The observed rate constants were 0.00398, 0.00308, 0.00207 and 0.00091 min^{-1} for the UV light intensities of 2.61×10^{-6}, 1.15×10^{-6}, 4.35×10^{-7} and 2.30×10^{-7} Einstein L^{-1} s^{-1} respectively. These values are much less compared to the observed rate constant of 0.608 min^{-1} for the experiment at 185 nm in figure 4.17.

Reproduced with permission of the copyright owner. Further reproduction prohibited without permission.

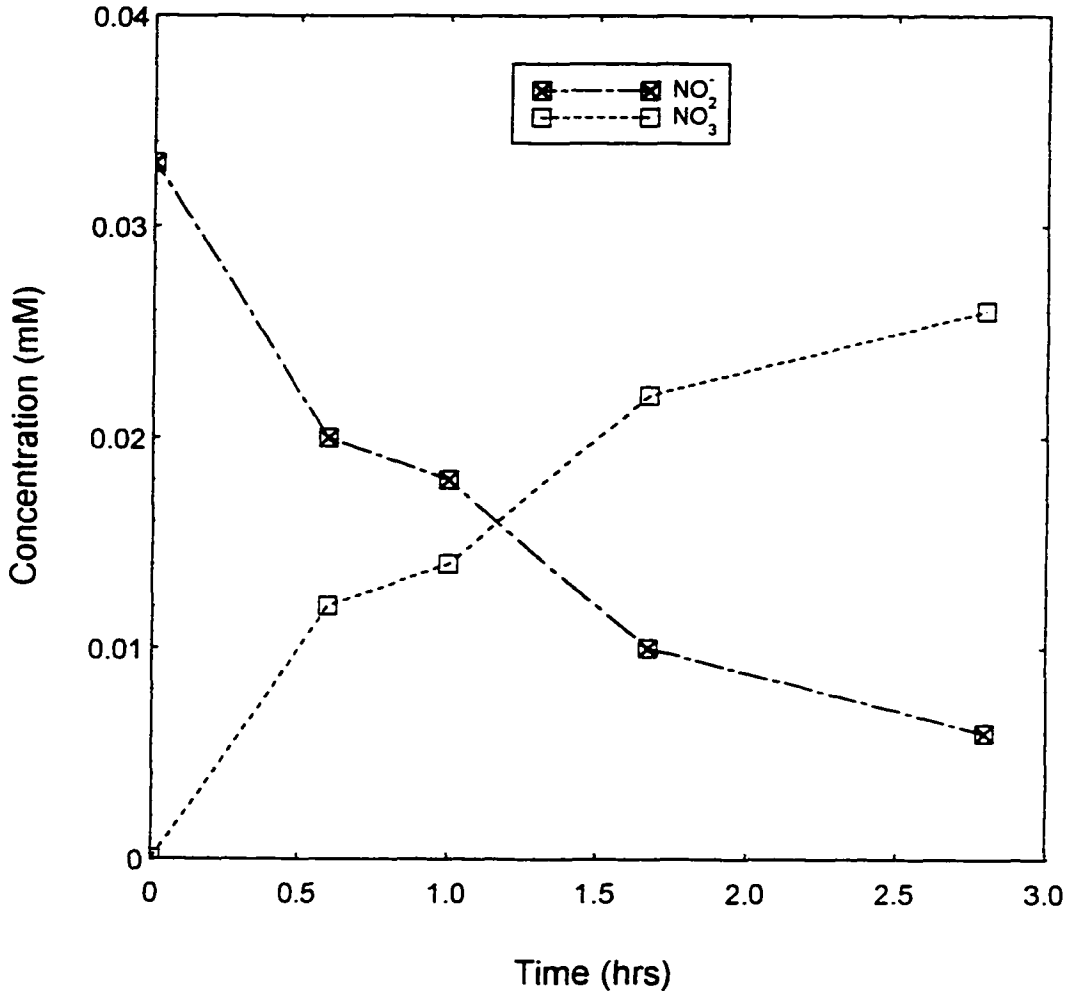

Figure 4.17. Species Profiles During UV Irradiation (185nm) of Nitrite with 8, 35W Lamps (NO_2^- = 0.033 mM, Initial pH = 7.23, T_i 25.5 °C).

Reproduced with permission of the copyright owner. Further reproduction prohibited without permission.

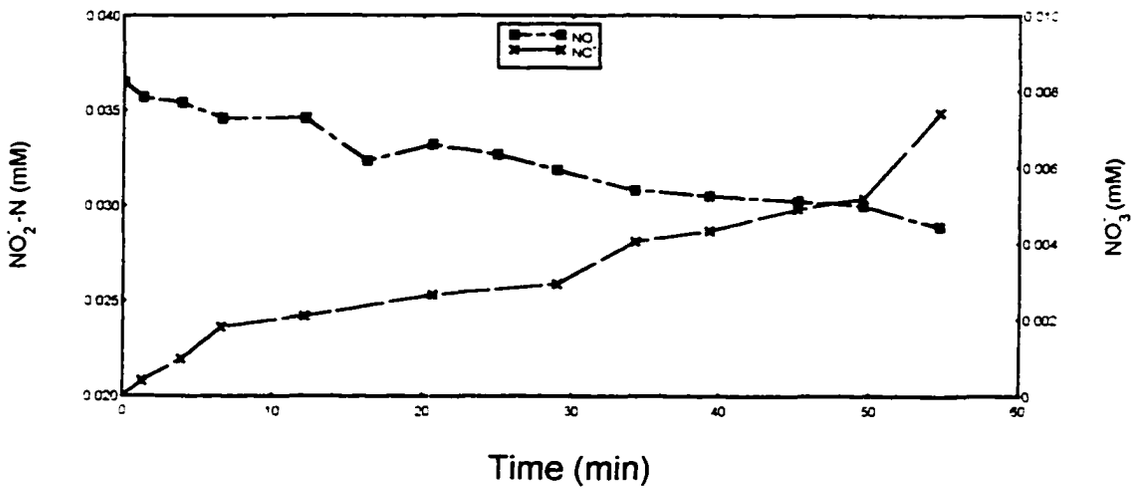

Figure 4.18. Species Profile During UV Irradiation of Aqueous Nitrite Solution (I= 2.61 x 10^{-6} Einstein / L*s, NO_2^-=0.036 mM,pH_i=6.70, T_i=25°; EXP 92).

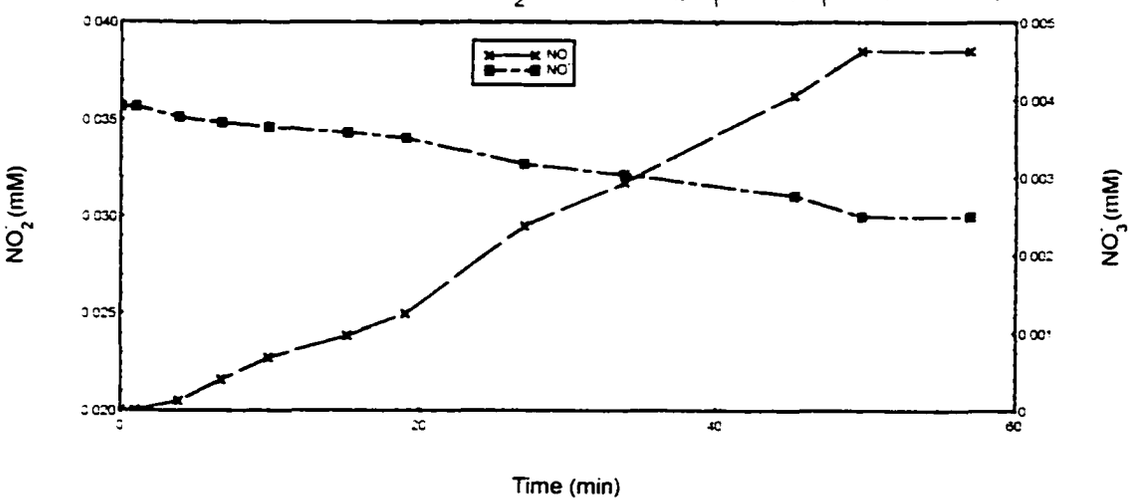

Figure 4.19. Species Profile During UV Irradiation of Aqueous Nitrite Solution (I= 1.15 x 10^{-6} Einstein/ L*s, NO_2^- = 0.036 mM, pH_i=6.76, T_i=25°C; EXP 93).

Reproduced with permission of the copyright owner. Further reproduction prohibited without permission.

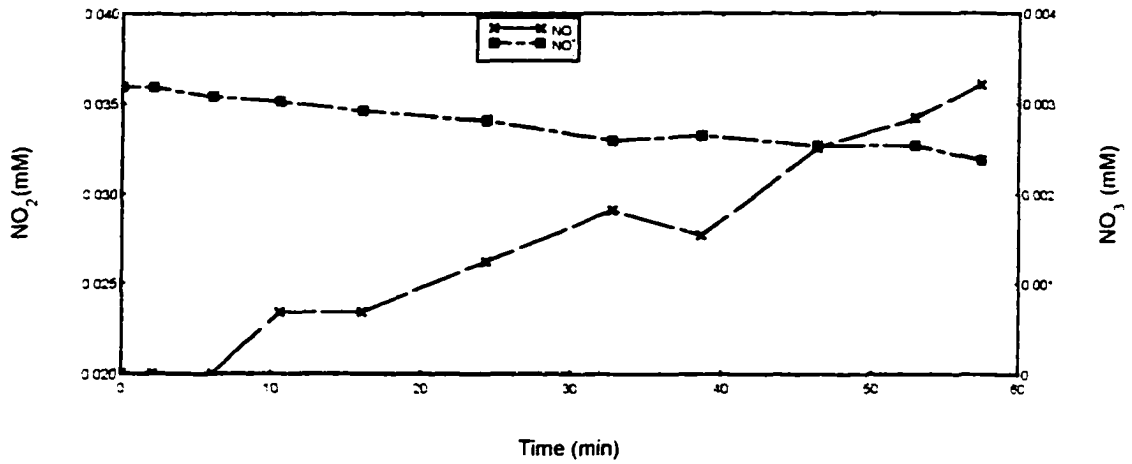

Figure 4.20. Species Profile During UV Irradiation of Aqueous Nitrite Solution (I = 4.35 x 10^{-7} Einstein/L*s, NO_2^- = 0.036 mM, pH_i=6.64, T_i=25°C; EXP 94).

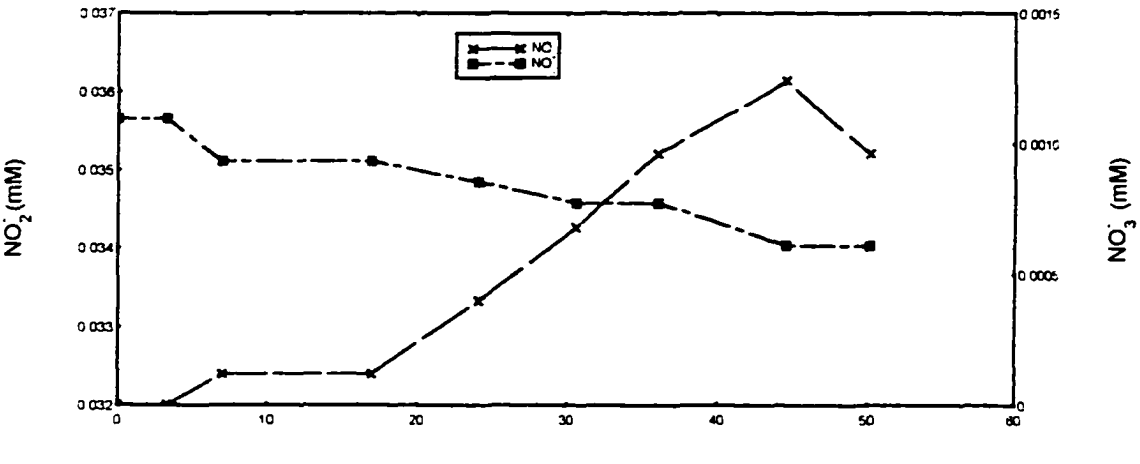

Figure 4.21. Species Profile During UV Irradiation of Aqueous Nitrite Solution (I = 2.30 x 10^{-7} Einstein/L*s, NO_2^-=0.036 mM, pH_i=6.68, T_i = 25°C; EXP 95).

Reproduced with permission of the copyright owner. Further reproduction prohibited without permission.

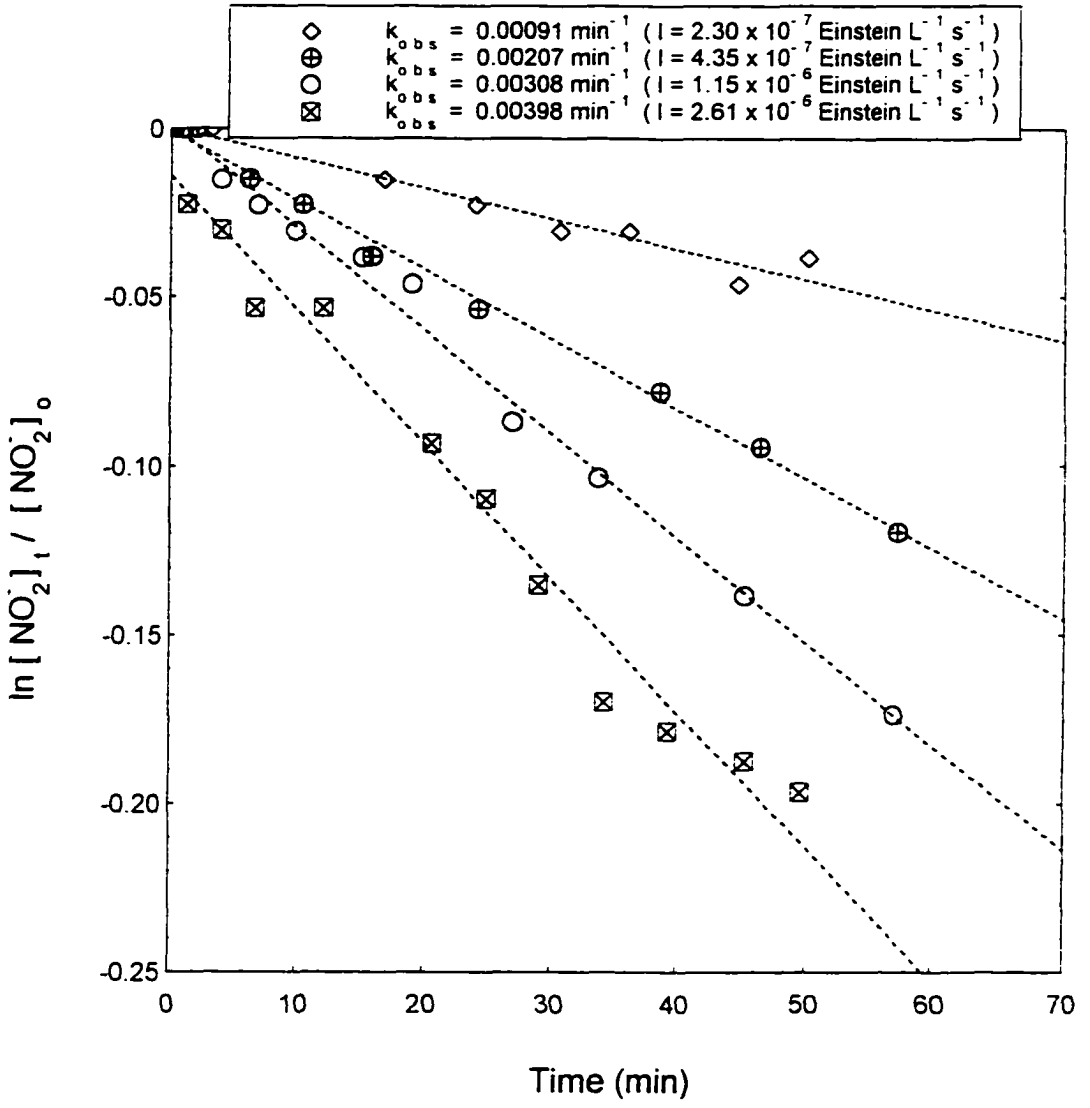

Figure 4.22. Pseudo-First Order Plots for UV Irradiation (254 nm) of Aqueous Nitrite (NO_2^- = 0.0357 mM, Range pH_i = 6.64 - 6.76, T_i = 25°C, EXP 92-95).

Reproduced with permission of the copyright owner. Further reproduction prohibited without permission.

4.4 Bromate Decomposition in the Presence of Nitrite

4.4.1 Experimental Observations

Typical concentration-time profiles of reactants and products during UV irradiation of aqueous bromate solution containing nitrite for four UV light intensities are shown in Figures 4.23 through 4.26. In all four experiments, bromate was observed to decay while bromide steadily formed and TFB formed and decayed. Except for a few deviations, the total bromine species (TBr_t) as defined by EQN (4-1) remained in relatively good agreement with the initial total bromine (TBr_i) depicted by the upper horizontal line.

In the case of the nitrogen species in the four experiments, nitrite was oxidized to nitrate. The rate of oxidation increeased with increasing UV light intensity. In the experiments depicted in Figure 4.23 and Figure 4.24,the total nitrogen as defined by EQN (4-7) was in good agreement with total initial nitrogen (TN_i) depicted by the lower horizontal line.

$$[TN]_t = [NO^-]_t + [NO_2^-]_t \qquad (4\text{-}7)$$

In Figure 4.25, TN_t deviates from TN_i at the onset and coincides with the nitrate profile after nitrite disappears. In Figure 4.26, TN_t is in fair agreement with TN_i until nitrite disappears, whereafter it coincides with the nitrate profile.

Reproduced with permission of the copyright owner. Further reproduction prohibited without permission.

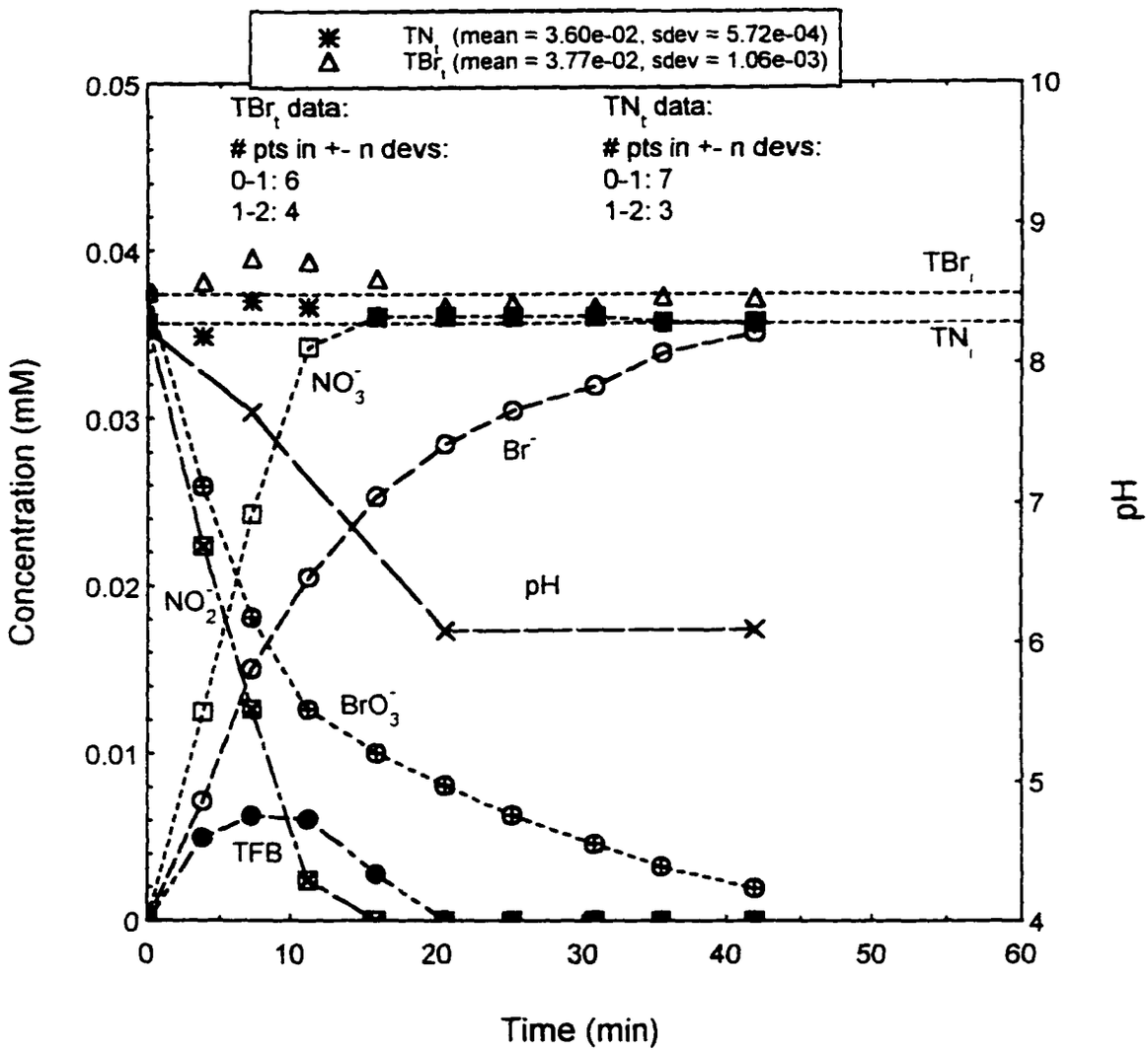

Figure 4.23. Species Profiles During UV Irradiation of Bromate/Nitrite Solution ($I = 2.61 \times 10^{-6}$ Einstein/L*s, BrO_3^- = 0.037 mM, NO_2^- = 0.036 mM, pH_i = 8.24, T_i = 22°C,; EXP 43).

Reproduced with permission of the copyright owner. Further reproduction prohibited without permission.

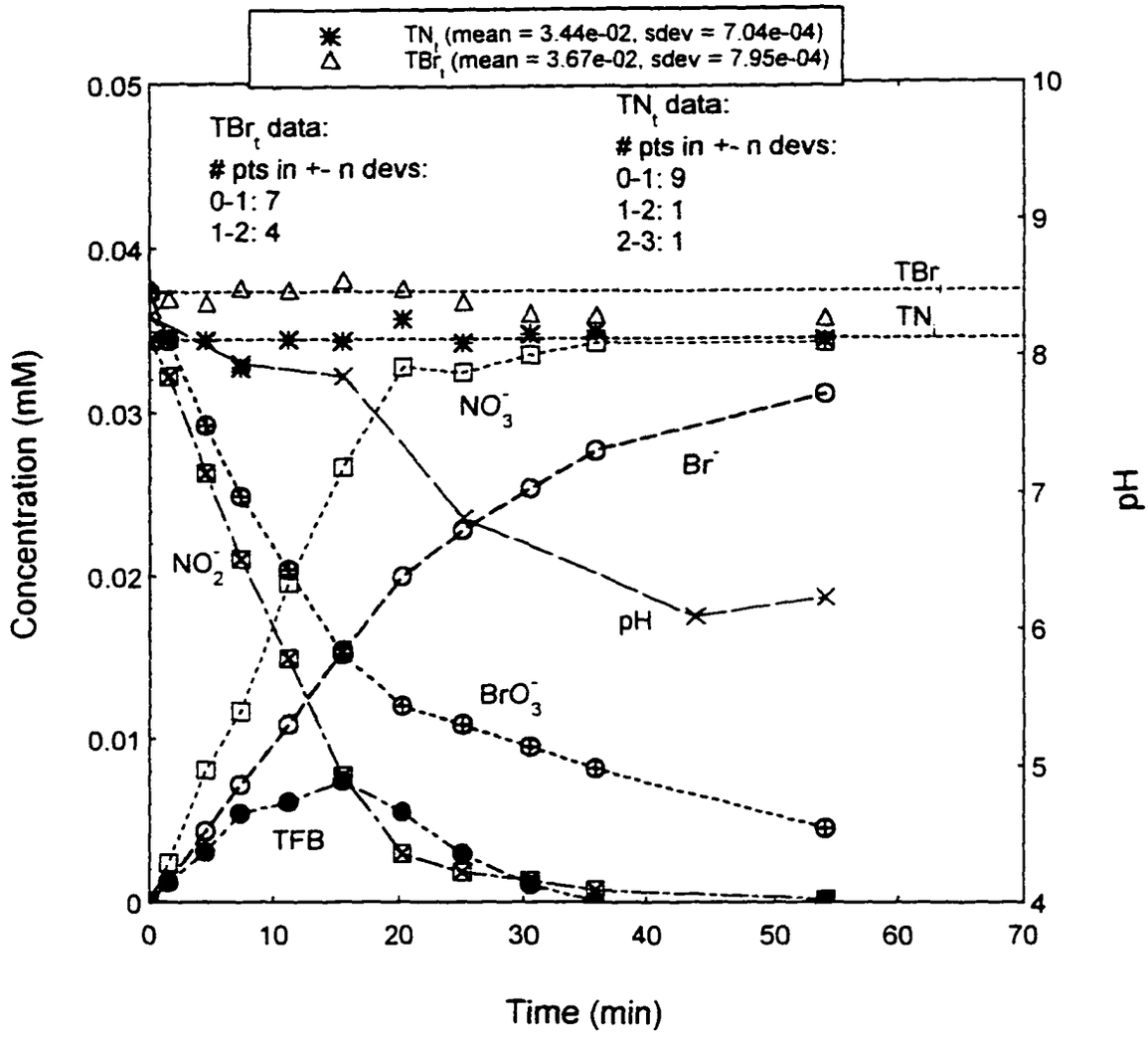

Figure 4.24. Species Profiles During UV Irradiation of Bromate/Nitrite Solution ($I = 1.15 \times 10^{-6}$ Einstein/L*s, BrO_3^- = 0.037 mM, NO_2^- = 0.034 mM, pH_i = 8.10, T_i = 20°C; EXP 49).

Reproduced with permission of the copyright owner. Further reproduction prohibited without permission.

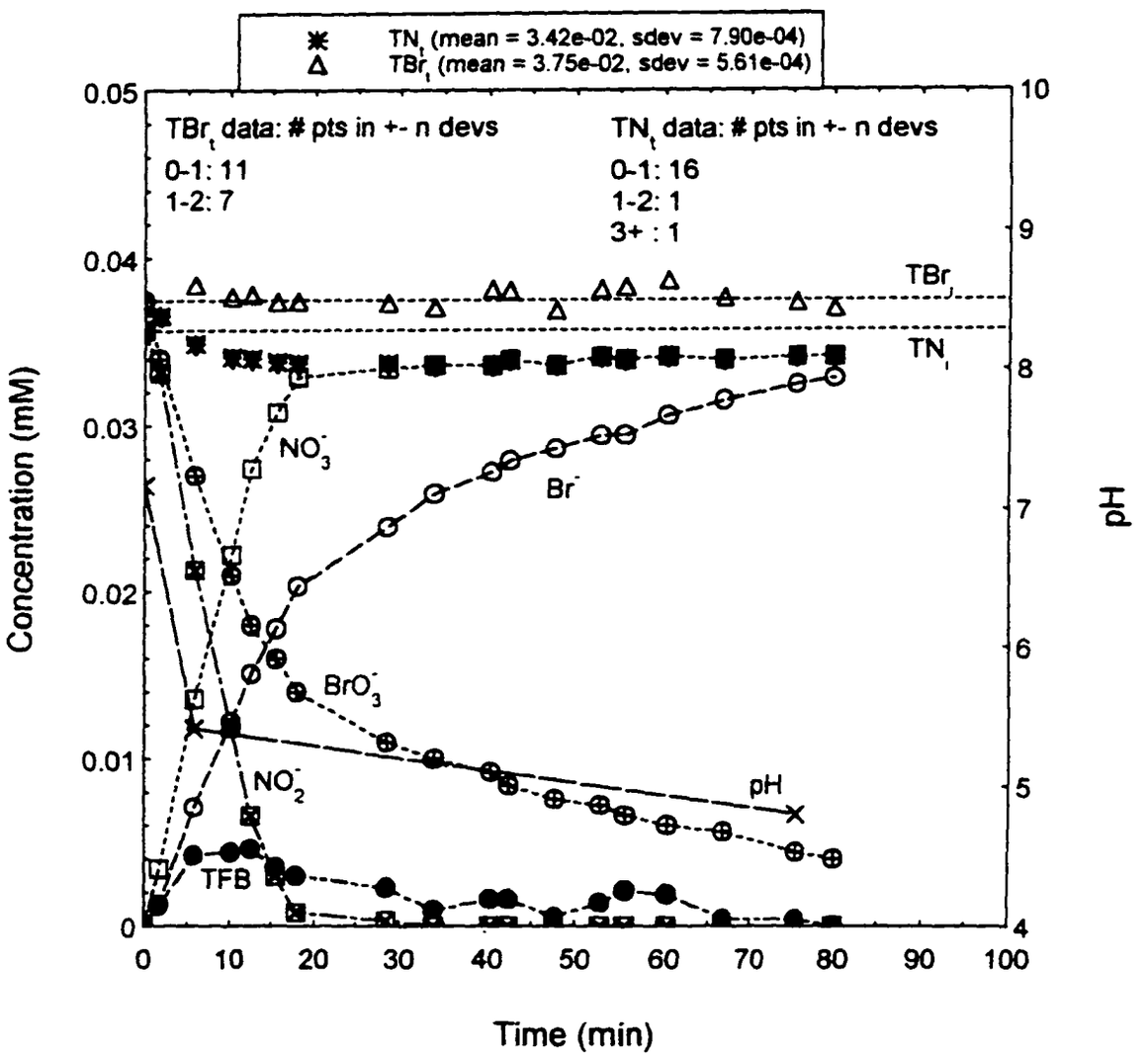

Figure 4.25. Species Profiles During UV Irradiation of Bromate/Nitrite Solution ($I = 4.35 \times 10^{-7}$ Einstein/L*s, BrO_3^- = 0.038 mM, NO_2^- = 0.036 mM, pH_i = 7.17, T_i = 24°C; EXP 24).

Reproduced with permission of the copyright owner. Further reproduction prohibited without permission.

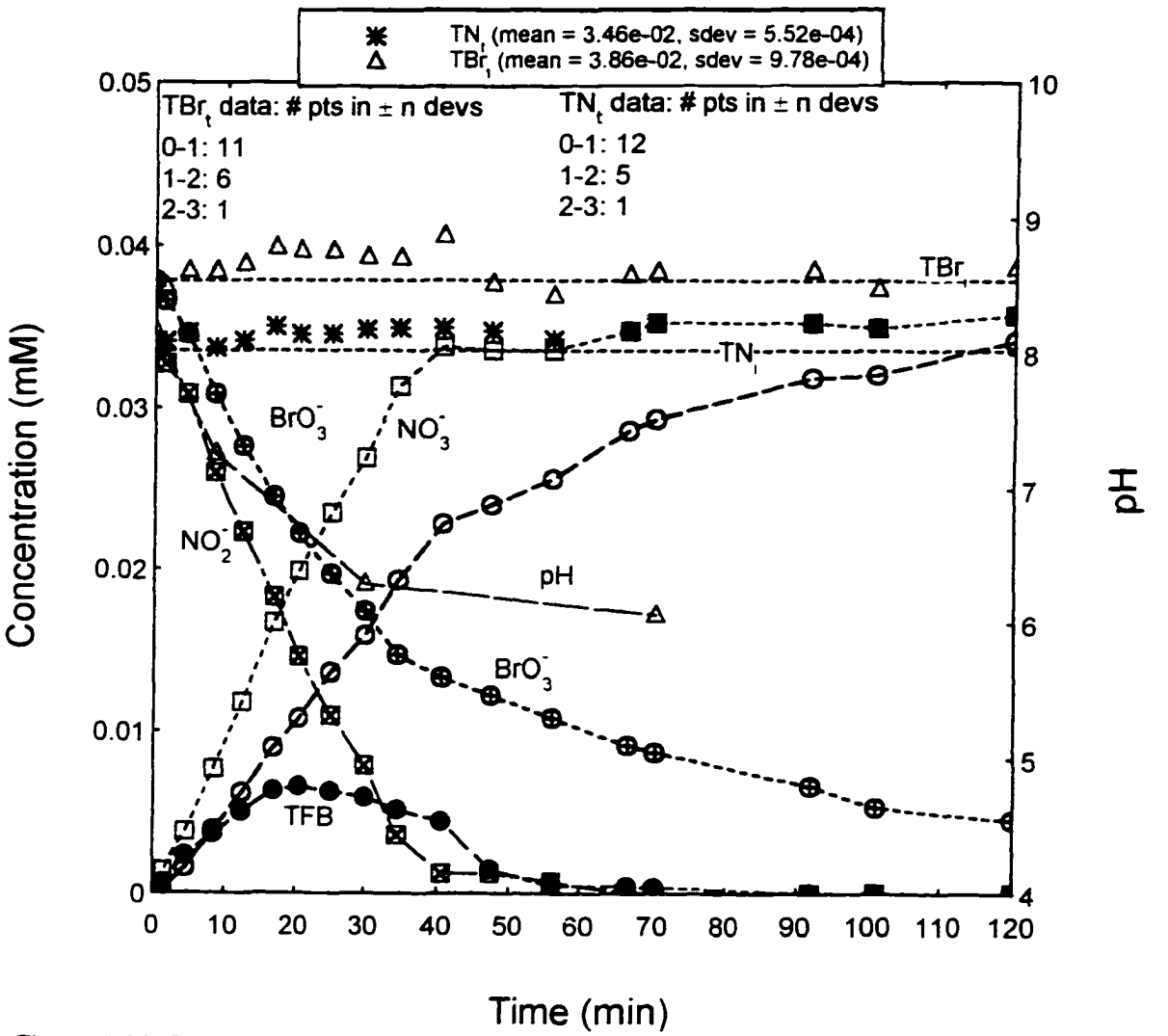

Figure 4.26. Species Profiles During UV Irradiation of Bromate/Nitrite Solution ($I = 2.30 \times 10^{-7}$ Einstein /L*s, BrO_3^- = 0.038 mM, NO_2^- = 0.034 mM, pH_i = 8.17, T_i = 23.3°C; EXP 18r).

Reproduced with permission of the copyright owner. Further reproduction prohibited without permission.

In all four previous experiments, total free bromine is formed in appreciable quantities compared to the experiments involving bromate alone. This diminishes the significance of the reaction between nitrite and free bromine (EQN 2-25) since the concentration of free bromine was expected to be significantly reduced in the presence of nitrite. It can be speculated that nitrite is oxidized principally by bromine species other than free bromine. The fact that there were no marked deviations in the bromine balance during the course of the experiments suggests that the species responsible for nitrite oxidation was a short-lived bromine intermediate that was undetected by the analytical methods used in the study. The bromine free radical species BrO• and BrO_2• fit this characteristic.

As was the case with the experiments involving bromate alone, solution pH decreases during UV irradiation by as much as 1.5 pH units of the initial values for solutions with initial pH < 9.0. Explanation of this result is as before with bromate alone solution, since during UV irradiation of aqueous nitrite solution, pH decrease was within 0.3 pH units of the initial levels. At pH > 9.0, the pH remained within 0.4 units of the initial value. Figure 4.27 depicts a typical UV irradiation experiment of bromate in presence of nitrite at initial pH > 9.0 at a UV light intensity of 2.61×10^{-6} Einstein L^{-1} s^{-1}. The species profiles are similar to that seen in Figure 4.23 with similar UV light intensity with the exception that the pH decrease is not as large.

Reproduced with permission of the copyright owner. Further reproduction prohibited without permission.

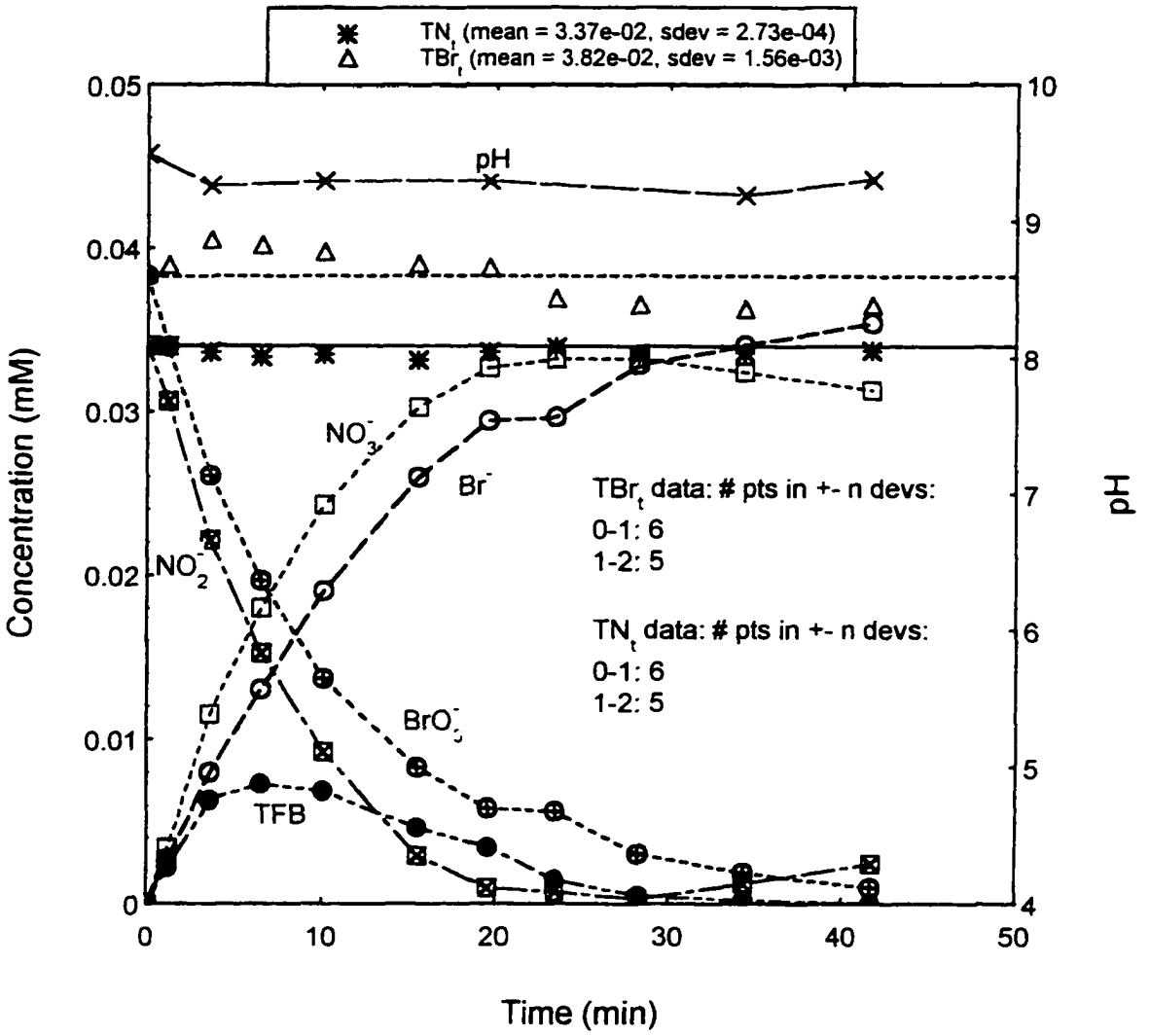

Figure 4.27. Species Profiles During UV Irradiation of Bromate/Nitrite Solution ($I = 2.61 \times 10^{-6}$ Einstein/L*s, $BrO_3^- = 0.038$ mM, $NO_2^- = 0.033$ mM, $pH_i = 9.49$, $T_i = 25°C$; EXP 63).

Reproduced with permission of the copyright owner. Further reproduction prohibited without permission.

4.4.2 Kinetics of Bromate Decomposition

A comparison of the profiles in these experiments and the profiles from the bromate alone experiments clearly depict much faster bromate decay and bromide formation kinetics and a more pronounced TFB profile. A control experiment conducted in the dark revealed no reaction between nitrite and bromate under similar pH and temperature conditions, over a reaction period of 45 hours. Figure 4.28 is a first order plot for bromate decay in the presence of nitrite for the experiment depicted in Figure 4.23. Nitrite concentration was plotted on the second y-axis. The figure clearly depicts two different decay rates for bromate with the transition occuring near the point when nitrite became limiting, at a concentration of approximately 0.002 mM. In the presence of nitrite, k_{obs} was 0.0976 min^{-1} which reduced to the value of 0.0623 min^{-1} in its subsequent absence. The latter rate was still much higher than corresponding experiments with bromate alone solution under similar experimental conditions. This suggests that the presence of nitrate in solution may also promote bromate decay after nitrite becomes limiting.

Reproduced with permission of the copyright owner. Further reproduction prohibited without permission.

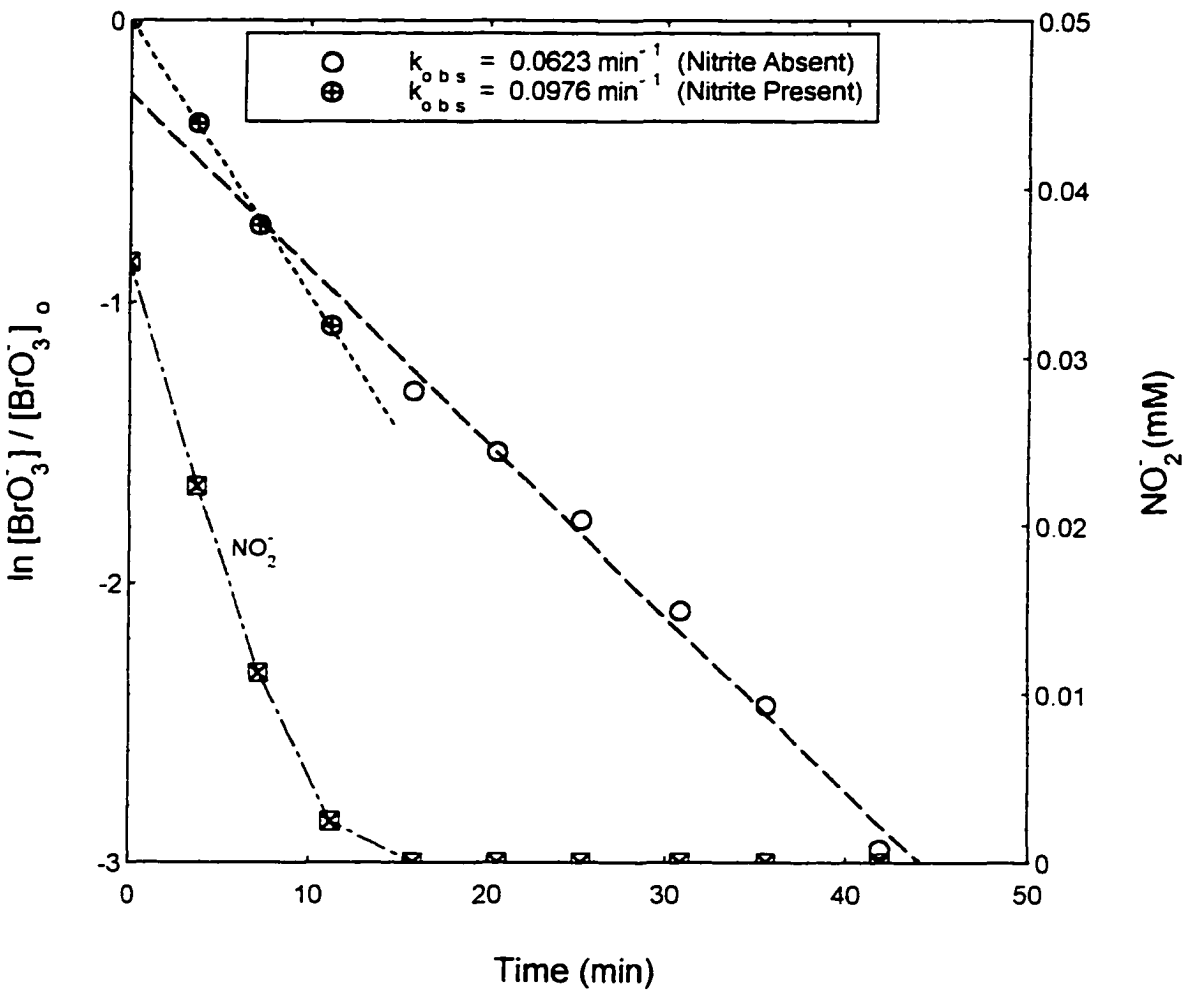

Figure 4.28. Bromate Decay First Order Plot in the Presence and Absence of Nitrite ($I = 2.61 \times 10^{-6}$ Einstein / L*s, BrO_3^- = 0.037 mM, NO_2^- = 0.036 mM, pH_i = 8.24, T_i = 22°C; EXP 43).

Reproduced with permission of the copyright owner. Further reproduction prohibited without permission.

Further kinetic analysis on bromate decay in the presence of nitrite was performed for various bromate/nitrite scenarios. The analysis in Figure 4.29 shows the first order plots for experiments in which the bromate/nitrite ratio < 1 (i.e., nitrite was in molar excess). Eight, four and sixteen UV lamps were used for experiments 28, 44 and 87 respectively. The figure shows that the data points are for the most part linear, indicating that bromate decay was pseudo-first order in presence of excess nitrite.

Figure 4.30 shows typical first order plots for experiments in which the bromate/nitrite > 1 (i.e., bromate in molar excess). Four and 16 lamps were used for experiments 17r and 67 respectively. The figure shows that bromate decay follows first order kinetics under these conditions. First order kinetics is more well defined, the higher the magnitude of the absolute bromate concentration. For lower bromate concentrations, the data points best approximate linearity in the early and later stages.

Figure 4.31 shows the case where the bromate/nitrite ≈ 1 (i.e., bromate and nitrite at equimolar concentrations). Twelve and four UV lamps were used for experiments 34 and 80 respectively. The overall data show linear bromate decay kinetics. As in Figure 4.29 for the lower bromate concentration, the data agrees well with the linear regression line in the early and later stages of the experiment. Nitrite disappears faster than bromate and the deviation from the straight line in the middle stages of the experiment, reflects the lower rate of bromate decay when nitrite becomes limiting.

Reproduced with permission of the copyright owner. Further reproduction prohibited without permission.

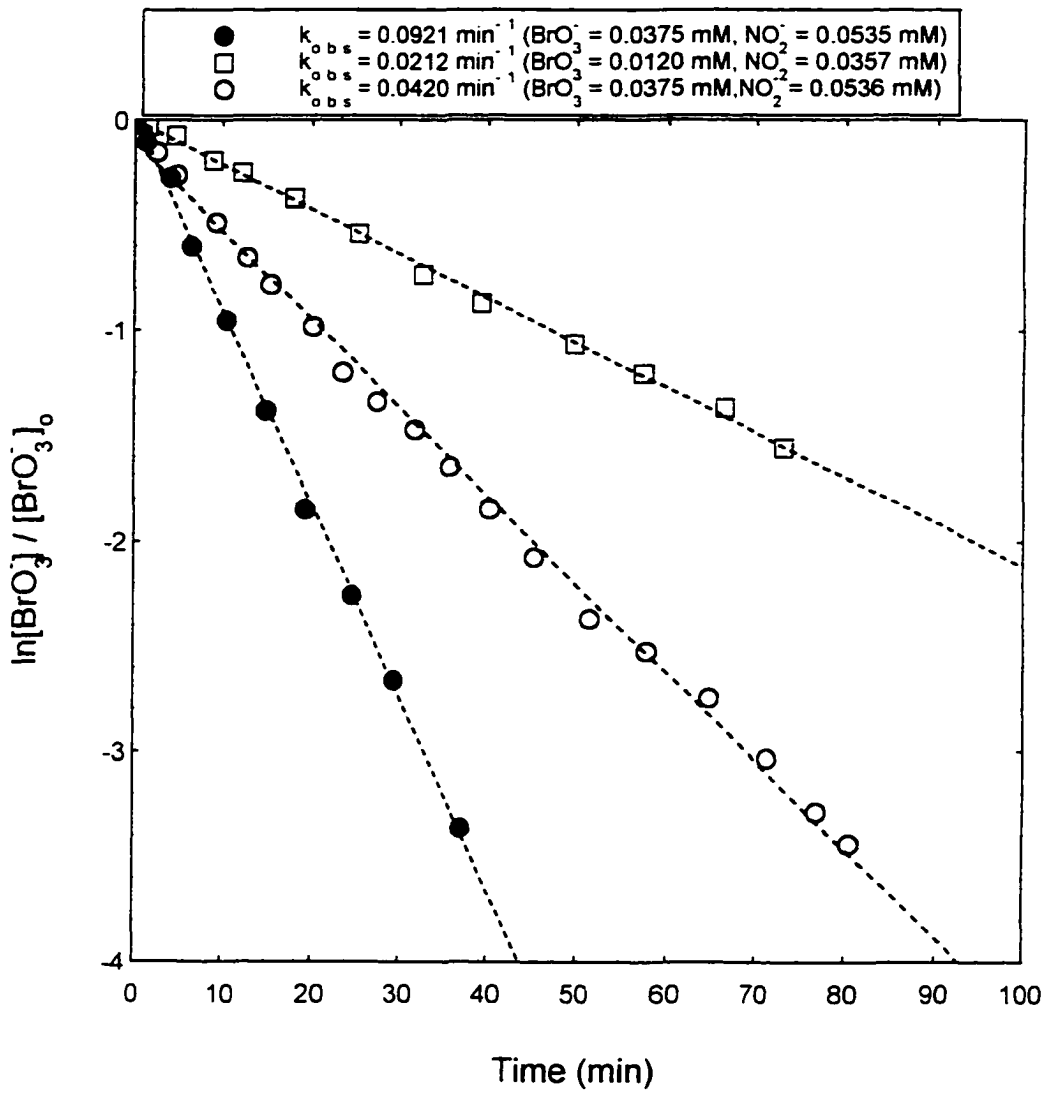

Figure 4.29. Bromate Decay First Order Plots for Bromate Solution Containing Excess Nitrite (EXP 28, 44, 87).

Reproduced with permission of the copyright owner. Further reproduction prohibited without permission.

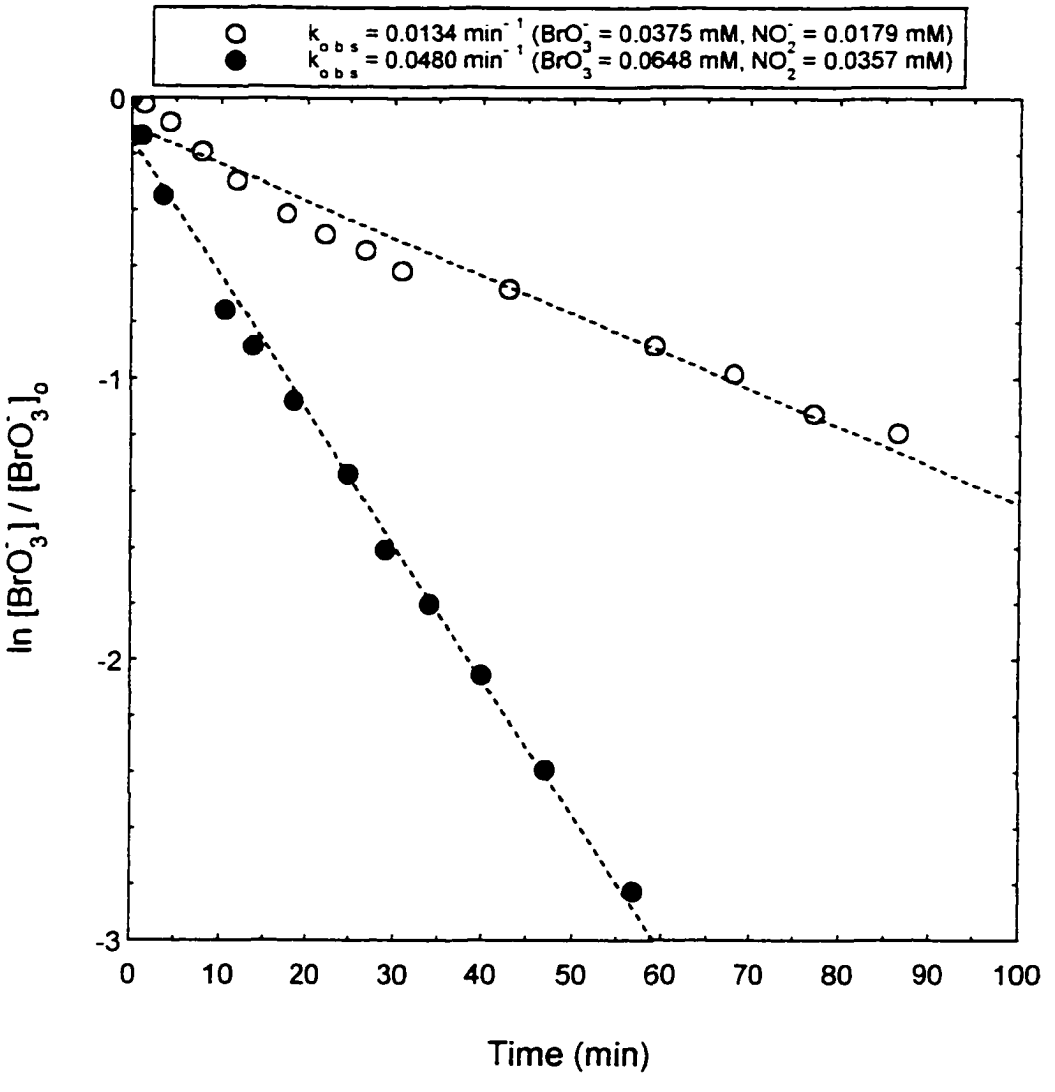

Figure 4.30. Bromate Decay First Order Plot for Bromate Solution in the Presence of Limiting Nitrite (EXP 17r, 67).

Reproduced with permission of the copyright owner. Further reproduction prohibited without permission.

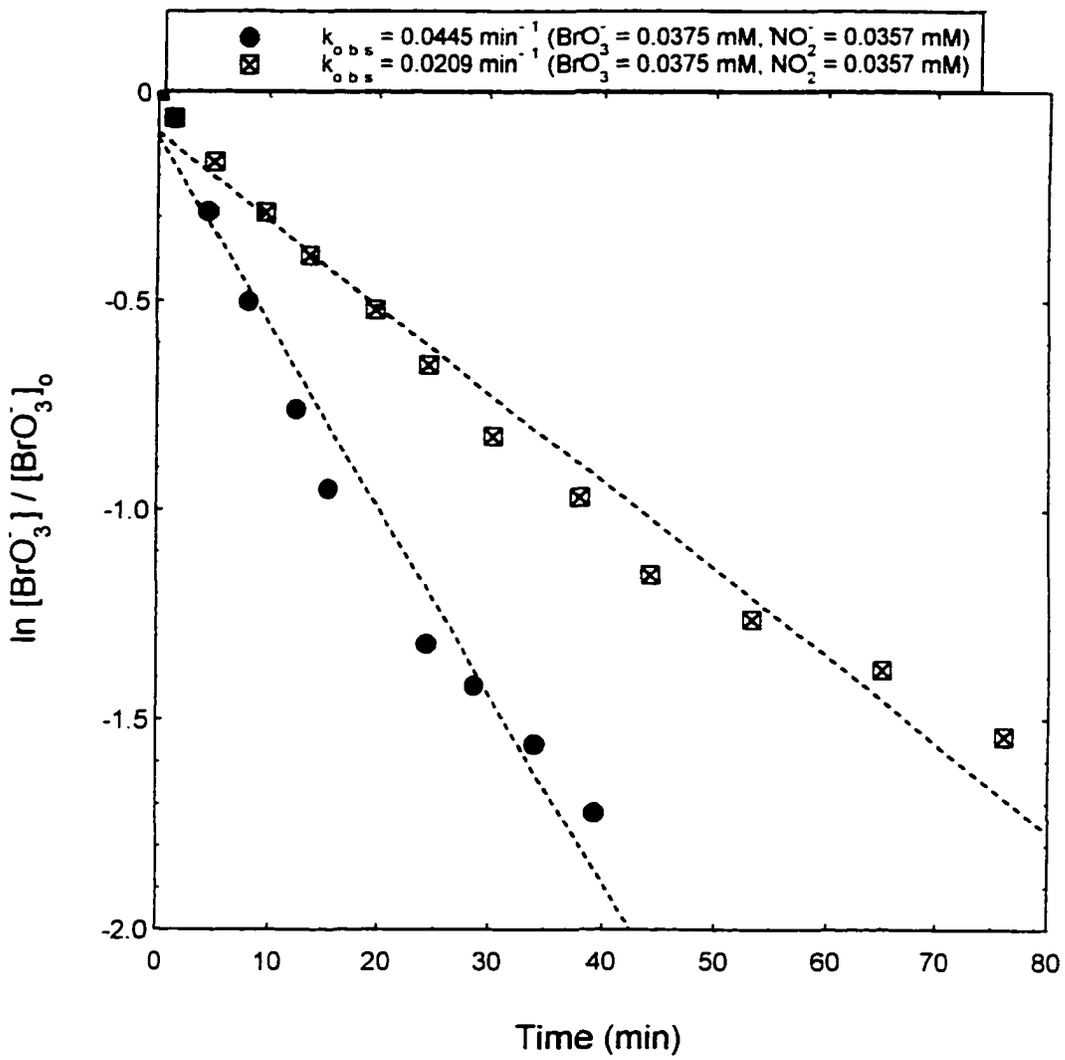

Figure 4.31. Bromate Decay First Order Plot for Bromate Solution Containing Equimolar Nitrite (EXP 34, 80).

Reproduced with permission of the copyright owner. Further reproduction prohibited without permission.

4.4.3 Kinetic Effect of Initial Bromate Concentration

The effect of initial bromate on k_{obs} was investigated for four UV light intensities over a narrow range of pH and temperature conditions for each set of experiments. Bromate was held constant at 0.038 mM (3 mg/L). The value of k_{obs} was determined only for those data points where the nitrite concentration was > 0.002 mM, since a marked decrease in k_{obs} was observed when nitrite concentration fell below this limiting value.

Figure 4.32 represents the plot of k_{obs} at various initial bromate concentrations for all four UV light intensities. The dashed horizontal lines represent the mean k_{obs} for each UV light intensity. As in the case of the bromate alone experiments, the figure shows that k_{obs} is relatively independent of initial bromate concentration in the presence of nitrite, though the rates are markedly higher than in the corresponding bromate alone experiments. The mean k_{obs} was 0.110 min^{-1} (16 UV lamps), 0.055 min^{-1} (12 UV lamps), 0.053 min^{-1} (8 UV lamps) and 0.023 min^{-1} (4 UV Lamps). Of the four lamp configurations, k_{obs} for the 12 lamp configuration had the highest standard deviation (σ). The ratio of the standard deviation for each of the four UV lamp configurations to σ for the 12 lamp configuration was 0.33, 1.0, 0.45 and 0.37 for the 16, 12, 8 and 4 UV lamp configurations respectively.

Reproduced with permission of the copyright owner. Further reproduction prohibited without permission.

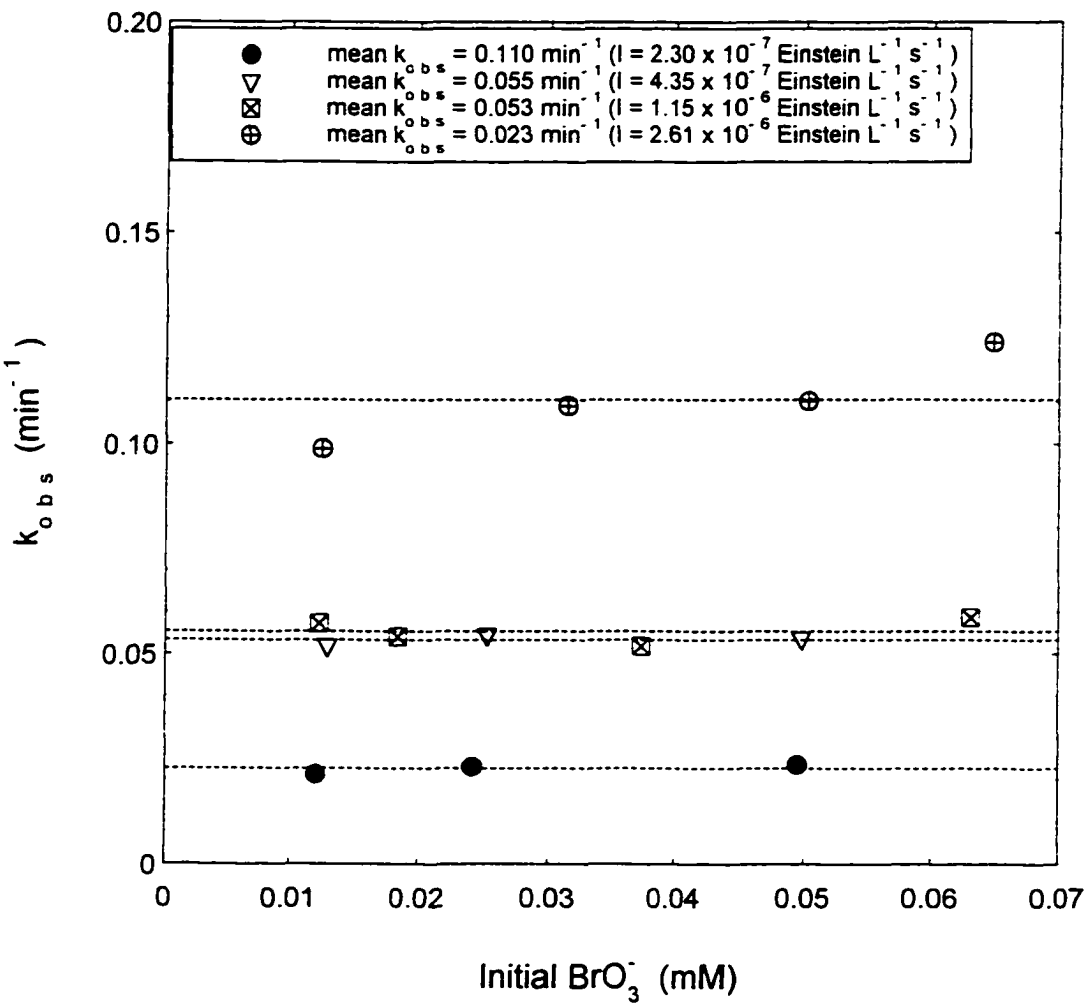

Figure 4.32. Dependency of Bromate Decay on Bromate in Presence of Nitrite (BrO_3^- = 0.038 mM, Range pH_i = 7.95 - 8.30, Range T_i = 20-25 °C, EXP 48-51, 66-69, 70-72, 85-87).

Reproduced with permission of the copyright owner. Further reproduction prohibited without permission.

4.4.4 Kinetic Effect of Initial Nitrite Concentration

The effect of initial nitrite on bromate decay was investigated for constant initial bromate concentration. Initial pH and initial temperature were held within a narrow range. Figure 4.33 shows k_{obs} as a function of initial nitrite for the four UV light intensities. The determination of k_{obs} was based only on the corresponding bromate data points where nitrite was in excess of 0.002 mM. The dashed horizontal lines represent the mean k_{obs} for each UV light intensity. The data for the UV light intensity of 4.35×10^{-7} Einstein L^{-1} s^{-1} (8 UV lamps) showed a relatively large scatter from the mean. However, the data for the other three UV light intensities showed that k_{obs} was basically independent of initial nitrite concentration in the range 0.01 mM to 0.06 mM. As in the previous figure, the rates were higher than the corresponding bromate alone experiments over the whole range of initial nitrite concentrations.

The mean k_{obs} was 0.091 min^{-1} (16 UV lamps), 0.061 min^{-1} (12 UV lamps), 0.057 min^{-1} (8 UV lamps) and 0.025 min^{-1} (4 UV Lamps). The k_{obs} for the 12 UV lamp configuration had a σ value of 0.017. The ratio of σ for each of the four UV lamp configurations to σ for the 8 lamp configuration was 0.46, 0.06 and 0.11 for the 16, 12 and 4 UV lamp configurations respectively.

Reproduced with permission of the copyright owner. Further reproduction prohibited without permission.

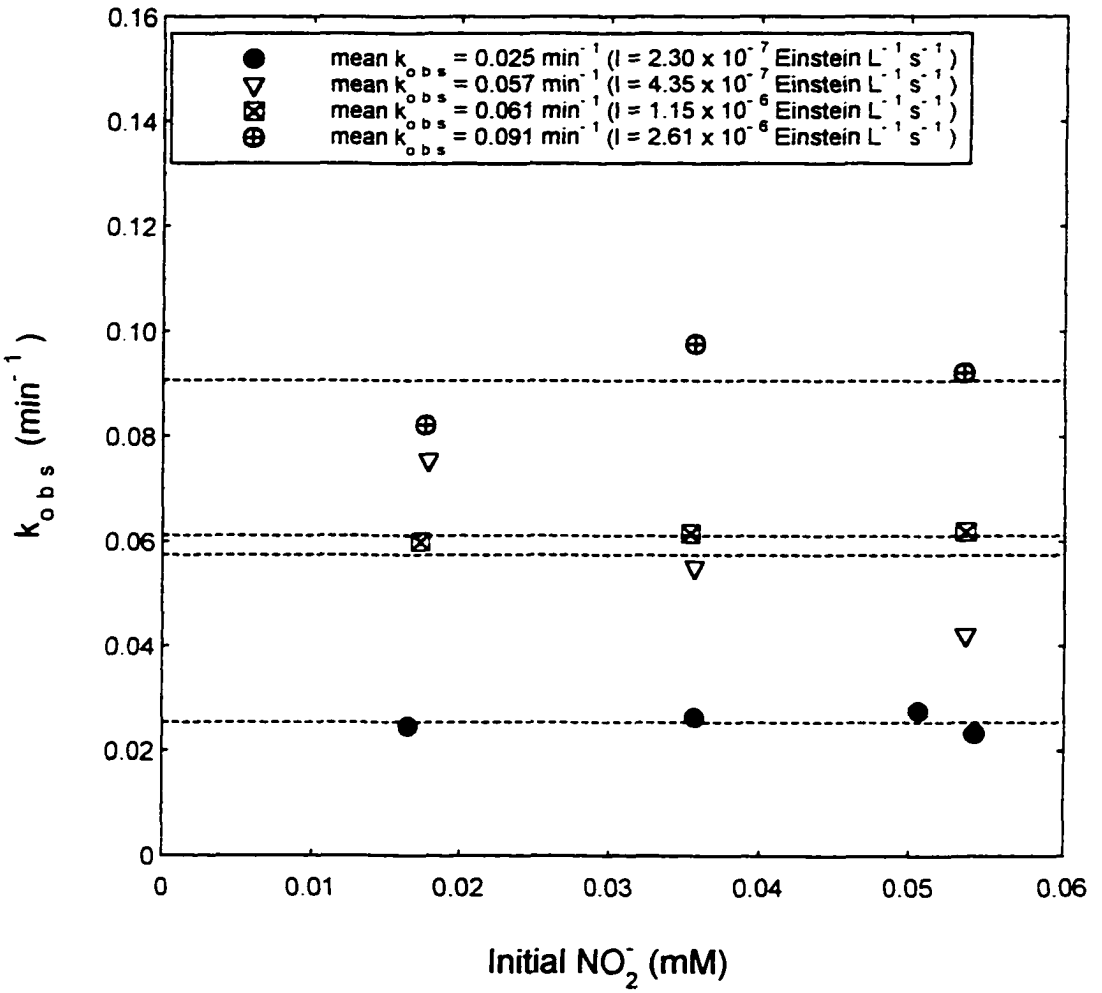

Figure 4.33. Dependency of Bomate Decay Observed Rate on Initial Nitrite (BrO_3^- = 0.038 mM, Range pH_i = 8.13-8.29, Range T_i = 22 - 24°C, EXP 14, 16, 17r, 19r, 25, 27, 28, 30-32, 42-44).

Reproduced with permission of the copyright owner. Further reproduction prohibited without permission.

4.4.5 Kinetic Effect of Initial pH

The effect of initial pH (range of 4 to 10) on bromate decay was investigated for constant initial bromate and nitrite concentrations and for temperature in a narrow range. Figures 4.34 shows the dependency of k_{obs} on initial solution pH the for four UV light intensities used in the this study. The determination of all k_{obs} values was based on bromate data points with corresponding nitrite concentration > 0.002 mM. The dashed horizontal lines represent the mean k_{obs} for each UV light intensity.

Except for one data point at the highest UV light intensity, the data shows that k_{obs} is relatively independent of initial pH in the range 7 to 10. For the UV light intensity of 1.15×10^{-6} Einstein L^{-1} s^{-1} , one data point at pH 4.9 also lies along the dashed horizontal line, indicating an extension of the range of pH over which k_{obs} is independent.

The reaction of free bromine and nitrite is a pH dependent reaction. Lengyel et al. (1989) reported a decrease in the the rate of the reaction of nitrous acid, which is in association with nitrite, and aqueous bromine solution for lower pH values. Pendlebury and Smith (1973) show that H^+ is a major product (EQN 2-25) from the reaction of nitrite and free bromine. Based on the reaction in EQN (4-6) where aqueous electrons are scavenged by H^+, a decrease in the rate of bromate decay was expected for bromate solution in presence of nitrite at lower pH.

Reproduced with permission of the copyright owner. Further reproduction prohibited without permission.

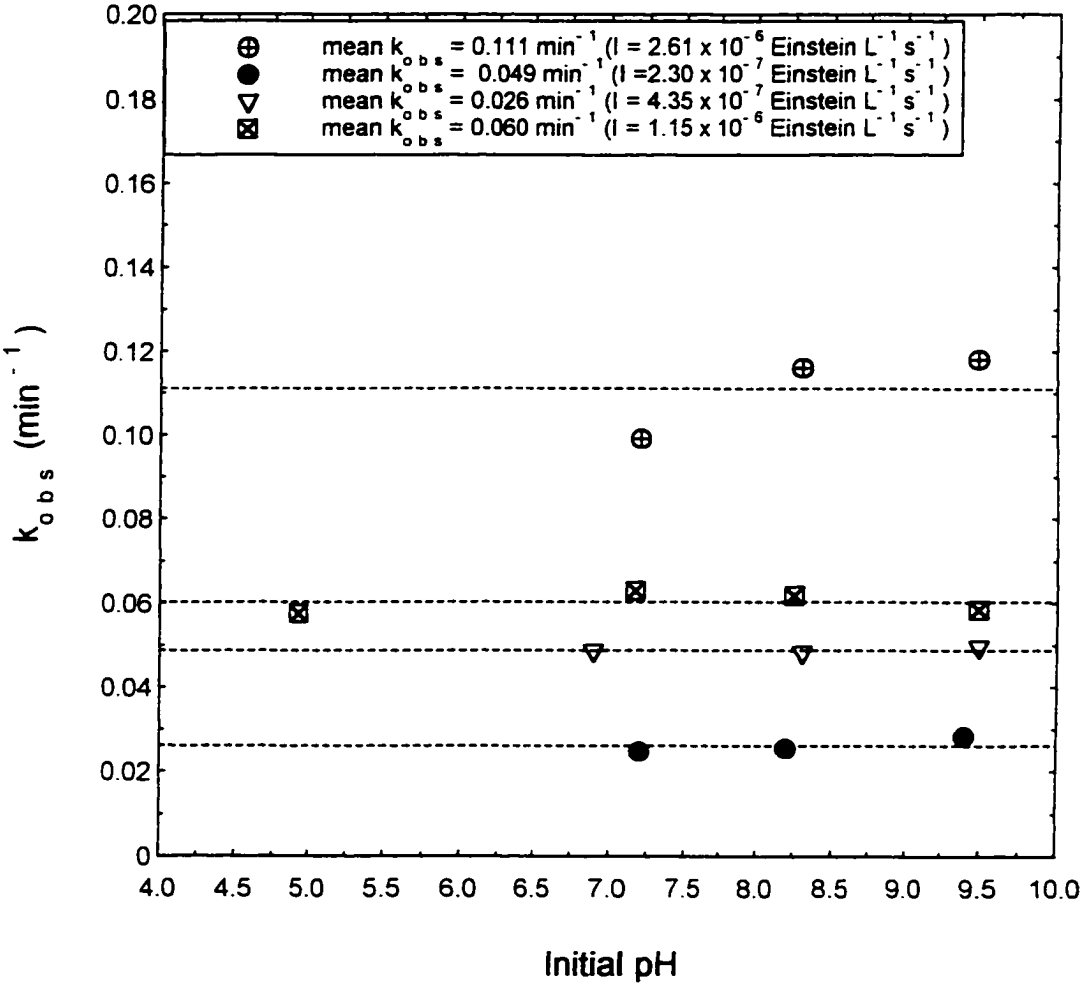

Figure 4.34. pH Dependency of Bromate Decay Constant in Presence of Nitrite (BrO_3^- = 0.038 mM, NO_2^- = 0.036 mM, Range T_i = 22.5 - 25 ^oC; EXP 33-36, 63-65, 73-75, 79-81).

Reproduced with permission of the copyright owner. Further reproduction prohibited without permission.

4.4.5 Effect of Light Intensity on Bromate Decay

The effect of light intensity on k_{obs} is shown in Figure 4.35 for constant initial bromate and nitrite and for temperature and pH within a narrow range. A linear regression analysis performed on the data found the following relationship

$$k_{obs}\ (\text{min}^{-1}) = 2.94 \times 10^{-4} * I + 0.0228 \qquad (4\text{-}8)$$

A change in instensity from 2.30 x 10^{-7} Einstein L^{-1} s^{-1} to 2.61 x 10^{-6} Einstein L^{-1} s^{-1} caused an increase in k_{obs} from 0.0230 min^{-1} to 0.0302 min^{-1}, a 30 % increase.

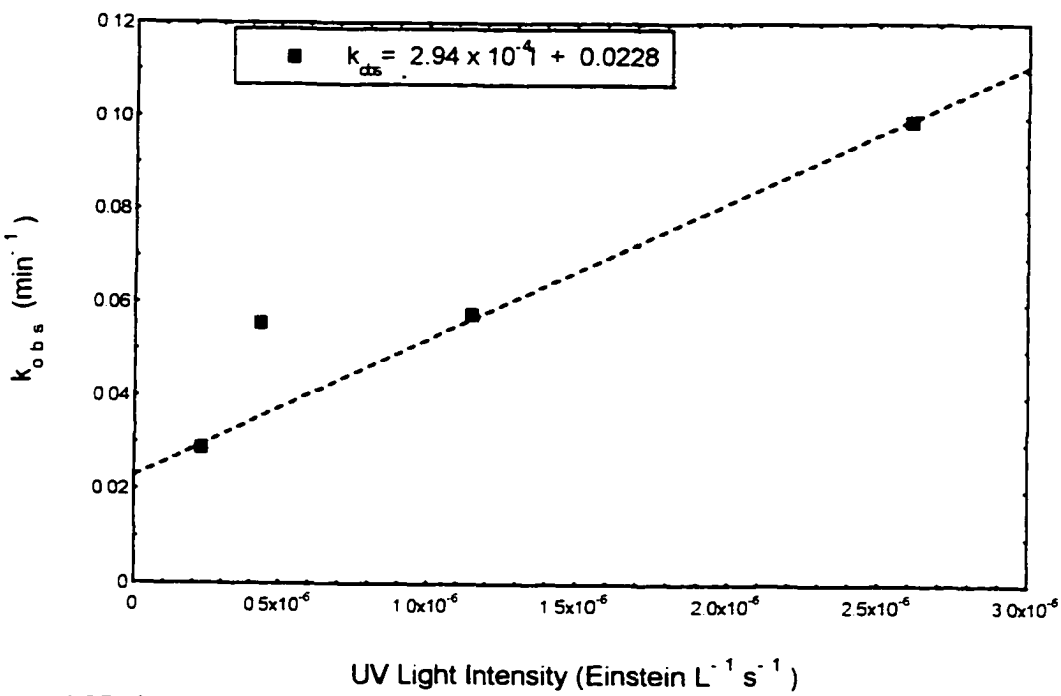

Figure 4.35. Light Dependency of Bromate Decay Constant in Presence of Nitrite (BrO_3^- =0.038 mM, NO_2^- =0.036 mM, Range pH_i = 9.37 - 9.49, Range T_i = 23 - 25°C; EXP 21r, 26, 36, 63).

Reproduced with permission of the copyright owner. Further reproduction prohibited without permission.

4.5 Bromate Decay in the Presence of Acetate

Bromate decomposition in the presence of acetate was investigated for the single UV light intensity of 4.35 x 10^{-6} Einstein L^{-1} s^{-1} with pH and temperature within a narrow range. Acetate concentrations ranged from 0.06 to 0.27 mM. Bromate concentration was held constant at 0.038 mM.

Figures 4.36 through 4.38 show the concentration-time profiles of species during UV irradiation of aqueous bromate solution containingin the presence of the varying acetate concentrations. As in the case of bromate alone solution, bromate decay was followed by bromide formation. Free bromine remained below the analytical detection limit throughout the experiments. Examination of the bromine species during UV irradiation showed that TBr_t as defined by EQN (4-1) was consistently below the initial bromine level (TBr_i) depicted by the dashed horizontal line in each figure. This could be attributed to the formation of brominated organic compounds at trace levels, and/or to possible error in determining very low levels of free bromine.

Acetate was converted to undetermined product(s) during each of the three experiments. Preliminary experiments with similar concentrations of solutions of acetate alone showed no change in acetate concentration during UV irradiation. This indicates that the product(s) of bromate decomposition is responsible for reaction of acetate. Acetate conversion ranged from 9.6% for the acetate concentration of 0.27 mM to 29% for the acetate concentration of 0.06 mM, for similar reaction times.

Reproduced with permission of the copyright owner. Further reproduction prohibited without permission.

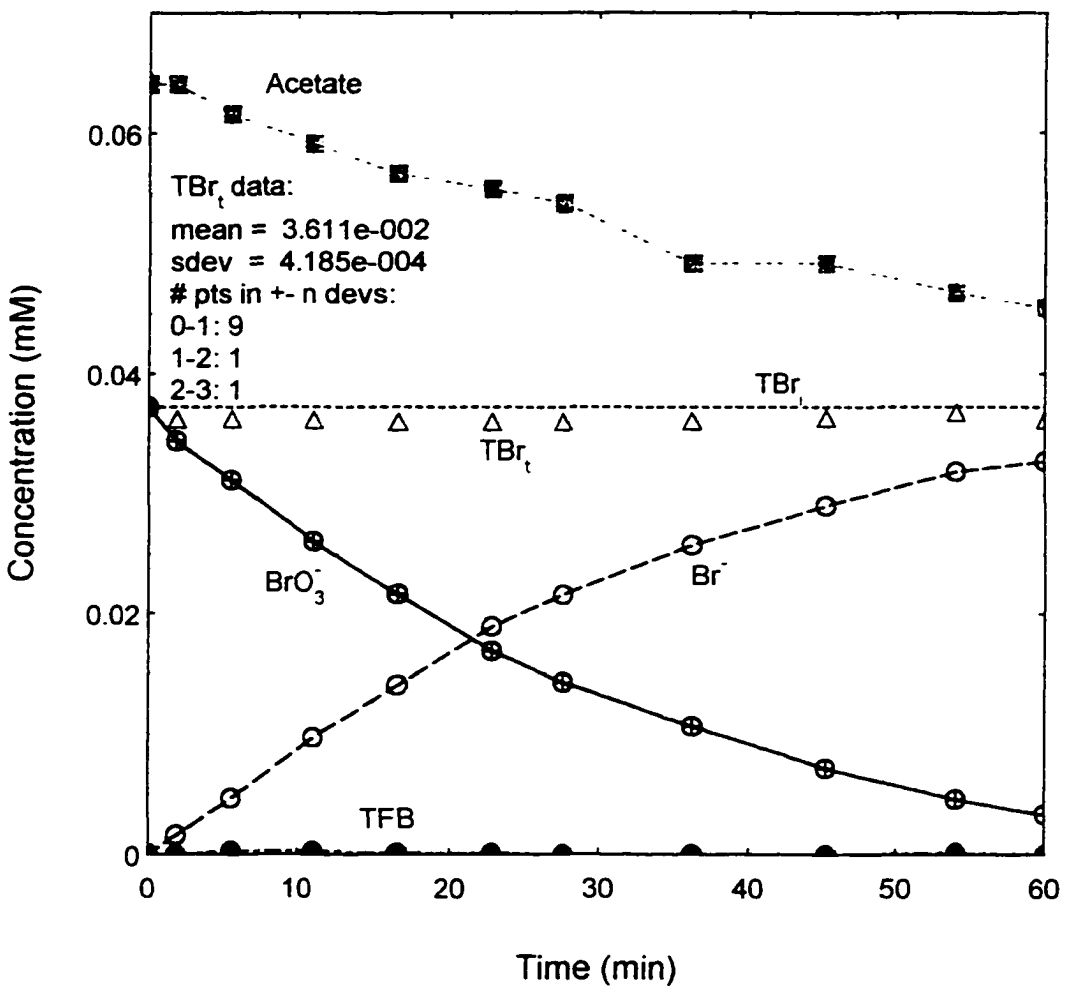

Figure 4.36. Species Profiles During UV Irradiation of Bromate/Acetate Solution ($I=4.35 \times 10^{-7}$ Einstein/L*s, BrO_3^- = 0.037mM, Acetate = 0.06 mM, pH_i = 7.96, T_i = 23°C; EXP 89).

Reproduced with permission of the copyright owner. Further reproduction prohibited without permission.

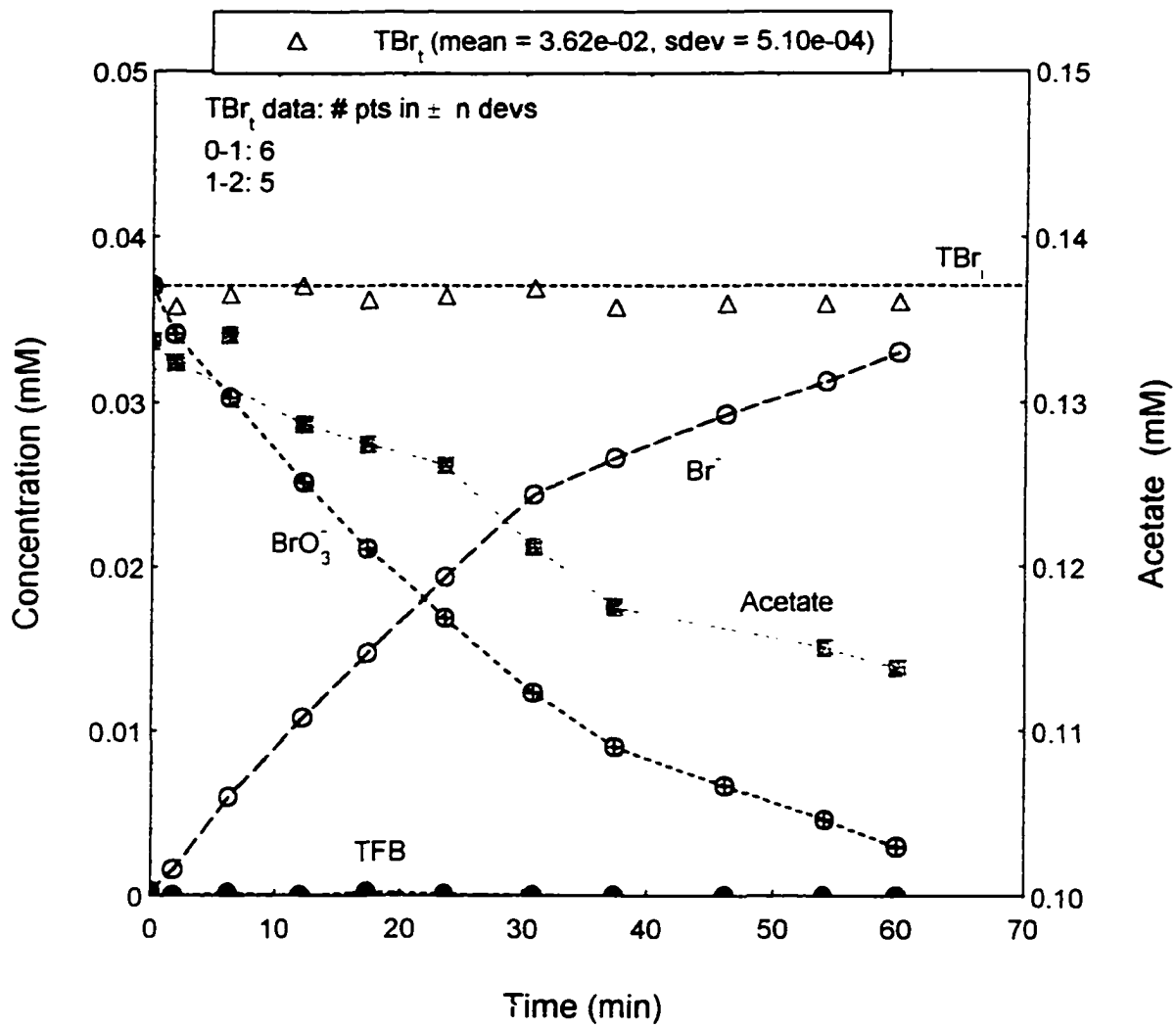

Figure 4.37. Species Profiles During UV Irradiation of Bromate/Acetate Solution ($I = 4.35 \times 10^{-7}$ Einstein / L*s, BrO_3^- = 0.038 mM, Acetate = 0.13 mM, pH_i = 8.10, T_i = 23°C; EXP 90).

Reproduced with permission of the copyright owner. Further reproduction prohibited without permission.

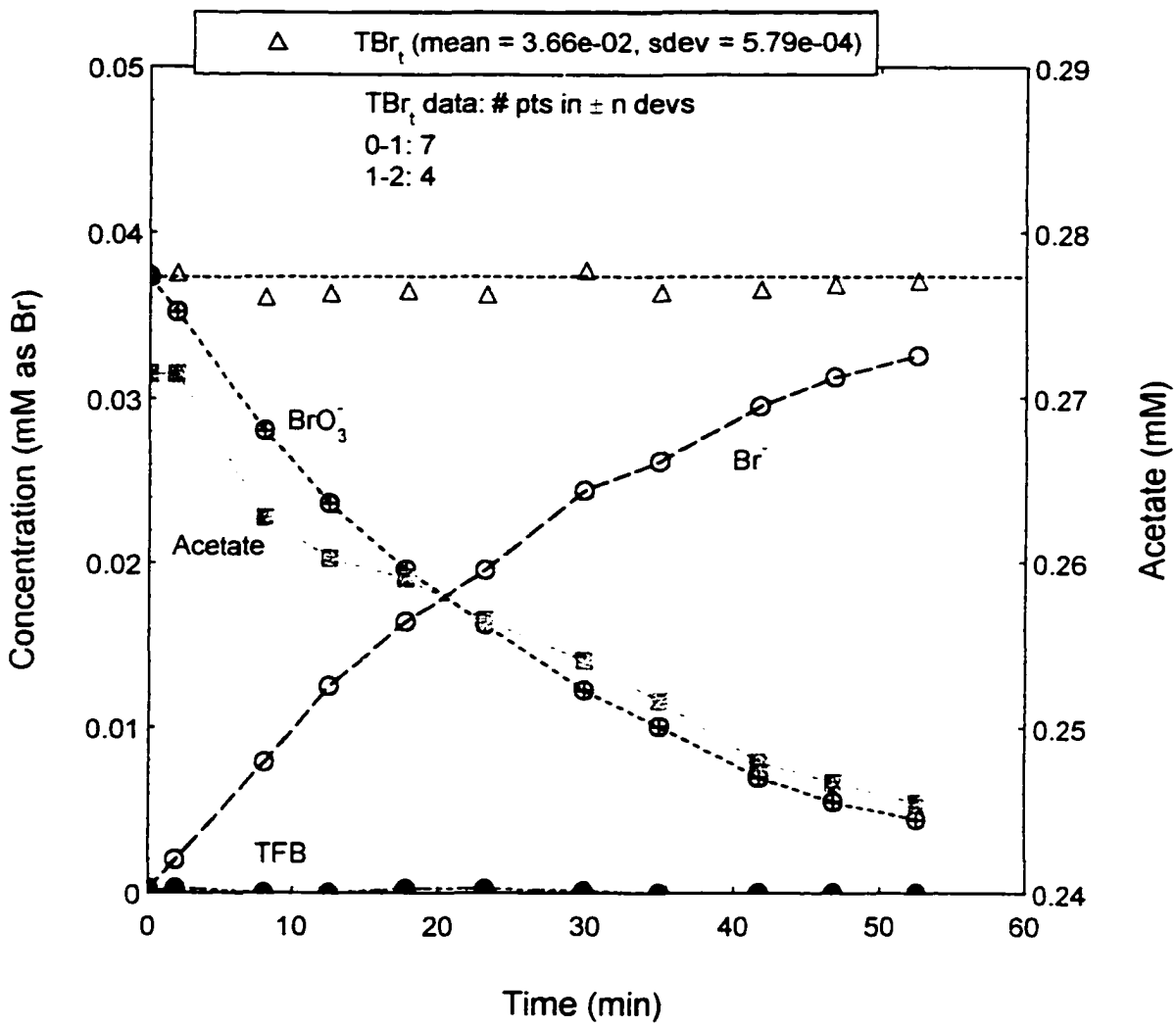

Figure 4.38. Species Profiles During UV Irradiation of Bromate/Acetate Solution ($I = 4.35 \times 10^{-7}$ Einstein / L*s, BrO_3^- = 0.037 mM, Acetate = 0.27 mM, pH_i = 8.02, T_i = 23°C; EXP 91).

Reproduced with permission of the copyright owner. Further reproduction prohibited without permission.

A comparison of the rates of bromate decay for an experiment with bromate alone and an experiment with bromate/acetate is in figure 4.39. The relative bromate ($[BrO_3^-]/[BrO_3^-]_o$) concentration is plotted as a function of UV irradiation time. The initial pH values ranged from 7.96 to 8.01 and temperature was held at 23°C for both experiments. The figure clearly shows faster bromate decay in the presence of acetate. The bromate decay half life was decreased from 32.9 minutes to 20.5 minutes by the presence of 0.06 mM acetate.

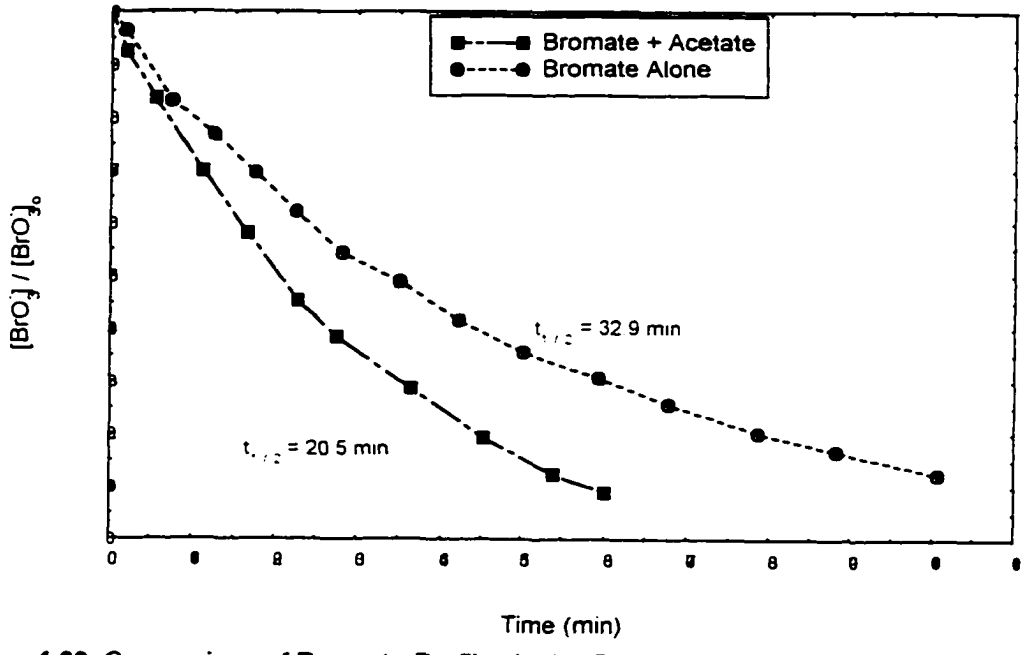

Figure 4.39. Comparison of Bromate Profiles in the Presence/Absence of Acetate ($I = 4.35 \times 10^{-7}$ Einstein $L^{-1} s^{-1}$, BrO_3^- = 0.038 mM, Acetate = 0.06 mM, Range pH_i = 8.01 - 8.10, T_i = 23°C; EXP 89-91).

Reproduced with permission of the copyright owner. Further reproduction prohibited without permission.

A first order plot for the three experiments depicted in figures 4.36 through 4.38 is shown in Figure 4.40. The figure shows first order kinetics for all three experiments. The value of k_{obs} remains relatively constant over a quadrupling of the acetate concentration. Also the rates are almost doubled that of a comparative bromate alone experiment under similar experimental conditions and are comparable to k_{obs} for the bromate alone experiments conducted at the highest UV light intensity of 2.61×10^{-6} Einstein L^{-1} s^{-1}.

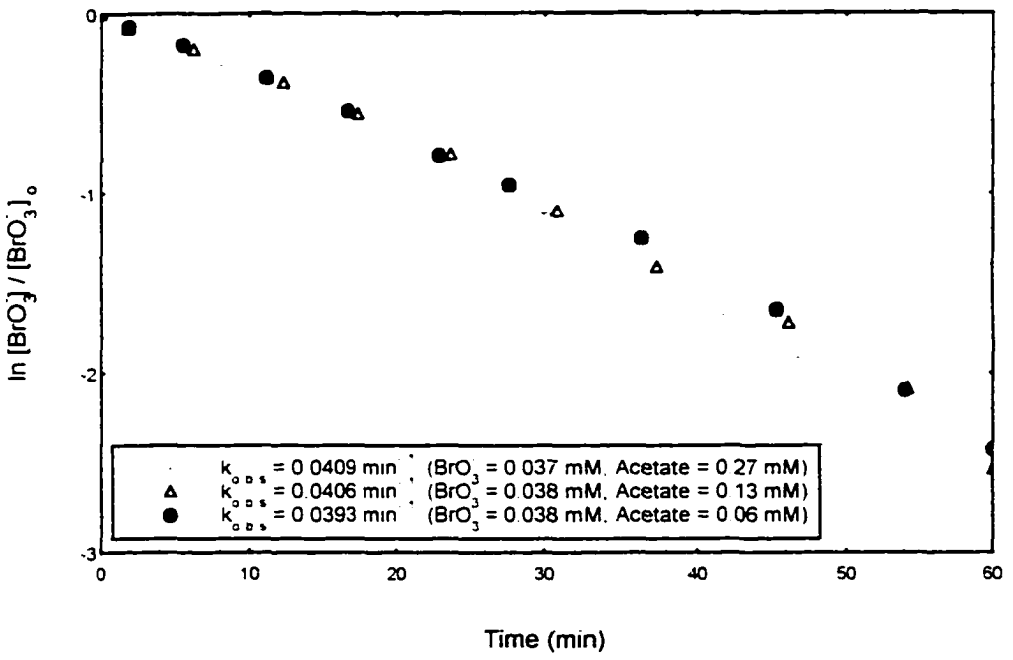

Figure 4.40. Bromate Decay Pseudo-First Order Plot for Bromate/Acetate Solution (I=4.35 x 10^{-7} Einstein/L*s, Range pH_i=7.96-8.02, T_i=23°C; EXP 89-91).

Reproduced with permission of the copyright owner. Further reproduction prohibited without permission.

CHAPTER 5

KINETIC MODEL DEVELOPMENT

A mechanism of chemical reactions based on literature studies and in part on this study, is proposed to describe bromate decay under UV irradiation. A numerical routine based on the Runge-Kutta fourth order method was used to solve the system of time dependent first order differential equations describing the change of species concentration for various experimental conditions (i.e., boundary conditions).

5.1 Bromate Decay Model

In the presence of nitrite, bromate decays to form bromide, oxygen and nitrate as end-products and free bromine as an intermediate. The following reaction scheme is proposed to explain bromate decay in solutions of bromate alone and of bromate in the presence of nitrite. The scheme is based in part on an extensive review of the literature and in part on the findings of this study.

Reproduced with permission of the copyright owner. Further reproduction prohibited without permission.

UV catalyzed decomposition of bromate

$$BrO_3^- + h\nu \rightarrow OBr^- + O_2 \qquad k_1 \qquad (5\text{-}1)$$

Hypobromite equilibrium reaction

$$OBr^- + H^+ \rightarrow HOBr \qquad pK_a \qquad (5\text{-}2)$$

UV catalyzed decomposition of hypobromite and hypobromous acid

$$OBr^- + h\nu \rightarrow Br^- + \frac{1}{2}O_2 \qquad k_2 \qquad (5\text{-}3)$$

$$HOBr + h\nu \rightarrow Br- + H^+ + \frac{1}{2}O_2 \qquad k_3 \qquad (5\text{-}4)$$

UV catalyzed disproportionation of hypobromite

$$3OBr^- + h\nu \rightarrow BrO_3^- + 2Br \qquad k_4 \qquad (5\text{-}5)$$

UV catalyzed nitrite decay

$$H_2O + NO_2^- + h\nu \rightarrow NO_3^- + 2H^+ \qquad k_5 \qquad (5\text{-}6)$$

Reaction of hypobromite and nitrite

$$OBr^- + NO_2^- \rightarrow Br^- + NO_3^- \qquad k_6 \qquad (5\text{-}7)$$

Reproduced with permission of the copyright owner. Further reproduction prohibited without permission.

The decomposition of bromate to form hypobromite and molecular oxygen in EQN (5-1) was first proposed by Farkas and Klein (1948) as the first step in the decomposition of bromate in a solution containing bromate alone. This reaction has been shown to have first order kinetics (this study and Siddiqui et al., 1997). Siddiqui et al. (1997) proposed the formation of bromite, BrO_2^-, (λ_{max} = 260 nm) as an intermediate product of bromate decomposition, though no experimental evidence was shown to support this claim.

EQN (5-2) is the equilibrium reaction for the hypobromite-hypobromous acid system (pK_a = 8.69). For pH values less than pK_a, hypobromous acid predominates while the reverse is true at pH values greater than pK_a. At any time, there will be a combination of hypobromite and hypobromous acid in a free bromine solution. Both species are light absorbing at 254 nm with molar absorptivities, ϵ, of 87.1 and 42.2 M^{-1} cm^{-1} for hypobromous acid and hypobromite respectively (Bridge and Matheson, 1960). Thus, at lower pH values, free bromine will decay at a faster rate due to the predominance of the more light absorbing hypobromous acid. Experimental evidence from this study and by Engel et al. (1953) have shown this to be generally true.

The reactions in EQNs (5-3) and (5-4) account for the decomposition of free bromine species during UV irradiation of bromate solution. These reactions are basically competitive when both species are represented in terms of total free bromine. The greater molar absorptivity of hypobromous acid suggests that k_3 is greater than k_2.

Reproduced with permission of the copyright owner. Further reproduction prohibited without permission.

The literature did not show any values of k_2 and k_3 at 254 nm. At UV wavelengths other than 254 nm, the rates will be different and would not be applicable to this model. The values of k_2 and k_3 were determined from the experimental results of the free bromine decomposition experiments in this study. Based on the experiments performed at the different pH values, the ratio of k_2 to k_3 used in the model was approximately 0.8.

EQN (5-5) depicts the UV catalyzed disproportionation reaction of hypobromite to form bromate and bromide according to Farkas and Klein (1948). The apparent order of the reaction was not reported however. The formation of bromate and bromide during UV irradiation of free bromine solution was also confirmed in the present study. The literature shows much debate about the mechanism and the apparent order of this reaction in the absence of UV radiation. Engel et al. (1953) represented the reaction as one involving hypobromite species with a reaction order of two. Chapin (1934) represented the reaction as one involving both hypobromous acid and hypobromite with a reaction order between two and three at pH 9.4. As recognized by Chapin (1934), the difficulty of establishing the order of the reaction may be due to the fact that the reaction consists of a mixture of concurrent reactions, the relative contributions of which may vary strongly with experimental conditions. In the model a third order reaction was assumed for the reaction in EQN (5-5).

Bromate decays in EQN (5-1) and forms in EQN (5-5), therefore the overall observed bromate decay rate constant is the difference between the observed bromate

Reproduced with permission of the copyright owner. Further reproduction prohibited without permission.

decay rate constant in EQN (5-1) and the observed bromate formation rate constant in EQN (5-5).

The reaction in EQN (5-6) was included in the model to account for the decay of nitrite itself under UV irradiation. The literature and also this study has shown that nitrite is oxidized during UV irradiation to form nitrate as the major product. The literature did not show any rates of nitrite decomposition at 254 nm and the rate for k_5 used in the model was that determined from the nitrite experiments in this study.

EQN (5-6) accounts for the reaction between nitrite and free bromine. Since this is a chemical and not a photochemical reaction, the value of k_6 remains constant for all UV light intensities in the model. Unlike the reaction between free chlorine and nitrite which is well documented (Diyamandoglu et al., 1990, Pendlebury and Smith, 1973b) the literature on the reaction between nitrite and free bromine is sparse. Following the work of Pendlebury and Smith (1973a), the reaction in EQN (5-7) was thus represented as third order overall and second order with respect to nitrite.

EQN (5-8) through EQN (5-15) expresses the concentration of each species in differential form. Where a species occurs as a reactant, a negative sign is placed to denote decreasing concentration with time and where it occurs as a product the opposite is true.

$$\frac{d[BrO_3^-]}{dt} = -k_1[BrO_3^-] + k_4[OBr^-]^3 \qquad (5\text{-}8)$$

Reproduced with permission of the copyright owner. Further reproduction prohibited without permission.

$$\frac{d[OBr^-]}{dt} = k_1[BrO_3^-] - k_2[OBr^-] - k_4[OBr^-]^3 - k_6[OBr^-][NO_2^-]^2 \quad (5\text{-}9)$$

$$\frac{d[HOBr]}{dt} = -k_3[HOBr] \quad (5\text{-}10)$$

$$\frac{d[Br^-]}{dt} = k_2[OBr^-] + k_3[HOBr] + \frac{2}{3}k_4[OBr^-]^3 + k_6[OBr^-][NO_2^-]^2 \quad (5\text{-}11)$$

$$\frac{d[NO_2^-]}{dt} = -k_5[NO_2^-] - k_6[OBr^-][NO_2^-]^2 \quad (5\text{-}12)$$

$$\frac{d[NO_3^-]}{dt} = k_5[NO_2^-] + k_6[OBr^-][NO_2^-]^2 \quad (5\text{-}13)$$

$$\frac{d[O_2]}{dt} = k_1[BrO_3^-] + \frac{1}{2}k_2[OBr^-] + \frac{1}{2}k_3[HOBr] \quad (5\text{-}14)$$

$$\frac{d[H^+]}{dt} = k_3[HOBr] + 2k_5[NO_2^-] \quad (5\text{-}15)$$

Total free bromine is the sum of hypobromite and hypobromous acid

$$[TFB] = [HOBr] + [OBr^-] \quad (5\text{-}16)$$

Reproduced with permission of the copyright owner. Further reproduction prohibited without permission.

Using the definition of K_a

$$K_a = \frac{[H^+][OBr^-]}{[HOBr]} \tag{5-17}$$

we get the following expressions for [HOBr] and [OBr$^-$]

$$[HOBr] = \frac{[H^+]}{K_a + [H^+]}[TFB] = K_{50}[TFB] \tag{5-18}$$

$$[OBr^-] = \frac{K_a}{K_a + [H^+]}[TFB] = K_{60}[TFB] \tag{5-19}$$

Differentiating (5-16) with respect to time we get

$$\frac{d[TFB]}{dt} = \frac{d[HOBr]}{dt} + \frac{d[OBr^-]}{dt} \tag{5-20}$$

Using EQNs (5-18), (5-19) and (5-20) we rewrite the system of differential equation:

$$\frac{d[BrO_3^-]}{dt} = -k_1[BrO_3^-] + \frac{1}{3}k_4K_{60}^3[TFB]^3 \tag{5-21}$$

$$\frac{d[TFB]}{dt} = k_1[BrO_3^-] - k_2K_{60}[TFB] - k_4K_{60}^3[TFB]^3 - k_6K_{60}[TFB][NO_2^-]^2 - k_3K_{50}[TFB] \tag{5-22}$$

$$\frac{d[Br^-]}{dt} = k_2K_{60}[TFB] + k_3K_{50}[TFB] + \frac{2}{3}k_4K_{60}[TFB]^3 + k_6K_{60}[TFB][NO_2^-]^2 \tag{5-23}$$

Reproduced with permission of the copyright owner. Further reproduction prohibited without permission.

$$\frac{d[NO_2^-]}{dt} = -k_5[NO_2^-] - k_6K_{60}[TFB][NO_2^-]^2 \quad (5\text{-}24)$$

$$\frac{d[NO_3^-]}{dt} = k_5[NO_2^-] + k_6K_{60}[TFB][NO_2^-]^2 \quad (5\text{-}25)$$

$$\frac{d[O_2]}{dt} = k_1[BrO_3^-] + \frac{1}{2}k_2K_{60}[TFB] + \frac{1}{2}k_3K_{50}[TFB] \quad (5\text{-}26)$$

$$\frac{d[H^+]}{dt} = k_3K_{50}[TFB] + 2k_5[NO_2^-] \quad (5\text{-}27)$$

Examination of the differential equations in EQN (5-21) through (5-27) show that for the case where nitrite is zero, the model describes the case of UV decomposition of a solution of bromate alone. The nomenclature used in the model is shown below:

y(1) = BrO_3^-	yprime(1)	=	$\frac{d[BrO_3^-]}{dt}$
y(2) = TFB	yprime(2)	=	$\frac{d[TFB]}{dt}$
y(3) = Br^-	yprime(3)	=	$\frac{d[Br^-]}{dt}$
y(4) = NO_2^-	yprime(4)	=	$\frac{d[NO_2^-]}{dt}$
y(5) = NO_3^-	yprime(5)	=	$\frac{d[NO_3^-]}{dt}$
y(6) = O_2	yprime(6)	=	$\frac{d[O_2]}{dt}$
y(7) = H^+	yprime(7)	=	$\frac{d[H^+]}{dt}$

Reproduced with permission of the copyright owner. Further reproduction prohibited without permission.

5.2 Runge-Kutta Numerical Method

The underlying idea of any numerical routine for solving boundary value problems is always to rewrite the dy/dt as finite steps Δy and Δt and multiply the equations by Δt (Kreyszig, 1983). This gives algebraic formulas for the change in the functions when the independent variable, t is stepped by one step size, h. Making the step size as small as mathematically possible ensures a good approximation to the true solution.

We consider the boundary value problem of the form:

$$y' = f(t,y), \qquad y(t_o)=y_o \tag{5-28}$$

Assuming f to be such that the problem has a unique solution on some interval containing t_o. The computation is started from $y_o = y(t_o)$ and proceeds in a stepwise manner. In the first step we compute an approximate value of y_1 of the solution y of (12) at $t = t_1 = t_o + h$. In the second step we compute an approximate value of y_2 at $t_2 = t_1+h$.

For the Runge-Kutta numerical method the solution takes the form of the expression in EQN (5-29):

$$y_{n+1} \approx y_n + \frac{1}{6}(K_1 + 2K_2 + 2K_3 + K_4) \tag{5-29}$$

It can be shown that the truncation error per step is of order h^5 (Collatz, 1966) and the

Reproduced with permission of the copyright owner. Further reproduction prohibited without permission.

method is therefore a fourth-order method. Four auxiliary quantities are computed in each step, K_1, K_2, K_3, K_4 and therefore in each step, the derivative is evaluated four times; once at the initial point (K_1), twice at midpoints (K_2, K_3), and once at trial endpoints(K_4).

$$K_1 = h f(t_n , y_n) \tag{5-30}$$

$$K_2 = h f(t_n + \frac{1}{2}h , y_n + \frac{1}{2}K_1) \tag{5-31}$$

$$K_3 = h f(t_n + \frac{1}{2}h , y_n + \frac{1}{2}K_2) \tag{5-32}$$

$$K_4 = h f(t_n + h , y_n + K_3) \tag{5-33}$$

The subroutines in the algorithm to describe bromate decay (**APPENDIX A**) have been adapted for the most part from from Press et al. (1992) and has been customized for this model. The algorithm has been organized into five levels. At the lowest level, there is the *algorithm* routine which implements the basic formulas of the method. It starts with dependent variables y_i at t, and returns new values of the dependent variables at the value t+h. It also provides information about the quality of the solution after each step. The routine, however, is unable to make decisions on the acceptability of the solution.

Reproduced with permission of the copyright owner. Further reproduction prohibited without permission.

That quality control decision is encoded is made by the *stepper* routine.It calls the algorithm routine and may reject the result, set a smaller step size and call the algorithm routine again, until compatibility with a predetermined accuracy criterion has been achieved. The principal function of the stepper is to take the largest step size consistent with the performance requirements specified by the user.

Above the stepper is the *driver* routine, which starts and stops integration, and stores intermediate results. Driver routines usually act as an interface with the user, but in the bromate decay routine, there is an *interface* routine which communicates with the user and passes the information on initial conditions to the driver routine.

Of the routines that follow, **rkck** is the algorithm routine, **rkqs** are the stepper routine and **odeint** is the driver routine. The interface routine was not coded as a subroutine and is therefore not named. It appears as the program code occurring before subroutine **odeint.** The subroutine **derivs** is a user supplied subroutine containing the system of differential equations derived for the model.

According to Press et al. (1992), a good differential equation integrator should be able to exert some measure of control over its progress, by making frequent changes to the step size. The function of this adaptive step size control is to achieve a predetermined accuracy with the minimum computational effort and result in gains in computational efficiency by factors of a hundred or more.

The most common form of adaptive step-size control is by step performing the

Reproduced with permission of the copyright owner. Further reproduction prohibited without permission.

computation simultaneously with step-size 2h (Press et al., 1992). This corresponds to increasing the truncation error by a factor of $2^5 = 32$, but since the number of steps decreases, the actual increase is by a factor of $2^5/2 = 16$. Hence the error of the first computation (with step h) equals about 1/15 times the difference,δ, of corresponding values of y (Kreyszig, 1983). We may now choose a number ϵ and leave h unchanged if $0.2\epsilon \leq |\delta| \leq 10\epsilon$, decrease h by 50% if $|\delta| > 10\epsilon$, and double h if $|\delta| < 0.2\epsilon$

The step size control routine used in **rkqs** is based on the embedded Runge-Kutta formulas developed by Fehlberg. For orders M higher than four, more than M function evaluations are required. However Fehlberg discovered a fifth order method with six function evaluations where another combination of the six functions gives a fourth order method. The difference between the two estimates of y(t+h) can then be used as an estimate of the truncation error to adjust the step size.

The general form of a fifth-order Runge-Kutta formula is

$$y_{n-1} = y_n + c_1K_1 + c_2K_2 + c_3K_3 + c_4K_4 + c_5K_5 + c_{6_6} + O(h^6) \qquad (5\text{-}34)$$

The embedded fourth-order formula is

$$y_{n-1}^{*} = y_n + c_1^{*}K_1 + c_2^{*}K_2 + c_3^{*}K_3 + c_4^{*}K_4 + c_5^{*}K_5 + c_6^{*}K_6 + O(h^5) \qquad (5\text{-}35)$$

and so the error estimate is

Reproduced with permission of the copyright owner. Further reproduction prohibited without permission.

$$\Delta \equiv y_{n+1} - y_{n+1}^{*} = \Sigma (c_i - c_i^{*}) K_i, \qquad i=1...6 \tag{5-36}$$

The particular values of the various constants used in **rkqs** are the Cash-Karp values (Cash and Karp, 1990).

To keep the error bounded we must examine the relationship between Δ and h. For a fourth-order method, Δ is of order h^5 . If a step h_1 is taken and produces an error Δ_1 , therefore the step h_0 that would have given some other value Δ_0 is estimated as the following (Press et al., 1992)

$$h_o = h_1 \left| \frac{\Delta_o}{\Delta_1} \right|^{0.2} \tag{5-37}$$

Δ_0 denotes the desired accuracy. EQN (5-37) is used in two ways: if Δ_1 is larger than Δ_0 in magnitude, the equation tells how much to decrease the stepsize when the failed step is retried. If Δ_1 is smaller than Δ_0 then the equation tells how much to safely increase the stepsize on the next try.

Reproduced with permission of the copyright owner. Further reproduction prohibited without permission.

CHAPTER 6

COMPARISON OF EXPERIMENTAL PROFILES AND MODEL PREDICTIONS FOR BROMATE SOLUTION

This chapter compares the experimentally derived species profiles for the bromate alone experiments with the species profiles predicted by the bromate decomposition kinetic model developed in Chapter 5.

The kinetic model was first calibrated with one experiment from each of the four UV intensities used in the study. Therefore a total of four calibration experiments were used. Selection of calibration experiments was based on smoothness of the experimental profiles and good balance of bromine species as defined by EQN (4-1). The initial experimental conditions of each of the four calibration experiments were used as input into the kinetic model and the values of the observed rate constants of k_1 through k_4 adjusted slightly to give a reasonably good fit between experimental profiles and kinetic model predictions. The calibrated model was then used to predict the concentration of reactants and products for other experiments. The experimental conditions of each experiment being modeled were used as initial conditions to run the model.

The kinetic model predictions for each of the experiments were plotted on the graph with the experimental profiles using EASYPLOT (Spiral Software,

Reproduced with permission of the copyright owner. Further reproduction prohibited without permission.

Massachussets Institute of Technology, MA). The kinetic model predictions for over twenty experiments are presented in this chapter.

6.1 Comparison of Profiles for Intensity of 2.61 x 10^{-6} Einstein L^{-1} s^{-1}

Figure 6.1 is the calibration experiment used for experiments with UV light intensity of 2.61 x 10^{-6} Einstein L^{-1} s^{-1}. The bromate concentration was 0.037 mM (3 mg/L) and the pH was 8.27. The figure shows a slight deviation in the bromide concentration between model and experiment during the first ten minutes. The bromate profile fits the experimental profiles well until it deviates slightly after 20 minutes reaction time. The free bromine profiles agrees reasonably well with the experimental profiles for the duration of the experiment.

Figures 6.2 through 6.4 present comparisons of some of the experimental data with the model predictions for experiments with similar UV light intensity as in Figure 6.1. The comparisons show good qualitative agreement between the experimental data and the model predictions. The concentration of free bromine in solution and the reaction time to achieve maximum concentration increases for higher initial bromate concentration, as found experimentally. The model also confirms the experimental finding that the decomposition of bromate is relatively independent of initial reaction pH. A change in pH from the calibration pH of 8.27 (Figure 6.1) to 9.47 (Figure 6.3) has little or no impact on model output.

Reproduced with permission of the copyright owner. Further reproduction prohibited without permission.

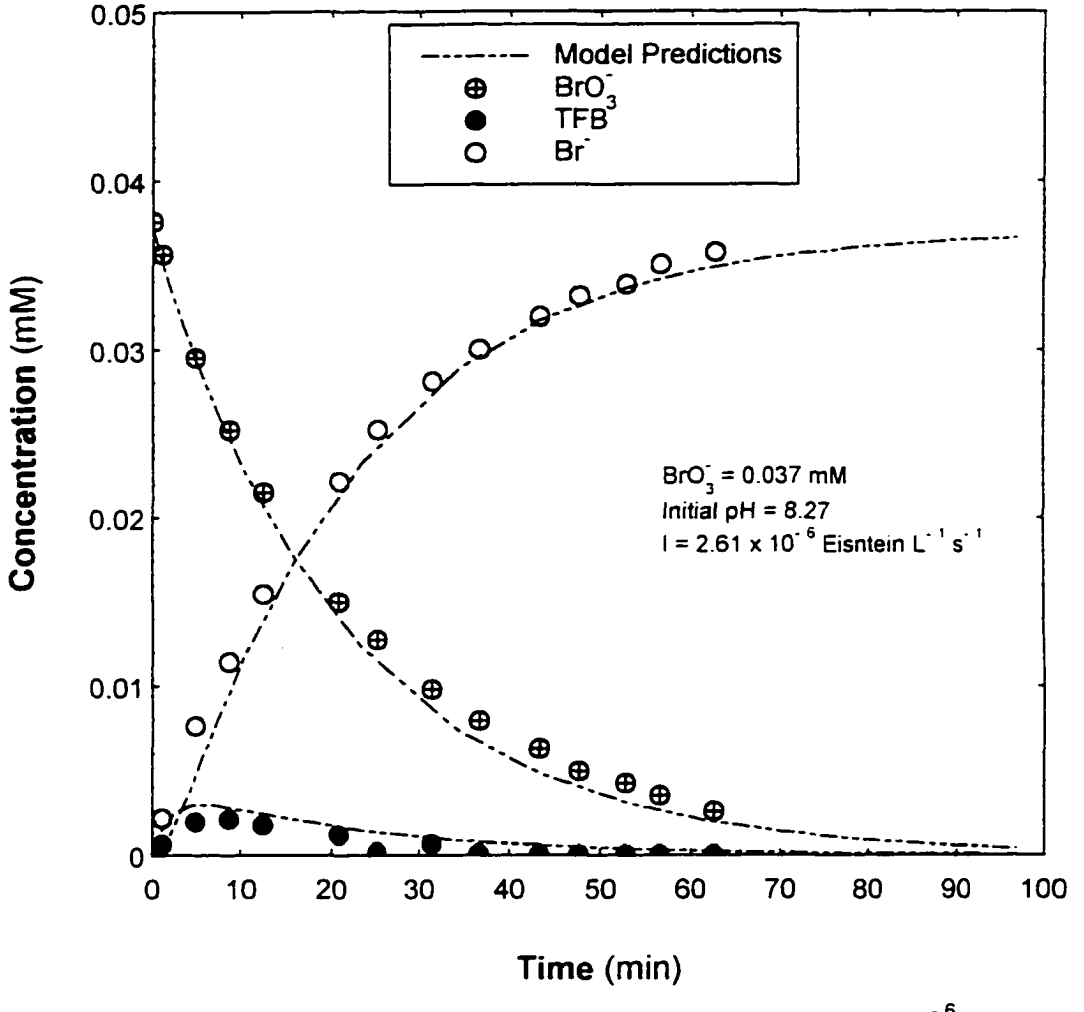

Figure 6.1. Calibration of Kinetic Model for UV Light Intensity of 2.61×10^{-6} Einstein / L*s (EXP 61).

Reproduced with permission of the copyright owner. Further reproduction prohibited without permission.

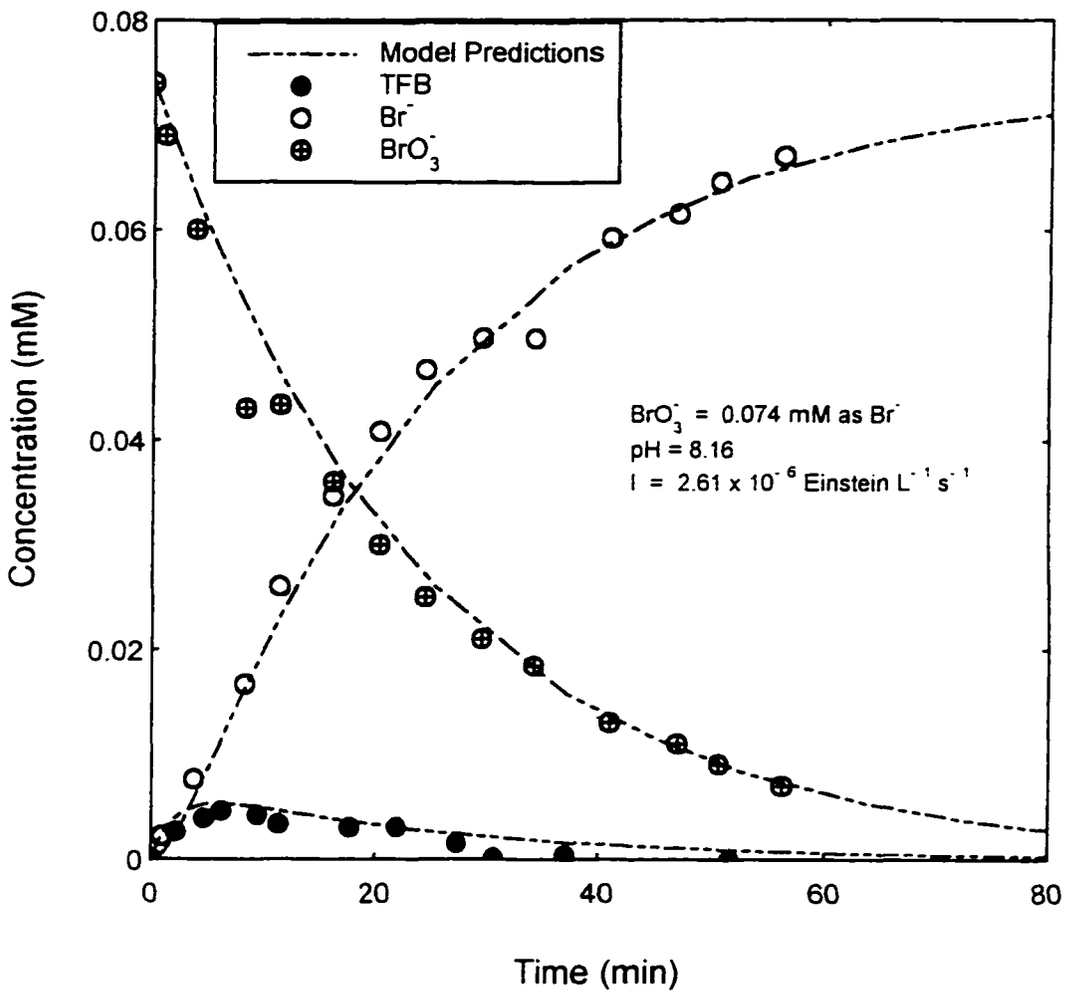

Figure 6.2. Comparison of Experimental Profiles and Kinetic Model Predictions (EXP 2)

Reproduced with permission of the copyright owner. Further reproduction prohibited without permission.

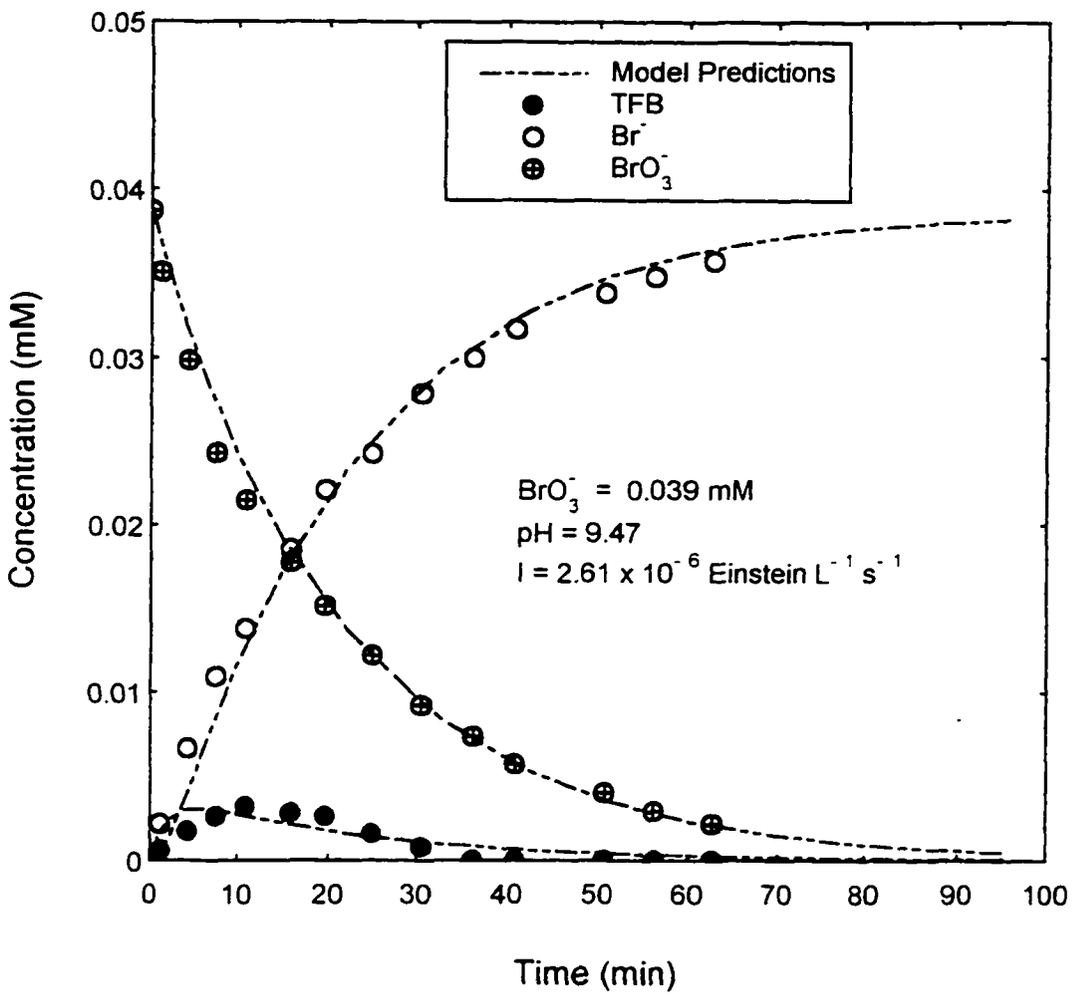

Figure 6.3. Comparison of Experimental Profiles and Kinetic Model Predictions (EXP 60).

Reproduced with permission of the copyright owner. Further reproduction prohibited without permission.

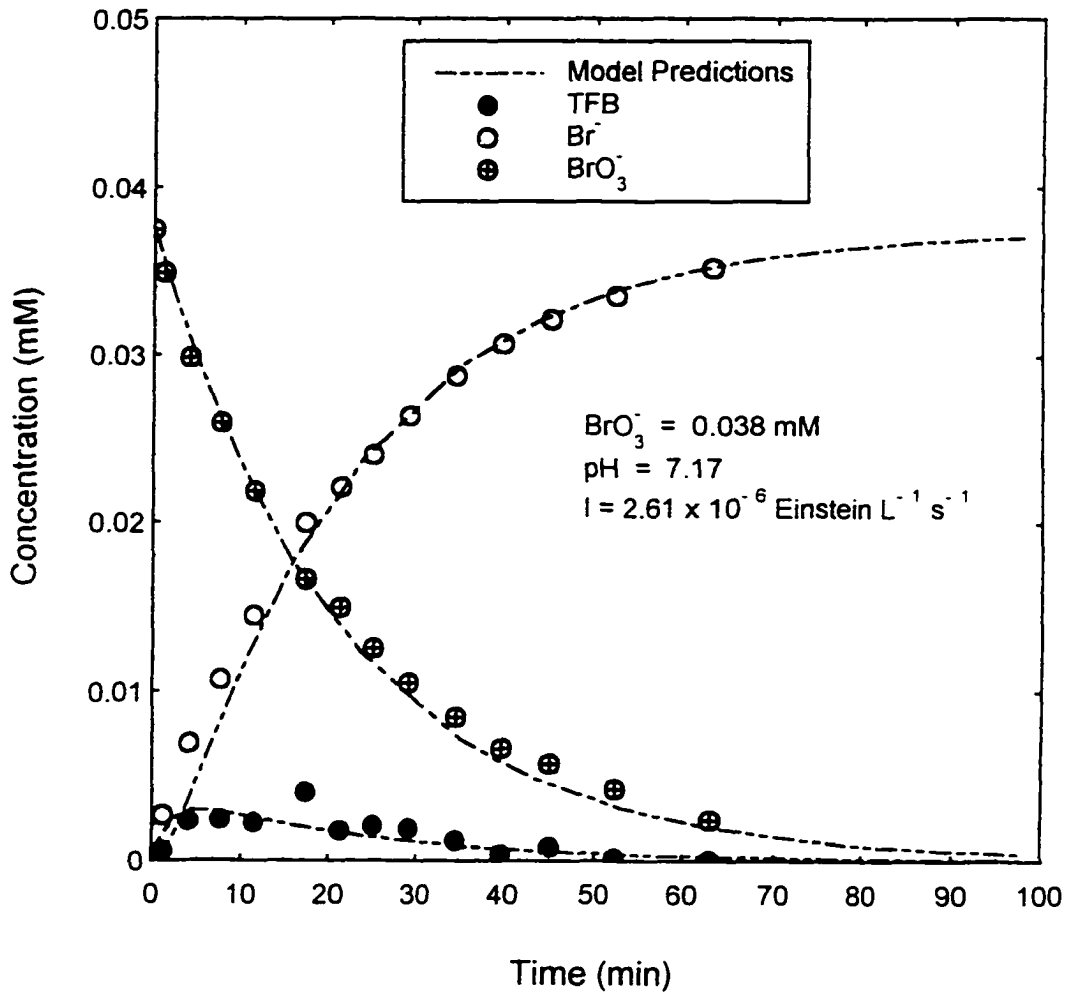

Figure 6.4. Comparison of Experimental Profiles and Kinetic Model Predictions (EXP 62).

Reproduced with permission of the copyright owner. Further reproduction prohibited without permission.

6.2 Comparison of Profiles for Intensity of 1.15 x 10^{-6} Einstein L^{-1} s^{-1}

The calibration of the kinetic model for the a UV light Intensity of 1.15 x 10^{-6} Einstein L^{-1} s^{-1} is shown in Figure 6.5. The bromate concentration of 0.0671 mM (5.4 mg/L) in the calibration experiment is much higher than in the experiments depicted above. The fitting of the model and the experimental profiles proved most difficult in the first 30 minutes of the experiment for bromate, bromide and free bromine. The fit between model and experiment was reasonable after that period.

Comparison of the experimental data and the model predictions in Figure 6.6 at approximately half the bromate concentration than in the calibration experiment shows good fit with the bromate profile. The bromide and free bromine profile on the other hand indicates that a larger value of k_2 and k_3 is required for a better fit. Recall that these rates govern the conversion of free bromine to bromide.

In Figure 6.7, for an initial bromate concentration of 0.0375 mM, the bromate and bromide profiles are in good agreement with the experimental profiles. However, model prediction of free bromine is in excess of that observed experimentally. Free bromine undergoes competitive reactions. It is produced by the decomposition of bromate and removed by its photodecomposition under UV irradaition. At lower UV light intensities, the residual free bromine concentration in solution will be low since bromate decomposition is slowed compared to the higher intensity. Its rate of decay may be higher at lower concentrations than at higher concentrations. The model does

Reproduced with permission of the copyright owner. Further reproduction prohibited without permission.

not take into account this apparent concentration effect and may explain the deviations in the predicted and experimental profiles.

Figures 6.8 shows the comparisons for initial bromate of 0.0118 mM. The model predicts a higher rate of bromate decomposition than found experimentally. The fit worsens for lower bromate concentrations. Figure 6.9 shows the comparison for an initial bromate of 0.0068 mM, almost halved that from the previous figure. The fit of all species deviates markedly from the experimental profiles. Only one experiment at this concentration was performed for each UV light intensity and the existence of a concentration dependence of bromate decay may account for the deviation between model and experiment.

Figure 6.10 shows the comparisons of an experiment similar to the one used for calibration. In the initial stages (<30 min), the model prediction for bromate and bromide agrees well with the experimental but diverge slightly thereafter. The model slightly overpredicts the free bromine concentration in the first 10 minutes of the experiments approaches it between 10 and 20 minutes and slightly over-predicts it again thereafter.

Reproduced with permission of the copyright owner. Further reproduction prohibited without permission.

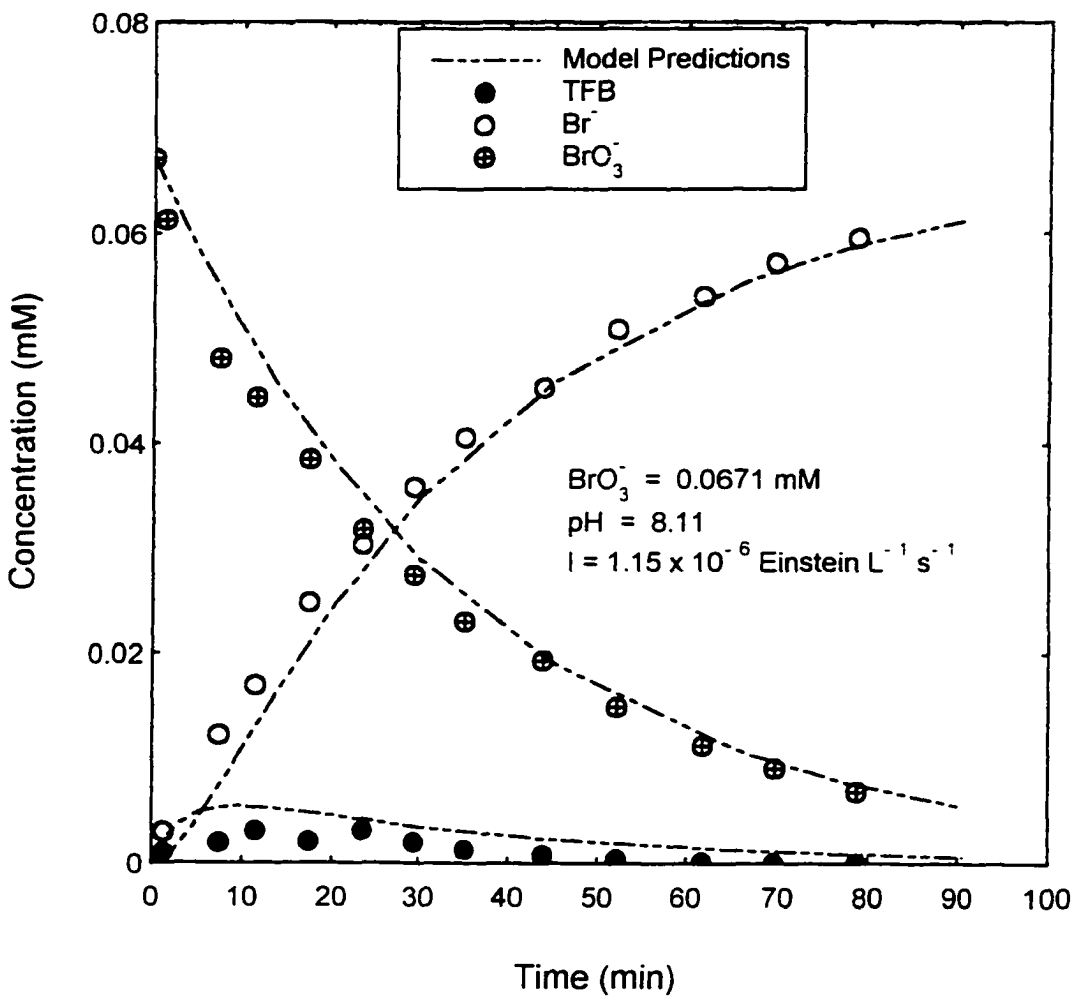

Figure 6.5. Calibration of Kinetic Model for UV Light Intensity of 1.15×10^{-6} Einstein/L*s (EXP 96).

Reproduced with permission of the copyright owner. Further reproduction prohibited without permission.

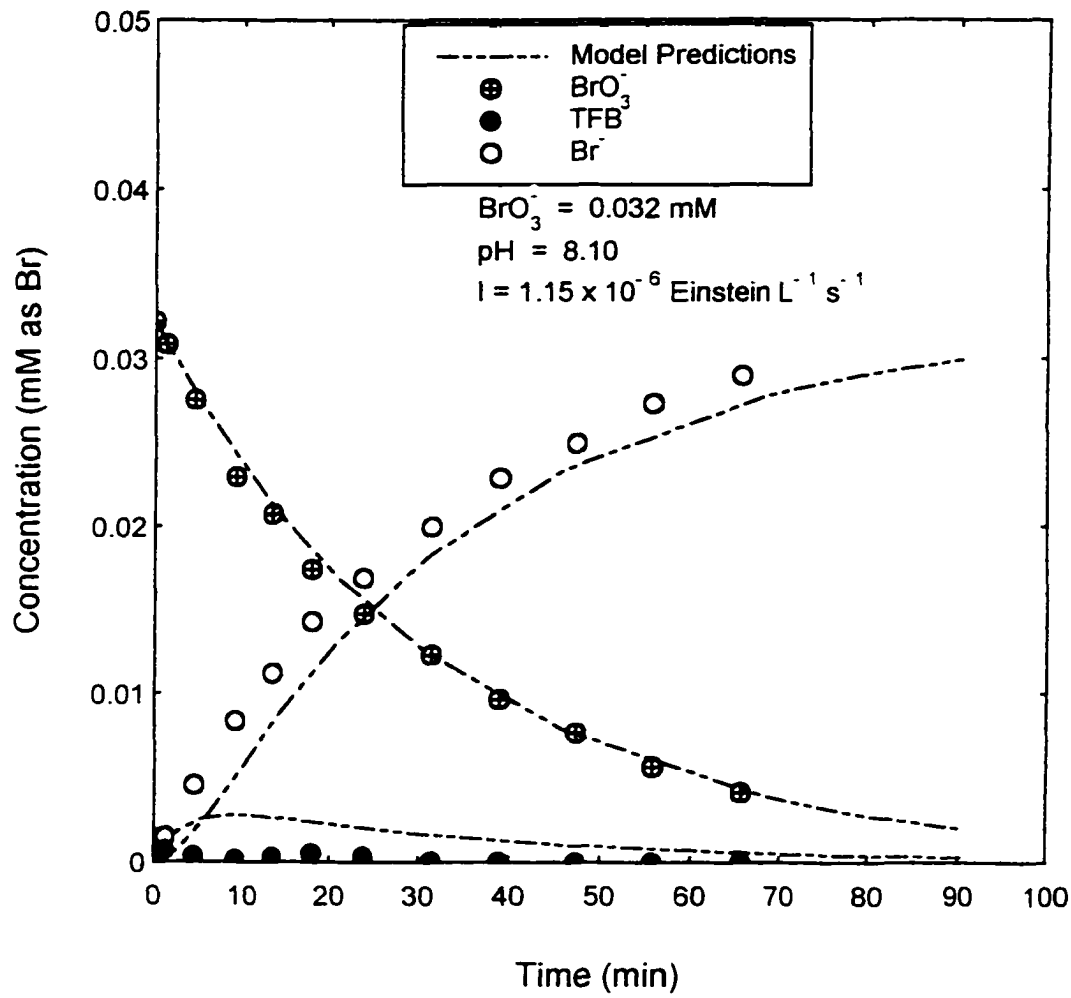

Figure 6.6. Comparison of Experimental Profiles and Kinetic Model Predictions (EXP 97).

Reproduced with permission of the copyright owner. Further reproduction prohibited without permission.

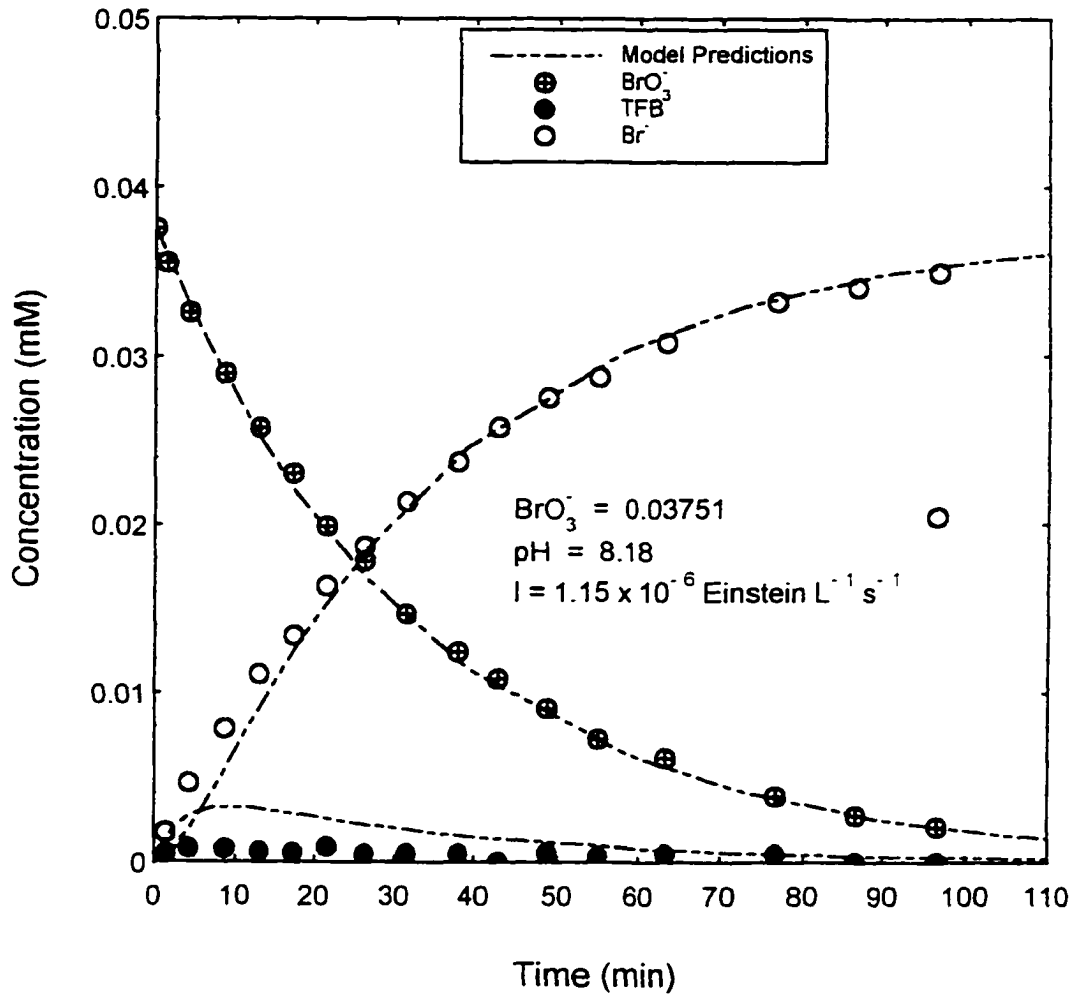

Figure 6.7. Comparison of Experimental Profiles and Kinetic Model Predictions (EXP 29).

Reproduced with permission of the copyright owner. Further reproduction prohibited without permission.

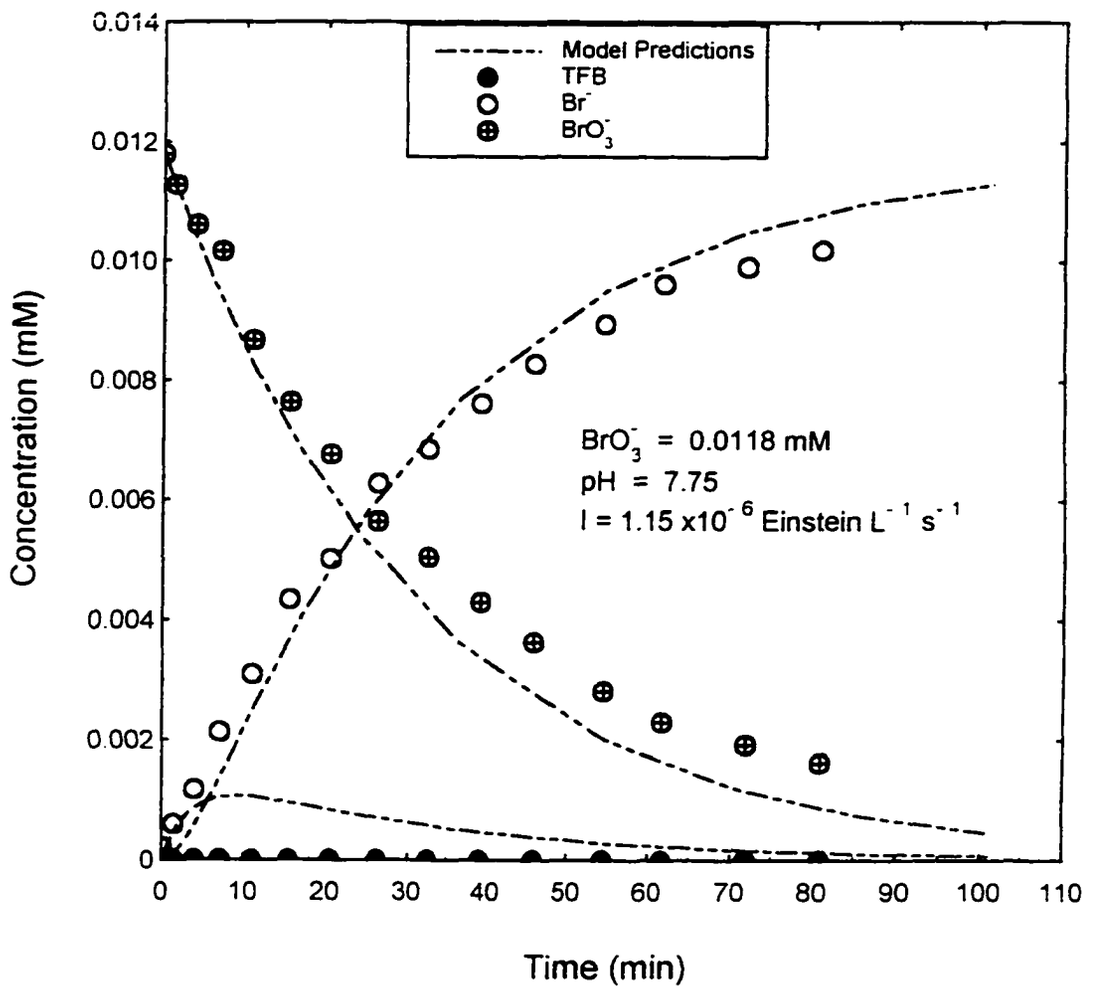

Figure 6.8. Comparison of Experimental Profiles and Kinetic Model Predictions (EXP 39).

Reproduced with permission of the copyright owner. Further reproduction prohibited without permission.

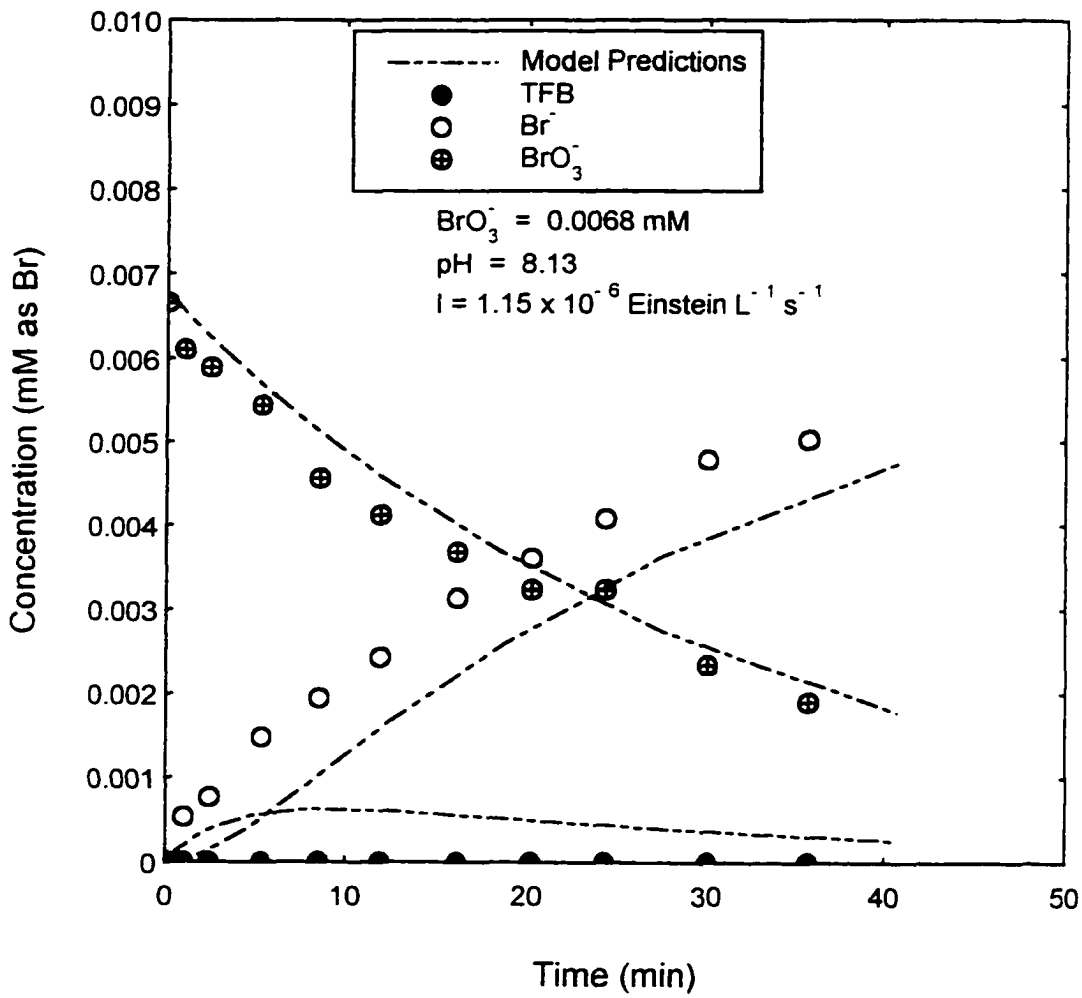

Figure 6.9. Comparison of Experimental Profiles and Kinetic Model Predictions (EXP 98).

Reproduced with permission of the copyright owner. Further reproduction prohibited without permission.

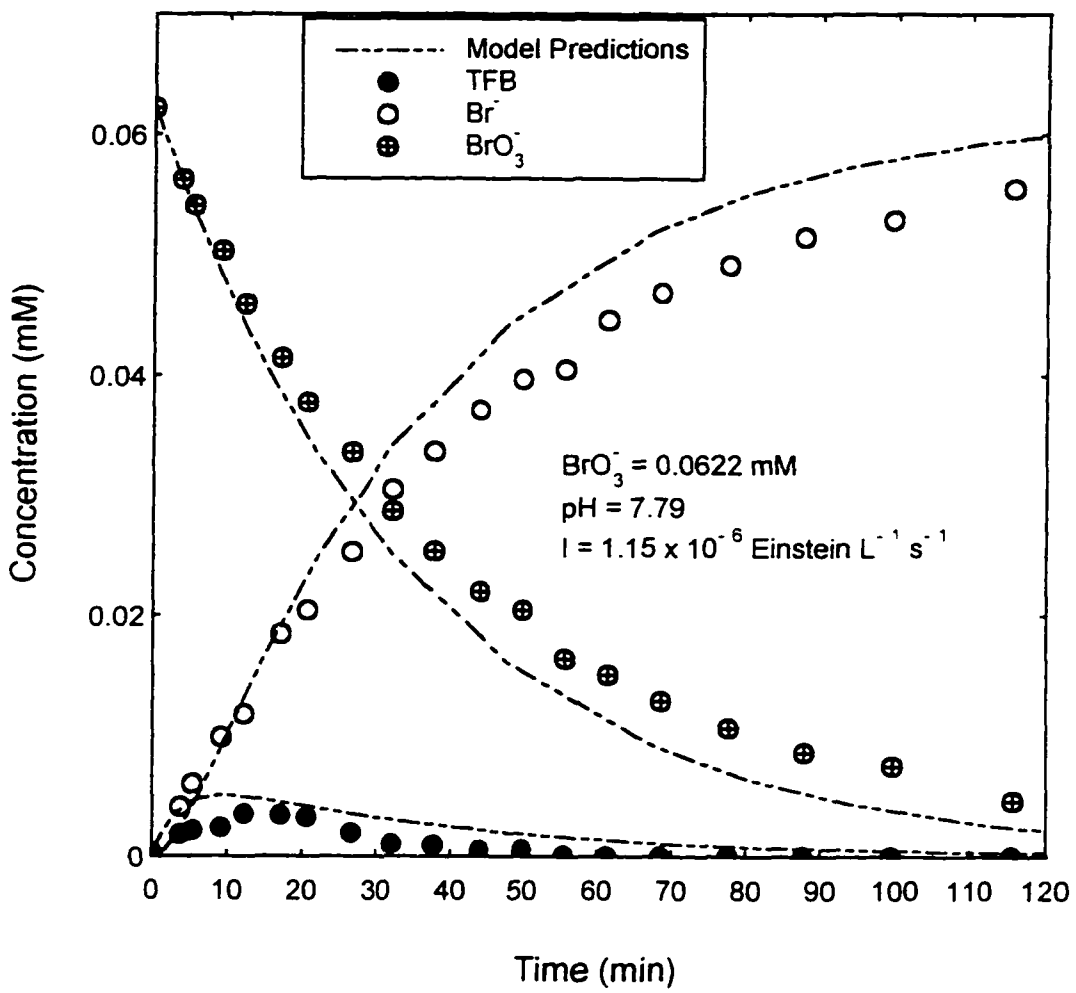

Figure 6.10. Comparison of Experimental Profiles and Kinetic Model Predictions (EXP 37).

Reproduced with permission of the copyright owner. Further reproduction prohibited without permission.

6.3 Comparison of Profiles for Intensity of 4.35 x 10^{-7} Einstein L^{-1} s^{-1}

Calibration of the kinetic model for a UV intensity of 4.35 x 10^{-7} Einstein L^{-1} s^{-1} is shown in Figure 6.11. Calibration provided a good fit with bromate and bromide profiles. The model overpredicted the free bromine concentration for the entire reaction period.

Figure 6.12 and 6.13 shows comparisons for bromate experimental conditons similar to those used in the calibration experiment in Figure 6.11. Both experiments show good qualitative agreement between the model predictions and the experimental profiles. The free bromine profile, though the model predicted free bromine conentrations exceeds that found experimentally. Again the same argument as was made in the previous experiments are valid here as well. Of import is the fact that the experiments depicted in Figure 6.12 and Figure 6.13 were performed approximately one year apart. The fact that model fits both experiments reasonably well, highlights the reproducibility of the experimental results.

For initial bromate concentrations greater than the calibration level the model shows good agreement with the experimental data (Figure 6.14). Figure 6.15 shows the comparisons for an initial bromate slightly less than that used in the calibration experiment. Again good fit is shown between the model output and the experimental data. However at much lower concentrations the model profiles and the experimental profiles deviate (Figure 6.16). This was also seen in the previous set of experiments at

Reproduced with permission of the copyright owner. Further reproduction prohibited without permission.

a UV intensity of 1.15 x 10^{-6} Einstein L^{-1} s^{-1}. The case of the intial bromate concentration of approximately 0.0067 mM (0.5 mg/L) appears to be the limiting case for the model.

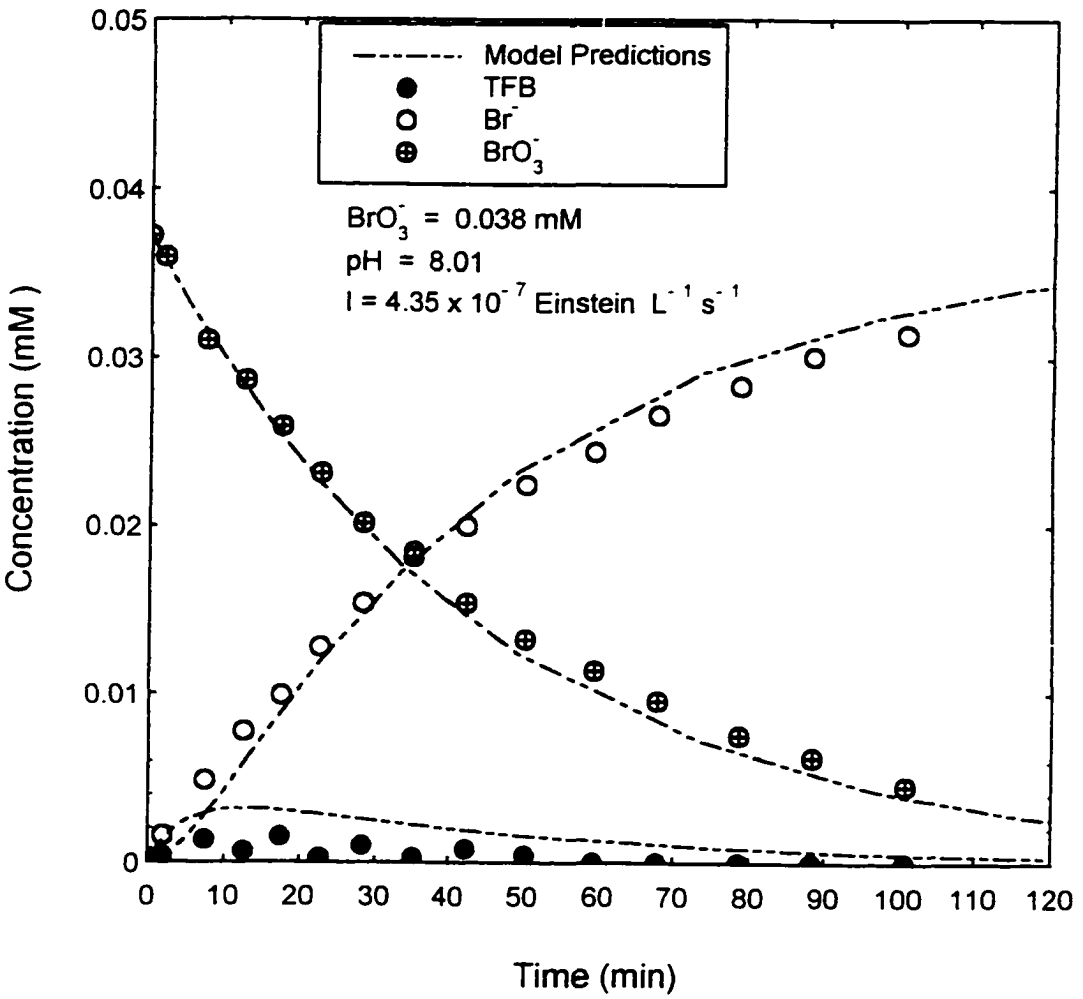

Figure 6.11. Calibration of Kinetic Model for UV Light Intensity of 4.35 x 10^{-7} Einstein / L*s (EXP 88).

Reproduced with permission of the copyright owner. Further reproduction prohibited without permission.

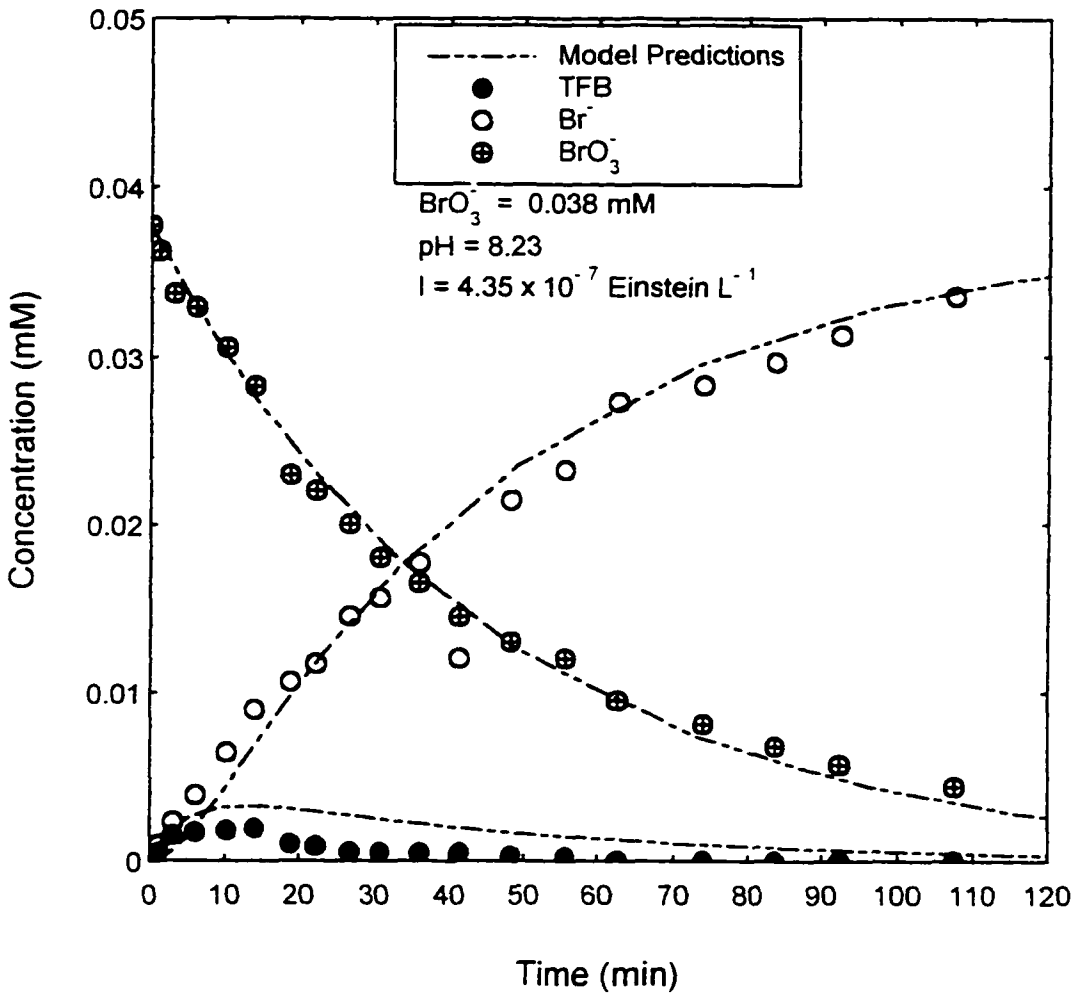

Figure 6.12. Comparison of Experimental Profiles and Kinetic Model Predictions (EXP 12).

Reproduced with permission of the copyright owner. Further reproduction prohibited without permission.

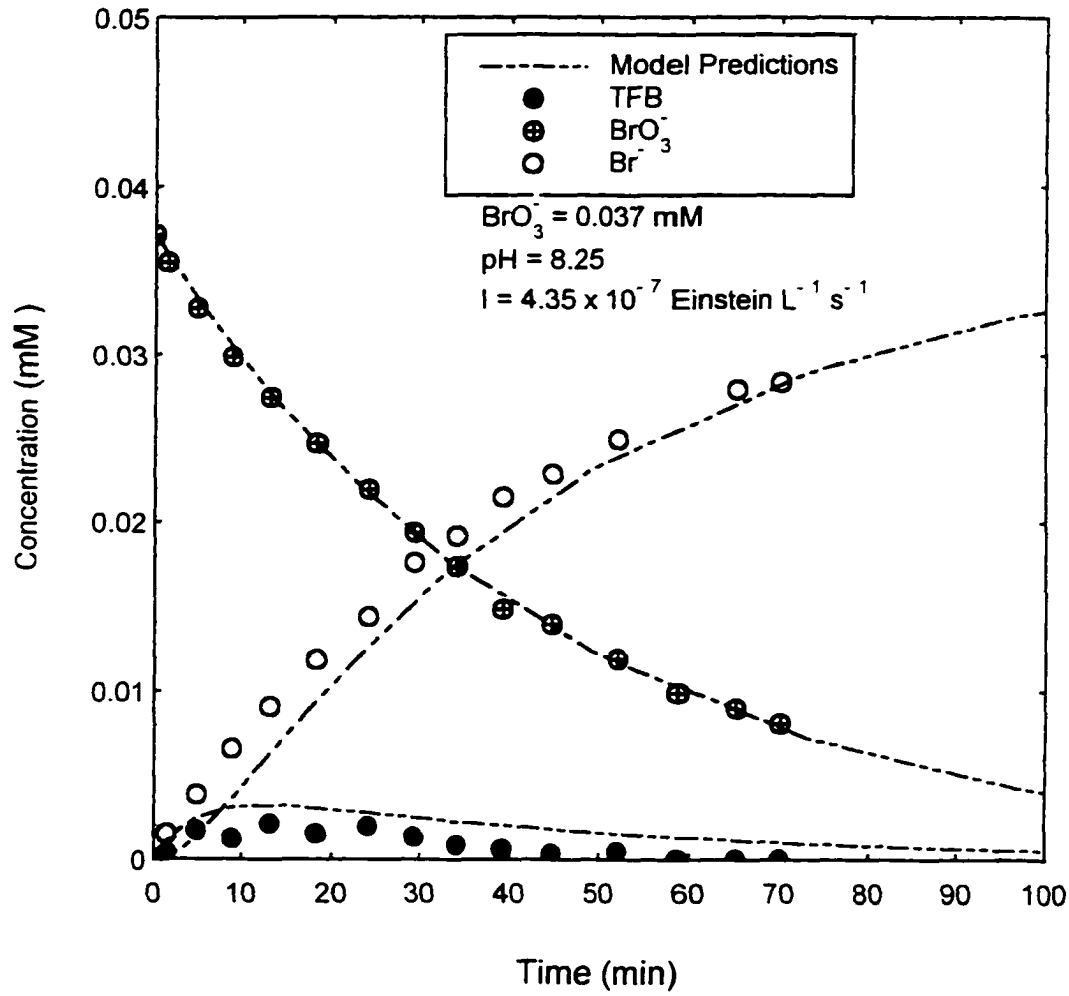

Figure 6.13. Comparison of Experimental Profiles and Kinetic Model Predictions (EXP 77).

Reproduced with permission of the copyright owner. Further reproduction prohibited without permission.

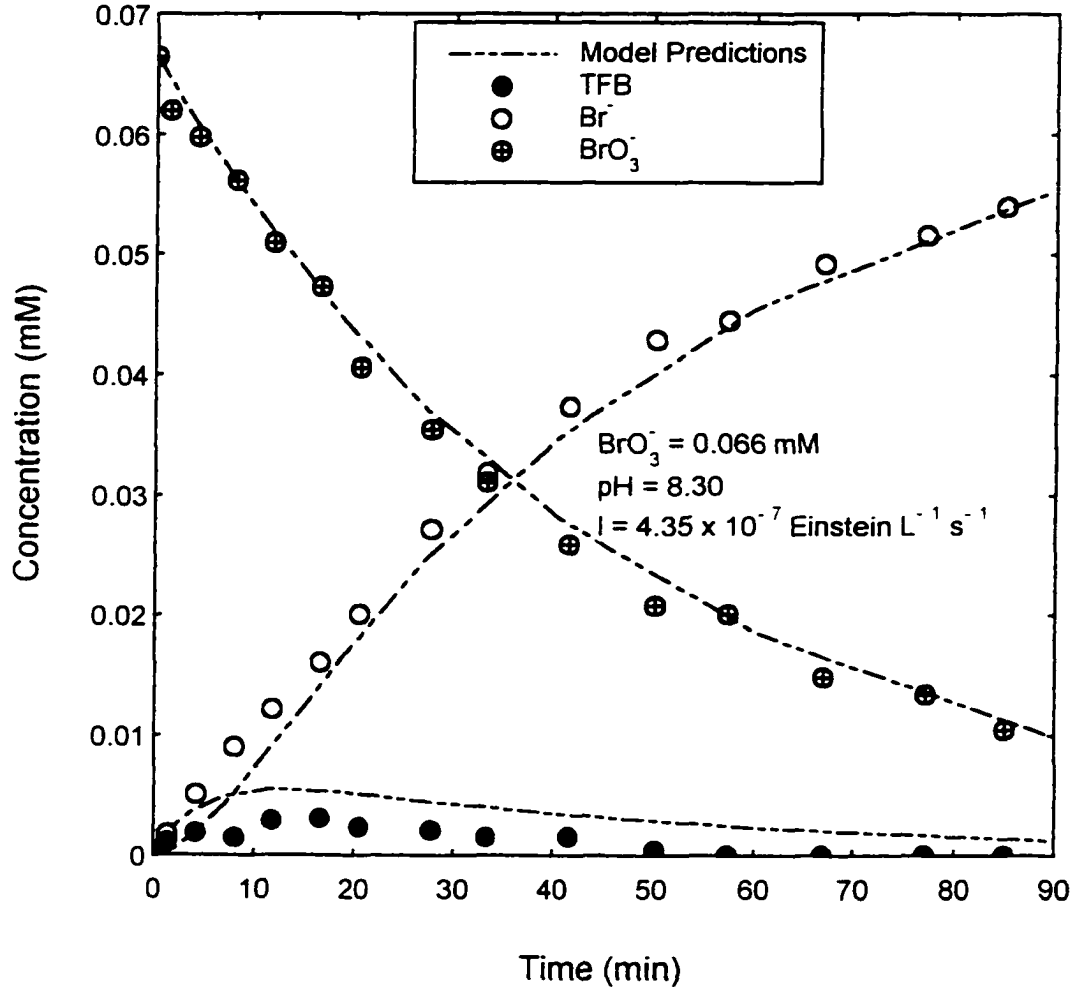

Figure 6.14. Comparison of Experimental Profiles and Kinetic Model Predictions (EXP 99).

Reproduced with permission of the copyright owner. Further reproduction prohibited without permission.

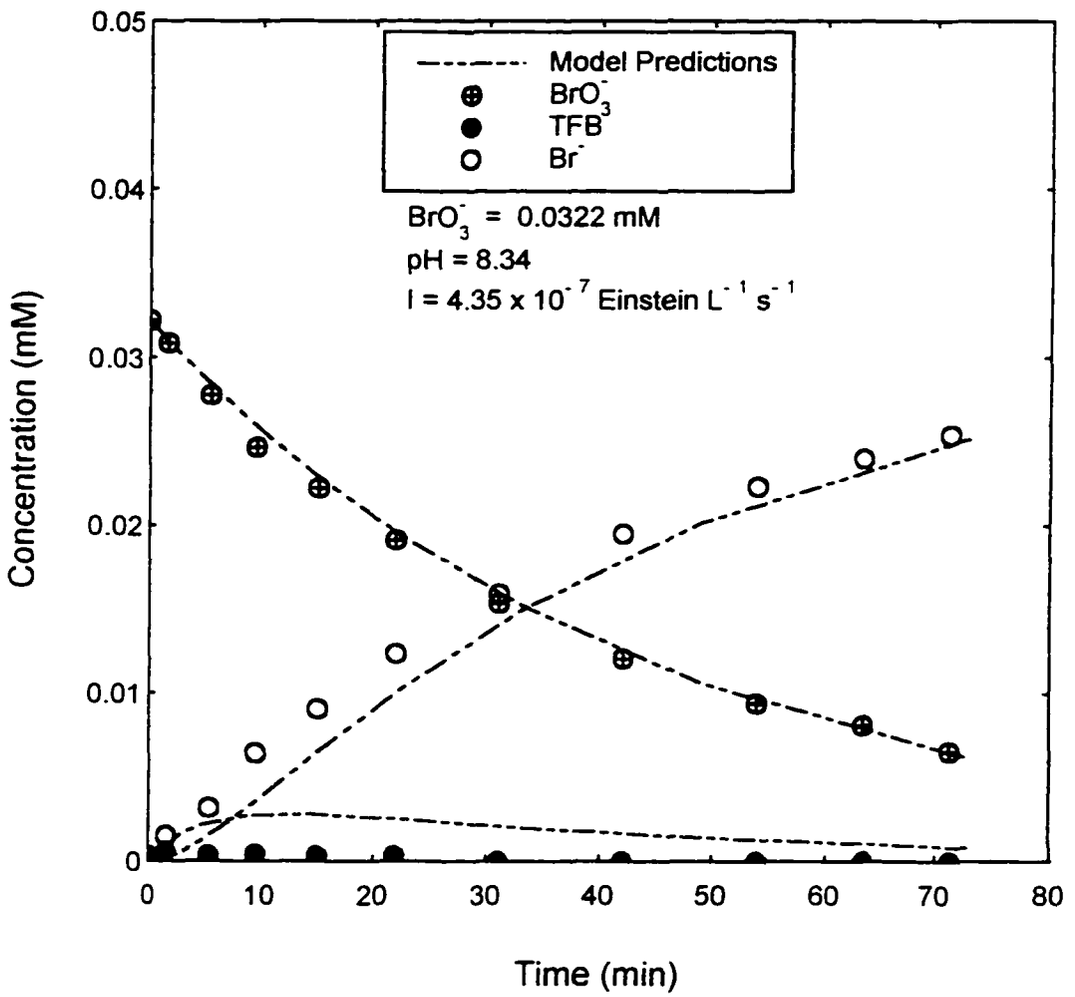

Figure 6.15. Comparison of Experimental Profiles and Kinetic Model Predictions (EXP100).

Reproduced with permission of the copyright owner. Further reproduction prohibited without permission.

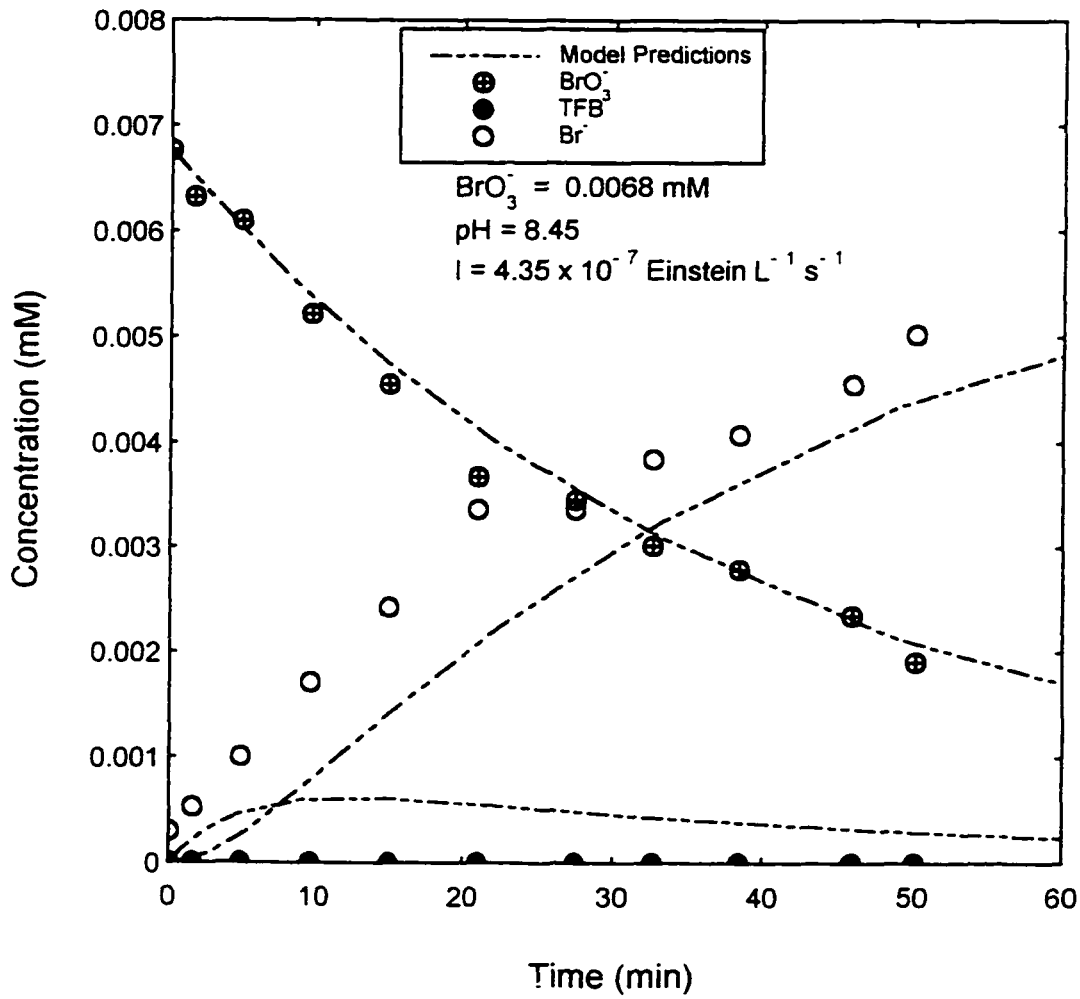

Figure 6.16. Comparison of Experimental Profiles and Kinetic Model Predictions (EXP 101).

Reproduced with permission of the copyright owner. Further reproduction prohibited without permission.

6.4 Comparison of Profiles for Intensity of 2.30 x 10^{-7} Einstein L^{-1} s^{-1}

Calibration of the kinetic model for a UV light intensity of 2.30 x 10^{-7} Einstein L^{-1} s^{-1} is shown in Figure 6.17. The bromate concentration was 0.037 mM (3 mg/) and the initial pH was 8.17. Calibration provided good fit between the bromate and bromide experimental profiles and the kinetic model predictions. The model gave a slightly higher free bromine concentration than observed experimentally.

Figure 6.18 shows the comparison for pH of 7.14. The model and the experiment are in good agreement for about 50 minutes of reaction time whereafter the profiles diverge slightly. At the higher pH value (Figure 6.19) the bromate and bromide profile are in good agreement. Though the model predicts higher free bromine than determined experimentally, the fits appear to be better than in the previous sets of experiments. This was acheived by changing the value of k_2 and k_3 slightly to remove free bromine at a faster rate and yet produce a good fit for all the species. The lower UV intensity allows more freedom in the choise of these values. For higher intensities, a slight change in k_2 and k_3 can have a more pronounced effect on the fit of the model.

Increasing the initial bromate produces relatively tight fits between the model and the experimental profiles (Figure 6.20). Decreasing the bromate level slightly from that used in the calibration equation still produces good agreement between the experimental and the model predictions (Figure 6.21). At initial bromate concentratrion of approximately 0.0067 mM (0.5 mg/L) in Figure 6.22, the model is in good

Reproduced with permission of the copyright owner. Further reproduction prohibited without permission.

agreement until approximately 40 minutes of reaction time and diverges deviates slightly thereafter. It appears that more experimental data at levels below 0.5 mg/L will be useful to calibrate the model more efficiently for low level bromate analysis.

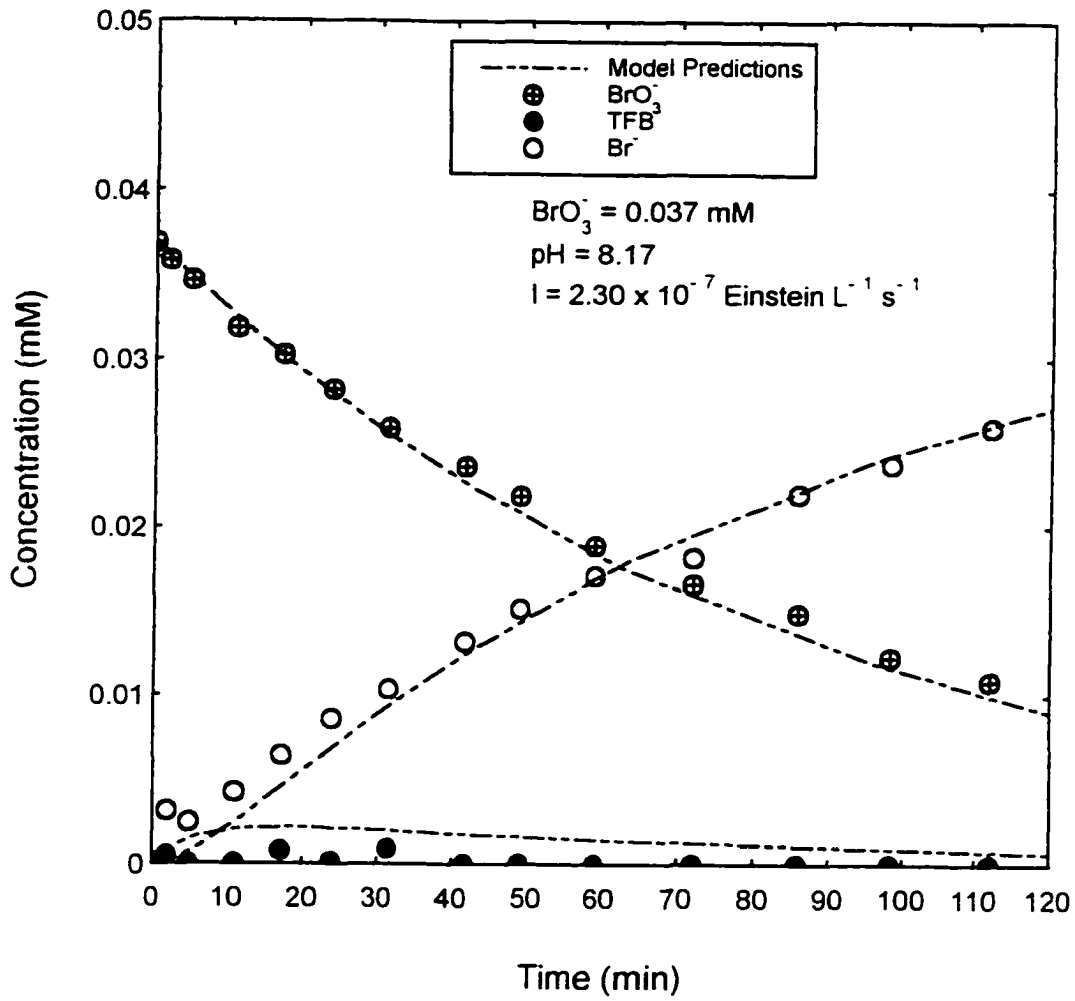

Figure 6.17. Calibration of Kinetic Model for UV Light Intensity of 2.30 x 10^{-7} Einstein / L*s (EXP 82).

Reproduced with permission of the copyright owner. Further reproduction prohibited without permission.

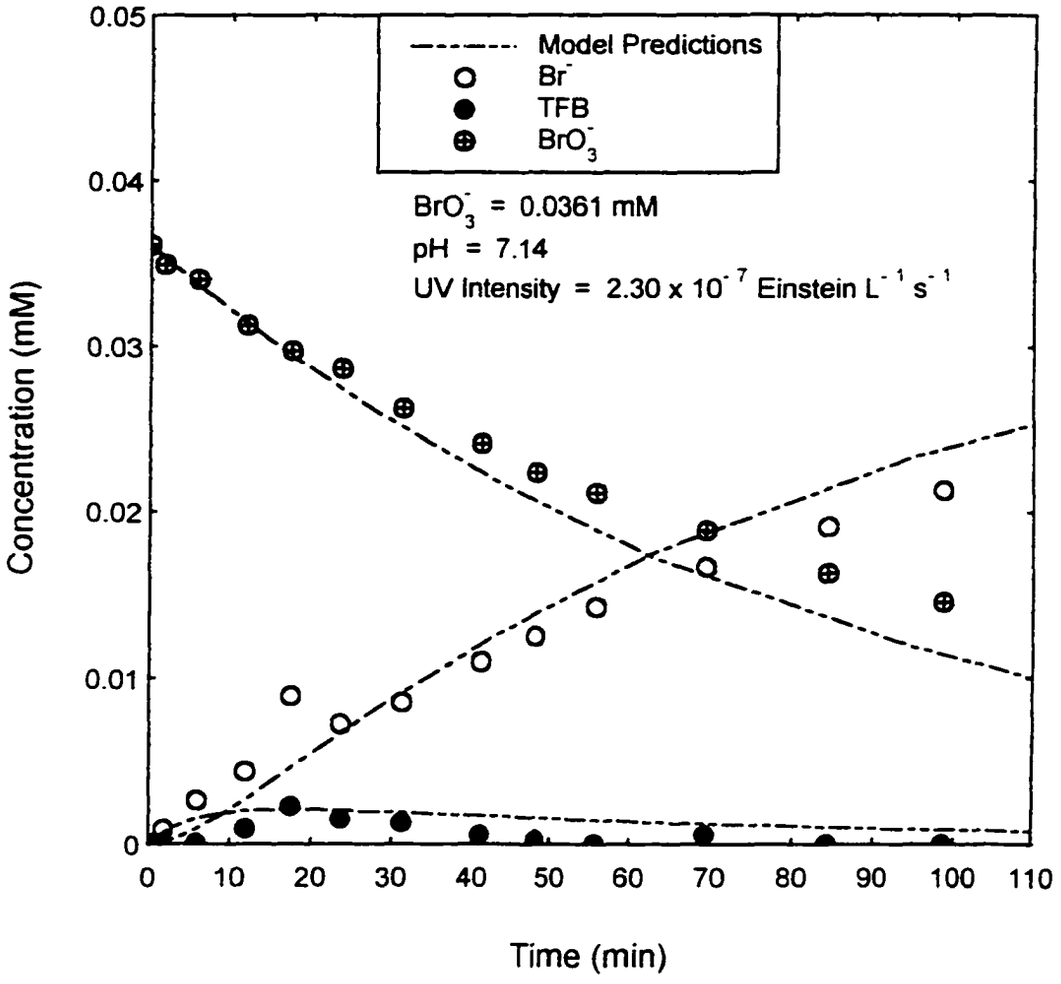

Figure 6.18. Comparison of Experimental Profiles and Kinetic Model Predictions (EXP83).

Reproduced with permission of the copyright owner. Further reproduction prohibited without permission.

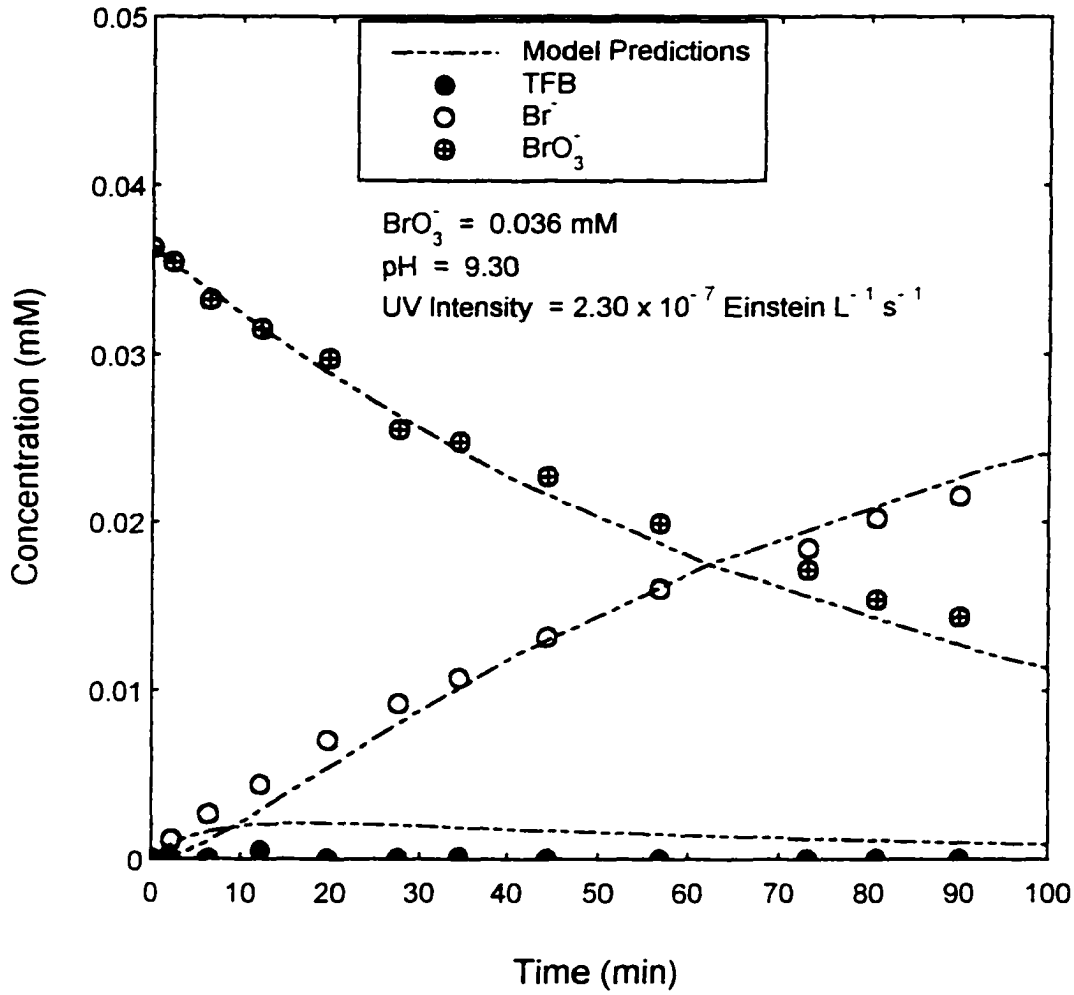

Figure 6.19. Comparison of Experimental Profiles and Kinetic Model Predictions (EXP 84).

Reproduced with permission of the copyright owner. Further reproduction prohibited without permission.

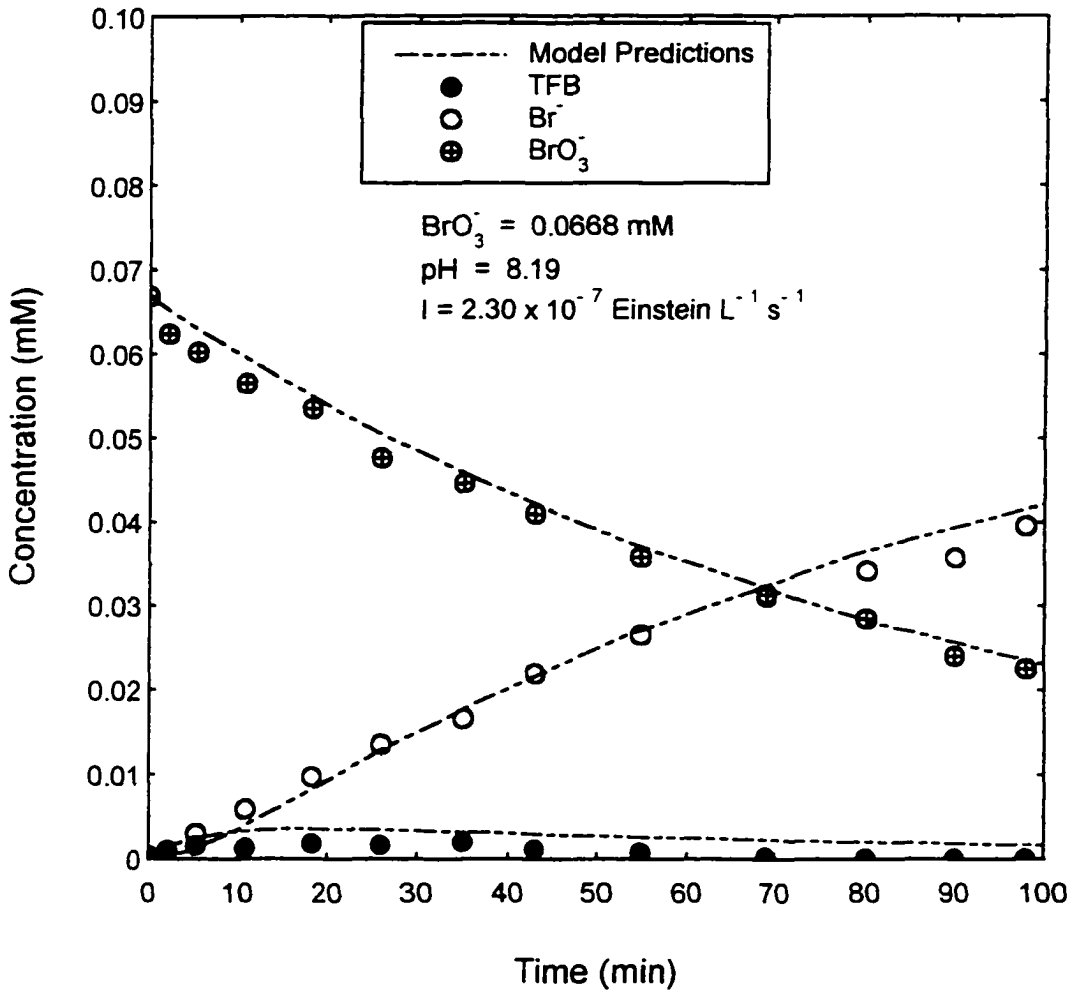

Figure 6.20. Comparison of Experimental Data and Kinetic Model Predictions (EXP102).

Reproduced with permission of the copyright owner. Further reproduction prohibited without permission.

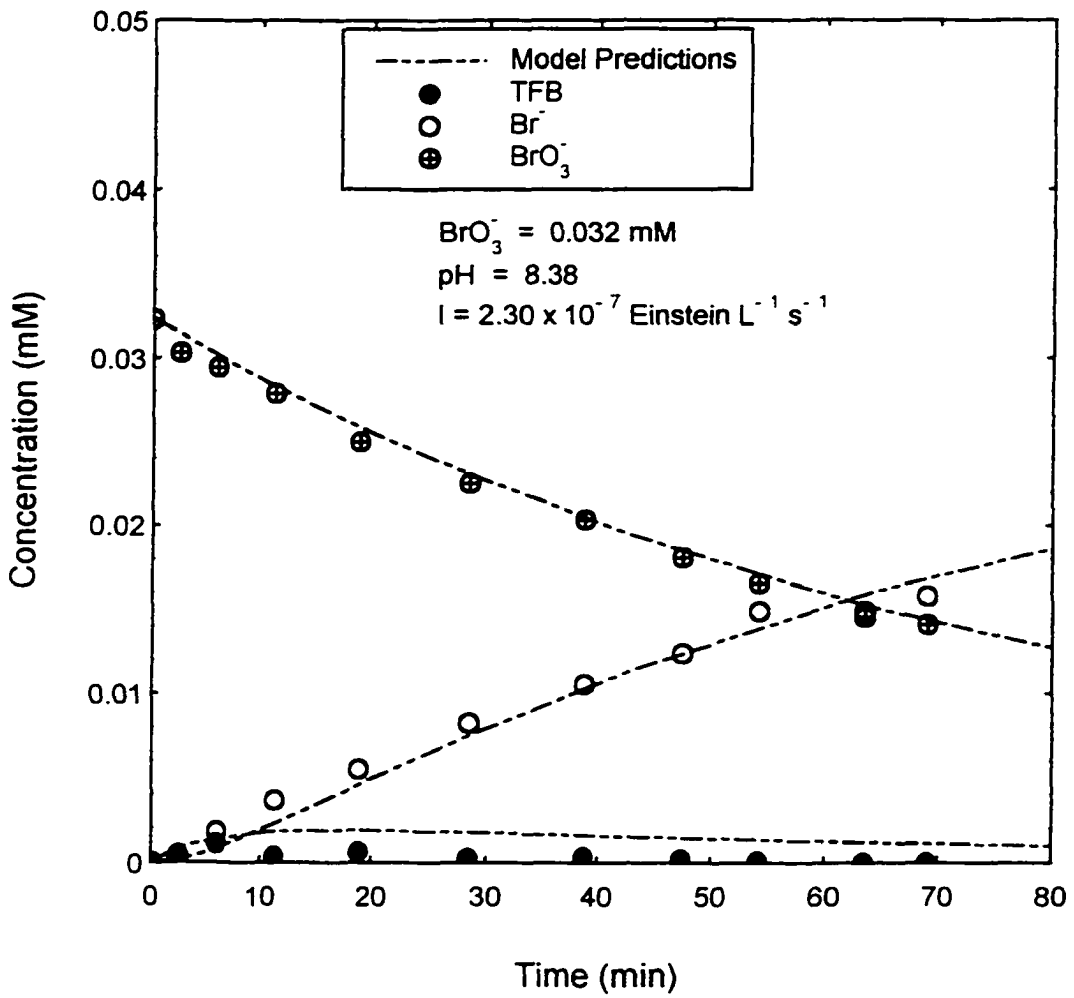

Figure 6.21. Comparison of Experimental Profiles and Kinetic Model Predictions (EXP 103).

Reproduced with permission of the copyright owner. Further reproduction prohibited without permission.

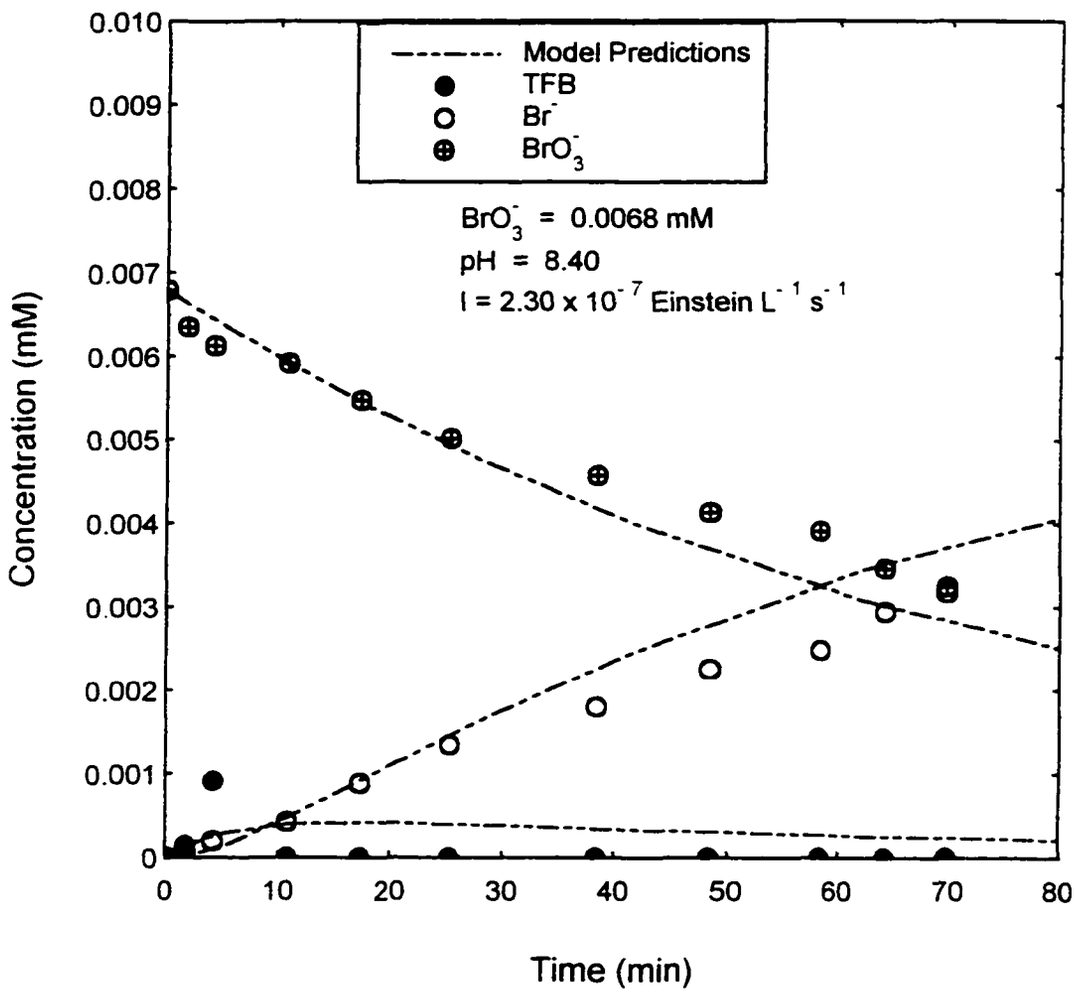

Figure 6.22. Comparison of Experimental Profiles and Kinetic Model Predictions (EXP 104).

Reproduced with permission of the copyright owner. Further reproduction prohibited without permission.

6.5 Summary

This section presents a comparison of the bromate decay rate constants from the bromate alone experimental observations and that used in calibrating the bromate decay kinetic model for the four UV light intensities used in this study.

The values of the rate constants (k_1, k_2, k_3, k_4) used in calibrating the kinetic model for the bromate alone cases are shown as a function of UV light intensity in Table 6.1. The observed rate constant could be regenerated by multiplying each value by the corresponding UV light intensity. The data shows that the value of the bromate

Table 6.1. Rate Constants Used in Calibration of Bromate Alone Kinetic Model.

# UV Lamps	I Einstein / L*min	k_1 L/Einstein	k_2 L/Einstein	k_3 L/Einstein	k_4 L/Einstein
16	1.57×10^{-4}	3.38×10^{2}	2.30×10^{3}	2.87×10^{3}	0.19×10^{2}
12	6.90×10^{-5}	4.78×10^{2}	2.90×10^{3}	3.77×10^{3}	0.36×10^{2}
8	2.61×10^{-5}	1.02×10^{3}	6.03×10^{3}	7.45×10^{3}	0.77×10^{2}
4	1.38×10^{-5}	1.09×10^{3}	7.72×10^{3}	9.25×10^{3}	1.09×10^{2}

decay rate constant, k_1, is almost an order of magnitude less than the free bromine decay constants, k_2 and k_3, and more than an order of magnitude greater than the bromate formation constant from free bromine disproportionation, k_4. The experimental apparatus used by Siddiqui et al. (1996) was more efficient in the transfer of UV light to the solution phase than the reactor used in this study, and the observed bromate decay rate found in their study was more than an order of magnitude greater than found here. The experimental values of the observed bromate decay rate from this study were

Reproduced with permission of the copyright owner. Further reproduction prohibited without permission.

used as a *first try* in the kinetic model and then adjusted to give a good fit with the species profiles of the experiments used for calibration. The literature did not show any values for k_2 and k_3 under similar experimental conditions at 254 nm. The values observed during UV decomposition of free bromine in this study were used to calibrate the model. Trial and error was used in determining k_4 to calibrate the model.

A comparison of the experimentally derived bromate decay rate constants with that from the calibration of the kinetic model for the four UV light intensities is shown in Table 6.2 and Table 6.3. Column (2) through (4) represent initial conditions for each experiment. Column (5) represents the bromate decay observed rate constant determined from the slopes of the bromate decay pseudo-first order plots for each experiment. It represents the overall bromate decay between EQN (5-1) and EQN (5-5)

$$k_{obs} = (k_1)_{obs} - (k_4)_{obs} \qquad (6\text{-}1)$$

Column (6) is the bromate decay universal rate constant, determined by dividing the values in column (5) by the UV light intensity for each experiment. The values in column (6) represents the net bromate decay rate or

$$(k_1 - k_4) = \frac{k_{obs}}{I} \qquad (6\text{-}2)$$

Column (7) represents the difference between k_1 and k_4 for each of the four calibration experiments, and is therefore constant for constant UV light intensity.

Reproduced with permission of the copyright owner. Further reproduction prohibited without permission.

Table 6.2. Comparison of the Bromate Decay Rate Constant from Experiments and Kinetic Model for the Two Highest UV Light Intensities.

(1) EXP #	(2) BrO_3^- (mM)	(3) pH	(4) I* (Einstein /L min)	(5) k_{obs} (min^{-1})	(6) $(k_1 - k_4)_{exp}$+ (L/Einstein)	(7) $(k_1 - k_4)_{mod}$+ (L/Einstein)
1	0.036	8.01	1.57×10^{-4}	0.0486	3.09×10^2	3.20×10^2
2	0.074	8.16	"	0.0402	2.56×10^2	3.20×10^2
3	0.049	8.10	"	0.0471	3.00×10^2	3.20×10^2
4	0.023	8.08	"	0.0495	3.15×10^2	3.20×10^2
7	0.038	6.90	"	0.0426	2.71×10^2	3.20×10^2
11	0.038	8.30	"	0.0368	2.34×10^2	3.20×10^2
41	0.037	8.26	"	0.0364	2.32×10^2	3.20×10^2
60	0.038	9.47	"	0.0447	2.85×10^2	3.20×10^2
61†	0.038	8.27	"	0.0419	2.67×10^2	**3.20×10^2**
62	0.038	7.17	"	0.0423	2.69×10^2	3.20×10^2
10	0.038	8.26	6.90×10^{-5}	0.0273	3.96×10^2	4.42×10^2
29	0.038	8.18	"	0.0300	4.35×10^2	4.42×10^2
38	0.038	7.77	"	0.0230	3.33×10^2	4.42×10^2
45	0.0326	6.90	"	0.0204	2.96×10^2	4.42×10^2
46	0.038	8.13	"	0.0210	3.04×10^2	4.42×10^2
47	0.038	9.37	"	0.0238	3.45×10^2	4.42×10^2
96†	0.067	8.06	"	0.0280	4.06×10^2	**4.42×10^2**
97	0.032	8.10	"	0.0307	4.45×10^2	4.42×10^2
98	0.0067	8.13	"	0.0339	4.91×10^2	4.42×10^2

† Calibration Experiment

* 2.61×10^{-6} Einstein L^{-1} s^{-1} = 1.57×10^{-4} Einstein L^{-1} min^{-1} (16 UV Lamps)

+ $(k_1 - k_4)_{exp} = k_{obs}/f(I) = k_{obs}/I$ ≡net experimental bromate decay rate constant

+ $(k_1 - k_4)_{mod}$ ≡net bromate decay constant derived from calibration of kinetic model

Reproduced with permission of the copyright owner. Further reproduction prohibited without permission.

Table 6.3. Comparison of the Bromate Decay Rate Constant from Experiments and Kinetic Model for the Two Lowest UV Light Intensities.

(1) EXP #	(2) BrO_3^- (mM)	(3) pH	(4) I^* (Einstein /L min)	(5) k_{obs} (min^{-1})	(6) $(k_1 - k_4)_{exp}$ (L/Einstein)	(7) $(k_1 - k_4)_{mod}$ (L/Einstein)
12	0.038	8.23	2.61×10^{-5}	0.0201	7.70×10^2	9.46×10^2
76	0.038	7.38	"	0.0205	7.85×10^2	9.46×10^2
77	0.038	8.25	"	0.0218	8.35×10^2	9.46×10^2
78	0.038	9.32	"	0.0201	7.70×10^2	9.46×10^2
88†	0.038	8.02	"	0.0203	7.78×10^2	**9.46×10^2**
99	0.066	8.30	"	0.0216	8.27×10^2	9.46×10^2
100	0.032	8.34	"	0.0220	8.43×10^2	9.46×10^2
101	0.0068	8.45	"	0.0239	9.16×10^2	9.46×10^2
13	0.038	8.17	1.38×10^{-5}	0.0105	7.61×10^2	9.86×10^2
15	0.037	8.26	"	0.0083	6.01×10^2	9.86×10^2
82†	0.037	8.17	"	0.0108	7.83×10^2	**9.86×10^2**
83	0.036	7.14	"	0.0097	7.03×10^2	9.86×10^2
84	0.036	9.30	"	0.0102	7.39×10^2	9.86×10^2
102	0.067	8.19	"	0.0107	7.75×10^2	9.86×10^2
103	0.032	8.38	"	0.0119	8.63×10^2	9.86×10^2
104	0.0068	8.37	"	0.0099	7.17×10^2	9.86×10^2

† Calibration Experiment

* 4.35×10^{-7} Einstein L^{-1} s^{-1} $= 2.61 \times 10^{-5}$ Einstein L^{-1} min^{-1} (16 UV Lamps)

*$(k_1 - k_4)_{exp} = k_{obs}/f(I) = k_{obs}/I$ ≡net experimental bromate decay rate constant

*$(k_1 - k_4)_{mod}$ ≡net bromate decay constant derived from calibration of kinetic model

Reproduced with permission of the copyright owner. Further reproduction prohibited without permission.

From observation, the data in Tables 6.2 and 6.3 show that the model derived overall bromate decay rate constants (column 7) are higher than the experimentally derived values (column 6) for the four UV light intensities. The mean experimental bromate decay rate constants for each group of experiments with constant UV light intensity was 273 ($\sigma = 28.8$), 383 ($\sigma = 67.7$), 816 ($\sigma = 50.5$), and 743 ($\sigma = 75.4$) for the 16, 12, 8 and 4 UV lamp configurations, respectively. The deviation between the experimental rate constant and the model rate constant for the calibration experiments were 19%, 8.9%, 21% and 25.9% for the 16, 12, 8 and 4 UV lamps respectively. This deviation had the most significance when modeling low concentration (~ 0.5 mg/L) bromate solution. There were marked deviations from the experiments for these conditions.

For each group of experiments with constant UV light intensity there was at least one experiment where the experimental rate constant and the model rate constant more closely approached each other. However, the approach used in selecting experiments for calibrating the model was to select experiments with smooth species profiles and good balance of total bromine species.

The bromate decay universal rate constant used in the kinetic model was clearly not constant over the range of UV light intensites used in this study. In the absence of any bromate decay pH dependencies, the realtionship between the experimental universal rate constant, k, and UV light intensity was plotted (Figure 6.23) over the

Reproduced with permission of the copyright owner. Further reproduction prohibited without permission.

complete range of experimental condition for the bromate alone experiments. The figure clearly shows that the relationship is nonlinear over the range of light intensities.

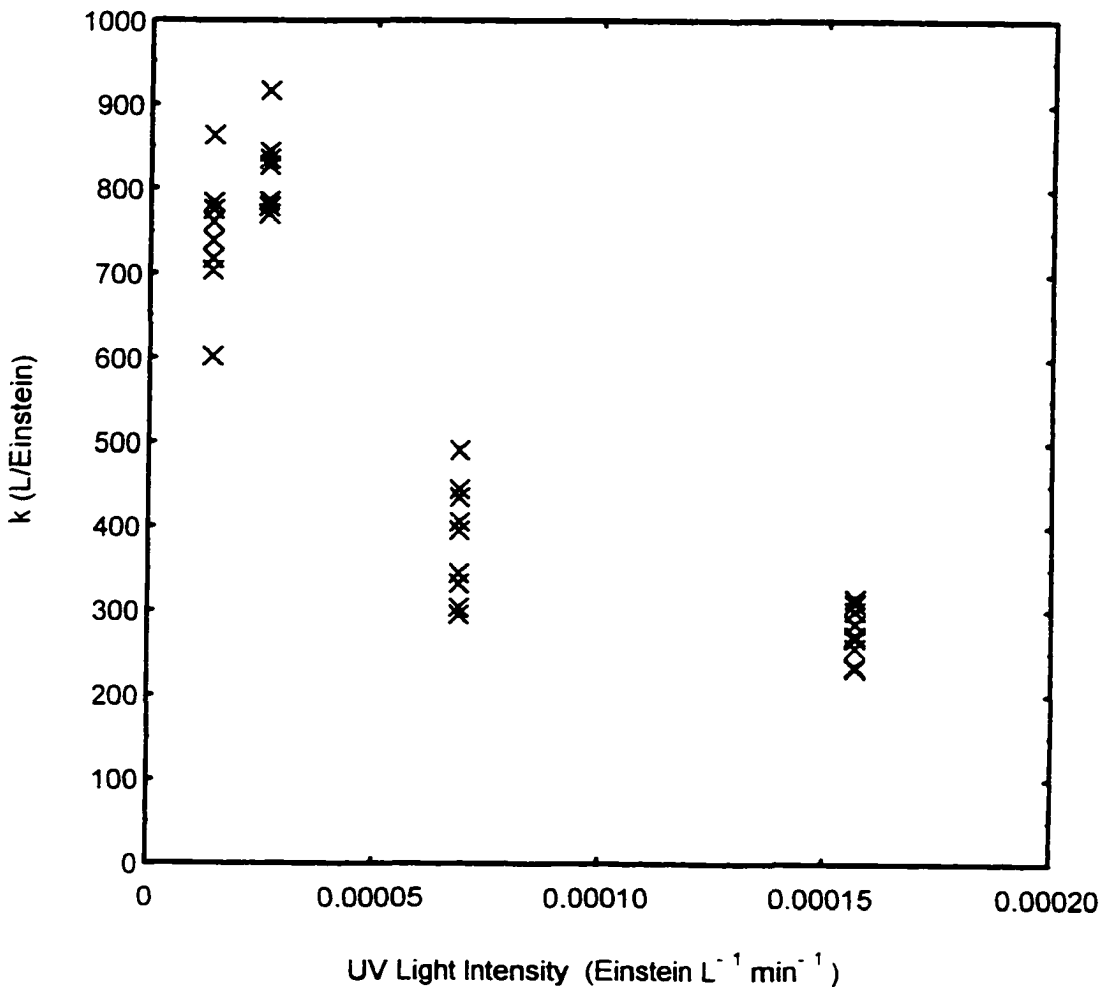

Figure 6.23. UV Light Dependency of Bromate Decay Universal Rate Constant (BrO_3^- = 0.038 mM, Range pH_i =6.90 - 9.47, Range T_i=21-25C EXP 1-4,7,10-15,29,38,41,45-47,60-62,76-78,82-84,88,96-104).

Reproduced with permission of the copyright owner. Further reproduction prohibited without permission.

CHAPTER 7

COMPARISON OF EXPERIMENTAL PROFILES AND MODEL PREDICTIONS: BROMATE/NITRITE SOLUTION

This chapter compares the experimental profiles for experiments involving the UV irradiation of bromate solution containing nitrite and the predictions of the kinetic model for the four UV light intensities used in this study.

Calibration of the kinetic model for the bromate solution containing nitrite was similar to that used for modeling the bromate alone experiments. One experiment for each UV light intensity was used as a calibration experiment. The initial conditions of each of the four experiments was input into the model and the predictions derived. The rate constants k_1 and k_5 were adjusted to give the best fit with the experimental profiles. The values of k_2, k_3, k_4 and k_6 were basically held constant.The calibrated model was then used to predict the species profiles for selected experiments with bromate/nitrite solution.The comparison of over 19 experiment are presented here.

Unlike the modeling of the bromate alone data, the modeling of bromate decay in the presence of nitrite proved more difficult. Examination of the experimental data for all UV light intensities showed a faster rate of bromate decay in the presence of nitrite and a more pronounced level of free bromine formation than experienced in the experiments involving bromate alone. Nitrite itself was also decomposed at a faster rate than in solutions of nitrite alone found in this study. The original belief was that nitrite

Reproduced with permission of the copyright owner. Further reproduction prohibited without permission.

reacted rapidly with free bromine to remove the more light absorbing free bromine species making more light available for bromate decay and increasing its rate of decay. However, the more pronounced free bromine formation in the presence of nitrite discounts this theory and points to the possible reaction of nitrite with an indeterminate bromine species.

Amikar et al. (1975) postulated that during gamma irradiation of water, radicals formed from the decomposition of bromate may directly attack nitrite ion converting it to nitrate. The reactions were thought to be

$$BrO_2\bullet + NO_2^- \rightarrow BrO\bullet + NO_3^- \qquad (7\text{-}1)$$

$$BrO\bullet + NO_2^- \rightarrow Br\bullet + NO_3^- \qquad (7\text{-}2)$$

Modeling the rapid disappearance of nitrite as a chemical reaction between free bromine and nitrite is only possible by having EQN (5-6) play a more prominent role. Herein lies one of the key limitations of the bromate model in the presence of nitrite. To achieve nitrite removal seen experimentally, k_5 for each UV intensity had to be increased by some two orders of magnitude from the experimentally determined values in nitrite alone solutions. More importantly, the experimental observed bromate decay rate, k_1, decreases dramatically when nitrite becomes limiting at around 0.002 mM and the model fails to account for this.

Reproduced with permission of the copyright owner. Further reproduction prohibited without permission.

7.1 Comparison of Profiles for Intensity of 2.61 x 10^{-6} Einstein L^{-1} s^{-1}

Figure 7.1 depicts the calibration of the bromate decay model in the presence of nitrite for experiments with UV light intensity of 2.61 x 10^{-6} Einstein L^{-1} s^{-1}. The model predictions and the experimental profiles fit well for nitrite concentrations > 0.002 mM. When nitrite approaches this limiting value, there is a marked deviation between model and experiment for the bromide and bromate profiles. Nitrite and nitrate fit well over the entire experimental reaction time. Except for the period around 10 minutes, the model predicted free bromine is in agreement with the experimental profile.

Figure 7.2 shows the predictions of the model for an experiment with nitrite concentration almost half the concentration of the calibration experiment in Figure 7.1. The predicted nitrogen profiles are in reasonable agreement with experiment. The model slightly over predicts free bromine. The bromate and bromide profiles agree well with the until nitrite becomes limiting. The predicted bromine species concentrations is in good agreement when nitrite is in excess of bromate as in Figures 7.3 and 7.5. The nitrogen species deviate markedly from the experimental profiles under this condition.In Figure 7.4 bromate is in excess of nitrite as in Figure 7.2. The same explanation is valid. The nitrogen species agree well with the experiment. Bromate and bromide fit well until nitrite becomes limiting. Bromate is under-predicted and bromide over-predicted thereafter. Free bromine is in good agreement with the experiment.

Reproduced with permission of the copyright owner. Further reproduction prohibited without permission.

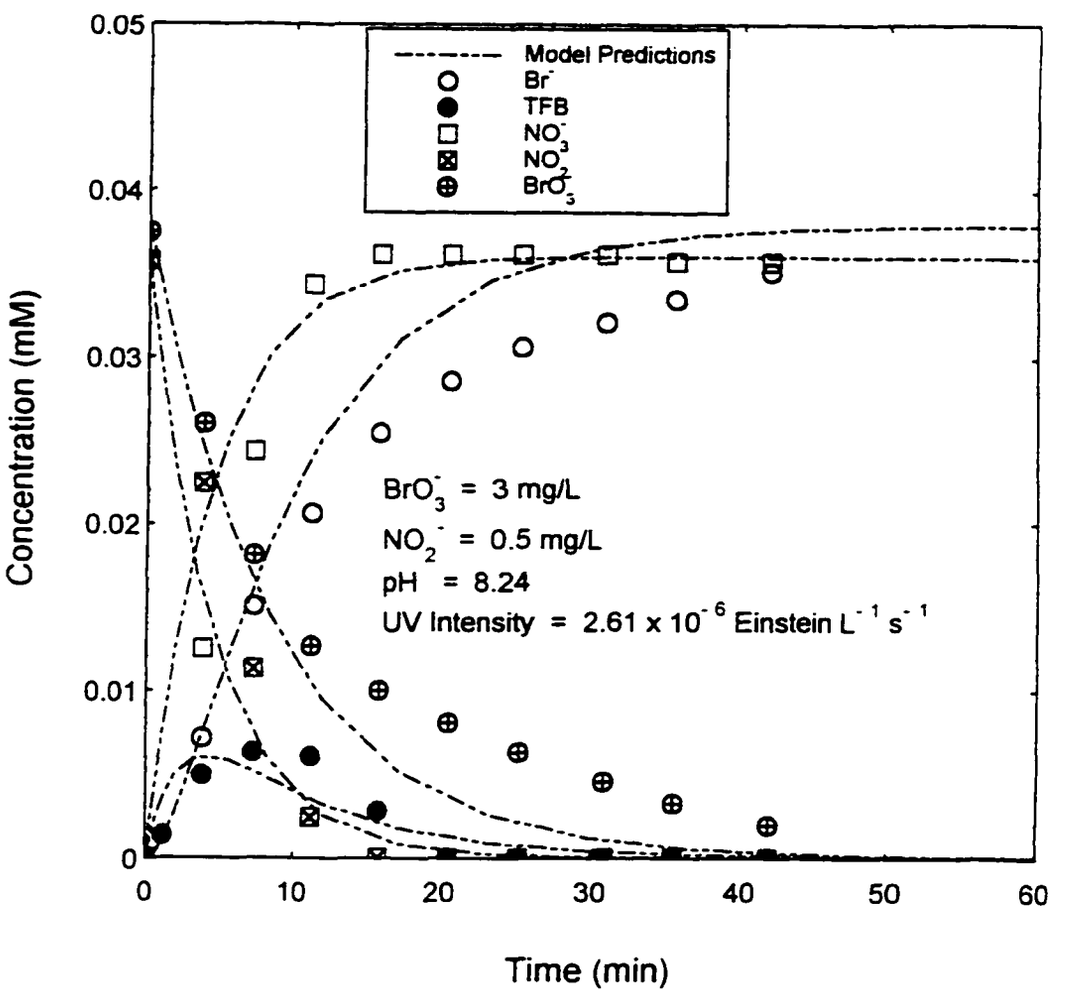

Figure 7.1. Calibration of Bromate Kinetic Model in Presence of Nitrite for I = 2.61 x 10^{-6} Einstein / L*s (EXP 43).

Reproduced with permission of the copyright owner. Further reproduction prohibited without permission.

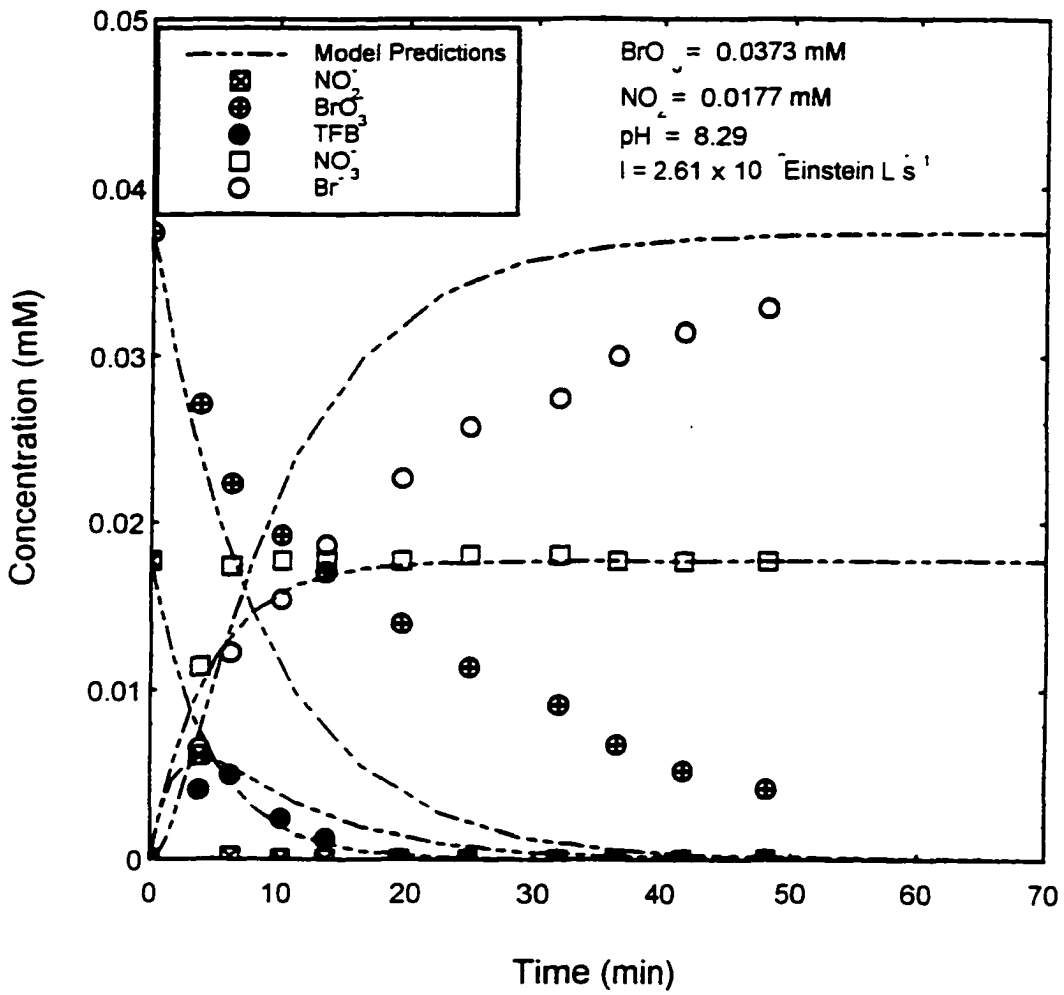

Figure 7.2. Comparison of Experimental Profiles and Kinetic Model Predictions (EXP 42).

Reproduced with permission of the copyright owner. Further reproduction prohibited without permission.

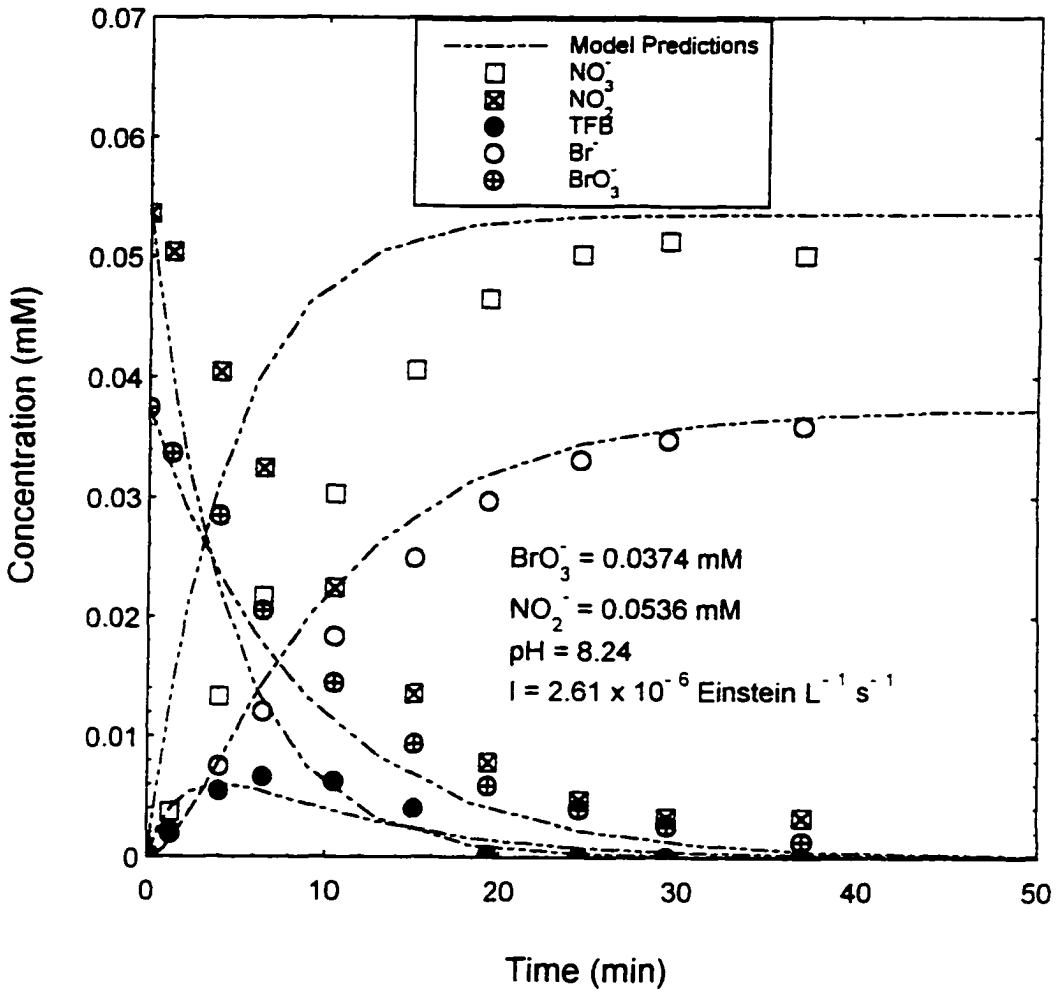

Figure 7.3. Comparison of Experimental Profiles and Kinetic Model Predictions (EXP 44).

Reproduced with permission of the copyright owner. Further reproduction prohibited without permission.

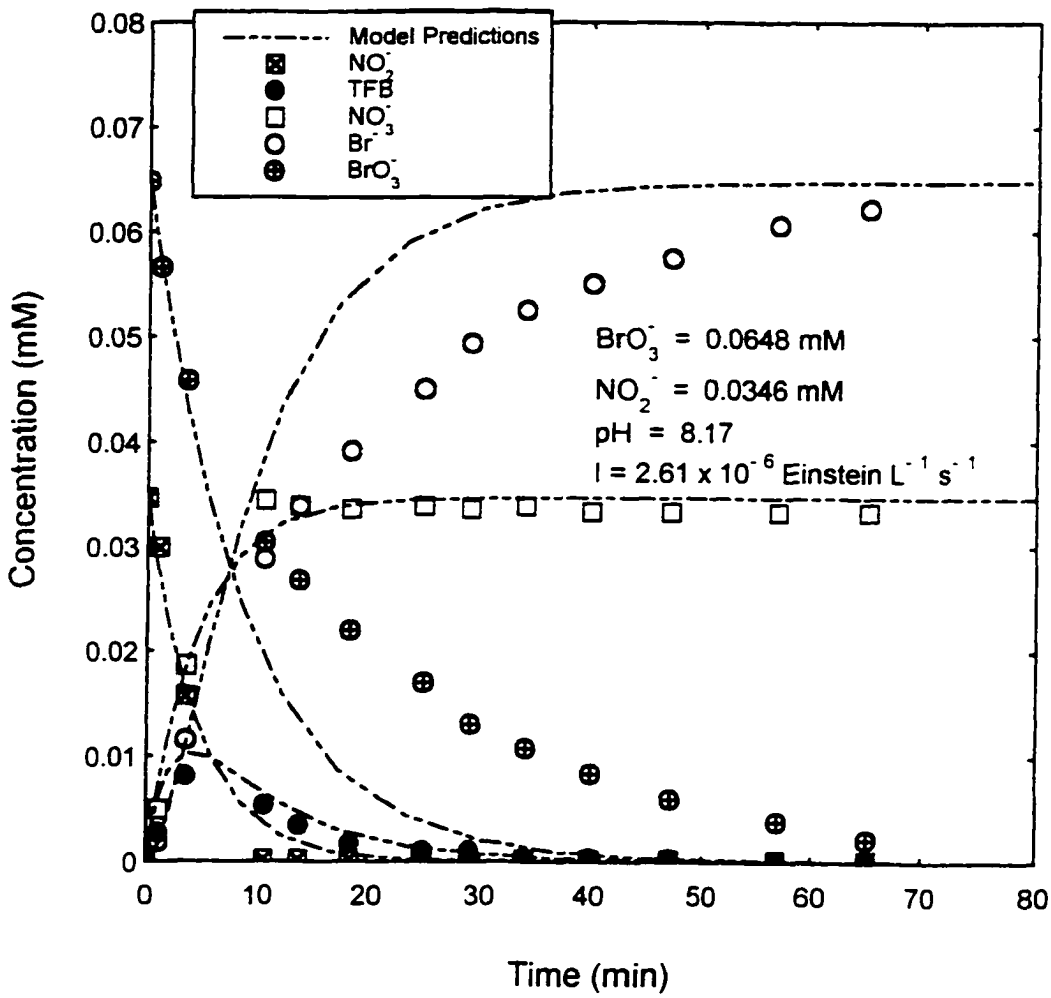

Figure 7.4. Comparison of Experimental Profiles and Kinetic Model Predictions (EXP 67).

Reproduced with permission of the copyright owner. Further reproduction prohibited without permission.

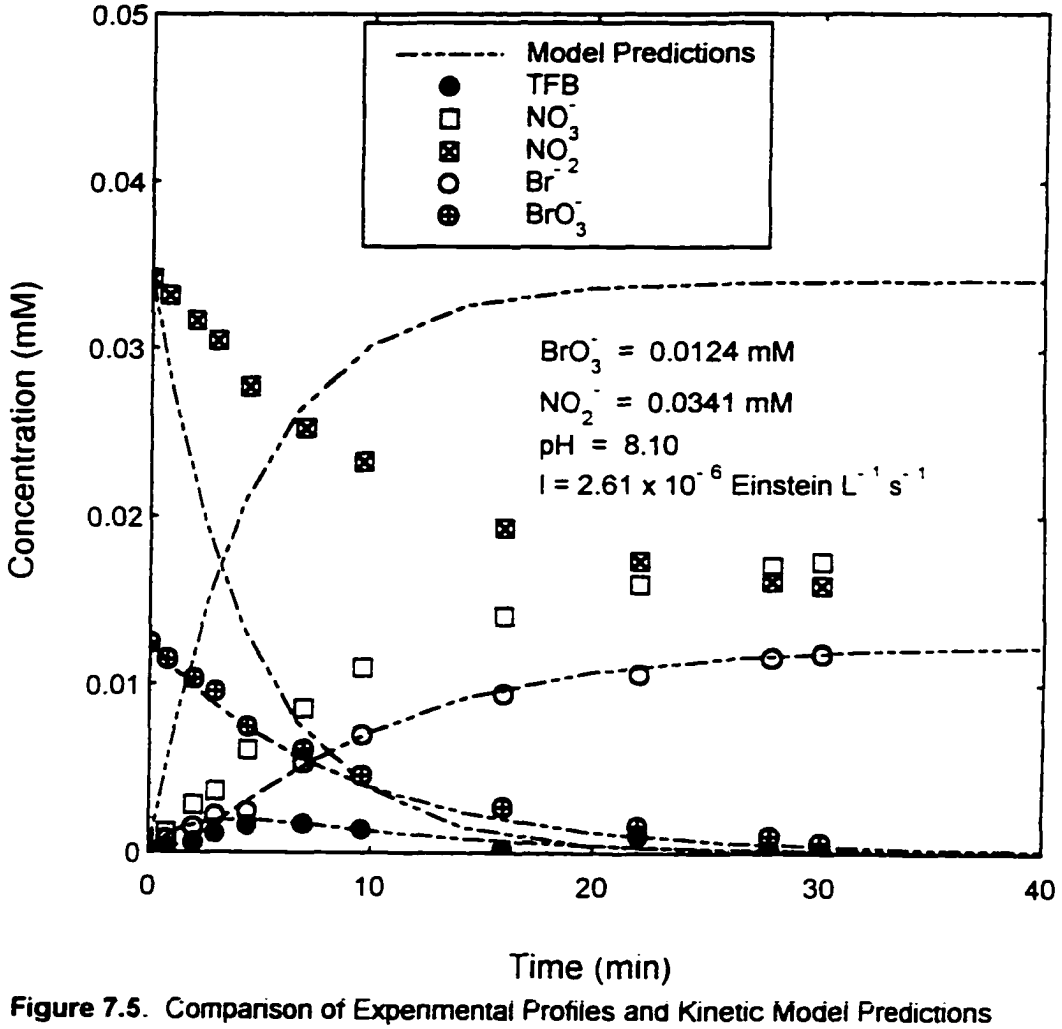

Figure 7.5. Comparison of Experimental Profiles and Kinetic Model Predictions (EXP 69).

Reproduced with permission of the copyright owner. Further reproduction prohibited without permission.

7.2 Comparison of Profiles for Intensity of 1.15 x 10^{-6} Einstein L^{-1} s^{-1}

Figure 7.6 represents the calibration of the bromate kinetic model in the presence of nitrite for experiments with UV intensity of 1.15 x 10^{-6} Einstein L^{-1} s^{-1}. Bromate and nitrite concentrations are approximately equimolar. The model predicted bromate, and bromide profiles fit well with the experimental profiles until the nitrite disappears around 20 minutes and deviates markedly thereafter. Nitrite and nitrate fit well with the experiment over the entire reaction period. Free bromine is slightly over predicted for the over the entire reaction period.

Prediction of an experiment with bromate/nitrite ratio similar to that in the previous figure, is shown in Figure 7.7. The nitrite and nitrate profiles are in good agreement with the experimental profiles. The free bromine profile agree well with the experiment except for the period between 10 and 20 minutes when the model under-predicts it. The bromate and bromide profiles are in good agreement with the experiment until nitrite becomes limiting, whereafter the model under-predicts bromate and over predicts bromide. For experiments with bromate in molar excess of nitrite (Figure 7.8 and 7.10), the nitrite and nitrate profiles are in good agreement with experiment. The bromate and bromide profiles agree well with the experiment until nitrite becomes limiting. Free bromine is over-predicted up until about 30 minutes of reaction time with the largest deviation occurring around 20 minutes. Figure 7.9 shows the case where nitrite is in molar excess of bromate. Like in the case of the higher UV

Reproduced with permission of the copyright owner. Further reproduction prohibited without permission.

intensity, bromate and bromide agree well over the entire reaction period while the nitrogen species profiles deviate markedly from the onset. Free bromine agrees well with the experiment until 10 minutes, whereafter the model under-predicts it.

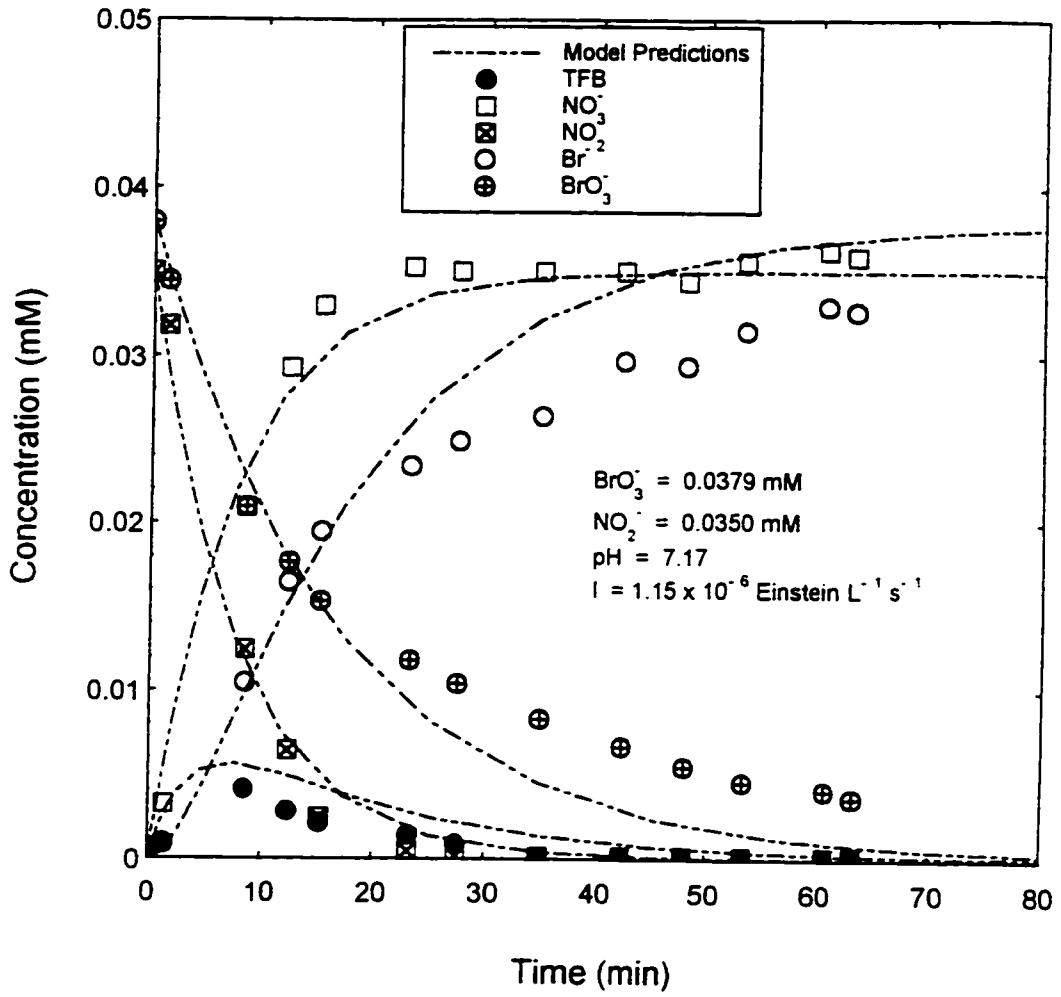

Figure 7.6. Calibration of Bromate Kinetic Model in Presence of Nitrite for I = 1.15 x 10^{-6} Eisntein / L*s (EXP35).

Reproduced with permission of the copyright owner. Further reproduction prohibited without permission.

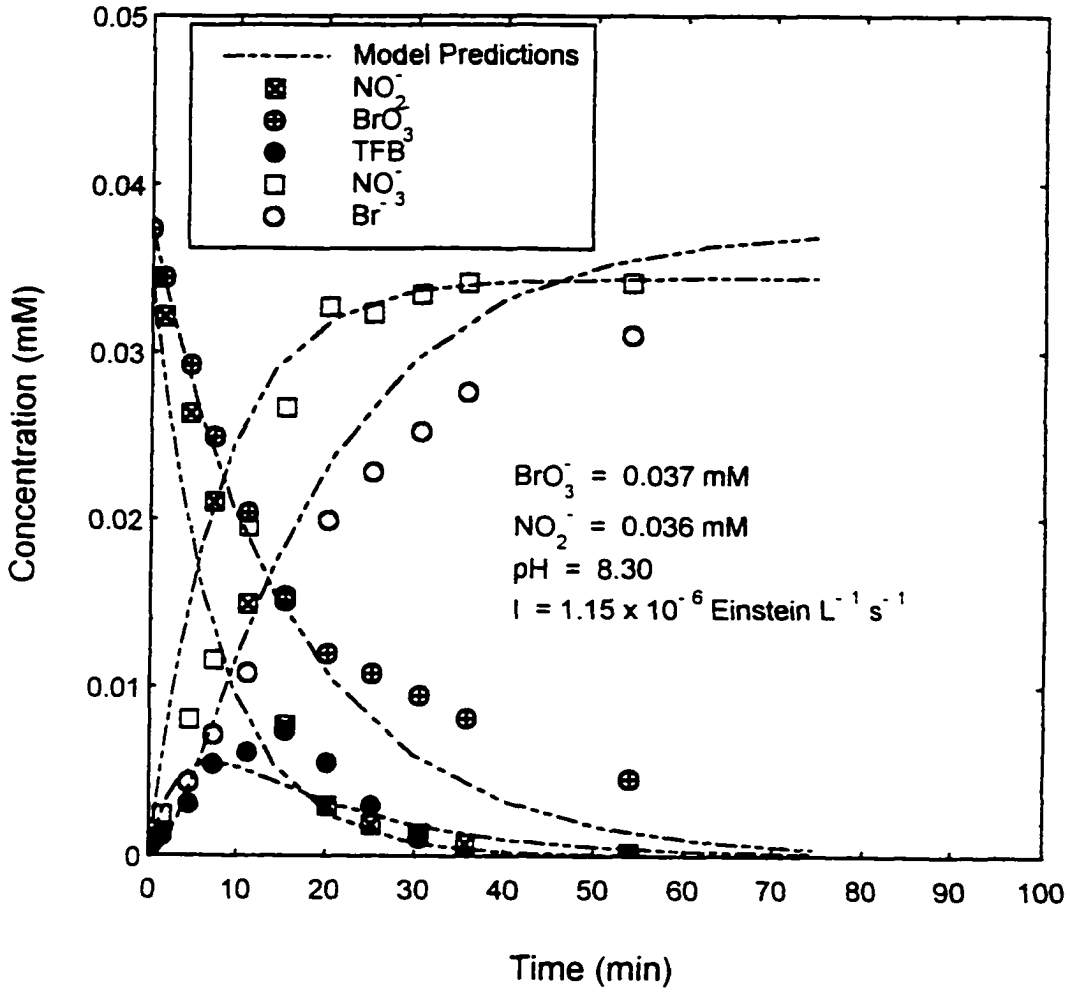

Figure 7.7. Comparison of Experimental Profiles and Kinetic Model Predictions (EXP 49).

Reproduced with permission of the copyright owner. Further reproduction prohibited without permission.

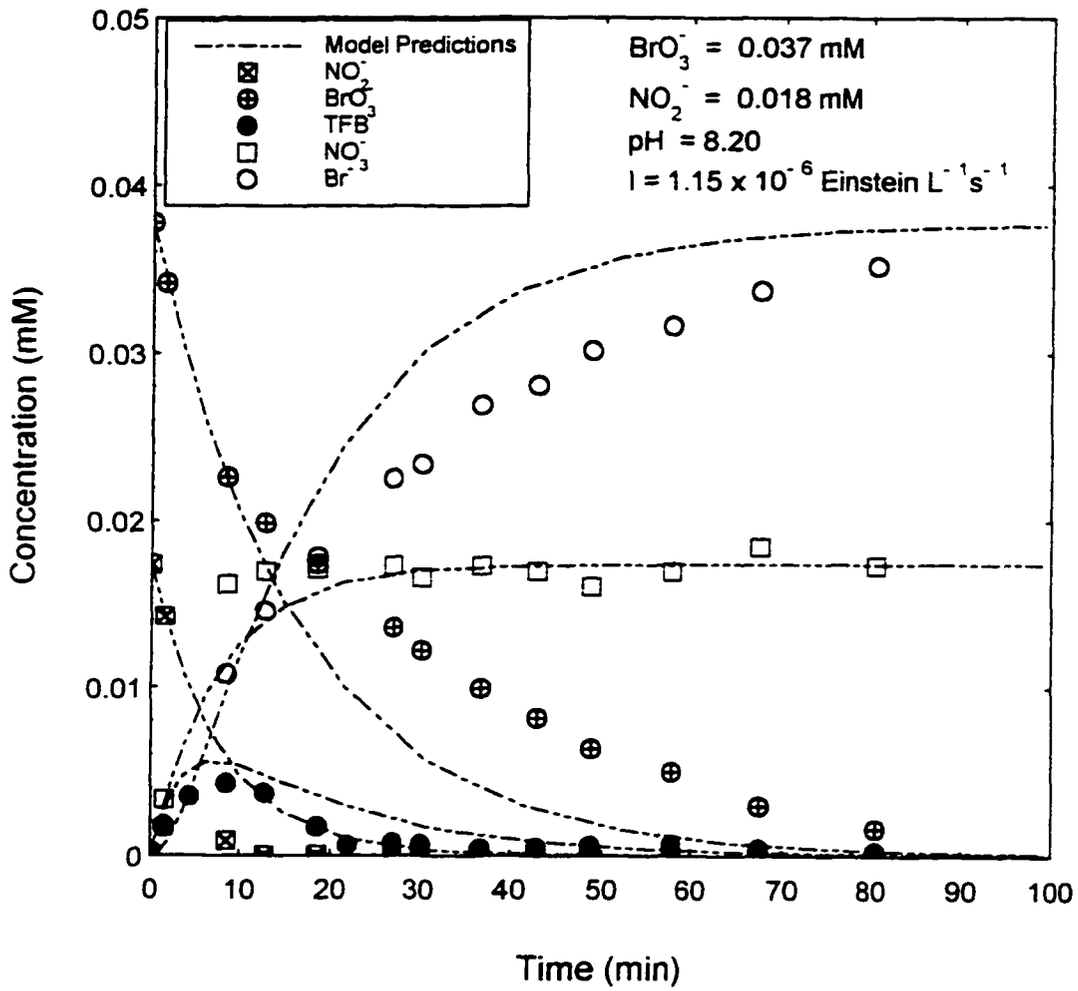

Figure 7.8. Comparison of Experimental Profiles and Kinetic Model Predictions (EXP 30).

Reproduced with permission of the copyright owner. Further reproduction prohibited without permission.

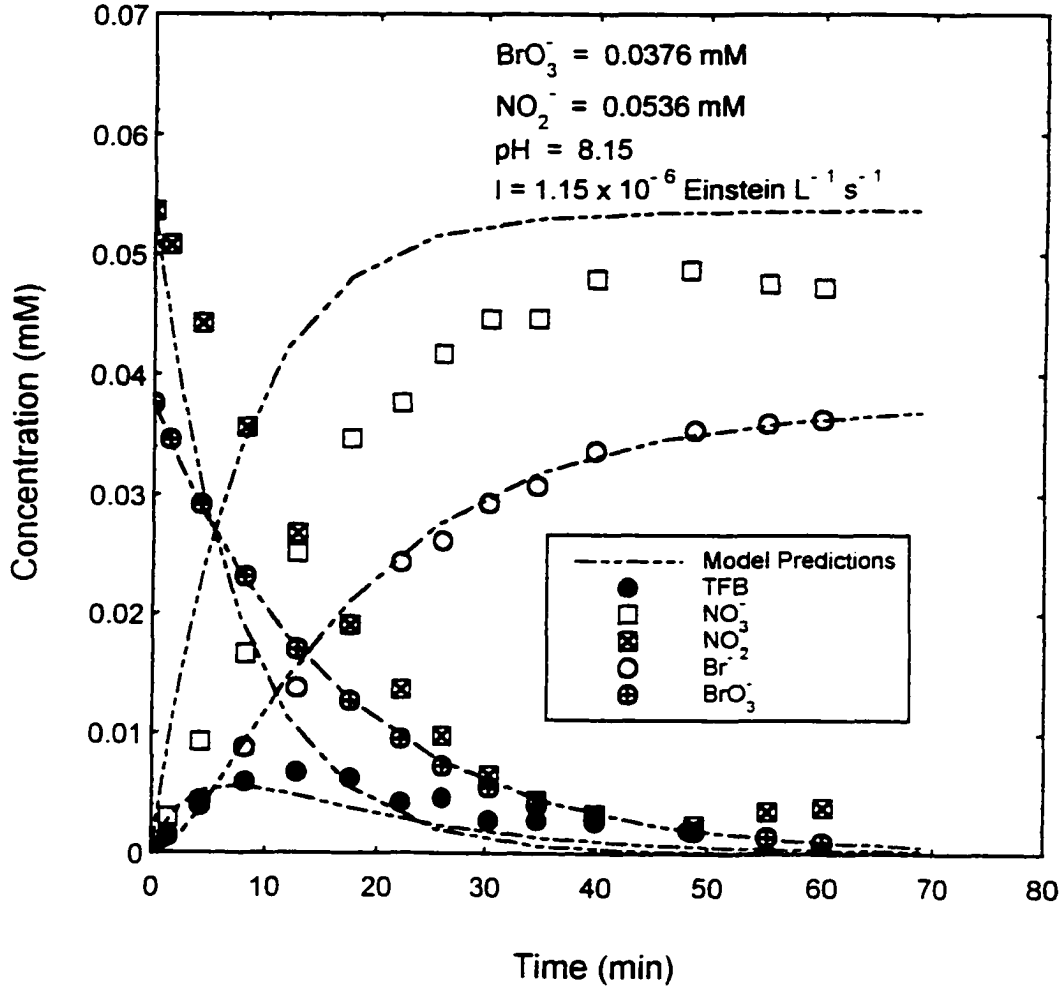

Figure 7.9. Comparison of Experimental Profiles and Kinetic Model Predictions (EXP 32).

Reproduced with permission of the copyright owner. Further reproduction prohibited without permission.

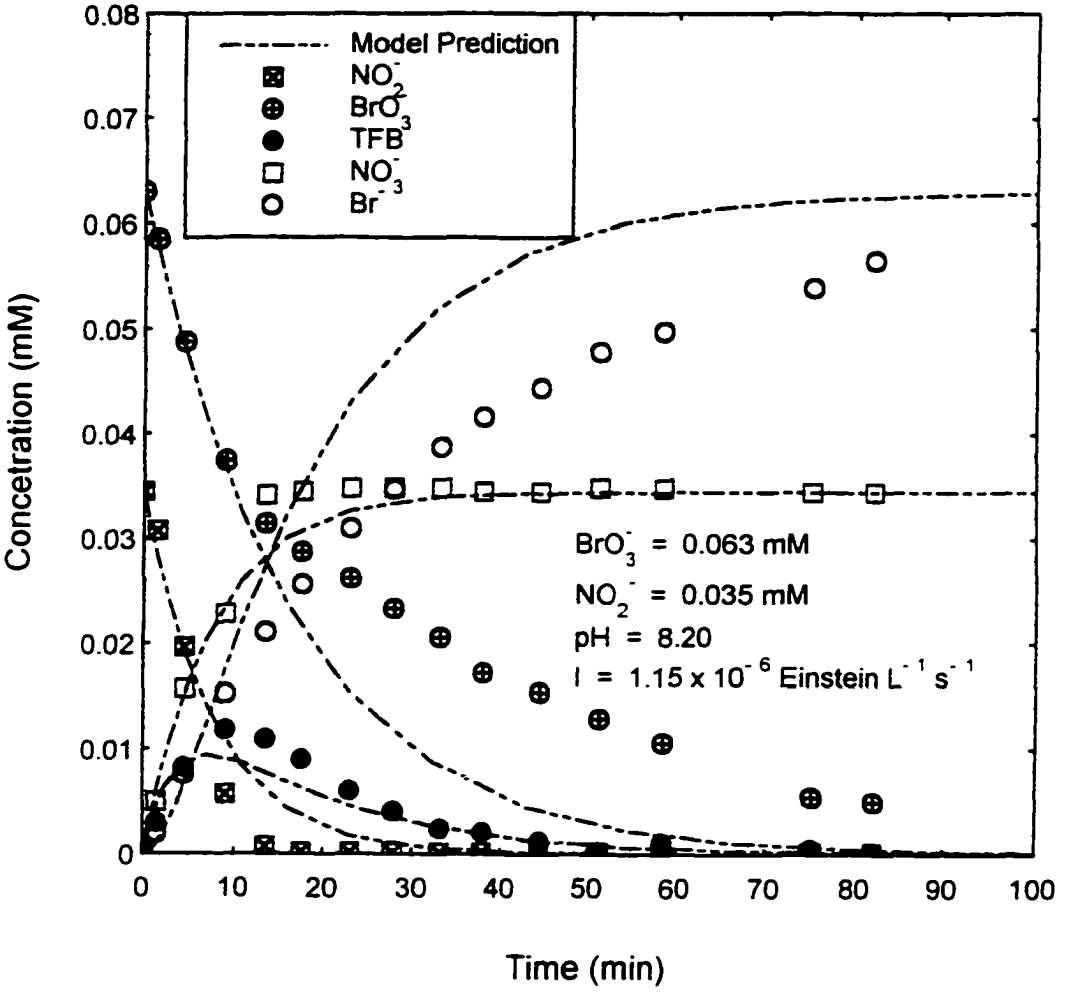

Figure 7.10. Comparison of Experimental Profiles and Kinetic Model Predictions (EXP 48).

Reproduced with permission of the copyright owner. Further reproduction prohibited without permission.

7.3 Comparison of Profiles for Intensity of 4.35 x 10^{-7} Einstein L^{-1} s^{-1}

Calibration of the bromate kinetic model in the presence of nitrite for the UV Intensity of 4.35 x 10^{-6} Einstein L^{-1} s^{-1} is shown in Figure 7.11. Bromate and nitrite concentrations are approximately equimolar. Bromate and bromide are shown to fit well with the experiment until the nitrite disappears around 25 minutes. Nitrate fits well with experiment over the entire reaction period. The nitrite fit is good up to about 20 minutes whereafter calibration of the model gives slighty higher concentrations than seen experimentally.

Figure 7.12 compares the model predictions with the experimental profiles for nitrite and bromate at equimolar concentrations. The predicted bromate and bromide profiles agree well with the experiment until nitrite disappears around 25 minutes. The model under-predicts their concentration thereafter. Free bromine is in good agreement with the experiment until around 20 minutes, whereafter the model over-predicts it. Nitrate agrees well with the experiment with the exception of the latter stages where the model slightly over-predicts its concentration.

Figure 7.13 depicts an experiment with similar bromate/nitrite ratio as in the two previous figures but with initial pH approximately 1.5 pH units higher.The bromate and free bromine profiles agrees well with the experiment for the entire period. Bromide deviates slightly after nitrite becomes limiting around 40 minutes. Nitrite is in good agreement with the experiment until after 70 minutes when the experimental

Reproduced with permission of the copyright owner. Further reproduction prohibited without permission.

nitrite concentration increases with a corresponding drop in nitrate concentration. The nitrate profile is over predicted over the entire reaction. The deviation is more marked in the end when the experimental profile decreases in response to the increase in nitrite concentration. This suggest that at high pH around 9.5, nitrate is reconverted to nitrite after continuous UV irradiation over a period of about an hour.

The model predictions for an experiment with bromate in molar excess of nitrite is shown in Figure 7.14. The model grossly under-predicts the bromate concentration after nitrite disappears around 10 minutes and over-predicts the bromide concentration. Free bromine agrees well with the model until about 12 minutes of reaction time, whereafter the model overpredicts its concentration. The model under-predicts the nitrate concentration until about 20 minutes of reaction time, whereafter it coincides with the model experimental profiles for the duration of the experiment.

Figure 7.15 shows the comparison of model and experiment for an experiment with excess nitrite. As in the case of the two previous UV light intensities under similar conditions, the model agrees well with the bromine species profiles over the entire reaction period. The nitrogen species profiles diverges markedly from the experimental profiles from the onset of the experiment.

Reproduced with permission of the copyright owner. Further reproduction prohibited without permission.

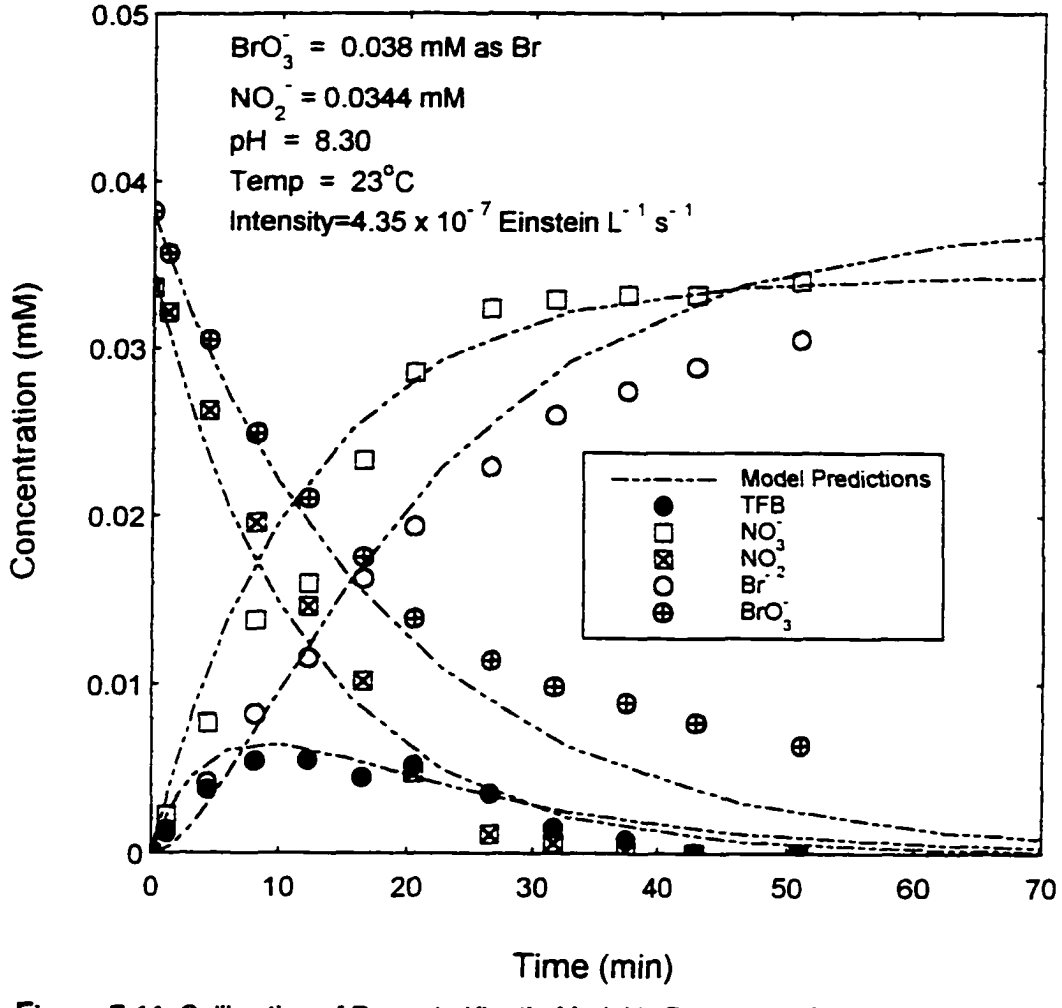

Figure 7.11. Calibration of Bromate Kinetic Model in Presence of Nitrite for I = 4.35 x 10^{-7} Eisntein / L*s (EXP 74).

Reproduced with permission of the copyright owner. Further reproduction prohibited without permission.

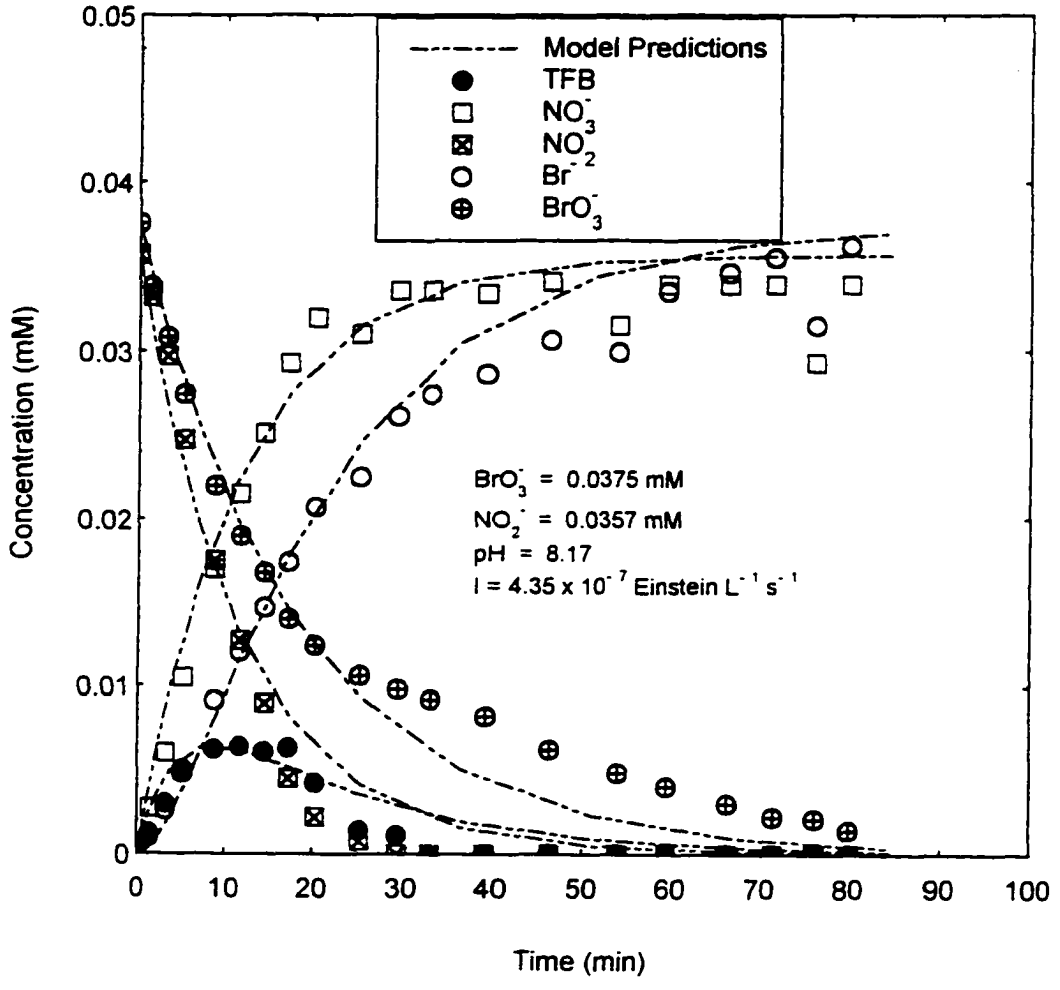

Figure 7.12. Comparison of Experimental Profiles and Kinetic Model Predictions (EXP 25).

Reproduced with permission of the copyright owner. Further reproduction prohibited without permission.

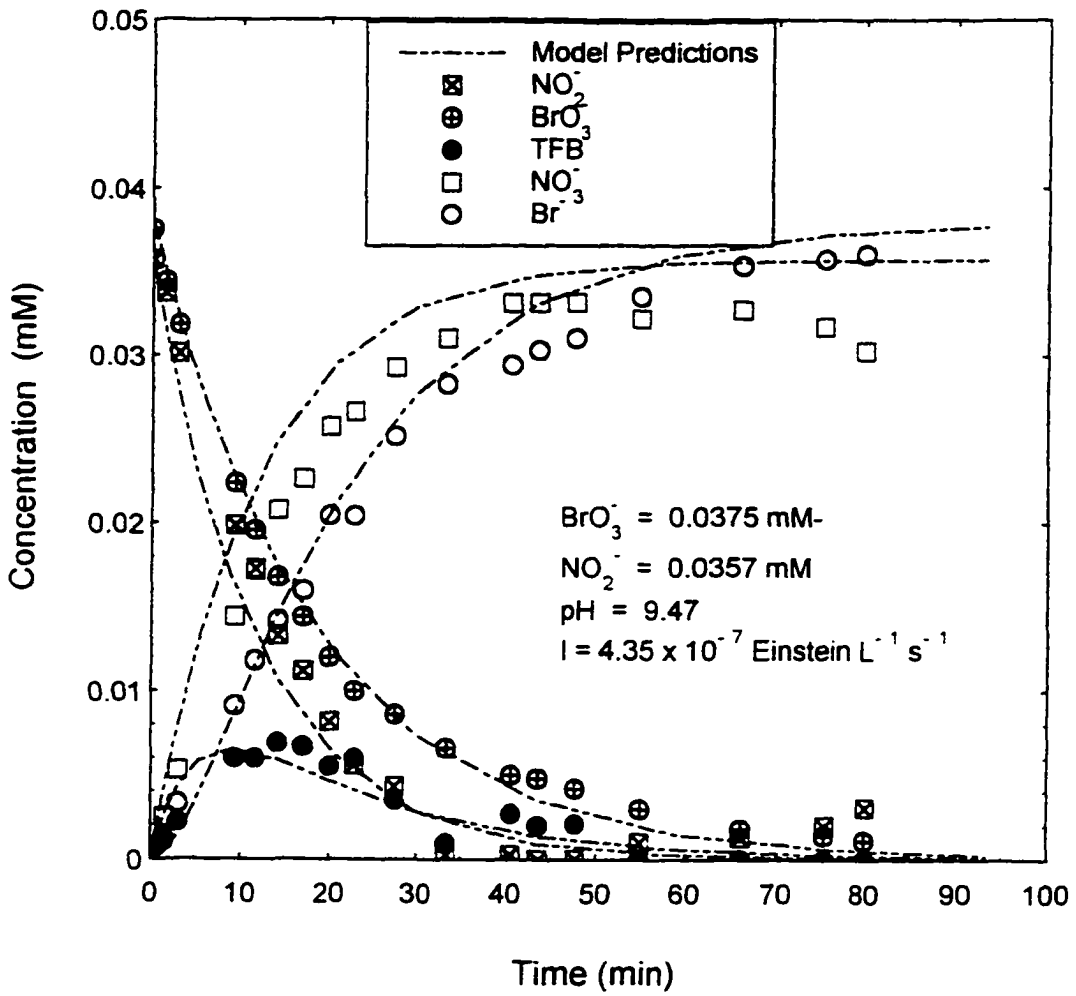

Figure 7.13. Comparison of Experimental Profiles and Kinetic Model Predictions (EXP 26).

Reproduced with permission of the copyright owner. Further reproduction prohibited without permission.

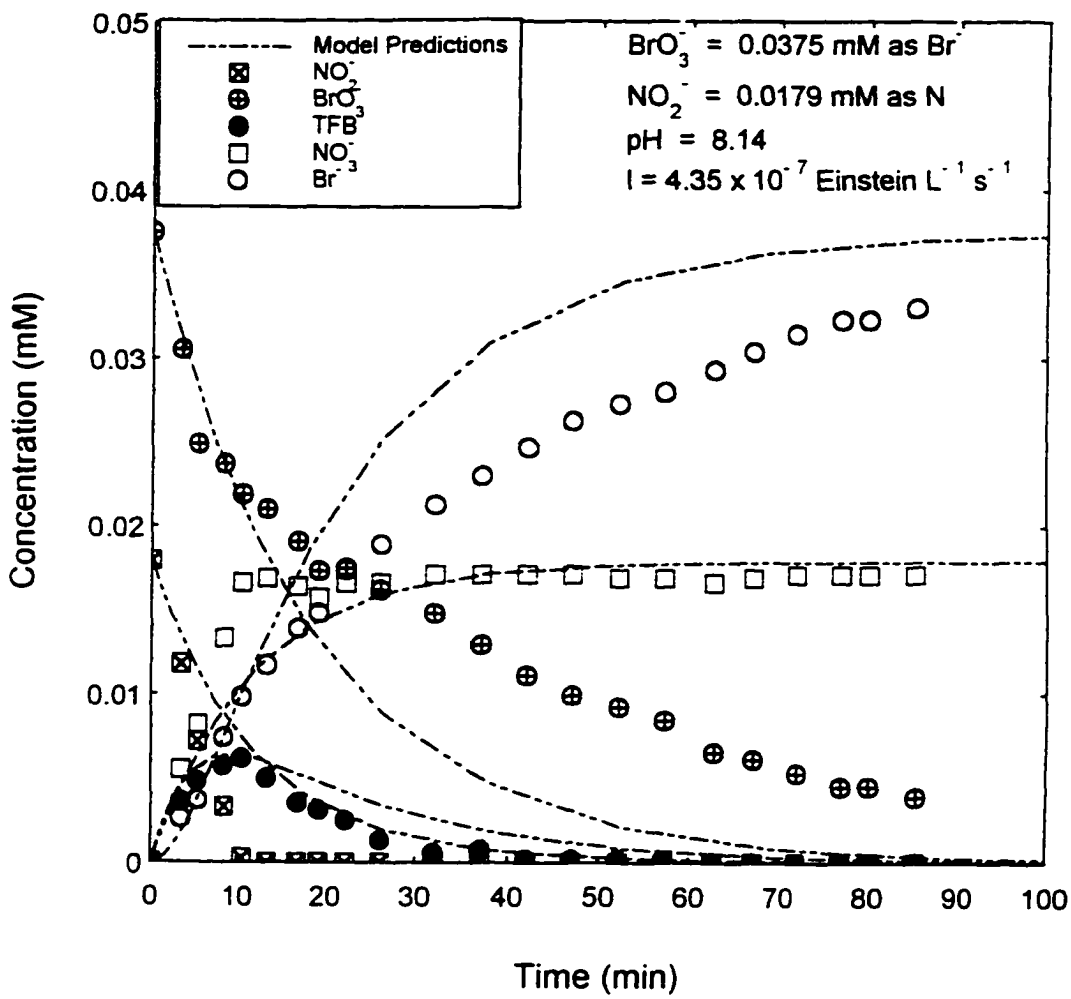

Figure 7.14. Comparison of Experimental Profiles and Kinetic Model Predictions (EXP 27).

Reproduced with permission of the copyright owner. Further reproduction prohibited without permission.

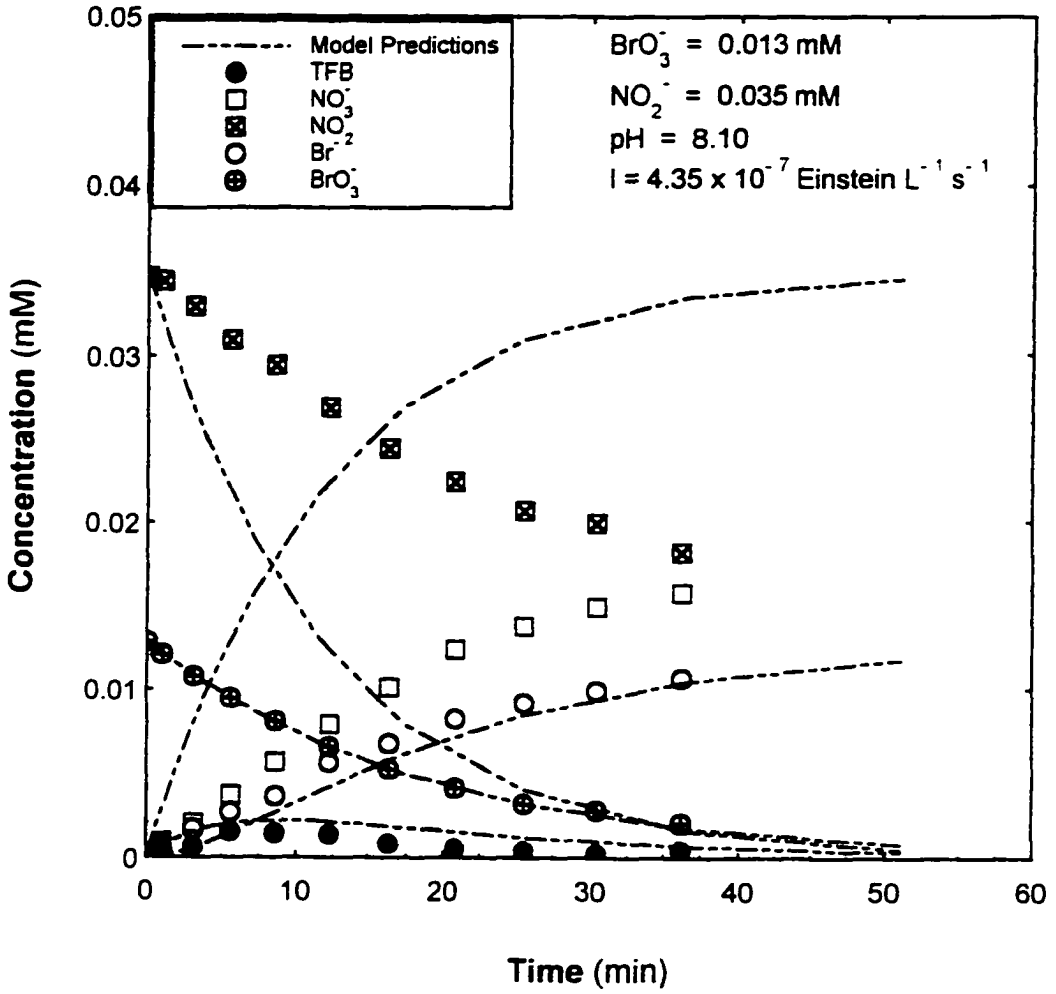

Figure 7.15. Comparison of Experimental Profiles and Kinetic Model Predictions (EXP 72).

Reproduced with permission of the copyright owner. Further reproduction prohibited without permission.

7.4 Comparison of Profiles for Intensity of 2.30 x 10^{-7} Einstein L^{-1} s^{-1}

Figure 7.16 shows the calibration experiment for the UV Light Intensity of 2.30 x 10^{-6} Einstein L^{-1} s^{-1}. Bromate and nitrite were at approximately equimolar concentration. The calibration fit for the bromine species was good up to about 40 minutes of reaction time. Thereafter, there is a marked deviation in the model predicted bromate and bromide profiles from the experimental profiles and a slight over prediction of free bromine. The fit of nitrogen species is good until approximately 30 minutes of reaction time, whereafter, there is a deviation between model and experiment, until 60 minutes. The model approaches the experimental thereafter.

The plot in Figure 7.17 compares the model with an experiment with similar bromate/nitrite ratio as in the calibration experiment. The model prediction of bromate is in good agreement with the experiment until about 60 minutes. The bromide profiles begins deviating from the experimental profiles around 30 minutes, before nitrite becomes limiting at 50 minutes. The model slightly over-predicts free bromine in the early stages (15 minutes) and then under-predicts it until the close to the termination of the experiment. The nitrogen species deviate from the experimental profiles from the onset until it approaches them when nitrite becomes limiting. The case of excess bromate is shown in Figure 7.18. The same observations can be made as in experiments with similar bromate/nitrite ratios for different UV light intensity. The bromine species profiles agree well with the experiment while the nitrogen species diverges from the

Reproduced with permission of the copyright owner. Further reproduction prohibited without permission.

onset. For the case of excess bromate, like in similar experiments at different UV light intensity, the nitrogen species are in good agreement with the experiment. The bromine species fit the experiment well initially, and diverge after nitrite becomes limiting.

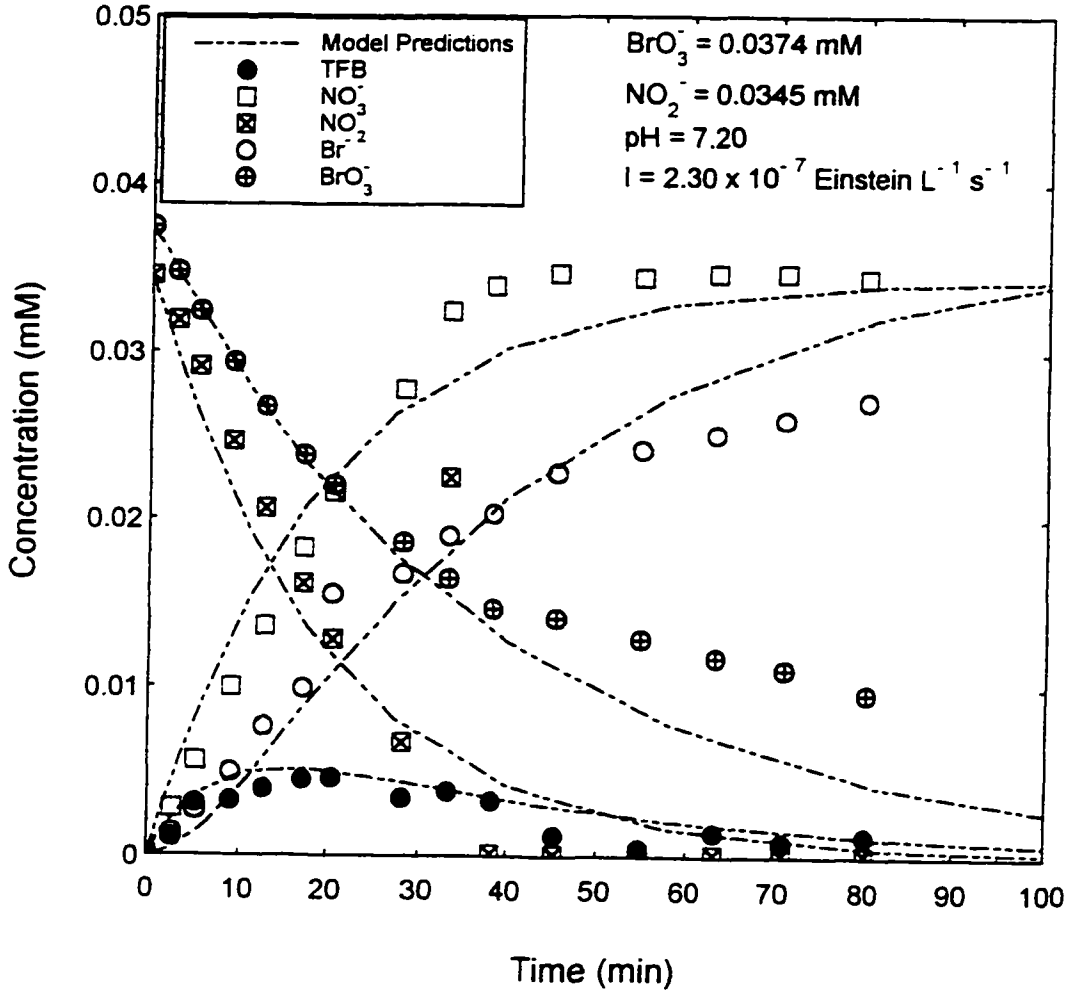

Figure 7.16. Calibration of Bromate Kinetic Model in Presence of Nitrite for I = 2.30 x 10^{-7} Einstein / L*s (EXP 79).

Reproduced with permission of the copyright owner. Further reproduction prohibited without permission.

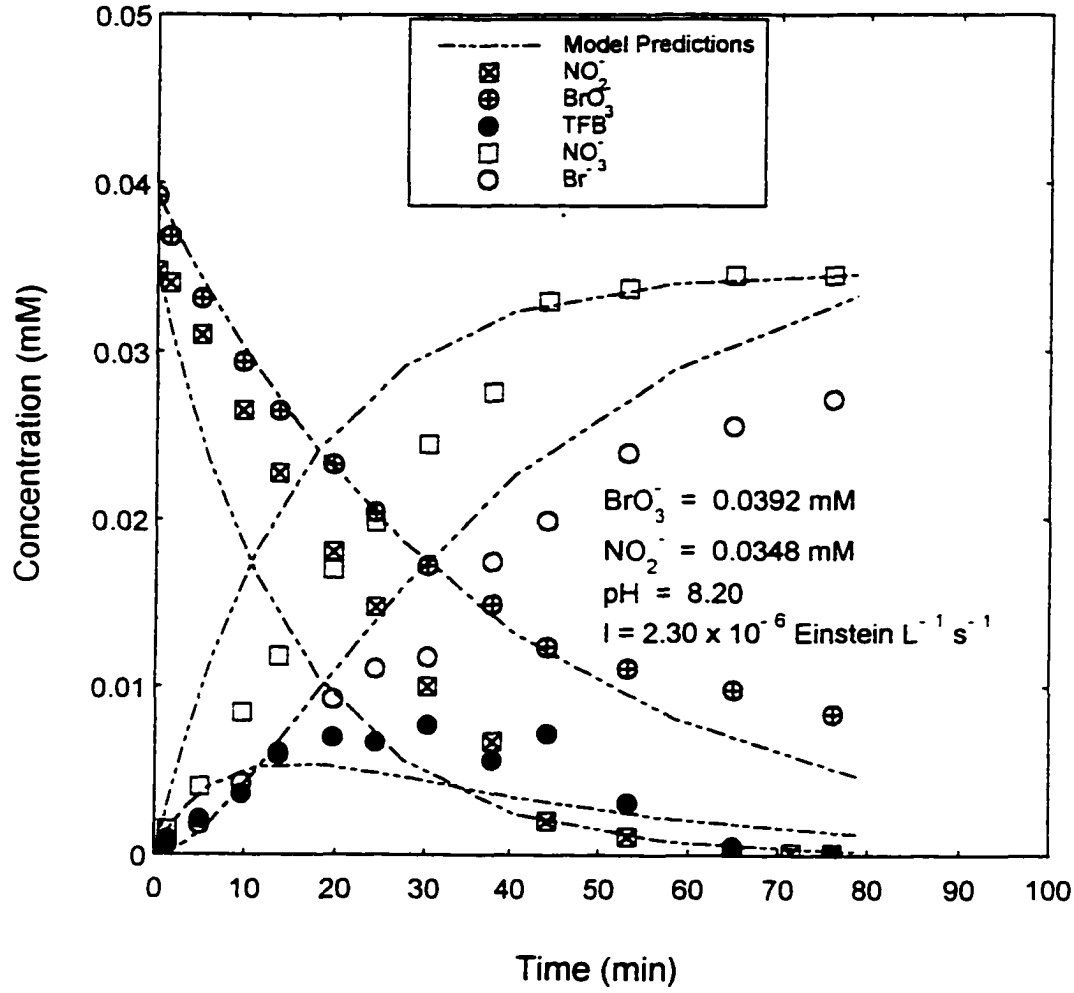

Figure 7.17. Comparison of Experimental Profiles and Kinetic Model Predictions (EXP 80).

Reproduced with permission of the copyright owner. Further reproduction prohibited without permission.

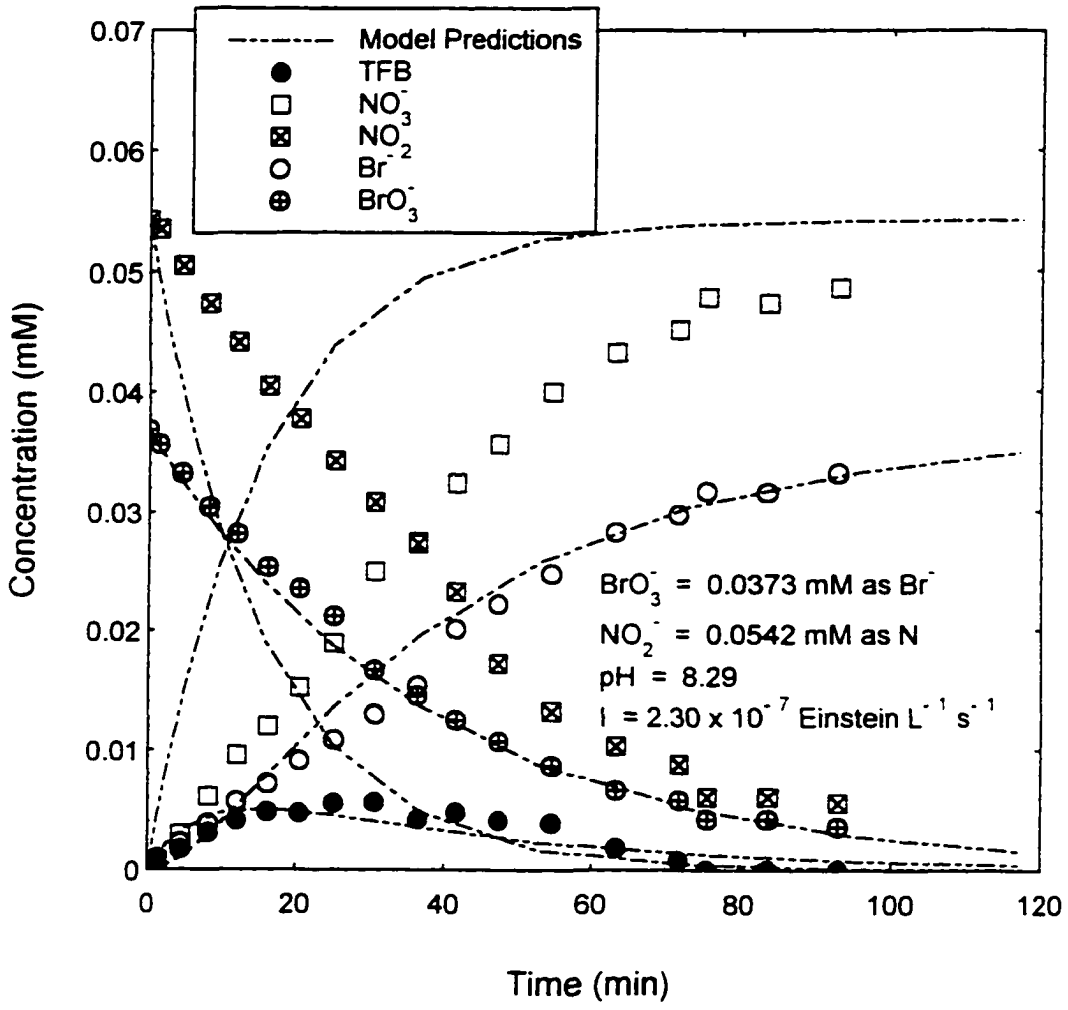

Figure 7.18. Comparison of Experimental Profiles and Kinetic Model Predictions (EXP 16).

Reproduced with permission of the copyright owner. Further reproduction prohibited without permission.

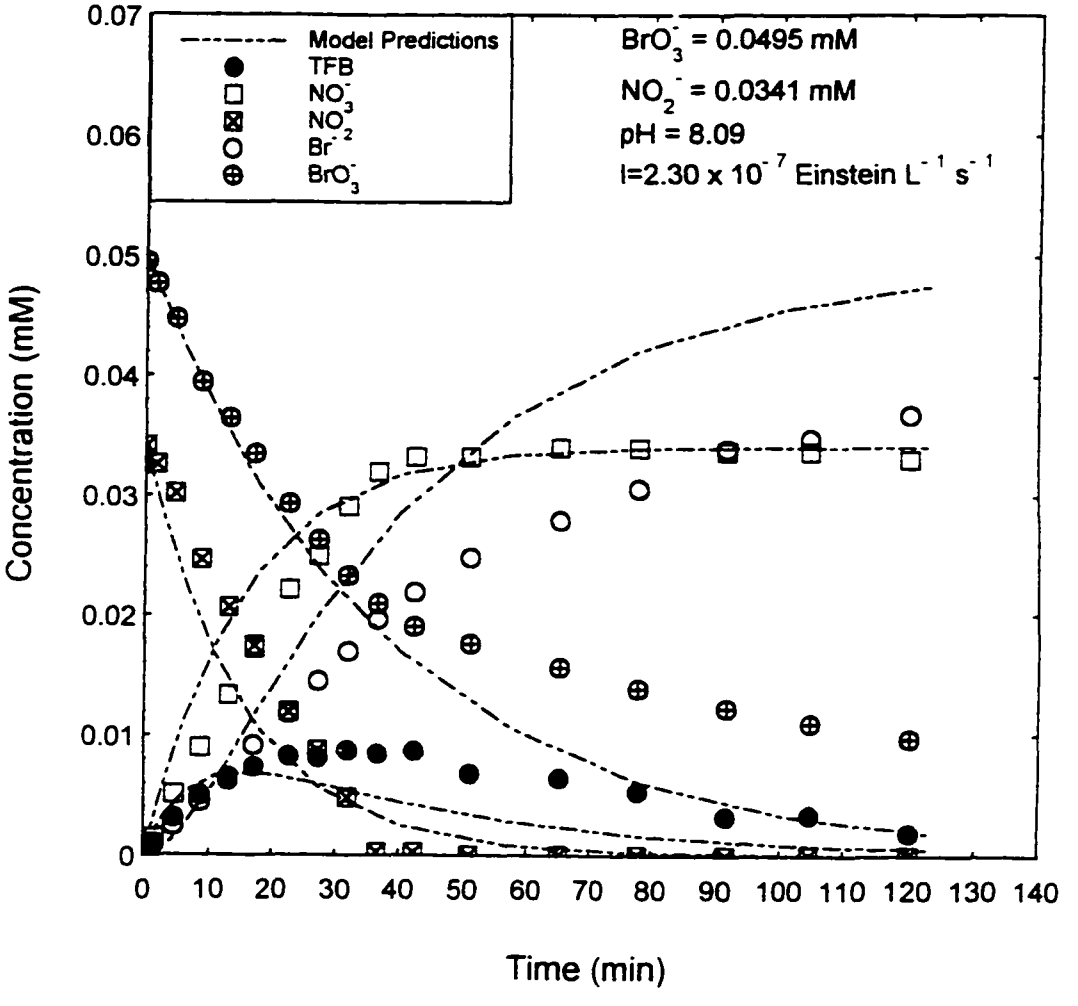

Figure 7.19. Comparison of Experimental Profiles and Kinetic Model Predictions (EXP 85).

Reproduced with permission of the copyright owner. Further reproduction prohibited without permission.

7.5 Summary

Comparisons have been presented between the bromate decay kinetic model and experimental observations when nitrite is present during UV irradiation of bromate solution. As has been outlined above, the model fails to account for the change in bromate decay rate observed when nitrite becomes a limiting reactant at about 0.002 mM and a detailed analysis of the comparisons will not be presented here.

The rate constants used in calibrating the kinetic model in the presence of nitrite are shown below. From experimental observations the value of k_1 was much higher in the presence of nitrite. However, when nitrite concentration approached zero, all the

Table 7.1. Kinetic Constants Used in Calibrating Bromate Kinetic Model in Presence of Nitrite.

# UV LAMPS	k_1 L/Einstein	k_2 L/Einstein	k_3 L/Einstein	k_4 L/Einstein	k_5 L/Einstein	k_6 L/Einstein *mM^{-3}
16	$7.38x10^2$	2.30×10^3	$2.87x\ 10^3$	0.19×10^2	$1.40 x10^3$	3.0×10^3
12	$8.91x10^2$	2.90×10^3	$3.77 x10^3$	0.36×10^2	$1.88 x10^3$	3.0×10^3
8	$2.10x10^3$	6.03×10^3	$7.45 x10^3$	0.77×10^2	$3.26 x10^3$	3.0×10^3
4	$1.96x10^3$	7.72×10^3	$9.25 x10^3$	1.09×10^2	$4.78 x10^3$	3.0×10^3

terms in the model involving nitrite approached zero and the model automatically reverted back to the case of bromate alone with k_1 as defined in Table 6.1. The values of k_2, k_3, k_4 were the same as in the bromate alone case. The reaction between free bromine and nitrite is chemical and not photochemical. Thus, k_6 was made independent of UV light intensity.

Reproduced with permission of the copyright owner. Further reproduction prohibited without permission.

CHAPTER 8

CONCLUSIONS

Experimental observation of bromate solution under UV irradiation (254 nm) has shown that bromate decomposes stoichiometrically to form bromide as a final product. Free bromine was an intermediate product of the reaction. A bromine balance performed during each of the photochemical experiments virtually eliminated the possibility of formation of other bromine final products in detectable quantities. The solution pH decreased up to 1.5 pH units in all photochemical experiments with initial pH < 9.0. This has been attributed to the reaction between H• and OH^-. No appreciable pH drop was observed during UV irradiation of a control solution of deionized water under experimental conditions similar to the bromate experiments. For experiments with bromate solution buffered at pH > 9.0 with sufficient 5N NaOH, pH remained within 0.5 pH units of the initial value during UV irradiation.

Bromate decay kinetics has been shown to be first order with respect to initial bromate concentration. Kinetic analysis of the data showed that k_{obs} was virtually independent of initial pH in the range of 6.5 to 9.5. Aqueous electrons are a product of UV irradiation of aqueous systems and can be scavenged by H^+ (Neta et al., 1988). This reduces the amount of electrons available for the reduction of bromate to bromide at lower pH values. However, the absence of a pH dependency in this study indicates that the concentration of aqueous electrons generated during UV irradiation was low.

Reproduced with permission of the copyright owner. Further reproduction prohibited without permission.

A number of experiments conducted with bicarbonate alkalinity varying between 0.05 and 1.0 mM and for fixed bromate concentration showed k_{obs} to be independent of alkalinity within this range. The solution pH for experiments with bicarbonate between 0.5 mM and 1.0 mM remained with 0.04 pH units of the initial value. The pH decrease for the experiment with bicarbonate concentration of 0.05 mM was similar to the bromate alone experiments when the initial pH < 9.0.

In the presence of nitrite, bromate was stoichiometrically decomposed to bromide as a final product at a much faster rate than in aqueous solutions of bromate alone. Nitrite was stoichiometrically oxidized to nitrate. Free bromine formation was more pronounced than in corresponding bromate alone solution, suggesting that one of the intermediate products of bromate decay is principally responsible for the oxidation of nitrite to nitrate. The solution pH was also found to decrease in the presence of nitrite suggesting that the same explanations as in the case of the bromate alone solutions are valid.

For bromate/nitrite ratios <1, ~1 and >1, bromate decomposition was shown to be first order. There was a change in the rate of the reaction when nitrite became limiting at a concentration of approximately 0.002 mM. In one case the rate changed from a value of 0.0976 to 0.0623 min^{-1}. This change in the bromate decay rate when nitrite became limiting was characteristic of all photochemical experiments with bromate/nitrite solution. The reduced bromate decay rate was still higher than the

Reproduced with permission of the copyright owner. Further reproduction prohibited without permission.

corresponding experiments involving only bromate. This indicates that bromate decay may also be catalyzed by the presence of nitrate in solution.

Kinetic analysis of the data showed that k_{obs} was basically independent of initial bromate, initial nitrite and initial pH, during UV irradiation of bromate solution in the presence of nitrite.

Experiments were performed only at the UV light intensity of 4.35×10^{-6} Einstein L^{-1} s^{-1} (8 UV lamps) for bromate solution containing acetate in the range of 0.06 mM to 0.27 mM solution. The bromate concentration was fixed and the initial pH and temperature were held within a narrow range. During UV irradiation, bromate was reduced to bromide and acetate was converted to an unidentified product. Preliminary experiments had shown that acetate solution was unreactive under UV irradiation for similar experimental conditions. Free bromine remained at trace levels throughout the course of the reaction. The bromine balance remained constantly below the initial bromine level throughout the course of the experiments suggesting the formation of organic by-products from the reaction of acetate with free bromine.

Kinetic analysis of bromate decay in the presence of acetate showed it followed pseudo-first order kinetics. The values of k_{obs} in the presence of varying amounts of acetate were comparable to those for the experiments involving bromate alone conducted at the higher UV light intensity of 2.61×10^{-6} Einstein L^{-1} s^{-1} (16 UV lamps). Bromate pseudo-first order decay rate was found to be unchanged by varying the

Reproduced with permission of the copyright owner. Further reproduction prohibited without permission.

acetate concentration in the range of 0.06 mM to 0.27 mM.

The kinetic model predictions were in good qualitative agreement with the experimental data involving bromate alone. The model deviated from the experimental data for low levels of initial bromate. The bromate decay rate constant used in the calibration of the kinetic model was higher than the experimentally derived values. The consequences were most evident for the model predictions of low concentrations of bromate solutions, where there were marked deviations between the experimental and model profiles.

The modeling of bromate decay in the presence of nitrite presented complications. The experimental observed bromate decay rate decreased markedly for limiting nitrite concentrations (NO_2^- < 0.002 mM). The lack of a reaction to account for this drop in the rate of bromate decay led to marked deviations between the bromate experimental profiles and the predicted bromate profiles after the limiting nitrite concentration for the case where bromate was either in molar excess of nitrite or at equimolar concentration. For these conditions, the predicted nitrogen species profiles was overall, in fair agreement with the experiments. In the case where nitrite was in molar excess of bromate, the predicted bromine species profiles closely approximated the experimental profiles, while the nitrogen species profiles deviated markedly.

Further experimental observations are required to identify bromate radical species produced during UV irradiation of bromate solutions and bromate solutions

Reproduced with permission of the copyright owner. Further reproduction prohibited without permission.

containing nitrite. These will aid in identifying bromine species that react with nitrite and promote the decomposition of bromate. Identification of the possible reactions between bromine species and nitrite will also enable better modeling of the reacting system during UV irradiation of bromate and bromate/nitrite solution and allow a greater role for the possible reaction between bromine radical species and nitrite, and less to the reaction between nitrite and free bromine.

Reproduced with permission of the copyright owner. Further reproduction prohibited without permission.

APPENDIX A

BROMATE DECAY ALGORITHM

Reproduced with permission of the copyright owner. Further reproduction prohibited without permission.

```
**********************************************************************
**     BROMATE DECAY MODEL: Model Predicts the Profiles of Species    **
**     During UV Irradiation of Bromate or Bromate/Nitrite Solution.  **
**     August 26, 1998                                                **
**********************************************************************
c
c
c    INTERFACE ROUTINE
c
c       prompts the user to input initial conditions for the model as well as info on the
c       the starting step size and on the accuracy desired by the user. The routine then
c       then passes control to the driver routine, odeint to calculate function values at
c       at each  step.
c
        character * 20 fname
        external derivs,rkqs
        integer maxsiz
        parameter (maxsiz=4)
        common initial(maxsiz)
        real initial
        real ystart(10),x1, x2, h1, hmin,eps,pH,DO,BrO3o,NO2o,numlamps
        integer nvar, nok, nbad
        print*,'enter output file name'
        read*,fname
        open(1,file=fname,status='new',form='formatted')
        print*,'enter the number of equations'
        read*,nvar
        print*,'enter the number of UV Lamps in operation'
        read*,numlamps
        initial(1) = numlamps
        print*,'enter the initial bromate in mM'
        read*, BrO3o
        initial(2) = BrO3o
        ystart(1) = BrO3o
        print*,'enter initial free bromine in mM'
        read*,ystart(2)
        print*,'enter initial bromide in mM'
        read*,ystart(3)
        print*,'enter initial nitrite in mM'
        read*,NO2o
```

Reproduced with permission of the copyright owner. Further reproduction prohibited without permission.

```
      ystart(4) = NO2o
      initial(3) = NO2o
      print*,'enter initial nitrate in mM'
      read*,ystart(5)
      print*,'enter initial D.O. in mg/L (5.0 is a good value)'
      read*,DO
      ystart(6) = DO/32.0
      print*,'enter initial pH'
      read*,pH
      initial(4) = pH
      print*,initial(1),initial(2),initial(3),initial(4)
      ystart(7) = 10.0**(-pH)
      x1 = 0.0
      print*,'enter the reaction time'
      read*, x2
      print*,'enter the initial step size (0.01 recommended)'
      read*,h1
      print*,'enter the minimum step size (0.001 recommended)'
      read*,hmin
      print*,'enter the required accuracy (0.005 recommended)'
      read*, eps
      call odeint(ystart,nvar,x1,x2,eps,h1,hmin,nok,nbad,derivs,rkqs)
      close(1)
      end
c
c
c     DRIVER SUBROUTINE
c
c     Runge-Kutta driver routine with adaptive stepsize control. Integrates the starting
c     value  ystart(1:nvar) over the specified time interval (x1 to x2) with accuracy
c     eps.  h1 should be set as a guessed first stepsize, hmin as the minimum allowed
c     stepsize.  On output,  nok and nbad are the number of good and bad (but retried)
c     steps taken,and ystart is replaced by values at the end of the integration interval,
c     derivs is the user supplied supplied subroutine for calculating the right hand side
c     derivative, while rkqs is the stepper rotuine to be used.
c
c
      subroutine odeint(ystart,nvar,x1,x2,eps,h1,hmin,nok,nbad,
     +derivs,rkqs)
      integer nbad, nok, nvar, KMAXX,MAXSTP,NMAX
```

Reproduced with permission of the copyright owner. Further reproduction prohibited without permission.

```
      real eps, h1, hmin,x1,x2,ystart(nvar),TINY,temp,pHf
      external derivs,rkqs
      parameter (maxsiz=4)
      common initial(maxsiz)
      real initial
      parameter(MAXSTP=100000000,NMAX=10,KMAXX=1000,TINY=1.0e-10)
      integer i, kmax, kount, nstp
      real dxsav,h,hdid,hnext,x,xsav,dydx(NMAX),xp(KMAXX),y(NMAX)
      real yp(NMAX,KMAXX), yscal(NMAX)
      common kmax,kount,dxsav,xp,yp
      x = x1
      kmax = 1000
      dxsav = 0.00001
      h=sign(h1,x2-x1)
      nok=0
      nbad=0
      kount=0
      do 11 i=1,nvar
      y(i) = ystart(i)
11    continue
      if (kmax .gt. 0) xsav=x-2.0*dxsav
      do 16 nstp = 1, MAXSTP
c     checking number of steps taken
      print*,nstp
      call derivs (x,y,dydx)
      temp = y(7)
c     determining pH from H+ concentration (pH = -log [H+])
      pHf = -alog10(temp)
c     writing model output to output file
      write (1, fmt = 999)x,y(1),y(2),y(3),y(4),y(5),y(6),pHf
999   format(E15.9,1x,E15.9,1x,E15.9,1x,E15.9,1x,E15.9,1x,E15.9,1x,
     +E15.9,1x,f5.1)
      do 12 i = 1,nvar
      yscal(i) = abs(y(i)) + abs(h*dydx(i)) + TINY
12    continue
      if (kmax .gt. 0) then
      if (abs(x-xsav) .gt. abs(dxsav)) then
      if (kount .lt. kmax-1) then
      kount = kount + 1
      xp(kount) = x
```

Reproduced with permission of the copyright owner. Further reproduction prohibited without permission.

```
      do 13 i = 1, nvar
      yp(i,kount)=y(i)
13    continue
      xsav = x
      endif
      endif
      endif
      if ((x+h-x2)*(x+h-x1) .gt. 0.0) h=x2-x
      call rkqs (y,dydx,nvar,x,h,eps,yscal,hdid,hnext,derivs)
      if (hdid .eq. h) then
      nok = nok + 1
      else
      nbad = nbad + 1
      endif
      if((x-x2)*(x2-x1) .ge. 0.0) then
      do 14 i = 1, nvar
      ystart(i) = y(i)
14    continue
      if (kmax .ne. 0) then
      kount = kount + 1
      xp(kount) = x
      do 15 i = 1, nvar
      yp(i,kount) = y(i)
15    continue
      endif
      return
      endif
      if (abs(hnext) .lt. hmin) print*,'stepsize smaller than min'
      h = hnext
16    continue
      print*,'too many steps'
      return
      end
c
c
c     STEPPER SUBROUTINE
c
c     Fifth-order Runge Kutta step with monitoring of local truncation error to ensure
c     accuracy and adjust stepsize. Input are the dependent variable vector y(1:n) and
c     its derivative dydx(1:n) at the starting value of the independent variable x. Also
```

Reproduced with permission of the copyright owner. Further reproduction prohibited without permission.

```
c       input are the stepsize to be attempted htry, the required accuracy, eps, and the
c       vector yscal(1:n) against which the error is scaled. On output, y and x are
c       replaced by their new values, hdid is the stepsize that was actually acheived,
c       and hnext is the estimated next stepsize. derivs is the user-supplied subroutine,
c       that computes the right hand side derivates.
c
c
        subroutine rkqs (y,dydx,n,x,htry,eps,yscal,hdid,hnext,derivs)
        integer n, NMAX
        real eps, hdid, hnext, htry, x, dydx(n),y(n),yscal(n)
        external derivs
        parameter (NMAX=10)
        parameter (maxsiz=4)
        common initial(maxsiz)
        real initial
        integer i
        real  errmax,h,htemp,xnew,yerr(NMAX),ytemp(NMAX),SAFETY
        real PSHRNK, ERRCON,PGROW
        parameter (SAFETY=0.9,PGROW=-0.2,PSHRNK=-0.25,ERRCON=1.89e-04)
        h = htry
1       call rkck (y, dydx,n,x,h,ytemp,yerr,derivs)
        errmax = 0.0
        do 33 i = 1,n
        errmax=max(errmax,abs(yerr(i)/yscal(i)))
33      continue
        errmax = errmax/eps
        if(errmax .gt. 1.0) then
        htemp=SAFETY*h*(errmax**PGROW)
        h=sign(max(abs(htemp),0.1*abs(h)),h)
        xnew = x + h
        if (xnew .eq. x) print*,'stepsize underflow in rkqs'
        goto 1
        elseif (errmax .gt. ERRCON) then
        hnext=SAFETY*h*(errmax**PGROW)
        else
        hnext =5.0 * h
        endif
        hdid = h
        x = x + h
        do 35 i = 1, n
```

Reproduced with permission of the copyright owner. Further reproduction prohibited without permission.

```
      y(i) = ytemp(i)
35    continue
      return
      end
c
c
c     ALGORITHM SUBROUTINE
c
c     Given values for n variables y and their derivatives dydx known at x, uses
c     the fifth order Cash-Karp Runge-Kutta method to advance the solution
c     over an interval h and return the incremented variables as yout. Also return an
c     estimate of the local truncation error in yout using the embedded fourth-order
c     method.The user supplies the subroutine derivs which return derivatives at x.
c
      subroutine rkck (y,dydx,n,x,h,yout,yerr,derivs)
      integer n, NMAX
      real h, x, dydx(n),y(n),yerr(n),yout(n)
      external derivs
      parameter (NMAX=10)
      parameter (maxsiz=4)
      common initial(maxsiz)
      real initial
      integer i
      real ak2(NMAX),ak3(NMAX), ak4(NMAX),AK5(NMAX), ak6(NMAX)
      real ytemp(NMAX), A2,A3,A4,A5,A6,B21,B31,B41,B42,B43,B51
      real B52,B53,B54,B61,B62,B63,B64,B65,C1,C3,C4,C6,DC1,DC3
      real DC4,DC5,DC6
c
c     initializing the Cash-Karp parameters
c
      parameter (A2=.2,A3=.3,A4=.6,A5=1.,A6=.875,B21=.2,B31=3./40.,
     +B32=9./40,B41=.3,B42=-.9,B43=1.2,B51=-11./54.,B52=2.5,
     +B53=-70./27.,B54=35./27.,B61=1631./55296.,B62=175./512.,
     +B63=575./13824.,B64=44275./110592.,B65=253./4096.,
     +C1=37./378.,C3=250./621.,C4=125./594.,C6=512./1771.,
     +DC1=C1-2825./27648.,DC3=C3-18575./48384.,
     +DC4=C4-13525./55296.,DC5=-277./14336.,DC6=C6-.25)
c
      do 44 i=1,n
      ytemp(i) = y(i)+B21*h*dydx(i)
```

Reproduced with permission of the copyright owner. Further reproduction prohibited without permission.

```
44      continue
        call derivs(x+A2*h,ytemp,ak2)
        do 46 i = 1, n
        ytemp(i) = y(i)+h*(B31*dydx(i)+B32*ak2(i))
46      continue
        call derivs(x+A3*h,ytemp,ak3)
        do 48 i = 1, n
        ytemp(i) = y(i)+h*(B41*dydx(i)+B42*ak2(i)+B43*ak3(i))
48      continue
        call derivs(x+A4*h,ytemp,ak4)
        do 50 i= 1, n
        ytemp(i)=y(i)+h*(B51*dydx(i)+B52*ak2(i)*ak3(i)+B54*ak4(i))
50      continue
        call derivs (x+A5*h,ytemp,ak5)
        do 52 i = 1, n
        ytemp(i) = y(i)+h*(B61*dydx(i)+B62*ak2(i)+B63*ak3(i)+B64*ak4(i)+
       +B65*ak5(i))
52      continue
        call derivs(x+A6*h,ytemp,ak6)
        do 54 i = 1, n
        yout(i)=y(i)+h*(C1*dydx(i)+C3*ak3(i)+C4*ak4(i)+c6*ak6(i))
54      continue
        do 56 i = 1, n
        yerr(i)=h*(DC1*dydx(i)+DC3*ak3(i)+DC4*ak4(i)+DC5*ak5(i)+
       +DC6*ak6(i))
56      continue
        return
        end
c
c       FIRST ORDER ODE SUBROUTINE
c
        subroutine derivs(x,y,dydx)
        integer maxsiz
        parameter (maxsiz=4)
        common initial(maxsiz)
        real initial
        real x, y(10),dydx(10),UVInt
        real k1, k2, k3, k4, k5, k6, K50, K60, Ka
c       initial(1) =# of UV LAMPS
c       initial(2) = INITIAL BROMATE
```

Reproduced with permission of the copyright owner. Further reproduction prohibited without permission.

```
c       initial(3) = INITIAL NITRITE
c       initial(4) = INITIAL pH
c       ------------------------------------------------------------
c       coding kinetic constants for bromate in the presence of nitrite
c
        if (initial(3) .ne. 0.0) then
        if (initial(1) .eq. 16) then
        k1 = 0.1160
        k2 = 0.3610
        k3 = 0.4510
        k4 = 0.0030
        elseif (initial(1) .eq. 12.0) then
        k1 = 0.0615
        k2 = 0.2128
        k3 = 0.2660
        k4 = 0.0025
        elseif (initial(1) .eq. 8.0) then
        k1 = 0.0549
        k2 = 0.1594
        k3 = 0.1950
        k4 = 0.0020
        else
        k1 = 0.0270
        k2 = 0.0800
        k3 = 0.1290
        k4 = 0.0015
        endif
        else
c
c       coding the bromate alone kinetic constants
c
        if (initial(1) .eq. 16.0) then
        k1 = 0.0530
        k2 = 0.3610
        k3 = 0.4510
        k4 = 0.003
        elseif (initial(1) .eq. 12.0) then
        k1 = 0.0320
        k2 = 0.2000
        k3 = 0.2600
```

Reproduced with permission of the copyright owner. Further reproduction prohibited without permission.

```
      k4 = 0.0025
      elseif (initial(1) .eq. 8.0) then
      k1 = 0.0266
      k2 = 0.1575
      k3 = 0.1945
      k4 = 0.0020
      else
      k1 = 0.0151
      k2 = 0.1065
      k3 = 0.1277
      k4 = 0.0015
      endif
      endif
c
      if (initial(1) .eq. 16.0) k5 = 0.220
      if (initial(1) .eq. 12.0) k5 = 0.130
      if (initial(1) .eq. 8.0)  k5 = 0.085
      if (initial(1) .eq. 4.0)  k5 = 0.066
c
c     The reaction between NO2- and TFB and is a chemical one and thus k6 is
c     independent of Light Intensity
c
      k6 = 3.0e03
c
      ka = 10.0**(-8.69)
c
      K50 = y(7)/(Ka + y(7))
      K60 = Ka/(Ka + y(7))
c
      dydx(1) = -k1*y(1) + 0.33*k4*(K60)*(y(2))
      dydx(2)=k1*y(1)-k2*K60*y(2)-k4*(K60)*y(2)-k6*K60*y(2)*y(4)**2.0
+ -k3*K50*y(2)
      dydx(3)= k2*K60*y(2)+k3*K50*y(2)+0.67*k4*(K60)*y(3)+k6*K60*y(2)*y(4)
     + **2.0
      dydx(4) = -k5*y(4) - k6*K60*y(2)*y(4)**2.0
      dydx(5) = k5*y(4) + k6*K60*y(2)*y(4)**2.0
      dydx(6) = k1*y(1) + 0.5*k2*K60*y(2) + 0.5*k3*K50*y(2)
      dydx(7) = k3*K50*y(2)
      return
      end
```

Reproduced with permission of the copyright owner. Further reproduction prohibited without permission.

APPENDIX B

TABLES OF EXPERIMENTAL DATA

Reproduced with permission of the copyright owner. Further reproduction prohibited without permission.

Table B-1. Results of Experiment # 1. The Initial Concentration of Reactants and Products are Shown at Time = 0.0 min. UV Light Intensity = 2.61 x 10^{-6} Einstein L^{-1} s^{-1}; λ = 2537Å; $\mu = 6.25 \times 10^{-5}$.

Time (min)	BrO_3^- (mM)	Br^- (mM)	TFB (mM)	pH	Temp (°C)
0.0	0.036	BDL	BDL	8.01	25.0
1.2	0.033	0.00162	0.000153(2.8)		
4.6	0.028	0.0063	0.00098(7.0)		
8.8	0.023	0.0107	0.00091(9.9)		
12.0	0.0199	0.0135	-		
15.3	0.0165	0.0187	0.00036(12.9)		
18.7	0.0153	0.0200	0.00057(16.7)		
22.1	0.0117	0.0233	0.00044(19.8)		
25.9	0.0106	0.0247	0.000084(28.5)		
31.0	0.0077	0.028	-		
37.0	0.0058	0.0298	-		
40.9	0.0052	0.0310	-		
45.0	0.00454	0.0317	-		
51.0	0.0029	0.0331	-		
62.0	0.0016	0.0357	-		26.8

Note: The bracketed term in the fourth column represents the reaction time for TFB.

Reproduced with permission of the copyright owner. Further reproduction prohibited without permission.

Table B-2. Results of Experiment # 2. The Initial Concentration of Reactants and Products are Shown at Time = 0.0 min. UV Light Intensity = 2.61 x 10^{-6} Einstein L^{-1} s^{-1}; λ = 2537Å; μ =1.00 x 10^{-4}.

Time (min)	BrO_3^- (mM)	Br^- (mM)	TFB (mM)	pH	Temp (°C)
0.0	0.074	BDL	BDL	8.16	24.0
1.0	0.069	0.0022	0.0026(2.2)		
3.8	0.060	0.0076	0.0039(4.7)		
8.3	0.053	0.0166	0.0046(6.2)		
11.4	0.0433	0.026	0.0042(9.5)		
16.1	0.036	0.0346	0.0033(11.4)		
20.3	0.030	0.0408	0.003(17.7)		
24.4	0.025	0.0467	0.003(21.9)		
29.5	0.021	0.0497	0.0015(27.3)		
34.3	0.0184	0.0497	9.02e-05(30.7)		
41.0	0.013	0.0593	0.00043(37.2		
46.9	0.011	0.0616	BDL (51.7)		
50.7	0.009	0.0646	-		
56.3	0.007	0.06704	-	6.38	26.5

Note: The bracketed term in the fourth column represents the reaction time for TFB.

Reproduced with permission of the copyright owner. Further reproduction prohibited without permission.

Table B-3. Results of Experiment #3. The Initial Concentration of Reactants andProducts are Shown at Time = 0.0 min. UV Light Intensity = 2.61 x 10^{-6} Einstein L^{-1} s^{-1}; λ = 2537Å; μ =7.5 x 10^{-5}.

Time (min)	BrO_3^- (mM)	Br^- (mM)	TFB (mM)	pH	Temp (°C)
0.0	0.0485	BDL	BDL	8.10	25.5
1.3	0.046	0.00214	0.00178(3.3)		
5.3	0.037	0.0089	0.00178(6.4)		
8.7	0.032	0.0152	0.00142(10.1)		
12.0	0.027	0.02014	0.0016(13.3)		
16.4	0.024	-	0.00148(17.4)		
20.0	0.018	0.0296	0.00118(21.2)		
24.8	0.015	0.0332	0.00154(26.9)		
29.2	0.012	0.0363	0.00123(31.4)		
33.7	0.0108	0.0388	0.00046(38.3)		
37.2	0.0092	0.00395	0.00076(43.4)		
42.1	0.0068	0.0424	0.00058(46.1)		
48.4	0.0052	0.0439	0.00017(52.5)		
55.1	0.0036	0.0460	-		
60.1	0.0026	0.0470	-		28.4

Note: The bracketed term in the fourth column represents the reaction time for TFB.

Reproduced with permission of the copyright owner. Further reproduction prohibited without permission.

Table B-4. Results of Experiment # 4. The Initial Concentration of Reactants and Products are Shown at Time = 0.0 min. UV Light Intensity = 2.61 x 10^{-6} Einstein L^{-1} s^{-1}; λ = 2537Å; $\mu = 5.0 \times 10^{-5}$.

Time (min)	BrO_3^- (mM)	Br^- (mM)	TFB (mM)	pH	Temp (°C)
0.0	0.0234	BDL	BDL	8.08	26.0
0.9	0.0220	0.00057	0.00022(2.0)		
4.3	0.0190	0.00417	0.00046(5.2)		
8.0	0.0160	0.00732	0.00011(8.9)		
11.1	0.0130	0.0100	0.00029(16)		
15.0	0.0112	0.01182	0.00011(31.2)		
18.6	0.0088	0.0145	0.00011(47.5)		
23.9	0.0074	0.0161	-		
26.7	0.0064	0.0172	-		
29.8	0.0058	0.0183	-		
36.0	0.0040	0.0201	-		
39.8	0.0032	0.0208	-		
44.7	0.0030	0.0213	-		
53.7	0.0018	0.0224	-		
58.5	0.0014	0.0224	-		27.8

Note: The bracketed term in the fourth column represents the reaction time for TFB.

Reproduced with permission of the copyright owner. Further reproduction prohibited without permission.

Table B-5. Results of Experiment # 6. The Initial Concentration of Reactants and Products are Shown at Time = 0.0 min. UV Light Intensity = 2.61 x 10^{-6} Einstein L^{-1} s^{-1}; λ = 2537Å; μ = 3.75 x 10^{-5}.

Time (min)	BrO_3^- (mM)	Br^- (mM)	TFB (mM)	pH	Temp (°C)
0.0	0.012	0	BDL	8.25	25.0
1.3	0.0107	0.00036	BDL		
4.1	0.0098	0.00161	BDL		
7.5	0.0085	0.00302	BDL		
11.1	0.0077	0.00388	BDL		
14.4	0.0068	0.00459	BDL		
18.3	0.0061	0.00537	BDL		
22.1	0.0049	0.00678	BDL		
25.0	0.0041	0.00749	BDL		
29.3	0.0035	0.00828	BDL		
32.5	0.0033	0.00867	BDL		
36.5	0.0032	0.00843	BDL		
40.0	0.0028	0.00914	BDL		
45.4	-		BDL		
48.5	0.0018	0.0101	BDL		
53.3	-	0.0103	BDL		
57.3	0.0015	0.0102	BDL		27.2

Reproduced with permission of the copyright owner. Further reproduction prohibited without permission.

Table B-6. Results of Experiment # 7. The Initial Concentration of Reactants and Products are Shown at Time = 0.0 min. UV Light Intensity =2.61 x 10^{-6} Einstein L^{-1} s^{-1}; λ = 2537Å; $\mu = 4.5 \times 10^{-5}$.

Time (min)	BrO_3^- (mM)	Br^- (mM)	TFB (mM)	pH	Temp (°C)
0.0	0.0375	BDL	BDL	6.90	22.5
1.3	0.0355	0.0014	0.00115		
3.8	0.0318	0.0049	0.0022		
7.2	0.0273	0.0085	0.0035		
10.5	0.0239	0.0125	0.0034		
14.0	0.0203	0.0156	0.0026		
19.5	0.0172	0.0193	0.0024		
24.8	0.0162	0.0245	0.0027		
30.0	0.0098	0.0272	0.0025		
36.0	0.0075	0.0298	0.0017		
42.2	0.0061	0.0317	0.0012		
46.5	0.0054	0.0327	0.0015		
55.7	0.0036	0.0350	0.00023	5.75	25.2
62.5	0.0034	0.0362	BDL		

Reproduced with permission of the copyright owner. Further reproduction prohibited without permission.

Table B-7. Results of Experiment # 8. The Initial Concentration of Reactants and Products are Shown at Time = 0.0 min. UV Light Intensity =2.61 x 10^{-6} Einstein L^{-1} s^{-1}; λ = 2537Å; $\mu = 2.38 \times 10^{-4}$.

Time (min)	BrO_3^- (mM)	Br^- (mM)	TFB (mM)	pH	Temp (°C)
0.0	0.0382	BDL	BDL	9.08	24.0
1.1	0.0353	0.0016	0.00048		
3.9	0.03099	0.0061	0.00048		
8.7	0.0248	0.0116	0.0016		
12.7	0.02048	0.0161	0.0017		
17.8	-	0.0206	0.0012		
21.8	0.0139	0.0241	0.0037		
26.3	0.0098	0.0282	0.00029		
31.4	0.0077	0.0308	0.00037		
34.0	0.0065	0.0327	0.00037		
42.3	0.0050	0.0331	-		
45.7	0.0042	0.0343	-		
47.1	0.0040	0.0355	4.72e-05		
55.0	0.0021	0.0367	BDL		26.2

Reproduced with permission of the copyright owner. Further reproduction prohibited without permission.

Table B-8. Results of Experiment # 10. The Initial Concentration of Reactants and Products are Shown at Time = 0.0 min. UV Light Intensity = 1.15 x 10^{-6} Einstein L^{-1} s^{-1}; λ = 2537Å; μ = 6.25 x 10^{-5}.

Time (min)	BrO_3^- (mM)	Br^- (mM)	TFB (mM)	pH	Temp (°C)
0.0	0.0377	BDL	BDL	8.26	22.0
1.2	0.0363	0.0013	0.00012		
4.4	0.0326	0.0044	0.00075		
8.3	0.0264	0.0080	0.0033		
12.1	0.0231	0.0112	0.0034		
14.8	0.0217	0.0126	0.00344		
19.7	0.0188	0.0153	0.00361		
24.2	0.0160	0.0174	0.00435		
29.5	0.0145	0.0194	0.0038		
34.5	0.0123	0.0221	0.00327		
43.3	0.0100	0.0246	0.00309		
47.2	0.0090	0.0258	0.0028		
60.5	0.0063	0.0313	0.0002		
65.3	0.0057	0.0319	BDL		
70.5	0.0049	0.0333	BDL		
77.0	0.0045	0.0335	BDL		
80.0	0.0040	0.0340	BDL		24.0

Reproduced with permission of the copyright owner. Further reproduction prohibited without permission.

Table B-9. Results of Experiment # 11. The Initial Concentration of Reactants and Products are Shown at Time = 0.0 min. UV Light Intensity = 2.61 x 10^{-6} Einstein L^{-1} s^{-1}; λ = 2537Å; $\mu = 6.25 \times 10^{-5}$.

Time (min)	BrO_3^- (mM)	Br^- (mM)	TFB (mM)	pH	Temp (°C)
0.0	0.0377	BDL	BDL	8.30	23.0
1.2	0.0346	0.0016	0.0015		
4.7	0.0312	0.0057	0.0008		
7.9	0.0273	0.0087	0.0017		
11.8	0.0215	0.0126	0.0036		
15.7	0.0184	0.0158	0.0035		
20.9	0.0156	0.0189	0.0032		
26.3	0.0127	0.0219	0.0031		
30.4	0.0110	0.0235	0.0032		
36.6	0.0092	0.0285	BDL		
40.3	0.0086	0.0292	BDL		
45.4	0.0063	0.0313	BDL		
51.2	0.0053	0.0326	BDL		
55.6	0.0047	0.0338	BDL		
59.0	0.0043	0.0340	BDL	7.5	25.0

Reproduced with permission of the copyright owner. Further reproduction prohibited without permission.

Table B-10. Results of Experiment # 12. The Initial Concentration of Reactants and Products are Shown at Time = 0.0 min. UV Light Intensity = 4.35 x 10^{-7} Einstein L^{-1} s^{-1}; λ = 2537Å; μ =6.25 x 10^{-5}.

Time (min)	BrO_3^- (mM)	Br^- (mM)	TFB (mM)	pH	Temp (°C)
0.0	0.0377	BDL	BDL	8.23	21.0
1.1	0.0362	0.00093	0.00047		
3.1	0.0337	0.0023	0.0015		
6.1	0.0329	0.0039	0.0017		
10.2	0.0305	0.0064	0.0018		
14.0	0.0282	0.0896	0.00192		
18.8	0.0229	0.0106	0.00099		
22.1	0.0220	0.0117	0.00085		
26.6	0.0200	0.0145	0.00050		
30.7	0.0180	0.0156	0.00048		
36.0	0.0165	0.0177	0.00045		
41.2	0.0145	0.0120	0.00049		
48.2	0.0130	0.0214	0.00030		
55.7	0.0120	0.0232	0.00023		
62.6	0.0095	0.0272	BDL		
73.9	0.0081	0.0282	BDL		
83.7	0.0068	0.0296	BDL		
92.4	0.0057	0.0312	BDL		
107.4	0.0044	0.0335	BDL		23.0

Reproduced with permission of the copyright owner. Further reproduction prohibited without permission.

Table B-11. Results of Experiment # 13. The Initial Concentration of Reactants and Products are Shown at Time = 0.0 min. UV Light Intensity = 2.30 x 10^{-7} Einstein L^{-1} s^{-1}; λ = 2537Å; μ = 6.25 x 10^{-5}.

Time (min)	BrO_3^- (mM)	Br^- (mM)	TFB (mM)	pH	Temp (°C)
0.0	0.0377	BDL	BDL	8.17	21.0
1.1	0.0374	0.00070	0.00011		
3.4	0.0366	0.00139	0.00016		
7.8	0.0352	0.00253	0.00022		
11.9	0.0327	0.00368	0.00153		
15.7	0.0323	0.00529	0.00164		
21.3	0.0305	0.00655	0.00132		
29.7	0.0284	0.0085	0.0011		
39.5	0.0238	0.0103	0.0010		
48.3	0.0206	0.0136	0.00108		
53.4	0.0190	0.0147	0.00075		
57.7	0.0196	0.0147	0.000667		
61.7	0.0183	0.0158	0.00070		
68.2	0.0173	0.0170	0.00023		
74.4	0.0169	0.0175	BDL		
83.2	0.0159	0.0181	BDL		
94.8	0.0136	0.0200	BDL		
109.3	0.0114	0.0250	BDL		
113.4	0.0112	0.02617	BDL		
121.5	0.0106	0.0264	BDL		
137.6	0.0094	0.0278	BDL		
154.5	0.0075	0.02940	BDL		
168.3	0.0077	0.02940	BDL		

Reproduced with permission of the copyright owner. Further reproduction prohibited without permission.

Table B-12. Results of Experiment # 14. The Initial Concentration of Reactants and Products are Shown at Time = 0.0 min. UV Light Intensity = 2.30 x 10^{-7} Einstein L^{-1} s^{-1}; λ = 2537Å; $\mu = 9.82 \times 10^{-5}$.

Time (min)	BrO_2^- (mM)	Br^- (mM)	TFB (mM)	NO_2^- (mM)	NO_3^- (mM)	pH	Temp (°C)
0.0	0.0373	BDL	BDL	0.0357	BDL	8.23	23.0
1.5	0.0356	0.00083	0.00057	0.0345	0.00047		
4.6	0.0326	0.00193	0.00204	0.0322	0.00292		
7.9	0.0316	0.00348	0.00344	0.0271	0.00562		
12.6	0.0283	0.00526	0.00463	0.0235	0.00881		
17.8	0.0231	0.00724	0.00603	0.0195	0.0112		
24.6	0.0202	0.0106	0.00715	0.0157	0.0174		
29.6	0.0179	0.0123	0.00603	0.0124	0.02035		
34.1	0.0163	0.0141	0.00568	0.00997	0.0228		
44.3	0.0133	0.0181	0.00428	0.00506	0.0309		
51.4	0.0116	0.0203	0.00372	0.00285	0.0334		
58.8	0.0104	0.0227	0.0010	BDL	0.0353		
63.6	0.0100	0.0263	0.00008	0.00138	0.0348		
78.3	0.0092	0.0271	BDL	0.00138	0.0346		
91.5	0.0076	0.02891	BDL	BDL	0.0348		
113.2	0.0057	0.0311	BDL	BDL	0.0348		
136.0	0.0043	0.0318	BDL	BDL	0.0341	6.28	22.0

Reproduced with permission of the copyright owner. Further reproduction prohibited without permission.

Table B-13 . Results of Experiment # 15. The Initial Concentration of Reactants and Products are Shown at Time = 0.0 min. UV Light Intensity =2.30 x 10^{-7} Einstein L^{-1} s^{-1}; λ = 2537Å; μ = 6.25 x 10^{-5}.

Time (min)	BrO_3^- (mM)	Br^- (mM)	TFB (mM)	pH	Temp (°C)
0.0	0.0373	BDL	BDL	8.26	21.6
1.5	0.0363	0.00083	0.00017		
4.3	0.0349	0.00171	0.00062		
9.4	0.0341	0.00304	0.0011		
15.1	0.0312	0.00437	0.0017		
21.6	0.0302	0.00591	0.0013		
31.7	0.0281	0.0079	0.00119		
42.8	0.0263	0.00967	0.00105		
51.7	0.0220	0.01122	0.00087		
58.1	0.0210	0.0126	0.00037		
68.3	0.0190	0.0148	BDL		
82.3	0.0176	0.0159	BDL		
101.8	0.0149	0.0190	BDL		
103.5	0.0139	0.0198	BDL		
108.5	0.0141	0.0205	BDL		
128.6	0.0128	0.0203	BDL		
133.6	0.0121	0.0216	BDL		
149.5	0.0112	0.0221	BDL		
160.3	0.0098	0.0265	BDL	6.38	22.0

Reproduced with permission of the copyright owner. Further reproduction prohibited without permission.

Table B-14. Results of Experiment # 16. The Initial Concentration of Reactants and Products are Shown at Time = 0.0 min. UV Light Intensity =2.30 x 10^{-7} Einstein L^{-1} s^{-1}; λ = 2537Å; μ = 1.16 x 10^{-4}.

Time (min)	BrO_3^- (mM)	Br^- (mM)	TFB (mM)	NO_2^- (mM)	NO_3^- (mM)	pH	Temp (°C)
0.0	0.0368	BDL	BDL	0.0542	BDL	8.29	23.0
1.5	0.0356	0.00094	0.00062	0.0535	0.00071		
4.6	0.0332	0.00223	0.00169	0.0505	0.00292		
8.2	0.0304	0.00384	0.00308	0.0473	0.00611		
12.1	0.0281	0.00567	0.00409	0.0441	0.00956		
16.2	0.0253	0.00717	0.00484	0.0404	0.0120		
20.5	0.0235	0.0091	0.00472	0.0377	0.0152		
25.2	0.0212	0.0108	0.00554	0.0342	0.0189		
30.6	0.0167	0.01297	0.00560	0.0308	0.0250		
36.4	0.0145	0.01533	0.00421	0.0273	0.0275		
41.6	0.0125	0.0201	0.00478	0.0233	0.0324		
47.6	0.0107	0.0222	0.00409	0.0172	0.0356		
54.8	0.0087	0.02478	0.00390	0.0132	0.0399		
63.3	0.0066	0.0282	0.00182	0.0103	0.04317		
71.9	0.0058	0.02972	0.000748	0.00879	0.0451		
75.7	0.0042	0.03166	BDL	0.00607	0.0478		
83.7	0.0042	0.03159	BDL	0.00607	0.0473		
92.9	0.0036	0.0332	BDL	0.00558	0.0486	6.02	24.0

Reproduced with permission of the copyright owner. Further reproduction prohibited without permission.

Table B-15. Results of Experiment # 17r. The Initial Concentration of Reactants and Products are Shown at Time = 0.0 min. UV Light Intensity = 2.30 x 10^{-7} Einstein L^{-1} s^{-1}; λ = 2537Å; μ = 8.04 x 10^{-5}.

Time (min)	BrO_3^- (mM)	Br^- (mM)	TFB (mM)	NO_2^- (mM)	NO_3^- (mM)	pH	Temp (°C)
0.0	0.0383	BDL	BDL	0.0166	BDL	8.22	23.5
1.4	0.0374	0.00019	0.00065	0.0159	0.00141		
4.3	0.0351	0.00157	0.00214	0.0137	0.00404		
7.9	0.0316	0.00137	0.00338	0.0101	0.0094		
11.8	0.0285	0.0055	0.00381	0.0069	0.0104		
17.5	0.0253	0.0094	0.00424	0.00286	0.0152		
22.0	0.0235	0.0110	0.00517	BDL	0.01767		
26.6	0.0222	0.0129	0.00362	BDL	0.0179		
30.8	0.0206	0.0150	0.00183	BDL	0.01742		
42.9	0.0193	0.0182	0.00027	BDL	0.0179		
59.1	0.0158	0.0210	0.00083	BDL	0.0179		
68.1	0.0143	0.0237	0.00065	BDL	0.0182	6.49	
77.2	0.0124	0.0256	BDL	BDL	0.0179		
86.4	0.0116	0.0265	BDL	BDL	0.0182		
102.3	0.0099	0.0281	BDL	BDL	0.0182	5.96	
115.1	0.0083	0.0306	BDL	BDL	0.0182		
122.5	0.0058	0.0309	BDL	BDL	0.0182		24.0

Reproduced with permission of the copyright owner. Further reproduction prohibited without permission.

Table B-16. Results of Experiment # 18r. The Initial Concentration of Reactants and Products are Shown at Time = 0.0 min. UV Light Intensity = 2.30 x 10^{-7} Einstein L^{-1} s^{-1}; λ = 2537Å; $\mu = 9.82 \times 10^{-5}$.

Time (min)	BrO_3^- (mM)	Br^- (mM)	TFB (mM)	NO_2^- (mM)	NO_3^- (mM)	pH	Temp (°C)
0.0	0.0378	BDL	BDL	0.0335	BDL	8.17	23.3
1.5	0.03655	0.00019	0.00065	0.0327	0.00136		
4.6	0.0345	0.00157	0.00232	0.0308	0.0038		
8.5	0.0308	0.00388	0.00368	0.0260	0.00769	7.26	
12.4	0.0276	0.00619	0.00499	0.0223	0.0118		
16.9	0.0245	0.0090	0.00635	0.0183	0.0167		
20.5	0.0222	0.0108	0.0066	0.0146	0.0199		
25.1	0.0197	0.0136	0.00629	0.0110	0.0235		
30.0	0.0174	0.0159	0.0059	0.00791	0.0269	6.29	
34.6	0.0147	0.0193	0.00517	0.0036	0.0313		
40.5	0.0133	0.0228	0.0044	0.0012	0.0337		
47.3	0.0122	0.0240	0.00145	0.0012	0.0335		
56.1	0.0108	0.0256	0.00046	0.00069	0.0335		
66.4	0.0091	0.0286	0.000399	BDL	0.0347		
70.1	0.0087	0.0293	0.00034	BDL	0.0352	6.06	
81.8	-	-	0.00046	-	-		
91.9	0.0066	0.0318	BDL	BDL	0.0352		
100.8	0.0053	0.032	BDL	BDL	0.0349		
119.9	0.0045	0.0341	BDL	BDL	0.0357		24

Reproduced with permission of the copyright owner. Further reproduction prohibited without permission.

Table B-17. Results of Experiment # 19r. The Initial Concentration of Reactants and Products are Shown at Time = 0.0 min. UV Light Intensity = 2.30 x 10^{-7} Einstein L^{-1} s^{-1}; λ = 2537Å; μ = 1.16 x 10^{-4}.

Time (min)	BrO_3^- (mM)	Br^- (mM)	TFB (mM)	NO_2^- (mM)	NO_3^- (mM)	pH	Temp (°C)
0.0	0.0380	BDL	BDL	0.0506	BDL	8.17	23.1
1.5	0.0368	0.00019	0.00046	0.0500	0.00136		
5.0	0.0349	0.0016	0.00195	0.0481	0.00428	7.75	
9.3	0.0306	0.00342	0.00437	0.0433	0.0082		
13.5	0.0276	0.0050	0.00529	0.0397	0.0118		
17.6	0.0253	0.0076	0.00493	0.0368	0.0143		
21.7	0.0231	0.0097	0.00505	0.0341	0.0172		
26.7	0.0193	0.0117	0.0067	0.0286	0.0228	7.80	
30.8	0.0174	0.0147	0.0059	0.0257	0.0260		
36.7	0.0147	0.0170	0.0067	0.0211	0.0303		
42.0	0.0124	0.0214	0.0050	0.0173	0.0345		
46.9	0.0105	0.0221	0.0061	0.0144	0.0379		
51.8	0.0095	0.0228	0.00486	0.0127	0.0393	7.65	
58.9	0.0087	0.0267	0.00207	0.0115	0.0405		
64.7	0.0064	0.0290	0.00257	0.0074	0.0449		
70.9	0.0055	0.0306	0.00195	0.0062	0.0461	7.46	
80	0.0051	0.0323	BDL	0.0062	0.0461		
87.3	0.0037	0.0321	BDL	0.0038	0.0459		
100.3	0.0032	0.0348	BDL	0.00478	0.0478		
108.5	0.0022	0.0357	BDL	0.0033	0.0491		
118.5	0.0014	0.0371	BDL	0.0021	0.0503	7.19	23.7

Reproduced with permission of the copyright owner. Further reproduction prohibited without permission.

Table B-18. Results of Experiment # 20r. The Initial Concentration of Reactants and Products are Shown at Time = 0.0 min. UV Light Intensity = 2.30 x 10^{-7} Einstein L^{-1} s^{-1}; λ = 2537Å; μ = 8.75 x 10^{-5}.

Time (min)	BrO_3^- (mM)	Br^- (mM)	TFB (mM)	NO_2^- (mM)	NO_3^- (mM)	pH	Temp (°C)
0.0	0.0380	BDL	BDL	0.0335	BDL	7.10	23.5
1.6	0.037	0.00019	0.0016	0.0325	0.0016		
5.1	0.0335	0.0034	0.0060	0.0281	0.0060	5.32	
9.2	0.0299	0.0055	0.0118	0.0228	0.0118		
13.4	0.0266	0.0087	0.0282	0.0173	0.0166		
16.8	0.0237	0.0108	0.00325	0.0130	0.0216		
21.3	0.0210	0.0136	0.00306	0.00935	0.0247		
26.3	0.0183	0.0168	0.00338	0.0061	0.0301		
30.4	0.0162	0.0187	0.00375	0.00093	0.0342	5.38	
38.5	0.0145	0.0214	0.00145	BDL	0.03445		
46.9	0.0133	0.0233	0.00251	BDL	0.0352		
56.4	0.0128	0.0235	0.00257	BDL	0.0354		
63.5	0.0110	0.0260	0.00065	BDL	0.0354		
71.2	0.0099	0.02672	0.00034	BDL	0.03543		
86.5	0.0089	0.0286	0.00102	BDL	0.0362	5.06	
98.7	0.0076	0.0302	BDL	BDL	0.0357		
110.4	0.0068	0.0309	BDL	BDL	0.0359	4.87	24.8

Reproduced with permission of the copyright owner. Further reproduction prohibited without permission.

Table B-19. Results of Experiment # 21r. The Initial Concentration of Reactants and Products are Shown at Time = 0.0 min. UV Light Intensity = 2.30 x 10^{-7} Einstein L^{-1} s^{-1}; λ = 2537Å; μ = 2.73 x 10^{-4}.

Time (min)	BrO_3^- (mM)	Br^- (mM)	TFB (mM)	NO_2^- (mM)	NO_3^- (mM)	pH	Temp (°C)
0.0	0.0386	BDL	BDL	0.0332	BDL	9.43	24.1
1.4	0.0372	0.00019	0.00071	0.0322	0.00136		
4.4	0.0347	0.0018	0.00102	0.0298	0.0036		
7.7	0.0318	0.0041	0.00257	0.0281	0.0065		
11.5	0.0289	0.0060	0.00276	0.0245	0.00891	9.20	
16.0	0.0243	0.00942	0.00344	0.0204	0.0128		
20.3	0.0217	0.0115	0.00505	0.0175	0.0165		
24.7	0.0187	0.0124	0.00747	0.0127	0.0203	9.23	
29.5	0.0168	0.0140	0.00697	0.0113	0.0228		
34.1	0.0151	0.0182	0.00381	0.0106	0.0233		
40.1	0.0130	0.0191	0.00567	0.0070	0.0276		
45.1	0.0105	0.0207	0.00747	0.0036	0.0308		
48.3	0.0093	0.0228	0.00647	0.0021	0.0325		
54.4	0.0074	0.0249	0.00586	0.00045	0.0340		
61.8	0.0068	0.0274	0.00468	0.00021	0.0347		
69.5	0.0066	0.0290	0.00220	0.00053	0.0337		
79.3	0.0053	0.0320	0.00021	0.00021	0.0345	9.20	
90.9	0.0043	0.0330	BDL	0.00045	0.0345		
104.8	0.0032	0.0339	BDL	0.00093	0.0345	9.16	25.1

Reproduced with permission of the copyright owner. Further reproduction prohibited without permission.

Table B-20. Results of Experiment # 24. The Initial Concentration of Reactants and Products are Shown at Time = 0.0 min. UV Light Intensity = 4.35 x 10^{-7} Einstein L^{-1} s^{-1}; λ = 2537Å; μ = 8.75 x 10^{-4}.

Time (min)	BrO_3^- (mM)	Br^- (mM)	TFB (mM)	NO_2^- (mM)	NO_3^- (mM)	pH	Temp (°C)
0.0	0.0380	BDL	BDL	0.0357	BDL	7.17	24.0
1.7	0.034	0.0013	0.0012	0.0332	0.0034		
3.3	-	-	0.0028	-	-		
5.8	0.0270	0.0071	0.0042	0.0213	0.0136	5.42	
10.1	0.0210	0.0122	0.0044	0.0119	0.0222		
12.5	0.0180	0.0151	0.0046	0.0066	0.0274		
15.5	0.0160	0.0178	0.0035	0.0030	0.0308		
17.9	0.0140	0.0203	0.0030	0.0008	0.0329		
28.5	0.0110	0.0239	0.0023	0.0003	0.0334		
33.8	0.0100	0.0259	0.0010	BDL	0.0336		
40.3	0.0092	0.0272	0.0016	BDL	0.0336		
42.3	0.0084	0.0279	0.0016	BDL	0.0339		
47.6	0.0076	0.0286	0.00053	BDL	0.0336		
52.8	0.0072	0.0294	0.0014	BDL	0.0341		
55.5	0.0066	0.0294	0.0021	BDL	0.0339		
60.3	0.0060	0.0306	0.0019	BDL	0.0341		
66.8	0.0056	0.0315	0.0004	BDL	0.0339		
75.5	0.0044	0.0324	BDL	BDL	0.0341		
80	0.0040	0.0328	0.00005	BDL	0.0341	4.72	25.0

Reproduced with permission of the copyright owner. Further reproduction prohibited without permission.

Table B-21. Results of Experiment # 25. The Initial Concentration of Reactants and Products are Shown at Time = 0.0 min. UV Light Intensity = 4.35 x 10^{-7} Einstein L^{-1} s^{-1}; λ = 2537Å; $\mu = 9.82 \times 10^{-5}$.

Time (min)	BrO_3^- (mM)	Br^- (mM)	TFB (mM)	NO_2^- (mM)	NO_3^- (mM)	pH	Temp (°C)
0.0	0.0375	BDL	BDL	0.0357	BDL	8.17	24
1.5	0.0338	0.0010	0.0012	0.0332	0.0027		
3.4	0.0308	0.0026	0.0030	0.0297	0.00602		
5.3	0.0274	0.0048	0.0050	0.0247	0.0105	7.58	
8.8	0.0220	0.0091	0.0062	0.0175	0.0170		
11.7	0.0190	0.0120	0.0064	0.0127	0.0215		
14.5	0.0168	0.0147	0.0061	0.0090	0.0251		
17.3	0.0140	0.0174	0.0063	0.0045	0.0293		
20.3	0.0124	0.0207	0.0042	0.0022	0.0320		
25.3	0.0106	0.0225	0.0014	0.00075	0.0310		
29.5	0.0098	0.0261	0.0011	BDL	0.0336		
33.1	0.0092	0.0274	BDL	BDL	0.0336		
39.3	0.0082	0.0286	BDL	BDL	0.0334		
46.3	0.0062	0.0306	BDL	BDL	0.0341		
54.0	0.0048	0.0299	BDL	BDL	0.0315		
59.5	0.0040	0.0335	BDL	BDL	0.0339		
66.3	0.0030	0.0346	BDL	BDL	0.0339		
71.5	0.0022	0.0355	BDL	BDL	0.0339		
76.1	0.0021	0.0315	BDL	BDL	0.0293		
80.0	0.0014	0.0364	BDL	BDL	0.0339	7.34	25.5

Reproduced with permission of the copyright owner. Further reproduction prohibited without permission.

Table B-22. Results of Experiment # 26. The Initial Concentration of Reactants and Products are Shown at Time = 0.0 min. UV Light Intensity = 4.35 x 10^{-7} Einstein L^{-1} s^{-1}; λ = 2537Å; $\mu = 2.73 \times 10^{-4}$.

Time (min)	BrO_3^- (mM Br)	Br^- (mM Br)	TFB (mM Br)	NO_2^- (mM N)	NO_3^- (mM N)	pH	Temp (°C)
0.0	0.038	BDL	BDL	0.0357	BDL	9.47	24.0
1.5	0.0344	0.00125	0.0010	0.0337	0.0025	9.30	
3.0	0.0318	0.0033	0.0022	0.0301	0.0053		
7.0	-	-	0.0051	-	-		
9.3	0.0224	0.0091	0.0060	0.0199	0.0144		
11.6	0.0196	0.0118	0.0060	0.0173	0.0172		
14.2	0.0168	0.0142	0.0069	0.0133	0.0208		
17.0	0.0144	0.0160	0.0067	0.0112	0.0227		
20.0	0.0120	0.0205	0.0055	0.0082	0.0258		
22.8	0.0100	0.0205	0.0060	0.0056	0.0267		
27.6	0.0086	0.0252	0.0035	0.00434	0.0293		
33.3	0.0066	0.0283	0.00096	0.0026	0.0310		
40.5	0.0050	0.0294	0.0027	0.00026	0.0331		
43.5	0.0048	0.0303	0.0020	BDL	0.03314		
47.7	0.0042	0.0310	0.0021	BDL	0.03314		
54.9	0.0030	0.0335	BDL	0.0012	0.0322		
66.0	0.0018	0.0353	BDL	0.0013	0.0327		
75.3	0.0014	0.0357	BDL	0.0020	0.0317		
80.0	0.0011	0.0360	BDL	0.0031	0.0303	9.20	25.5

Reproduced with permission of the copyright owner. Further reproduction prohibited without permission.

Table B-23. Results of Experiment # 27. The Initial Concentration of Reactants and Products are Shown at Time = 0.0 min. UV Light Intensity = 4.35 x 10^{-7} Einstein L^{-1} s^{-1}; λ = 2537Å; $\mu = 8.04 \times 10^{-4}$.

Time (min)	BrO_3^- (mM)	Br^- (mM)	TFB (mM Br)	NO_2^- (mM N)	NO_3^- (mM N)	pH	Temp (°C)
0.0	0.0375	BDL	0.00134	0.0179	BDL	8.14	23.8
1.7	-	-	-0.0036	-	-		
3.4	0.0308	0.0026	0.0048	0.0118	0.0055		
5.3	0.0249	0.0037	0.00568	0.0072	0.0082		
8.4	0.0237	0.0074	0.00615	0.0033	0.0133		
10.5	0.0219	0.0098	0.00496	0.00026	0.0166		
13.3	0.0210	0.0117	0.00354	BDL	0.0169		
16.8	0.0191	0.0139	0.0031	BDL	0.0164		
19.2	0.0173	0.0148	0.00247	BDL	0.0157	7.51	
22.2	0.0175	0.0174	0.0013	BDL	0.0166		
26.1	0.0162	0.0189	0.00057	BDL	0.0166		
32.0	0.0148	0.0213	0.00075	BDL	0.0171		
37.0	0.0129	0.0230	0.00015	BDL	0.0171		
42.0	0.0111	0.0247	0.0002	BDL	0.0171		
47.0	0.0099	0.0263	0.00015	BDL	0.0171		
52.1	0.0092	0.0273	BDL	BDL	0.0169		
57.2	0.0084	0.0280	BDL	BDL	0.0169		
62.6	0.0065	0.0293	BDL	BDL	0.0166		
67.0	0.0061	0.0304	BDL	BDL	0.0169		
72.0	0.0053	0.0315	BDL	BDL	0.0171		
77.0	0.0045	0.0323	BDL	BDL	0.0171		
80.0	0.0045	0.0323	BDL	BDL	0.0171		
85.2	0.0039	0.0330	BDL	BDL	0.0171	6.28	24.7

Reproduced with permission of the copyright owner. Further reproduction prohibited without permission.

Table B-24. Results of Experiment # 28. The Initial Concentration of Reactants and Products are Shown at Time = 0.0 min. UV Light Intensity = 4.35 x 10^{-7} Einstein L^{-1} s^{-1}; λ = 2537Å; μ = 1.16 x 10^{-4}.

Time (min)	BrO_3^- (mM)	Br^- (mM)	TFB (mM)	NO_2^- (mM)	NO_3^- (mM)	pH	Temp (°C)
0.0	0.0375	BDL	BDL	0.0536	BDL	8.18	23.8
1.0	0.0344	0.00088	0.00134	0.0523	0.0018		
2.5	0.0321	0.0022	0.0023	0.0496	0.0039		
4.8	0.0288	0.0037	0.0046	0.0453	0.0084	7.90	
8.3	0.0230	0.0080	0.0066	0.0370	0.0157		
12.9	0.0195	0.0111	0.0074	0.0317	0.0204		
15.5	0.0171	0.0135	0.0078	0.0280	0.0030		
20.1	0.0140	0.0171	0.0066	0.0232	0.0291		
23.4	0.0113	0.0195	0.00645	0.0181	0.0329		
27.4	0.0098	0.0221	0.0061	0.0154	0.0364		
31.7	0.0086	0.0252	0.0038	0.0136	0.0376		
35.7	0.0072	0.0265	0.00288	0.0108	0.0394		
40.2	0.0059	0.0293	0.00288	0.0081	0.0430		
45.2	0.0047	0.0313	0.00127	0.0068	0.0441		
51.6	0.0035	0.0330	0.00051	0.0055	0.0456		
57.8	0.0030	0.0334	0.00009	0.0045	0.0453		
64.7	0.0024	0.0347	0.00015	0.0043	0.0470		
71.4	0.0018	0.0358	0.00003 2	0.0048	0.0465	7.63	
77.0	0.0014	0.0356	BDL	0.0050	0.0458		
80.5	0.0012	0.0356	BDL	0.0055	0.0446		24.7

Reproduced with permission of the copyright owner. Further reproduction prohibited without permission.

Table B-25. Results of Experiment # 29. The Initial Concentration of Reactants and Products are Shown at Time = 0.0 min. UV Light Intensity = 1.15 x 10^{-6} Einstein L^{-1} s^{-1}; λ = 2537Å; $\mu = 6.25 \times 10^{-5}$.

Time (min)	BrO_3^- (mM)	Br^- (mM)	TFB (mM)	pH	Temp (°C)
0.0	0.0375	BDL	BDL	8.18	22.0
1.4	0.03548	0.00169	0.00045		
4.3	0.03254	0.00463	0.00077	7.75	
8.7	0.02893	0.00785	0.00072		
13.0	0.02576	0.01108	0.00056	7.19	
17.4	0.02305	0.01343	0.00057		
21.5	0.01989	0.01636	0.00087		
26.2	0.01786	0.01871	0.00045	6.06	
31.5	0.0147	0.02135	0.00045		
37.9	0.01243	0.02370	0.00045		
42.9	0.01085	0.02575	BDL	5.76	
48.7	0.00905	0.0275	0.00051		
54.9	0.00724	0.02868	0.00030		
63.4	0.00611	0.03073	0.00045		
76.6	0.00385	0.0331	0.00045	5.01	
86.5	0.00272	0.03397	BDL		
96.5	0.00204	0.03485	BDL	6.27	23.5

Reproduced with permission of the copyright owner. Further reproduction prohibited without permission.

Table B-26. Results of Experiment # 30. The Initial Concentration of Reactants and Products are Shown at Time = 0.0 min. UV Light Intensity = 1.15 x 10^{-6} Einstein L^{-1} s^{-1}; λ = 2537Å; $\mu = 8.04 \times 10^{-5}$.

Time (min)	BrO_2^- (mM)	Br^- (mM)	TFB (mM)	NO_2^- (mM)	NO_3^- (mM)	pH	Temp (°C)
0.0	0.0377	BDL	BDL	0.0174	BDL	8.20	22
1.5	0.03412	0.00169	0.0018	0.01425	0.00332		
4.3	-	-	0.0035	--	-		
8.5	0.0226	0.0108	0.00496	0.00087	0.01624	7.89	
12.8	0.0199	0.0146	0.0037	BDL	0.01697		
18.5	0.0174	0.0178	0.0017	BDL			
21.9	-	-	0.00061	BDL		7.04	
27.0	0.01356	0.0225	0.00076	BDL	0.01734		
30.3	0.01221	0.0234	0.0006	BDL	0.0166		
36.9	0.00995	0.0269	0.00040	BDL	0.01734	6.56	
42.9	0.00814	0.0281	0.00045	BDL	0.01697		
48.8	0.00634	0.03015	0.00056	BDL	0.01697		
57.8	0.00498	0.03161	0.00066	BDL	0.01697		
67.4	0.00295	0.03367	0.00040	BDL	0.0185		
80.5	0.00159	0.03514	0.00024	BDL	0.01734	6.61	23

Reproduced with permission of the copyright owner. Further reproduction prohibited without permission.

Table B-27. Results of Experiment # 31. The Initial Concentration of Reactants and Products are Shown at Time = 0.0 min. UV Light Intensity = 1.15 x 10^{-6} Einstein L^{-1} s^{-1}; λ = 2537Å; $\mu = 9.82 \times 10^{-5}$.

Time (min)	BrO_3^- (mM)	Br^- (mM)	TFB (mM Br)	NO_2^- (mM N)	NO_3^- (mM N)	pH	Temp (°C)
0.0	0.03706	BDL	BDL	0.0354	BDL	8.13	22.0
1.5	0.03344	0.0014	0.0025	0.03209	0.00214		
4.7	0.0278	0.00521	0.0052	0.02465	0.00963		
9.0	0.0203	0.00991	0.0067	0.01484	0.01845		
13.3	0.01628	0.01548	0.0064	0.008	0.02768		
18.4	0.01198	0.02047	0.0055	0.00146	0.0332	7.75	
23.8	0.00995	0.02458	0.0032	BDL	0.03432		
27.7	0.0088	0.02722	0.00077	BDL	0.03506	7.32	
32.3	0.00747	0.02840	0.00072	BDL	0.03395		
37.6	0.00611	0.03044	BDL	BDL	0.03395		
41.7	0.00543	0.03103	BDL	BDL	0.03395	7.20	
47.1	0.00453	0.03325	BDL	BDL	0.03395	7.01	
54.3	0.00317	0.03397	BDL	BDL	0.03395		
59.8	0.00182	0.03514	BDL	BDL	0.03395		
65.0	0.00140	0.03543	BDL	0.00027	0.03321	7.24	23.0

Reproduced with permission of the copyright owner. Further reproduction prohibited without permission.

Table B-28. Results of Experiment # 32. The Initial Concentration of Reactants and Products are Shown at Time = 0.0 min. UV Light Intensity = 1.15 x 10^{-6} Einstein L^{-1} s^{-1}; λ = 2537Å; $\mu = 1.16 \times 10^{-4}$.

Time (min)	BrO_3^- (mM)	Br^- (mM)	TFB (mM)	NO_2^- (mM)	NO_3^- (mM)	pH	Temp (°C)
0.0	0.0376	BDL	BDL	0.05364	BDL	8.15	22
1.5	0.0346	0.0014	0.0014	0.05081	0.00295		
4.3	0.0292	0.00433	0.0039	0.04427	0.00923	8.08	
8.2	0.02305	0.00878	0.0059	0.03565	0.01661		
12.8	0.0170	0.01372	0.0067	0.02673	0.02509		
17.5	0.0127	0.01900	0.0062	0.01900	0.03469	7.91	
22.1	0.00950	0.02428	0.0042	0.01365	0.03764		
26.0	0.00724	0.02604	0.0046	0.00979	0.0417	7.95	
30.3	0.00543	0.02927	0.0027	0.00652	0.04465		
34.6	0.00408	0.03074	0.0027	0.00444	0.04465	7.75	
39.9	0.00295	0.03367	0.0026	0.003247	0.04797		
48.3	0.00182	0.03543	0.0019	0.002355	0.04871	7.35	
55.2	0.00137	0.03602	BDL	0.003544	0.04760		
60.0	0.000914	0.03631	BDL	0.003841	0.04723	7.19	22.5

Reproduced with permission of the copyright owner. Further reproduction prohibited without permission.

Table B-29. Results of Experiment # 33. The Initial Concentration of Reactants and Products are Shown at Time = 0.0 min. UV Light Intensity = 1.15 x 10^{-6} Einstein L^{-1} s^{-1}; λ = 2537Å; $\mu = 2.73 \times 10^{-4}$.

Time (min)	BrO_3^- (mM)	Br^- (mM)	TFB (mM Br)	NO_2^- (mM N)	NO_3^- (mM N)	pH	Temp (°C)
0.0	0.0389	BDL	BDL	0.03329	BDL	9.49	21.8
1.4	0.03677	0.000847	0.00074	0.03324	0.00247		
4.3	0.03046	0.00384	0.0037	0.02644	0.00735	9.46	
8.6	0.02346	0.00869	0.0056	0.01958	0.0145		
13.0	0.01786	0.01315	0.00758	0.01358	0.0209		
17.4	0.01483	0.01705	0.0052	0.01073	0.0235		
19.7	0.01179	0.01855	0.00695	0.00673	0.0276		
24.3	0.00899	0.02184	0.0064	0.003874	0.0310	9.41	
31.0	0.006657	0.02665	0.0041	0.001875	0.0333		
33.3	0.00549	0.02665	0.0053	0.000733	0.0340		
37.9	0.00479	0.02845	0.0046	0.000161	0.0352		
43.3	0.00386	0.03115	0.0014	0.000161	0.0348		
47.9	0.00316	0.03205	0.0008	0.000732	0.0340		
53.6	0.00246	0.03355	BDL	0.000732	0.0348	9.40	
61.6	0.00152	0.03415	BDL	0.00130	0.0340	9.37	22.5

Reproduced with permission of the copyright owner. Further reproduction prohibited without permission.

Table B-30. Results of Experiment # 34. The Initial Concentrations of Reactants and Products are Shown at Time = 0.0 min. UV Light Intensity = 1.15 x 10^{-6} Einstein L^{-1} s^{-1}; λ = 2537Å; $\mu = 9.82 \times 10^{-5}$.

Time (min)	BrO_3^- (mM)	Br^- (mM)	TFB (mM Br)	NO_2^- (mM N)	NO_3^- (mM N)	pH	Temp (°C)
0.0	0.0372	BDL	BDL	0.0344	BDL	8.25	21.5
1.4	0.0349	0.00115	0.00149	0.0322	0.00284		
4.5	0.0279	0.00445	0.00425	0.0247	0.0115	8.02	
8.1	0.0225	0.00865	0.00632	0.0176	0.0179		
12.5	0.0174	0.0135	0.00701	0.0102	0.0254		
15.5	0.0144	0.0165	0.0066	0.00587	0.0292	7.90	
20.1	0.00852	0.0162	0.0053	0.00130	0.0269		
24.3	0.00992	0.0242	0.0032	0.000161	0.0352		
28.6	0.00899	0.0267	0.0017	0.000161	0.0359	7.59	
34.1	0.00782	0.0288	0.000051	0.000161	0.0356		
39.3	0.00656	0.0303	0.000051	0.000161	0.0359		
47.0	0.00456	0.0324	BDL	0.000161	0.0352	7.00	
55.9	0.00269	0.0339	BDL	0.000161	0.0356		
61.3	0.00222	0.0344	BDL	0.000161	0.0348		23.0

Reproduced with permission of the copyright owner. Further reproduction prohibited without permission.

Table B-31. Results of Experiment # 35. The Initial Concentration of Reactants and Products are Shown at Time = 0.0 min. UV Light Intensity =1.15 x 10^{-6} Einstein L^{-1} s^{-1}; λ = 2537Å; μ =8.07 x 10^{-5}.

Time (min)	BrO_3^- (mM)	Br^- (mM)	TFB (mM)	NO_2^- (mM)	NO_3^- (mM)	pH	Temp (°C)
0.0	0.0379	BDL	BDL	0.0350	BDL	7.17	22.0
1.4	0.0344	0.00848	0.00091	0.0318	0.00322		
4.5	-	-	0.0040	-	-		
8.5	0.0209	0.0105	0.0041	0.0124	0.0209	5.75	
12.4	0.0176	0.0165	0.0028	0.00644	0.0292		
15.2	0.0153	0.0195	0.0021	0.0245	0.0329		
19.4	-	-	0.0019	-	-		
23.2	0.0118	0.02331	0.0014	0.000447	0.0352	5.20	
27.5	0.0104	0.0249	0.00086	0.000161	0.0350		
34.8	0.00829	0.0264	BDL	0.000161	0.0350		
42.3	0.00666	0.0297	BDL	0.000161	0.0350	5.15	
48.0	0.00549	0.0293	BDL	0.000161	0.0344		
53.3	0.00456	0.03145	BDL	0.000161	0.0356		
60.7	0.00409	0.03295	BDL	0.000161	0.0363		
63.2	0.00363	0.0327	BDL	0.000161	0.0359	5.20	23.0

Reproduced with permission of the copyright owner. Further reproduction prohibited without permission.

Table B-32. Results of Experiment # 36. The Initial Concentration of Reactants and Products are Shown at Time = 0.0 min. UV Light Intensity =1.15 x 10^{-6} Einstein L^{-1} s^{-1}; λ = 2537Å; $\mu = 7.08 \times 10^{-5}$.

Time (min)	BrO_3^- (mM)	Br^- (mM)	TFB (mM)	NO_2^- (mM)	NO_3^- (mM)	pH	Temp (°C)
0.0	0.0377	BDL	BDL	0.0356	BDL	4.93	21
1.5	0.0344	0.00145	0.00074	0.0313	0.00397		
4.4	0.0291	0.00685	0.00172	0.0224	0.0141	4.93	
7.2	0.0242	0.0113	0.0028	0.0142	0.0220		
13.0	0.0179	0.01705	0.00206	0.00502	0.0307		
17.5	0.0148	0.0210	0.00206	0.0013	0.0371		
23.6	0.0130	0.0233	0.0012	0.000447	0.0367		
26.6	0.0113	0.0243	0.0026	0.000161	0.0378		
30.8	0.0104	0.0252	0.0025	0.000161	0.0367		
38.9	0.00852	0.0273	0.0021	0.000161	0.0363		
42.9	0.0076	0.0282	0.0011	0.000161	0.0359		
52.8	0.00619	0.0299	0.00097	0.000161	0.0367		
67.2	0.00409	0.03175	0.0008	0.000161	0.0359	4.99	22.3

Reproduced with permission of the copyright owner. Further reproduction prohibited without permission.

TableB-33. Results of Experiment # 37. The Initial Concentration of Reactants and Products are Shown at Time = 0.0 min. UV Light Intensity = 1.15 x 10^{-6} Einstein L^{-1} s^{-1}; λ = 2537Å; $\mu = 8.75 \times 10^{-5}$.

Time (min)	BrO_3^- (mM Br)	Br^- (mM Br)	TFB (mM Br)	pH	Temp (°C)
0.0	0.0622	0	0	7.79	24.0
3.7	0.0562	0.00405	0.0018		
5.3	0.0540	0.00597	0.0020		
9.1	0.0503	0.009811	0.0023	7.31	
12.2	0.0459	0.0117	0.0042		
17.0	0.0414	0.0185	0.0042		
20.6	0.0377	0.0204	0.0039		
26.5	0.0335	0.0253	0.0032		
32.1	0.0286	0.0304	0.0030	7.02	
37.7	0.0253	0.0336	0.0027		
43.9	0.0220	0.0371	0.0020	6.32	
49.9	0.0204	0.0397	0.0013		
55.6	0.0164	0.0405	0.00086		
61.4	0.0151	0.0446	0	6.30	
68.5	0.0128	0.0469	0		
77.6	0.0106	0.0492	0		
87.7	0.0086	0.0515	0	6.04	
99.4	0.00749	0.0529	0		
115.6	0.00459	0.0555	0		25.4

Reproduced with permission of the copyright owner. Further reproduction prohibited without permission.

Table B-34. Results of Experiment # 38. The Initial Concentration of Reactants and Products are Shown at Time = 0.0 min. UV Light Intensity = 1.15 x 10^{-6} Einstein L^{-1} s^{-1}; λ = 2537Å; $\mu = 6.25 \times 10^{-5}$.

Time (min)	BrO_3^- (mM)	Br^- (mM)	TFB (mM)	pH	Temp (°C)
0.0	0.0362	0	0	7.77	25.0
1.3	0.0351	0.00107	0.00003		
4.6	0.0324	0.00309	0.00069		
8.4	0.0295	0.00568	0.0011	7.68	
12.6	0.0264	0.00856	0.00122		
17.8	0.0237	0.0114	0.00106		
22.8	0.0208	0.0143	0.00076	6.27	
27.1	0.0188	0.0166	0.00054		
34.7	0.0155	0.0198	0.00023		
42.3	0.0131	0.0221	0.00002	5.95	
51.7	0.0106	0.0247	BDL		
61.3	0.0086	0.0267	BDL		
71.8	0.00682	0.0293	BDL		
85	0.00526	0.0310	BDL	5.90	25.9

Reproduced with permission of the copyright owner. Further reproduction prohibited without permission.

Table B-35. Results of Experiment # 39. The Initial Concentrations of Reactants and Products are Shown at Time = 0.0 min. UV Light Intensity = 1.15 x 10^{-6} Einstein L^{-1} s^{-1}; λ = 2537Å; μ =3.75 x 10^{-5}.

Time (min)	BrO_3^- (mM)	Br^- (mM)	TFB (mM)	pH	Temp (°C)
0.0	0.0118	BDL	BDL	7.75	23.2
1.5	0.0113	0.00059	BDL		
4.0	0.0106	0.00171	BDL		
7.1	0.0102	0.00213	BDL	7.42	
11.0	0.00867	0.00309	BDL		
15.5	0.00763	0.00434	BDL		
20.5	0.00674	0.00501	BDL	6.38	
26.1	0.00563	0.00626	BDL		
32.5	0.00504	0.00683	BDL		
39.1	0.00429	0.00760	BDL	6.42	
45.8	0.00363	0.00827	BDL		
54.4	0.00281	0.00894	BDL		
61.7	0.0229	0.00962	BDL	5.74	
71.8	0.00192	0.00990	BDL		
80.8	0.00162	0.01020	BDL		24.5

Reproduced with permission of the copyright owner. Further reproduction prohibited without permission.

Table B-36. Results of Experiment # 40. The Initial Concentration of Reactants and Products are Shown at Time = 0.0 min. UV Light Intensity = 1.15 x 10^{-6} Einstein L^{-1} s^{-1}; λ = 2537Å; μ =3.13 x 10^{-5}.

Time (min)	BrO_3^- (mM)	Br^- (mM)	TFB (mM)	pH	Temp (°C)
0.0	0.00608	BDL	BDL	7.78	24.0
1.5	0.00570	0.000495	BDL		
3.8	0.00526	0.000975	BDL	7.47	
8.4	0.00459	0.00165	BDL		
12.1	0.00407	0.00213	BDL		
17.9	0.00348	0.00280	BDL		
22.5	0.00296	0.00338	BDL	5.94	
27.8	0.00251	0.00376	BDL		
34.4	0.00214	0.00405	BDL		
42.8	0.00170	0.00443	BDL	5.74	
48.7	0.00147	0.00462	BDL		
56.0	0.00133	0.00491	BDL	6.1	
64.9	0.00110	0.00519	BDL		25.5

Reproduced with permission of the copyright owner. Further reproduction prohibited without permission.

Table B-37. Results of Experiment # 41. The Initial Concentration of Reactants and Products are Shown at Time = 0.0 min. UV Light Intensity = 2.61 x 10^{-6} Einstein L^{-1} s^{-1}; λ = 2537Å; $\mu = 6.25 \times 10^{-4}$.

Time (min)	BrO_3^- (mM)	Br^- (mM)	TFB (mM)	pH	Temp (°C)
0.0	0.03726	BDL	BDL	8.20	21.8
1.3	0.03493	0.00153	0.000176		
3.7	0.03034	0.00495	0.00185		
7.8	0.0275	0.00923	0.0023	6.21	
12.5	0.0234	0.01323	0.0015		
16.5	0.01986	0.01665	0.00091		
21.1	0.01680	0.01950	0.00075		
26.5	0.01462	0.02643	0.00064		
31.1	0.01778	0.02493	0.000176	5.67	
35.9	0.01025	0.02692	BDL		
40.6	0.00828	0.02863	BDL		
46.1	0.006973	0.0301	BDL		
51.3	0.00544	0.03149	BDL		
60.2	0.004134	0.03291	BDL	5.83	24
62.3	0.003697	0.03434	BDL		

Reproduced with permission of the copyright owner. Further reproduction prohibited without permission.

Table B-38. Results of Experiment # 42. The Initial Concentration of Reactants and Products are Shown at Time = 0.0 min. UV Light Intensity = 2.61 x 10^{-6} Einstein L^{-1} s^{-1}; λ = 2537Å; $\mu = 8.04 \times 10^{-5}$.

Time (min)	BrO_3^- (mM Br)	Br^- (mM Br)	TFB (mM Br)	NO_2^- (mM N)	NO_3^- (mM N)	pH	Temp (°C)
0.0	0.03733	BDL	BDL	0.01769	BDL	8.29	22
1.1	-	-	0.00119	-	-		
3.9	0.02707	0.00657	0.00409	0.00613	0.01412		
6.7	0.02226	0.01228	0.00495	0.000129	0.01732		
10.3	0.01920	0.01542	0.00237	0.000157	0.01769		
13.8	0.01702	0.01855	0.00119	0.000157	0.01769	6.98	
19.5	0.01396	0.02264	BDL	0.000157	0.01769		
24.9	0.01134	0.02569	BDL	0.000157	0.01805	5.94	
31.8	0.00916	0.02740	BDL	0.000157	0.01805		
36.3	0.00676	0.0300	BDL	0.000157	0.01769		
41.7	0.00523	0.03139	BDL	0.000157	0.01769		
48.0	0.00414	0.03282	BDL	0.000157	0.01769	5.70	24.5

Reproduced with permission of the copyright owner. Further reproduction prohibited without permission.

Table B-39. Results of Experiment # 43. The Initial Concentration of Reactants and Products are Shown at Time = 0.0 min. UV Light Intensity =2.61 x 10^{-6} Einstein L^{-1} s^{-1}; λ = 2537Å; $\mu = 9.82 \times 10^{-5}$.

Time (min)	BrO_3^- (mM)	Br^- (mM)	TFB (mM)	NO_2^- (mM)	NO_3^- (mM)	pH	Temp (°C)
0.0	0.03744	BDL	BDL	0.0357	BDL	8.24	22
1.2	-	-	0.00135	0.0224	-		
3.8	0.02597	0.00714	0.00495	0.01267	0.01252		
7.2	0.01811	0.01504	0.0063	0.00241	0.02433	7.65	
11.2	0.01265	0.02055	0.00607	BDL	0.03429		
15.8	0.001003	0.02540	0.0028	BDL	0.03614		
20.5	0.008065	0.02854	BDL	BDL	0.03614	6.08	
25.2	0.006318	0.03054	BDL	BDL	0.03614		
30.8	0.004571	0.03196	BDL	BDL	0.03614		
35.5	0.00326	0.03339	BDL	BDL	0.0357		
41.9	0.001950	0.03510	BDL	BDL	0.0357	6.09	24.5

Reproduced with permission of the copyright owner. Further reproduction prohibited without permission.

Table B-40. Results of Experiment # 44. The Initial Concentration of Reactants and Products are Shown at Time = 0.0 min. UV Light Intensity = 2.61 x 10^{-6} Einstein L^{-1} s^{-1}; λ = 2537Å; $\mu = 1.16 \times 10^{-4}$.

Time (min)	BrO_3^- (mM)	Br^- (mM)	TFB (mM)	NO_2^- (mM)	NO_3^- (mM)	pH	Temp (°C)
0.0	0.03744	BDL	BDL	0.0536	BDL	8.24	22.0
1.3	0.03362	0.00201	0.00189	0.05039	0.00366		
4.0	0.02838	0.00743	0.00538	0.0404	0.01326		
6.5	0.0205	0.01199	0.00661	0.0324	0.0217	7.55	
10.5	0.0144	0.01827	0.0062	0.02241	0.03023		
15.0	0.00938	0.02483	0.00398	0.01355	0.0406		
19.3	0.00588	0.02968	0.00017	0.00784	0.0465	6.30	
24.5	0.00392	0.03311	BDL	0.0047	0.0502		
29.4	0.002605	0.03482	BDL	0.00327	0.0513		
37.0	0.001295	0.03596	BDL	0.00327	0.05016	6.35	24.0

Reproduced with permission of the copyright owner. Further reproduction prohibited without permission.

Table B-41. Results of Experiment # 45. The Initial Concentration of Reactants and Products are Shown at Time = 0.0 min. UV Light Intensity = 1.15 x 10^{-6} Einstein L^{-1} s^{-1}; λ = 2537Å; μ = 4.50 x 10^{-5}.

Time (min)	BrO_3^- (mM Br)	Br^- (mM Br)	TFB (mM Br)	pH	Temp (°C)
0.0	0.03617	BDL	BDL	6.90	21.0
1.3	0.03525	0.00104	BDL		
3.3	0.03342	0.00257	0.00015		
7.3	0.03043	0.00463	0.0012	5.24	
11.4	0.02814	0.00726	0.00131		
15.2	0.02493	0.00961	0.0015	5.01	
20.4	0.02217	0.01225	0.0019		
25.8	0.02011	0.014894	0.0011		
30.7	0.01781	0.01695	0.00065	4.5	
35.9	0.01643	0.01871	0.00023		
42.0	0.01437	0.02047	BDL	4.5	
50.5	0.01139	0.02370	BDL		
60.1	0.01023	0.02428	BDL		
67.1	0.00932	0.02604	BDL	4.40	
75.2	0.00771	0.02722	BDL		
80.0	0.00703	0.02868	BDL	4.39	22.0

Reproduced with permission of the copyright owner. Further reproduction prohibited without permission.

Table B-42. Results of Experiment # 46. The Initial Concentration of Reactants and Products are Shown at Time = 0.0 min. UV Light Intensity = 1.15 x 10^{-6} Einstein L^{-1} s^{-1}; λ = 2537Å; $\mu = 6.25 \times 10^{-5}$.

Time (min)	BrO_3^- (mM Br)	Br^- (mM Br)	TFB (mM Br)	pH	Temp (°C)
0.0	0.0378	BDL	BDL	8.13	21.0
1.4	0.03617	0.001104	0.000493		
4.0	0.03434	0.00257	0.00109		
7.4	0.0311	0.004918	0.00165	7.38	
11.1	0.02860	0.006972	0.00212		
16.2	0.02630	0.0102	0.0015		
21.8	0.02332	0.01255	0.00185	7.24	
26.7	0.02125	0.01460	0.0019		
31.6	0.01896	0.01665	0.0012		
36.6	0.01712	0.01812	0.0011	7.23	
42.0	0.01552	0.01988	0.00054		
49.3	0.01391	0.02282	BDL		
56.1	0.01162	0.02487	BDL	6.37	
62.8	0.01047	0.02634	BDL		
68.8	0.00863	0.02722	BDL		
75.0	0.00726	0.02868	BDL	7.13	22.5

Reproduced with permission of the copyright owner. Further reproduction prohibited without permission.

Table B-43. Results of Experiment # 47. The Initial Concentration of Reactants and Products are Shown at Time = 0.0 min. UV Light Intensity = 1.15 x 10^{-6} Einstein L^{-1} s^{-1}; λ = 2537Å; μ = 2.38 x 10^{-5}.

Time (min)	BrO_3^- (mM Br)	Br^- (mM Br)	TFB (mM Br)	pH	Temp (°C)
0.0	0.0403	BDL	BDL	9.37	21.0
1.2	0.03847	0.001104	0.00070		
3.8	0.03502	0.002864	0.0020		
8.8	0.03089	0.00639	0.0026	9.01	
14.1	0.02699	0.00991	0.00321		
18.4	0.02516	0.01225	0.00270		
25.0	0.02148	0.015187	0.00250	9.06	
29.0	0.01919	0.01753	0.0020		
34.2	0.01666	0.01988	0.00195		
39.3	0.01428	0.02164	0.00180	9.10	
45.6	0.01207	0.02135	0.00034		
51.6	0.1162	0.024576	BDL		
56.3	0.0107	0.02546	BDL	9.01	
62.3	0.00861	0.02663	BDL	9.00	
70.5	0.00725	0.02898	BDL		22.0

Reproduced with permission of the copyright owner. Further reproduction prohibited without permission.

Table B-44. Results of Experiment # 48. The Initial Concentration of Reactants and Products are Shown at Time = 0.0 min. UV Light Intensity = 1.15 x 10^{-6} Einstein L^{-1} s^{-1}; λ = 2537Å; μ = 1.23 x 10^{-4}.

Time (min)	BrO_3^- (mM)	Br^- (mM)	TFB (mM Br)	NO_2^- (mM N)	NO_3^- (mM N)	pH	Temp (°C)
0.0	0.06301	BDL	BDL	0.034456	BDL	8.20	21.0
1.5	0.0544	0.019407	0.00294	0.030748	0.00497		
4.5	0.04868	0.076167	0.00822	0.01962	0.01568	8.14	
9.0	0.03738	0.015184	0.0118	0.00572	0.02282		
13.5	0.03142	0.02105	0.0109	0.000713	0.03413		
17.6	0.028705	0.02559	0.00899	0.000157	0.03448	7.99	
23.0	0.02622	0.03098	0.00604	0.000157	0.03484	7.69	
27.9	0.02328	0.03467	0.00401	0.000157	0.03484		
33.0	0.020562	0.03865	0.00238	0.000157	0.03484		
37.9	0.01717	0.04148	0.00203	0.000157	0.03484		
44.5	0.01536	0.04432	0.0012	0.000157	0.03448	6.68	
51.2	0.01287	0.047727	0.0002	0.000157	0.03484		
58.5	0.01061	0.049714	0.00106	0.000157	0.03484	6.57	
75.0	0.00541	0.05539	0.000451	0.000157	0.03448		
82.0	0.00495	0.05653	BDL	0.000157	0.03448	6.39	22.0

Reproduced with permission of the copyright owner. Further reproduction prohibited without permission.

Table B-45. Results of Experiment # 49. The Initial Concentration of Reactants and Products are Shown at Time = 0.0 min. UV Light Intensity = 1.15 x 10^{-6} Einstein L^{-1} s^{-1}; λ = 2537Å; μ = 9.82 x 10^{-5}.

Time (min)	BrO_3^- (mM)	Br^- (mM)	TFB (mM)	NO_2^- (mM)	NO_3^- (mM)	pH	Temp (°C)
0.0	0.0373	BDL	BDL	0.03436	BDL	8.30	20.0
1.5	0.03436	0.001184	0.0012	0.03214	0.002354		
4.5	0.02916	0.004306	0.00304	0.026298	0.008066		
7.3	0.02486	0.007144	0.00538	0.021014	0.01636	7.95	
11.2	0.02034	0.01083	0.00609	0.014896	0.01949		
15.4	0.01513	0.01537	0.00736	0.00767	0.02663	7.86	
20.2	0.011966	0.01991	0.00548	0.00294	0.03270		
25.2	0.010835	0.22753	0.00294	0.001826	0.03234	6.82	
30.5	0.00948	0.0253	0.00101	0.00127	0.03341		
35.7	0.00812	0.02758	BDL	0.000713	0.03413		
43.8	-	-	BDL	-	-	6.07	
54.0	0.00450	0.03098	BDL	0.000157	0.03413	6.23	21.0

Reproduced with permission of the copyright owner. Further reproduction prohibited without permission.

Table B-46. Results of Experiment # 50. The Initial Concentration of Reactants and Products are Shown at Time = 0.0 min. UV Light Intensity = 1.15 x 10^{-6} Einstein L^{-1} s^{-1}; λ = 2537Å; $\mu = 7.95 \times 10^{-5}$.

Time (min)	BrO_3^- (mM Br)	Br^- (mM Br)	TFB (mM Br)	NO_2^- (mM N)	NO_3^- (mM N)	pH	Temp (°C)
0.0	0.0184	BDL	BDL	0.0344	BDL	8.30	20.0
1.1	0.01740	0.000616	0.00035	0.03353	0.00111		
3.5	0.01536	0.00148	0.00132	0.0310	0.003425	7.81	
7.7	0.01197	0.00402	0.00264	0.02658	0.007352		
12.0	0.00993	0.00629	0.00253	0.02352	0.01092		
16.0	0.00790	0.00856	0.00198	0.02074	0.01342	7.58	
20.9	0.00609	0.01083	0.00142	0.01768	0.01699		
28.2	0.00360	0.01339	0.00142	0.01351	0.02247	7.35	
34.7	0.00292	0.01481	0.00030	0.01239	0.0227		
40.3	0.00201	0.01424	BDL	0.01286	0.02342	6.35	21.0

Reproduced with permission of the copyright owner. Further reproduction prohibited without permission.

Table B-47. Results of Experiment # 51. The Initial Concentration of Reactants and Products are Shown at Time = 0.0 min. UV Light Intensity = 1.15 x 10^{-6} Einstein L^{-1} s^{-1}; λ = 2537Å; $\mu = 7.32 \times 10^{-5}$.

Time (min)	BrO_3^- (mM)	Br^- (mM)	TFB (mM)	NO_2^- (mM)	NO_3^- (mM)	pH	Temp (°C)
0.0	0.01219	BDL	BDL	0.0344	BDL	8.30	20.0
1.2	0.01513	0.00033	0.000096	0.03353	0.00093		
3.6	0.01016	0.00118	0.00055	0.03214	0.00235	8.15	
7.8	0.00835	0.00260	0.00110	0.02936	0.00485		
12.5	0.00676	0.00431	0.000604	0.02741	0.00735		
17.8	0.00518	0.00601	0.000198	0.02519	0.00949	7.67	
22.7	0.00382	0.00771	BDL	0.02268	0.01163		
29.7	0.00224	0.00941	BDL	0.01935	0.01449		
35.5	0.00156	0.00970	BDL	0.01879	0.01521		21.4

Reproduced with permission of the copyright owner. Further reproduction prohibited without permission.

Table B-48. Results of Experiment # 52. The Initial Concentration of Reactants and Products are Shown at Time = 0.0 min. UV Light Intensity = 2.30×10^{-7} Einstein L^{-1} s^{-1}; $\lambda = 2537$Å; $Cl^- = 0.072$ mM; $\mu = 1.19 \times 10^{-4}$.

Time (min)	TFB (mM)	Br^- (mM)	BrO_3^- (mM)	pH	Temp (°C)
0.0	0.0146	0.0066	BDL	8.15	25.0
6.0	0.0093	0.0099	0.0009	8.01	
11.9	0.0058	0.0116	0.0019	7.94	
20.0	0.0031	-	0.0021	7.86	
25.3	BDL	0.0173	0.0021	7.81	26.0

Table B-49. Results of Experiment # 53. The Initial Concentration of Reactants and Products are Shown at Time = 0.0 min. UV Light Intensity = 4.35×10^{-7} Einstein L^{-1} s^{-1}; $\lambda = 2537$Å; $Cl^- = 0.072$ mM; $\mu = 1.19 \times 10^{-4}$.

Time (min)	TFB (mM)	Br^- (mM)	BrO_3^- (mM)	pH	Temp (°C)
0.0	0.0146	0.0071	BDL	8.15	25.0
3.4	0.0079	0.0099	0.0012	7.89	
8.9	0.0045	0.0126	0.0021		
13.1	0.0016	0.0137	0.0023		
16.2	0.0006	0.0140	0.0023	7.76	

Reproduced with permission of the copyright owner. Further reproduction prohibited without permission.

Table B-50. Results of Experiment # 54. The Initial Concentration of Reactants and Products are Shown at Time = 0.0 min. UV Light Intensity = 1.15 x 10^{-6} Einstein L^{-1} s^{-1}; λ = 2537Å; Cl^- = 0.072 mM; $\mu = 1.19 \times 10^{-4}$.

Time (min)	TFB (mM)	Br^- (mM)	BrO_3^- (mM)	pH	Temp (°C)
0.0	0.0146	0.0073	BDL	8.15	25.0
2.3	0.0092	0.0099	0.0009		
6.7	0.0025	0.0133	0.0023		
11.0	BDL	0.0139	0.0075	7.50	

Table B-51. Results of Experiment # 55. The Initial Concentration of Reactants and Products are Shown at Time = 0.0 min. UV Light Intensity = 2.61 x 10^{-6} Einstein L^{-1} s^{-1}; λ = 2537Å; Cl^- = 0.072 mM; $\mu = 1.19 \times 10^{-4}$.

Time (min)	TFB (mM)	Br^- (mM)	BrO_3^- (mM)	pH	Temp (°C)
0.0	0.0146	0.0073	BDL	8.15	25.0
1.5	0.0088	0.0099	0.0009		
3.8	0.0027	0.0128	0.0021		
7.3	BDL	0.0142	0.0019		
8.3	BDL	-	-		

Reproduced with permission of the copyright owner. Further reproduction prohibited without permission.

Table B-52. Results of Experiment # 56. The Initial Concentrations of Reactants and Products are Shown at Time = 0.0 min. UV Light Intensity = 1.15 x 10^{-6} Einstein L^{-1} s^{-1}; λ = 2537Å; Cl^- = 0.074 mM; μ = 1.18 x 10^{-4}.

Time (min)	TFB (mM)	Br^- (mM)	BrO_3^- (mM)	pH	Temp (°C)
0.0	0.0144	0.0054	BDL	8.22	19.0
3.6	0.0088	0.0084	0.0009		
8	0.0047	0.0114	0.0013		
15.2	0	0.0140	0.0015		

Table B-53. Results of Experiment # 57. The Initial Concentrations of Reactants and Products are Shown at Time = 0.0 min. UV Light Intensity = 1.15 x 10^{-6} Einstein L^{-1} s^{-1}; λ = 2537Å; Cl^- = 0.072 mM; μ =2.92 x 10^{-4}.

Time (min)	TFB (mM)	Br^- (mM)	BrO_3^- (mM)	pH	Temp (°C)
0.0	0.0151	0.0490	BDL	9.37	19.0
2.2	0.0133	0.0057	BDL		
6.8	0.0096	0.0084	0.00057		
13.2	0.0054	0.0110	0.0009		
18.4	0.0035	0.0125	0.0012	9.26	19.8

Reproduced with permission of the copyright owner. Further reproduction prohibited without permission.

Table B-54. Results of Experiment # 58. The Initial Concentrations of Reactants and Products are Shown at Time = 0.0 min. UV Light Intensity = 1.15 x 10^{-6} Einstein L^{-1} s^{-1}; λ = 2537Å; Cl^- = 0.075 mM; μ = 1.99 x 10 -4.

Time (min)	TFB (mM)	Br^- (mM)	BrO_3^- (mM)	pH	Temp (°C)
0.0	0.0150	0.0052	BDL	8.35	21.0
2.7	0.0095	0.0065	0.00076		
7.8	0.0071	0.0082	0.0019		
12.8	0.0042	0.0110	0.0021		
14.5	0.0035	0.0122	0.0021	8.28	22.0

Table B-55. Results of Experiment # 59. The Initial Concentrations of Reactants and Products are Shown at Time = 0.0 min. UV Light Intensity = 2.30 x 10^{-7} Einstein L^{-1} s^{-1}; λ = 2537Å; Cl^- = 0.072 mM; μ = 1.20 x 10^{-4}.

Time (min)	TFB (mM)	Br^- (mM)	BrO_3^- (mM)	pH	Temp (°C)
0.0	0.01500	0.0054	BDL	8.18	21.0
9.0	0.00920	0.0079	0.0004		
14.7	0.00410	0.0120	0.0018		
22.2	0.00130	0.0140	0.0015		
28.2	0.00035	0.0140	0.0017	7.94	22.1

Reproduced with permission of the copyright owner. Further reproduction prohibited without permission.

Table B-56. Results of Experiment # 60. The Initial Concentration of Reactants and Products are Shown at Time = 0.0 min. UV Light Intensity = 2.61 x 10^{-6} Einstein L^{-1} s^{-1}; λ = 2537Å; $\mu = 2.38 \times 10^{-4}$.

Time (min)	BrO_3^- (mM)	Br^- (mM)	TFB (mM)	pH	Temp (°C)
0.0	0.0387	BDL	BDL	9.47	25
1.2	0.03504	0.00214	0.00057		
4.3	0.02984	0.0067	0.00171	8.99	
7.6	0.02427	0.01094	0.0026		
10.9	0.02148	0.01378	0.0032	8.96	
15.9	0.01777	0.0186	0.0028		
19.6	0.01517	0.0221	0.0026	9.01	
25	0.01220	0.02426	0.0016		
30.5	0.00922	0.02783	0.00076	8.97	
36.1	0.00737	0.02997	BDL		
40.8	0.00570	0.03164	BDL		
50.7	0.00403	0.03378	BDL		
56.3	0.00291	0.03473	BDL		
62.6	0.00217	0.0388	BDL	8.96	26.5

Reproduced with permission of the copyright owner. Further reproduction prohibited without permission.

Table B-57. Results of Experiment # 61. The Initial Concentration of Reactants and Products are Shown at Time = 0.0 min. UV Light Intensity = 2.61 x 10^{-6} Einstein L^{-1} s^{-1}; λ = 2537Å; $\mu = 6.25 \times 10^{-5}$.

Time (min)	BrO_3^- (mM Br)	Br^- (mM Br)	TFB (mM Br)	pH	Temp (°C)
0.0	0.03754	BDL	BDL	8.27	25.0
1.1	0.03559	0.00214	0.00062	7.78	
4.9	0.02947	0.00761	0.00191		
8.7	0.02519	0.01142	0.00206	7.82	
12.4	0.02148	0.01546	0.00171		
17.3	0.01795	0.0236	0.00131		
20.8	0.01498	0.02212	0.00116	7.73	
25.2	0.01275	0.02521	0.000168		
31.4	0.00978	0.02807	0.00062	7.90	
36.6	0.00792	0.02997	0.000069		
43.3	0.00625	0.03188	BDL		
47.6	0.00495	0.03307	BDL	7.82	
52.8	0.00421	0.03378	BDL		
56.6	0.00347	0.03497	BDL		
62.6	0.00254	0.03568	BDL	7.74	26.5

Reproduced with permission of the copyright owner. Further reproduction prohibited without permission.

Table B-58. Results of Experiment # 62. The Initial Concentration of Reactants and Products are Shown at Time = 0.0 min. UV Light Intensity = 2.61 x 10^{-6} Einstein L^{-1} s^{-1}; λ = 2537Å; $\mu = 4.50 \times 10^{-5}$.

Time (min)	BrO_3^- (mM)	Br^- (mM)	TFB (mM)	pH	Temp (°C)
0.0	0.03745	BDL	BDL	7.17	25
1.2	0.03485	0.00261	0.00052	5.98	
4.1	0.02984	0.00690	0.0023		
7.6	0.02594	0.01070	0.0024	5.89	
11.4	0.02185	0.01451	0.00221		
17.4	0.01665	0.01998	0.0040	5.93	
21.2	0.01498	0.02212	0.00171		
25.0	0.01257	0.02403	0.00201		
29.1	0.01052	0.02640	0.00186	5.94	
34.5	0.00848	0.02878	0.00116		
39.7	0.00662	0.03069	0.00032		
45.0	0.00570	0.03211	0.00076	5.96	
52.3	0.00421	0.03354	0.000131		
58.1	-	-	0.000069		
63.0	0.00235	0.03521	BDL	5.75	26.5

Reproduced with permission of the copyright owner. Further reproduction prohibited without permission.

TableB-59. Results of Experiment # 63. The Initial Concentration of Reactants and Products are Shown at Time = 0.0 min. UV Light Intensity = 2.61 x 10^{-6} Einstein L^{-1} s^{-1}; λ = 2537Å; μ = 2.73 x 10^{-4}.

Time (min)	BrO_3^- (mM)	Br^- (mM)	TFB (mM)	NO_2^- (mM)	NO_3^- (mM)	pH	Temp (°C)
0.0	0.03827	0.00038	BDL	0.03402	BDL	9.49	25
1.2	0.03396	0.00268	0.00221	0.03062	0.00341		
3.6	0.02608	0.00799	0.00632	0.02211	0.01154	9.26	
6.5	0.01971	0.01306	0.00730	0.01531	0.01805		
10.1	0.01371	0.01906	0.00684	0.00923	0.02429	9.29	
15.5	0.00827	0.02598	0.00464	0.00292	0.03026		
19.6	0.00583	0.02944	0.00343	0.00097	0.03270	9.29	
23.5	0.00564	0.02967	0.00146	0.00073	0.03324		
28.3	0.00342	0.03290	0.00048	0.00024	0.03324		
34.4	0.00189	0.03406	0.00019	0.000121	0.03243	9.18	
41.7	0.00096	0.03544	BDL	0.000243	0.03134	9.30	26.8

Reproduced with permission of the copyright owner. Further reproduction prohibited without permission.

Table B-60. Results of Experiment # 64. The Initial Concentration of Reactants and Products are Shown at Time = 0.0 min. UV Light Intensity = 2.61 x 10^{-6} Einstein L^{-1} s^{-1}; λ = 2537Å; $\mu = 9.82 \times 10^{-5}$.

Time (min)	BrO_3^- (mM)	Br^- (mM)	TFB (mM)	NO_2^- (mM)	NO_3^- (mM)	pH	Temp (°C)
0.0	0.03733	0.00038	BDL	0.03402	BDL	8.30	
1.2	0.03321	0.00291	0.0024	0.03013	0.00422		
3.7	0.02496	0.00822	0.00603	0.02041	0.01344	8.18	
6.7	0.01746	0.01445	0.0078	0.00923	0.02456		
9.6	0.01239	0.01999	0.00759	0.00146	0.03270	8.23	
13.4	0.01052	0.02483	0.00314	BDL	0.03405		
17.0	0.00902	0.02506	0.00192	BDL	0.03405	8.05	
21.7	0.00696	0.02967	0.00019	BDL	0.03351		
27.3	0.00471	0.03221	BDL	BDL	0.03405		
31.7	0.00339	0.03383	BDL	BDL	0.03405	7.60	
40.2	0.00152	0.03567	BDL	BDL	0.03324	7.64	

Reproduced with permission of the copyright owner. Further reproduction prohibited without permission.

Table B-61. Results of Experiment # 65. The Initial Concentration of Reactants and Products are Shown at Time = 0.0 min. UV Light Intensity = 2.61 x 10^{-6} Einstein L^{-1} s^{-1}; λ = 2537Å; $\mu = 8.07 \times 10^{-5}$.

Time (min)	BrO_3^- (mM)	Br^- (mM)	TFB (mM)	NO_2^- (mM)	NO_3^- (mM)	pH	Temp (°C)
0.0	0.03789	BDL	BDL	0.03451	BDL	7.20	25
1.0	0.03414	0.0022	0.00170	0.03062	0.00395	5.83	
3.3	0.02664	0.00845	0.0043	0.01944	0.01507		
6.1	0.01837	0.01629	0.00464	0.00559	0.02863	5.75	
9.4	0.01483	0.02091	0.00262	0.00073	0.03378		
13.8	0.01221	0.02368	0.0022	BDL	0.03432	5.63	
17.4	0.01052	0.02575	0.00192	BDL	0.03460		
22.0	0.00846	0.02806	0.00233	BDL	0.03460		
26.7	0.00696	0.02944	0.00140	BDL	0.03460	5.60	
35.4	0.00568	0.03198	0.00094	BDL	0.03460		
41.5	0.00377	0.03314	0.00042	BDL	0.03432	5.48	
47.5	0.00264	0.03452	BDL	BDL	0.03405	5.36	26.5

Reproduced with permission of the copyright owner. Further reproduction prohibited without permission.

Table B-62. Results of Experiment # 66. The Initial Concentration of Reactants and Products are Shown at Time = 0.0 min. UV Light Intensity = 2.61 x 10^{-6} Einstein L^{-1} s^{-1}; λ = 2537Å; μ = 1.11 x 10^{-4}.

Time (min)	BrO_3^- (mM Br)	Br^- (mM Br)	TFB (mMBr)	NO_2^- (mM N)	NO_3^- (mM N)	pH	Temp (°C)
0.0	0.0503	0.00021	BDL	0.03421	BDL	7.95	25.0
1.4	0.04398	0.00343	0.0036	0.02887	0.00582	7.82	
4.7	0.03019	0.01227	0.0098	0.01163	0.02046		
8.3	0.02266	0.02023	0.011	0.00235	0.03135	7.80	
11.5	0.01796	0.02505	0.0085	0.00014	0.03245		
16.2	0.0153	0.03277	0.0047	0.00014	0.03327	7.79	
32.0	0.00649	0.04338	0.0012	0.00014	0.03354	7.80	
36.9	0.00498	0.04507	BDL	0.00014	0.03327		
41.6	0.00348	0.04676	BDL	0.00014	0.0330		
49.1	0.00216	0.04845	BDL	0.00014	0.0330	7.69	
55.0	0.00122	0.04893	BDL	0.00137	0.03190	7.70	27.0

Reproduced with permission of the copyright owner. Further reproduction prohibited without permission.

TableB-63. Results of Experiment # 67. The Initial Concentration of Reactants and Products are Shown at Time = 0.0 min. UV Light Intensity = 2.61 x 10^{-6} Einstein L^{-1} s^{-1}; λ = 2537Å; $\mu = 1.23 \times 10^{-4}$.

Time (min)	BrO_3^- (mM)	Br^- (mM)	TFB (mM)	NO_2^- (mM)	NO_3^- (mM N)	pH	Temp (°C)
0.0	0.0648	BDL	BDL	0.03462	BDL	8.17	23
1.1	0.05654	0.00185	0.00269	0.002986	0.00491	7.65	
3.5	0.04575	0.01151	0.0081	0.01574	0.01863		
6.7	0.03495	-	0.0088	-	-		
10.5	0.03032	0.02874	0.0053	0.00014	0.03437		
13.7	0.02670	0.03381	0.0034	0.00014	0.03382	6.73	
18.4	0.02194	0.03912	0.0017	0.00014	0.03354	6.20	
24.8	0.01698	0.04492	0.00095	0.00014	0.03382		
29.0	0.01298	0.04926	0.0010	0.00014	0.03354	6.41	
34.0	0.0107	0.05240	0.00033	0.00014	0.03382		
40.0	0.0083	0.05498	0.00029	0.00014	0.03327		
47.0	0.00593	0.0574	0.00024	0.00014	0.03327	5.80	
56.9	0.00384	0.06062	BDL	0.00014	0.03327	5.80	
65.0	0.00212	0.06223	BDL	0.00014	0.03327		25

Reproduced with permission of the copyright owner. Further reproduction prohibited without permission.

Table B-64. Results of Experiment # 68. The Initial Concentration of Reactants and Products are Shown at Time = 0.0 min. UV Light Intensity = 2.61 x 10^{-6} Einstein L^{-1} s^{-1}; λ = 2537Å; $\mu = 9.20 \times 10^{-5}$.

Time (min)	BrO_3^- (mM)	Br^- (mM)	TFB (mM)	NO_2^- (mM)	NO_3^- (mM)	pH	Temp (°C)
0.0	0.03146	BDL	BDL	0.0344	BDL	8.15	23.0
1.0	0.02803	0.00169	0.00099	0.03117	0.00307		
2.5	0.02441	0.00410	0.0032	0.02698	0.00664	7.60	
4.6	0.01927	0.00845	0.0048	0.02009	0.01405		
6.9	0.01451	0.01256	0.0052	0.01319	0.02064	7.30	
9.8	0.01089	0.0167	0.0045	0.00753	0.02641		
17.4	0.00574	0.02487	0.0007	0.00063	0.03327	6.63	
21.5	0.00441	0.02656	BDL	0.00014	0.03327		
27.9	0.00289	0.02825	BDL	0.00014	0.03354		
32.8	0.00212	0.02970	BDL	0.00063	0.03354	5.70	
40.8	0.00117	0.03019	BDL	0.00112	0.03217	5.65	25.0

Reproduced with permission of the copyright owner. Further reproduction prohibited without permission.

Table B-65. Results of Experiment # 69. The Initial Concentration of Reactants and Products are Shown at Time = 0.0 min. UV Light Intensity = 2.61 x 10^{-6} Einstein L^{-1} s^{-1}; λ = 2537Å; $\mu = 7.32 \times 10^{-5}$.

Time (min)	BrO_2^- (mM)	Br^- (mM)	TFB (mM)	NO_2^- (mM)	NO_3^- (mM)	pH	Temp (°C)
0.0	0.01241	BDL	BDL	0.03413	BDL	8.10	23
0.8	0.01146	0.00072	0.00029	0.03314	0.00115		
2.0	0.01032	0.00145	0.00057	0.03166	0.00280		
3.0	0.00955	0.00217	0.0011	0.03043	0.00362		
4.5	0.00746	0.00241	0.0016	0.02772	0.00609		
7.0	0.00613	0.00531	0.0017	0.02526	0.00857		
9.6	0.0046	0.00700	0.00137	0.02230	0.01104		
16.0	0.0027	0.00942	0.00019	0.01935	0.01405	6.93	
22.0	0.00155	0.01062	0.000098	0.01738	0.01598		
27.8	0.00098	0.01159	0.000146	0.01615	0.01707		
30.0	0.00060	0.01183	BDL	0.01590	0.01735	6.43	24.5

Reproduced with permission of the copyright owner. Further reproduction prohibited without permission.

Table B-66. Results of Experiment # 70. The Initial Concentrations of Reactants and Products are Shown at Time = 0.0 min. UV Light Intensity = 4.35 x 10^{-7} Einstein L^{-1} s^{-1}; λ = 2537Å; $\mu = 1.11 \times 10^{-4}$.

Time (min)	BrO_3^- (mM)	Br^- (mM)	TFB (mM)	NO_2^- (mM)	NO_3^- (mM)	pH	Temp (°C)
0.0	0.04981	BDL	BDL	0.03361	BDL	8.12	22.5
1.5	0.04727	0.00184	0.00178	0.03154	0.00282	7.10	
4.7	0.04092	0.00668	0.00465	0.02324	0.01127		
8.6	0.03140	0.01233	0.0067	0.01245	0.02066		
12.3	0.02632	0.01798	0.00728	0.00498	0.03099	7.2	
17.1	0.02219	0.02443	0.00436	0.00075	0.03409		
22.1	0.02009	0.02806	0.00207	BDL	0.03409	6.30	
26.5	0.01819	0.03048	0.000805	BDL	0.03386	5.89	
31.5	0.01628	0.03339	0.00076	BDL	0.03386		
37.0	0.01457	0.03484	0.00042	BDL	0.03386	5.92	
43.8	0.01190	0.03726	0.00027	BDL	0.03386		
49.8	0.01076	0.03920	0.00046	BDL	0.03409	5.70	
57.3	0.00866	0.04114	BDL	BDL	0.03409	5.50	
65.2	0.00695	0.04259	BDL	BDL	0.03380		
74.4	0.00542	0.04428	BDL	BDL	0.03380	5.60	
83.9	0.00409	0.04574	BDL	BDL	0.03409		
93.7	0.0033	0.04719	BDL	BDL	0.03409	5.54	25.0

Reproduced with permission of the copyright owner. Further reproduction prohibited without permission.

Table B-67. Results of Experiment # 71. The Initial Concentration of Reactants and Products are Shown at Time = 0.0 min. UV Light Intensity = 4.35 x 10^{-7} Einstein L^{-1} s^{-1}; λ = 2537Å; $\mu = 8.57 \times 10^{-5}$.

Time (min)	BrO_3^- (mM)	Br^- (mM)	TFB (mM)	NO_2^- (mM)	NO_3^- (mM)	pH	Temp (°C)
0.0	0.02524	BDL	BDL	0.03436	BDL	8.0	22
1.2	0.02352	0.00095	0.0011	0.03312	0.00141	7.45	
7.3	0.01647	0.00603	0.0033	0.02415	0.01014	7.10	
11.4	0.01304	0.00918	0.0032	0.01892	0.01521		
15.8	0.01019	0.01257	0.0027	0.01419	0.0200		
20.2	0.00809	0.01547	0.0017	0.01021	0.02394	6.60	
24.8	0.00619	0.01765	0.00183	0.00672	0.02761		
31.6	0.0048	0.02032	0.00090	0.00374	0.03071	6.73	
36.3	0.00352	0.02153	0.00032	0.00224	0.03183		
40.8	0.00276	0.02250	0.000269	0.00100	0.03296		
46.8	0.00219	0.02346	BDL	BDL	0.03380	6.51	24

Reproduced with permission of the copyright owner. Further reproduction prohibited without permission.

Table B-68. Results of Experiment # 72. The Initial Concentration of Reactants and Products are Shown at Time = 0.0 min. UV Light Intensity = 4.35 x 10^{-7} Einstein L^{-1} s^{-1}; λ = 2537Å; μ = 7.32 x 10^{-5}.

Time (min)	BrO_3^- (mM)	Br^- (mM)	TFB (mM)	NO_2^- (mM)	NO_3^- (mM)	pH	Temp (°C)
0.0	0.01285	BDL	BDL	0.03486	BDL	8.10	22.5
1.0	0.01209	0.00046	0.00073	0.03436	0.00085		
3.1	0.01076	0.00167	0.00061	0.03287	0.00197	8.16	
5.6	0.00943	0.00264	0.0015	0.03088	0.00367		
8.6	0.00809	0.00361	0.0014	0.02938	0.00563		
12.3	0.00657	0.0056	0.00134	0.02689	0.00789		
16.4	0.00523	0.00676	0.0008	0.02440	0.01014	7.99	
20.8	0.00409	0.00821	0.00051	0.02241	0.01239		
25.5	0.00314	0.00918	0.00037	0.02067	0.01380	7.81	
30.4	0.00276	0.00991	0.00022	0.01992	0.01493		
36.2	0.0200	0.01063	0.00042	0.01818	0.01578	7.80	25.0

Reproduced with permission of the copyright owner. Further reproduction prohibited without permission.

Table B-69. Results of Experiment # 73. The Initial Concentration of Reactants and Products are Shown at Time = 0.0 min. UV Light Intensity = 4.35 x 10^{-7} Einstein L^{-1} s^{-1}; λ = 2537Å; $\mu = 8.07 \times 10^{-5}$.

Time (min)	BrO_3^- (mM)	Br^- (mM)	TFB (mM)	NO_2^- (mM)	NO_3^- (mM)	pH	Temp (°C)
0.0	0.03817	BDL	BDL	0.03410	BDL	6.90	22.5
4.2	0.03085	0.00489	0.002599	0.02540	0.00855	5.50	
8.4	0.02796	0.00988	0.00286	0.01809	0.01651		
13.0	0.02026	0.01511	0.00318	0.00898	0.02557	5.65	
17.2	0.01602	0.01915	0.002599	0.00282	0.03106		
20.8	0.01409	0.02176	0.00239	0.00011	0.03380		
24.9	0.01294	0.02224	0.00297	0.00013	0.03480	5.38	
29.9	0.01159	0.02414	0.00223	BDL	0.03408		
35.8	0.01043	0.02580	0.0016	BDL	0.03408		
43.0	0.00909	0.02723	0.00149	BDL	0.03408	5.48	
53.5	0.00677	0.02960	0.0019	BDL	0.03408		
63.2	0.00581	0.03127	0.00060	BDL	0.03463		
73.7	0.00466	0.03198	0.000285	BDL	0.03408	5.28	24.5

Reproduced with permission of the copyright owner. Further reproduction prohibited without permission.

Table B-70. Results of Experiment # 74. The Initial Concentration of Reactants and Products are Shown at Time = 0.0 min. UV Light Intensity = 4.35 x 10^{-7} Einstein L^{-1} s^{-1}; λ = 2537Å; $\mu = 9.82 \times 10^{-5}$.

Time (min)	BrO_3^- (mM)	Br^- (mM)	TFB (mM)	NO_2^- (mM)	NO_3^- (mM)	pH	Temp (°C)
0.0	0.03817	BDL	BDL	0.03361	BDL	8.30	23
1.2	0.03566	0.00133	0.001179	0.03213	0.00223	8.16	
4.5	0.03046	0.00418	0.00376	0.02622	0.00772		
8.2	0.02488	0.00822	0.00544	0.01957	0.01376	8.20	
12.2	0.02103	0.01155	0.0055	0.01464	0.01596		
16.5	0.01756	0.01630	0.00449	0.01021	0.02337		
20.5	0.01390	0.01939	0.00523	0.00479	0.02859		
26.7	0.01140	0.02295	0.00255	0.00110	0.03243		
31.6	0.00986	0.02604	0.001495	0.00060	0.03298		
37.4	0.00889	0.02747	0.00081	0.00011	0.03325	7.39	
42.9	0.00774	0.02889	BDL	BDL	0.03325		
51.0	0.00639	0.03055	BDL	BDL	0.03408	7.25	24.5

Reproduced with permission of the copyright owner. Further reproduction prohibited without permission.

Table B-71. Results of Experiment #75. The Initial Concentration of Reactants and Products are Shown at Time = 0.0 min. UV Light Intensity = 4.35 x 10^{-7} Einstein L^{-1} s^{-1}; λ = 2537Å; $\mu = 2.73 \times 10^{-4}$.

Time (min)	BrO_3^- (mM)	Br^- (mM)	TFB (mM)	pH	Temp (°C)
0.0	0.03875	BDL	BDL	9.49	22.5
1.2	0.03701	0.00109	0.00060	9.41	
3.9	0.03220	0.00394	0.00302		
7.7	0.02603	0.00798	0.00502	9.32	
11.7	0.02180	0.01202	0.0055		
15.6	0.01814	0.01511	0.0052		
19.8	0.01467	0.01867	0.0056	9.34	
23.7	0.01197	0.02105	0.0049		
28.9	0.00947	0.02438	0.0045		
33.2	0.00735	0.02580	0.00061		
38.4	0.00620	0.02889	0.000423		24.0

Reproduced with permission of the copyright owner. Further reproduction prohibited without permission.

Table B-72. Results of Experiment # 76. The Initial Concentration of Reactants and Products are Shown at Time = 0.0 min. UV Light Intensity = 4.35 x 10^{-7} Einstein L^{-1} s^{-1}; λ = 2537Å; $\mu = 6.25 \times 10^{-5}$.

Time (min)	BrO_3^- (mM)	Br^- (mM)	TFB (mM)	pH	Temp (°C)
0.0	0.03741	BDL	BDL	7.38	22.0
1.3	0.03564	0.00151	0.00012	6.20	
4.2	0.03345	0.00404	0.00071	5.64	
8.8	0.02980	0.00794	0.0011		
12.4	0.02742	0.00977	0.00124	5.44	
17.0	0.02468	0.01230	0.0010		
22	0.02231	0.01459	0.0018	5.45	
26.8	0.02030	0.01666	0.0023	5.25	
33.0	0.01792	0.01849	0.0011		
37.9	0.01646	0.02079	0.00215		
43.4	0.01500	0.02217	0.00124	5.35	
49.6	0.01262	0.02400	0.00049		
54.9	0.01153	0.02538	0.00081		
60.0	0.01052	0.02653	0.00076		
71.7	0.00842	0.02859	BDL		
80.0	0.00696	0.03020	BDL	5.18	
85.0	0.00641	0.03020	BDL	5.12	23.0

Reproduced with permission of the copyright owner. Further reproduction prohibited without permission.

Table B-73. Results of Experiment # 77. The Initial Concentration of Reactants and Products are Shown at Time = 0.0 min. UV Light Intensity = 4.35 x 10^{-7} Einstein L^{-1} s^{-1}; λ = 2537Å; $\mu = 6.25 \times 10^{-5}$.

Time (min)	BrO_3^- (mM Br)	Br^- (mM Br)	TFB (mM Br)	pH	Temp (°C)
0.0	0.03711	BDL	BDL	8.25	22.0
1.4	0.03546	0.00151	0.00039	8.01	
4.8	0.03272	0.00381	0.0017		
8.9	0.02980	0.00656	0.0012	7.99	
13.2	0.02742	0.00908	0.0021		
18.3	0.02468	0.01184	0.0015	7.92	
24.0	0.02194	0.01436	0.00193		
29.3	0.01938	0.01758	0.0013		
34.1	0.01737	0.01918	0.00087	8.0	
39.1	0.01482	0.02148	0.00060		
44.6	0.01390	0.02285	0.00033		
52.1	0.01189	0.02492	0.00044	7.60	
58.8	0.00988	0.02423	BDL		
65.1	0.00897	0.02790	BDL	7.79	
70.0	0.00806	BDL	BDL		24.0

Reproduced with permission of the copyright owner. Further reproduction prohibited without permission.

Table B-74. Results of Experiment # 78. The Initial Concentration of Reactants and Products are Shown at Time = 0.0 min. UV Light Intensity = 4.35 x 10^{-7} Einstein L^{-1} s^{-1}; λ = 2537Å; $\mu = 2.38 \times 10^{-4}$.

Time (min)	BrO_3^- (mM Br)	Br^- (mM Br)	TFB (mM Br)	pH	Temp (°C)
0.0	0.03820	BDL	BDL	9.32	22.0
1.5	0.03656	0.00128	0.00039	9.26	
4.8	0.03345	0.00335	0.00092		
8.6	0.03108	0.00564	0.00097	9.22	
12.5	0.02602	0.00771	0.00044		
18.2	0.02503	0.01115	0.0017		
26.3	0.02176	0.01436	0.0013		
32.2	0.01884	0.01735	0.00017	9.26	
36.6	0.01756	0.01872	0.00145		
44.4	0.01518	0.02102	0.0014	9.20	
49.6	0.01354	0.02262	0.00097		
54.9	0.01244	0.02423	0.00081	9.19	
59,7	0.01134	0.02492	0.00103		
67.0	0.00933	0.02794	0.000013		23.5

Reproduced with permission of the copyright owner. Further reproduction prohibited without permission.

Table B-75. Results of Experiment # 79. The Initial Concentration of Reactants and Products are Shown at Time = 0.0 min. UV Light Intensity = 2.30 x 10^{-7} Einstein L^{-1} s^{-1}; λ = 2537Å; $\mu = 8.07 \times 10^{-5}$.

Time (min)	BrO_3^- (mM)	Br^- (mM)	TFB (mM)	NO_2^- (mM)	NO_3^- (mM)	pH	Temp (°C)
0.0	0.03741	0	0	0.03451	0	7.20	24.0
2.7	0.03472	0.00132	0.00104	0.03192	0.00277	5.5	
5.2	0.03239	0.00267	0.0031	0.02910	0.00561		
9.0	0.02935	0.00494	0.00324	0.02462	0.00999	5.53	
12.8	0.0267	0.00766	0.00394	0.02062	0.01360		
17.2	0.02380	0.00992	0.0045	0.01615	0.01825		
20.5	0.02201	0.01551	0.00458	0.01285	0.02160	5.39	
28.1	0.01860	0.01672	0.0034	0.00673	0.02779		
33.1	0.01645	0.01898	0.0038	0.00225	0.03244		
38.2	0.01466	0.02034	0.00324	0.00013	0.03398		
45.4	0.01413	0.02283	0.0012	0.00013	0.03476		
54.7	0.01287	0.02419	0.00045	0.00013	0.03450		
63.2	0.01180	0.02510	0.0014	0.00013	0.03476	5.31	
70.9	0.01108	0.02600	0.000829	0.00013	0.03476		
80.0	0.00965	0.02714	0.00012	0.00013	0.03450		24.5

Reproduced with permission of the copyright owner. Further reproduction prohibited without permission.

Table B-76. Results of Experiment # 80. The Initial Concentration of Reactants and Products are Shown at Time = 0.0 min. UV Light Intensity = 2.30 x 10^{-7} Einstein L^{-1} s^{-1}; λ = 2537Å; $\mu = 9.82 \times 10^{-5}$.

Time (min)	BrO_3^- (mM)	Br^- (mM)	TFB (mM)	NO_2^- (mM)	NO_3^- (mM)	pH	Temp (°C)
0.0	0.03920	BDL	BDL	0.03475	BDL	8.20	24
1.4	0.03681	0.00064	0.00088	0.03404	0.00148		
5.0	0.03311	0.00177	0.0021	0.03098	0.00406	7.88	
9.6	0.02935	0.00426	0.0036	0.02651	0.00844	7.90	
13.7	0.02648	0.00607	0.00592	0.0227	0.01180		
19.7	0.02326	0.00924	0.00699	0.01803	0.01696	7.70	
24.4	0.02039	0.01105	0.0067	0.01473	0.01980		
30.3	0.01717	0.01173	0.0077	0.01002	0.02444	7.60	
37.9	0.01484	0.01740	0.0056	0.00673	0.02753		
44.1	0.01233	0.01989	0.0072	0.00202	0.03295		
53.2	0.01108	0.02397	0.00311	0.00107	0.03373	7.40	
64.9	0.00983	0.02555	0.00233	0.00013	0.03424	7.70	
71.5	0.00911	0.02714	0.00051	0.00013	0.03450		
76.0	0.00839	0.02714	BDL	0.00013	0.03450	7.65	24.5

Reproduced with permission of the copyright owner. Further reproduction prohibited without permission.

Table B-77. Results of Experiment # 81. The Initial Concentration of Reactants and Products are Shown at Time = 0.0 min. UV Light Intensity = 2.30 x 10^{-7} Einstein L^{-1} s^{-1}; λ = 2537Å; $\mu = 2.73 \times 10^{-4}$.

Time (min)	BrO_3^- (mM)	Br^- (mM)	TFB (mM)	NO_2^- (mM)	NO_3^- (mM)	pH	Temp (°C)
0.0	0.03812	BDL	BDL	0.0336	BDL	9.37	24.0
1.7	0.03633	0.00064	0.00083	0.03263	0.00148	9.26	
5.7	0.03293	0.0029	0.00233	0.02933	0.00483		
9.9	0.02863	0.00562	0.0042	0.02486	0.00896	9.12	
14.3	0.02577	0.0084	0.0097	0.02203	0.01205		
21.5	0.02057	0.01128	0.00614	0.01638	0.01696		
26.2	0.01807	0.0140	0.0062	0.01356	0.02057	9.28	
32.0	0.01574	0.01830	0.0059	0.01073	0.02289		
45.0	0.01072	0.0208	0.00796	0.00437	0.02908	9.28	
52.0	0.00875	0.02238	0.0080	0.00202	0.03244		
58.2	0.00732	0.02442	0.0066	0.00084	0.03269		
66.1	0.00678	0.02736	0.0045	0.00037	0.03347	9.33	
71.1	0.00607	0.02940	0.00016	0.00013	0.03321		24.5

Reproduced with permission of the copyright owner. Further reproduction prohibited without permission.

Table B-78. Results of Experiment # 82. The Initial Concentration of Reactants and Products are Shown at Time = 0.0 min. UV Light Intensity = 2.30 x 10^{-7} Einstein L^{-1} s^{-1}; λ = 2537Å; $\mu = 6.25 \times 10^{-5}$.

Time (min)	BrO_3^- (mM)	Br^- (mM)	TFB (mM)	pH	Temp (°C)
0.0	0.03680	BDL	BDL	8.17	24.0
1.9	0.03576	0.00306	0.00044	7.80	
4.9	0.03454	0.00240	BDL		
10.9	0.03175	0.00416	BDL		
17.1	0.03019	0.00636	0.00073		
23.7	0.02810	0.00855	0.00009		
31.4	0.02584	0.01031	0.00085	7.60	
41.5	0.02358	0.01316	BDL		
48.9	0.02184	0.01514	BDL		
59.3	0.0189	0.01712	BDL		
72.0	0.01662	0.01821	BDL		
85.6	0.01488	0.02195	BDL	6.61	
98.2	0.01227	0.0237	BDL		
112.0	0.01087	0.0259	BDL	6.53	25.5

Reproduced with permission of the copyright owner. Further reproduction prohibited without permission.

Table B-79. Results of Experiment # 83. The Initial Concentration of Reactants and Products are Shown at Time = 0.0 min. UV Light Intensity = 2.30 x 10^{-7} Einstein L^{-1} s^{-1}; λ = 2537Å; $\mu = 4.50 \times 10^{-5}$.

Time (min)	BrO_3^- (mM)	Br^- (mM)	TFB (mM)	pH	Temp (°C)
0.0	0.03610	BDL	BDL	7.14	24.0
1.8	0.03487	0.00087	BDL	6.02	
6.0	0.0340	0.00262	0.00003	5.90	
11.9	0.03123	0.00438	0.00091		
17.5	0.02967	0.00592	0.00225	6.06	
23.6	0.02862	0.00723	0.00149		
31.2	0.02619	0.00855	0.00126	5.72	
40.9	0.02410	0.01097	0.00055		
48.1	0.02236	0.01250	0.00026	5.53	
55.8	0.02114	0.01421	BDL		
69.4	0.01888	0.01668	0.00055	5.26	
84.2	0.01627	0.01909	BDL	5.15	
98.5	0.01453	0.02129	BDL	5.66	25.0

Reproduced with permission of the copyright owner. Further reproduction prohibited without permission.

Table B-80. Results of Experiment # 84. The Initial Concentration of Reactants and Products are Shown at Time = 0.0 min. UV Light Intensity = 2.30 x 10^{-7} Einstein L^{-1} s^{-1}; λ = 2537Å; $\mu = 2.38 \times 10^{-4}$.

Time (min)	BrO_3^- (mM Br)	Br^- (mM Br)	TFB (mM Br)	pH	Temp (°C)
0.0	0.03628	BDL	BDL	9.30	24.0
2.3	0.03541	0.00108	BDL	9.25	
6.4	0.03315	0.00262	BDL	9.24	
12.2	0.03141	0.00438	0.00044	9.28	
19.7	0.02967	0.00701	BDL		
27.6	0.02549	0.00921	0.00003	9.23	
34.5	0.02479	0.01075	0.00014		
44.3	0.02271	0.01316	BDL		
56.8	0.01992	0.01602	BDL	9.35	
73.2	0.01714	0.01843	BDL		
80.9	0.01540	0.02019	BDL	9.26	
90.0	0.01435	0.02151	BDL	9.30	24.8

Reproduced with permission of the copyright owner. Further reproduction prohibited without permission.

Table B-81. Results of Experiment # 85. The Initial Concentration of Reactants and Products are Shown at Time = 0.0 min. UV Light Intensity = 2.30 x 10^{-7} Einstein L^{-1} s^{-1}; λ = 2537Å; $\mu = 1.11 \times 10^{-4}$.

Time (min)	BrO_3^- (mM Br)	Br^- (mM Br)	TFB (mM Br)	NO_2^- (mM N)	NO_3^- (mM N)	pH	Temp (°C)
0.0	0.0498	BDL	BDL	0.03410	BDL	8.09	23.5
1.6	0.04769	0.00086	0.00096	0.03251	0.00144	7.90	
4.6	0.04471	0.00242	0.00306	0.03013	0.00505		
8.6	0.03935	0.00443	0.00493	0.02458	0.00892	7.82	
13.0	0.03637	0.00644	0.00615	0.02062	0.01330		
17.2	0.03339	0.00911	0.00731	0.01745	0.01717	7.81	
22.6	0.02922	0.01178	0.00820	0.01189	0.02207	7.76	
27.2	0.02624	0.01446	0.00806	0.00872	0.02491		
31.8	0.02326	0.01691	0.00867	0.00476	0.02904	7.71	
36.5	0.02093	0.01951	0.00839	0.00021	0.03188		
42.3	0.01897	0.02182	0.00862	0.00024	0.03317		
51.0	0.01754	0.02471	0.00675	BDL	0.03317		
65.2	0.01557	0.02783	0.00638	BDL	0.03394	7.82	
77.8	0.01378	0.03051	0.00527	BDL	0.03394	7.82	
91.5	0.01217	0.03385	0.00320	BDL	0.03368		
104.7	0.01092	0.03474	0.00334	BDL	0.03368	7.73	
120.0	0.00967	0.03675	0.00185	BDL	0.03317	7.70	24.0

Reproduced with permission of the copyright owner. Further reproduction prohibited without permission.

Table B-82. Results of Experiment # 86. The Initial Concentration of Reactants and Products are Shown at Time = 0.0 min. UV Light Intensity = 2.30 x 10^{-7} Einstein L^{-1} s^{-1}; λ = 2537Å; $\mu = 8.57 \times 10^{-5}$.

Time (min)	BrO_3^- (mM)	Br^- (mM)	TFB (mM)	NO_2^- (mM)	NO_3^- (mM)	pH	Temp (°C)
0.0	0.02415	BDL	BDL	0.03307	BDL	8.08	22.8
1.7	0.02362	0.00042	0.00078	0.03259	0.00066	7.88	
4.7	0.02183	0.00131	0.00096	0.03093	0.00247	7.83	
8.9	0.01933	0.00242	0.00236	0.02807	0.00453	7.83	
14.0	0.01736	0.00376	0.00339	0.02569	0.00763	7.81	
19.1	0.01557	0.00510	0.00358	0.02379	0.00918	7.89	
25.2	0.01414	0.00688	0.00339	0.02189	0.01124		
31.7	0.01182	0.00889	0.00302	0.01903	0.01305		
38.3	0.01021	0.01022	0.00386	0.01665	0.01588		
46.2	0.00842	0.01223	0.00423	0.01356	0.01872	7.79	
55.2	0.00699	0.01134	0.00423	0.01166	0.02130		
64.4	0.00520	0.01557	0.00418	0.00880	0.02440	7.74	
84.5	0.00359	0.01892	0.00134	0.00666	0.02595		
90.0	0.00252	0.01959	0.000204	0.00500	0.02723		23.9

Reproduced with permission of the copyright owner. Further reproduction prohibited without permission.

Table B-83. Results of Experiment # 87. The Initial Concentration of Reactants and Products are Shown at Time = 0.0 min. UV Light Intensity = 2.30 x 10^{-7} Einstein L^{-1} s^{-1}; λ = 2537Å; $\mu = 4.5 \times 10^{-4}$.

Time (min)	BrO_3^- (mM)	Br^- (mM)	TFB (mM)	NO_2^- (mM)	NO_3^- (mM)	pH	Temp (°C)
0.0	0.01199	BDL	BDL	0.03378	BDL	8.00	23.0
1.5	0.01164	0.00042	0.00012	0.03354	0.00066	7.72	
4.6	0.01110	0.00086	0.00031	0.03283	0.00118		
8.9	0.00985	0.00131	0.00101	0.03093	0.00247	7.60	
12.2	0.00931	0.00198	0.00096	0.03021	0.00324	7.70	
18.0	0.00824	0.00287	0.00134	0.02926	0.00479	7.74	
25.2	0.00699	0.00376	0.00190	0.02783	0.00660		
32.6	0.00574	0.00465	0.00148	0.02546	0.00763		
39.2	0.00502	0.00577	0.00101	0.02450	0.00892	7.50	
49.7	0.00413	0.00710	0.000959	0.02355	0.01021		
57.4	0.00359	0.00777	0.00045	0.02260	0.01124	7.74	
66.4	0.00305	0.00844	0.00073	0.02141	0.01227		
73.3	0.00252	0.00911	0.00045	0.02070	0.01279	7.43	23.7

Reproduced with permission of the copyright owner. Further reproduction prohibited without permission.

Table B-84. Results of Experiment # 88. The Initial Concentration of Reactants and Products are Shown at Time = 0.0 min. UV Light Intensity = 4.35 x 10^{-7} Einstein L^{-1} s^{-1}; λ = 2537Å; μ = 6.25 x 10^{-5}.

Time (min)	BrO_3^- (mM Br)	Br^- (mM Br)	TFB (mM Br)	pH	Temp (°C)
0.0	0.03719	BDL	BDL	8.01	23.0
1.9	0.0359	0.001549	0.00037	7.80	
7.5	0.03096	0.004843	0.00130		
12.5	0.02858	0.00770	0.00064	7.75	
17.5	0.02583	0.009893	0.00154		
22.6	0.02308	0.01275	0.00021		
28.2	0.02015	0.01538	0.00100	7.75	
35.0	0.01813	0.018458	0.00026		
42.2	0.01538	0.01999	0.00075		
50.2	0.01318	0.02241	0.00042	7.80	
59.3	0.01349	0.02439	BDL		
67.7	0.009516	0.02658	BDL		
78.6	0.007500	0.02834	BDL		
88.3	0.006217	0.03010	BDL		
100.7	0.00457	0.031414	BDL	6.40	25.0

Reproduced with permission of the copyright owner. Further reproduction prohibited without permission.

Table B-85. Results of Experiment # 89. The Initial Concentration of Reactants and Products are Shown at Time = 0.0 min. UV Light Intensity = 4.35 x 10^{-7} Einstein L^{-1} s^{-1}; λ = 2537Å; μ = 1.31 x 10^{-4}.

Time (min)	BrO_3^- (mM Br)	Br^- (mM Br)	TFB (mM Br)	Acetate (mM)	pH	Temp (°C)
0.0	0.03719	BDL	BDL	0.06407	7.96	23.0
1.9	0.03444	0.001549	BDL	0.06407		
5.5	0.03115	0.004623	0.00026	0.06159	7.89	
11.1	0.026013	0.009674	0.00026	0.05911		
16.6	0.02161	0.01407	0.000098	0.05662		
22.8	0.016848	0.01890	0.000098	0.05538	7.71	
27.6	0.01428	0.02153	BDL	0.054138		
36.3	0.01062	0.02527	BDL	0.04917		
45.3	0.00713	0.02899	BDL	0.04917	6.80	
54.0	0.00457	0.03185	0.000153	0.04669		
60.0	0.00328	0.03273	BDL	0.04544	6.90	25.0

Reproduced with permission of the copyright owner. Further reproduction prohibited without permission.

Table B-86. Results of Experiment # 90. The Initial Concentration of Reactants and Products are Shown at Time = 0.0 min. UV Light Intensity = 4.35 x 10^{-7} Einstein L^{-1} s^{-1}; λ = 2537Å; $\mu = 1.99 \times 10^{-4}$.

Time (min)	BrO_3^- (mM)	Br^- (mM)	TFB (mM)	Acetate (mM)	pH	Temp (°C)
0.0	0.0370	BDL	BDL	0.133630	8.10	23.0
1.8	0.03408	0.001549	BDL	0.013238		
6.2	0.03023	0.005941	0.000153	0.133626	8.60	
12.1	0.02510	0.01077	BDL	0.12866	8.58	
17.3	0.02106	0.014725	0.00021	0.12742	8.47	
23.6	0.01685	0.019336	0.000098	0.126174		
30.8	0.01227	0.024387	0.000044	0.121206		
37.3	0.00897	0.026583	BDL	0.11748	8.16	
46.1	0.00658	0.029218	BDL	0.121206	8.26	
54.1	0.00457	0.031195	BDL	0.114996	8.24	
60.0	0.00292	0.032951	BDL	0.113754		25.0

Reproduced with permission of the copyright owner. Further reproduction prohibited without permission.

Table B-87. Results of Experiment # 91. The Initial Concentration of Reactants and Products are Shown at Time = 0.0 min. UV Light Intensity = 4.35 x 10^{-7} Einstein L^{-1} s^{-1}; λ = 2537Å; $\mu = 3.45 \times 10^{-4}$.

Time (min)	BrO_3^- (mM)	Br^- (mM)	TFB (mM)	Acetate (mM)	pH	Temp (°C)
0.0	0.03729	BDL	BDL	0.27149	8.01	23.0
1.9	0.03518	0.001988	0.00026	0.27149	8.06	
8.1	0.02803	0.007917	BDL	0.26280	7.89	
12.5	0.02363	0.01253	BDL	0.26031		
17.8	0.019597	0.01648	0.00021	0.25907		
23.2	0.016298	0.019556	0.00021	0.25658	6.56	
29.9	0.01227	0.02439	0.000982	0.25410		
35.1	0.01007	0.02614	BDL	0.25162		
41.7	0.00695	0.029438	BDL	0.24789		
46.8	0.005483	0.031195	BDL	0.24665		
52.6	0.004384	0.03251	BDL	0.24541	6.50	25.0

Reproduced with permission of the copyright owner. Further reproduction prohibited without permission.

Table B-88. Results of Experiment 92, UV Irradiation of Aqueous Nitrite. The Initial Concentration of Reactants and Products are Shown at Time = 0.0 min. UV Light Intensity = 2.61 x 10^{-6} Einstein L^{-1} s^{-1}; λ = 2537Å; $\mu = 4.32 \times 10^{-5}$.

Time (min)	NO_2^- (mM)	NO_3^- (mM)	pH	Temp (°C)
0.0	0.03647	BDL	6.65	25.0
1.3	0.03565	0.000401	6.54	
4.0	0.03538	0.000964	6.70	
6.7	0.03457	0.001807	6.70	
12.1	0.03457	0.00209	6.69	
16.2	0.03234	0.004337	6.60	
20.6	0.03321	0.002650	-	
25.0	0.03267	0.004618	6.58	
29.0	0.03186	0.00293	6.63	
34.2	0.030777	0.00406	6.66	
39.3	0.03050	0.00434	-	
45.2	0.03023	0.00489	-	
49.6	0.02996	0.00518	-	
54.8	0.02887	0.00743	6.46	26.3

Reproduced with permission of the copyright owner. Further reproduction prohibited without permission.

Table B-89. Results of Experiment 93, UV Irradiation of Aqueous Nitrite. The Initial Concentration of Reactants and Products are Shown at Time = 0.0 min. UV Light Intensity = 1.15 x 10^{-6} Einstein L^{-1} s^{-1}; λ = 2537Å; $\mu = 4.32 \times 10^{-5}$.

Time (min)	NO_2^- (mM)	NO_3^- (mM)	pH	Temp (°C)
0.0	0.03565	BDL	6.59	25.0
1.0	0.03565	BDL	6.63	
4.0	0.03511	0.00012	6.56	
6.9	0.03484	0.00040	6.58	
9.9	0.03457	0.00068	6.58	
15.1	0.03430	0.00096	6.58	
19.0	0.03403	0.00124	6.60	
27.0	0.03267	0.00237	6.53	
33.7	0.03213	0.00293	6.55	
45.2	0.03104	0.00406	6.49	
49.7	0.02996	0.00462	6.49	
57.0	0.02996	0.00462	6.49	26.2

Reproduced with permission of the copyright owner. Further reproduction prohibited without permission.

Table B-90. Results of Experiment 94, UV Irradiation of Aqueous Nitrite. The Initial Concentration of Reactants and Products are Shown at Time = 0.0 min. UV Light Intensity = 4.35×10^{-7} Einstein L^{-1} s^{-1}; $\lambda = 2537$Å; $\mu = 4.32 \times 10^{-5}$.

Time (min)	NO_2^- (mM)	NO_3^- (mM)	pH	Temp (°C)
0.0	0.03592	BDL	6.73	25.0
2.1	0.03592	BDL	6.70	
6.2	0.03538	BDL	-	
10.5	0.03511	0.00068	6.59	
15.9	0.03457	0.00068	6.56	
24.3	0.03403	0.00124	6.58	
32.8	0.03294	0.00181	6.46	
38.6	0.03321	0.00153	-	
46.4	0.03267	0.00251	6.48	
52.8	0.03267	0.00284	6.55	
57.3	0.03186	0.00321	6.50	25.8

Reproduced with permission of the copyright owner. Further reproduction prohibited without permission.

Table B-91. Results of Experiment 95, UV Irradiation of Aqueous Nitrite. The Initial Concentration of Reactants and Products are Shown at Time = 0.0 min. UV Light Intensity = 2.30×10^{-7} Einstein L^{-1} s^{-1}; $\lambda = 2537$Å; $\mu = 4.32 \times 10^{-5}$.

Time (min)	NO_2^- (mM)	NO_3^- (mM)	pH	Temp (°C)
0.0	0.03565	BDL	6.67	25.0
3.3	0.03565	BDL	6.73	
7.1	0.03511	0.00012	6.74	
16.8	0.03511	0.00012	6.69	
24.1	0.03484	0.00040	6.60	
30.6	0.03457	0.00068	6.56	
36.1	0.03457	0.00096	6.54	
44.6	0.03403	0.00124	-	
50.1	0.03403	0.00096	6.57	25.9

Reproduced with permission of the copyright owner. Further reproduction prohibited without permission.

Table B-92. Results of Experiment # 96. The Initial Concentration of Reactants and Products are Shown at Time = 0.0 min. UV Light Intensity = 1.15 x 10^{-6} Einstein L^{-1} s^{-1}; λ = 2537Å; $\mu = 8.75 \times 10^{-5}$.

Time (min)	BrO_3^- (mM)	Br^- (mM)	TFB (mM)	pH	Temp (°C)
0.0	0.06711	BDL	BDL	8.06	25.0
1.3	0.06122	0.00289	0.00098	8.04	
7.4	0.04797	0.01212	0.00188	7.96	
11.4	0.04430	0.01686	0.00300		
17.4	0.03841	0.02475	0.00198	7.39	
23.4	0.03178	0.03027	0.00307		
29.4	0.02737	0.03579	0.00193	7.58	
35.1	0.02295	0.04053	0.00123		
43.8	0.01927	0.04526	0.00078	7.05	
52.1	0.01486	0.05078	0.00038	7.06	
61.8	0.01118	0.05394	.00008		
69.6	0.00897	0.05709	BDL	6.92	
78.7	0.00676	0.05946	BDL	6.54	26.5

Reproduced with permission of the copyright owner. Further reproduction prohibited without permission.

Table B-93. Results of Experiment # 97. The Initial Concentration of Reactants and Products are Shown at Time = 0.0 min. UV Light Intensity = 1.15 x 10^{-6} Einstein L^{-1} s^{-1}; λ = 2537Å; $\mu = 5.62 \times 10^{-5}$.

Time (min)	BrO_3^- (mM)	Br^- (mM)	TFB (mM)	pH	Temp (°C)
0.0	0.03215	BDL	BDL	8.10	25.0
1.3	0.03083	0.00147	0.00068		
4.5	0.02751	0.00455	0.00033	8.07	
9.1	0.02288	0.00833	0.00013	7.49	
13.5	0.02067	0.01118	0.00028	7.28	
18.0	0.01736	0.01425	0.00048		
23.8	0.01471	0.01686	0.00033		
31.4	0.01228	0.01993	0.00003	7.09	
38.9	0.00963	0.02277	BDL	6.95	
47.3	0.00764	0.02490	BDL		
55.9	0.0565	0.02727	BDL	6.86	
65.6	0.0411	0.02893	BDL	6.80	26.3

Reproduced with permission of the copyright owner. Further reproduction prohibited without permission.

Table B-94. Results of Experiment # 98. The Initial Concentration of Reactants and Products are Shown at Time = 0.0 min. UV Light Intensity = 1.15 x 10^{-6} Einstein L^{-1} s^{-1}; λ = 2537Å; $\mu = 3.13 \times 10^{-5}$.

Time (min)	BrO_3^- (mM)	Br^- (mM)	TFB (mM)	pH	Temp (°C)
0.0	0.00665	BDL	BDL	8.13	25.0
1.0	0.00610	0.00052	BDL		
2.4	0.00588	0.00076	BDL		
5.3	0.00543	0.00147	BDL	8.10	
8.5	0.00455	0.00194	BDL		
11.9	0.00411	0.00242	BDL	7.79	
16.1	0.00367	0.00313	BDL	7.40	
20.2	0.00323	0.00360	BDL	7.15	
24.3	0.00323	0.00407	BDL		
30.0	0.00234	0.00478	BDL		
35.7	0.00190	0.00502	BDL	7.20	26.5

Reproduced with permission of the copyright owner. Further reproduction prohibited without permission.

Table B-95. Results of Experiment # 99. The Initial Concentration of Reactants and Products are Shown at Time = 0.0 min. UV Light Intensity = 4.35 x 10^{-7} Einstein L^{-1} s^{-1}; λ = 2537Å; $\mu = 8.75 \times 10^{-5}$.

Time (min)	BrO_3^- (mM)	Br^- (mM)	TFB (mM)	pH	Temp (°C)
0.0	0.06638	BDL	BDL	8.30	25.0
1.4	0.06196	0.00171	0.00108	8.28	
4.2	0.05975	0.00502	0.00183	8.19	
8.0	0.05607	0.00897	0.00143		
11.7	0.05092	0.01212	0.00287	8.17	
16.5	0.04724	0.01607	0.00302	7.73	
20.5	0.04061	0.02001	0.00232	7.46	
27.8	0.03546	0.02711	0.00203		
33.3	0.03105	0.03185	0.00148	7.01	
41.6	0.02589	0.03737	0.00153		
50.3	0.02074	0.04289	0.00038	6.94	
57.4	0.02001	0.04447	BDL		
67.0	0.01486	0.04920	BDL	6.77	
77.0	0.01338	0.05157	BDL		
85.0	0.01044	0.05394	BDL	6.59	26.0

Reproduced with permission of the copyright owner. Further reproduction prohibited without permission.

Table B-96. Results of Experiment # 100. The Initial Concentration of Reactants and Products are Shown at Time = 0.0 min. UV Light Intensity = 4.35 x 10^{-7} Einstein L^{-1} s^{-1}; λ = 2537Å; $\mu = 5.62 \times 10^{-5}$.

Time (min)	BrO_3^- (mM)	Br^- (mM)	TFB (mM)	pH	Temp (°C)
0.0	0.03215	BDL	BDL	8.34	25.0
1.7	0.03083	0.00147	0.00053		
5.5	0.02774	0.00313	0.00033	8.25	
9.6	0.02464	0.00644	0.00043		
15.1	0.02221	0.00904	0.00028	8.10	
21.9	0.01912	0.01236	0.00033		
31.1	0.01537	0.01591	BDL	8.05	
42.1	0.01210	0.01946	BDL	7.84	
54.0	0.00940	0.02230	BDL		
63.4	0.00810	0.02396	BDL		
71.3	0.00654	0.02538	BDL	7.55	25.8

Reproduced with permission of the copyright owner. Further reproduction prohibited without permission.

Table B-97. Results of Experiment # 101. The Initial Concentration of Reactants and Products are Shown at Time = 0.0 min. UV Light Intensity = 4.35 x 10^{-7} Einstein L^{-1} s^{-1}; λ = 2537Å; μ = 3.13 x 10^{-5}.

Time (min)	BrO_3^- (mM)	Br^- (mM)	TFB (mM)	pH	Temp (°C)
0.0	0.00676	BDL	BDL	8.45	25.0
1.6	0.00632	0.00052	BDL	8.43	
4.8	0.00610	0.00100	BDL	8.35	
9.7	0.00521	0.00171	BDL		
15.0	0.00455	0.00242	BDL	8.23	
21.0	0.00367	0.00336	BDL		
27.5	0.00345	0.00336	BDL		
32.6	0.00301	0.00384	BDL		
38.4	0.00278	0.00407	BDL	8.25	
45.9	0.00234	0.00455	BDL		
50.1	0.00190	0.00502	BDL	8.25	26.4

Reproduced with permission of the copyright owner. Further reproduction prohibited without permission.

Table B-98. Results of Experiment # 102. The Initial Concentration of Reactants and Products are Shown at Time = 0.0 min. UV Light Intensity = 2.30 x 10^{-7} Einstein L^{-1} s^{-1}; λ = 2537Å; $\mu = 8.75 \times 10^{-5}$.

Time (min)	BrO_3^- (mM)	Br^- (mM)	TFB (mM)	pH	Temp (°C)
0.0	0.06678	BDL	BDL	8.19	25.0
2.2	0.06236	0.00088	0.00096	8.22	
5.4	0.06014	0.00294	0.00150	8.10	
10.8	0.05645	0.00585	0.00130	8.06	
18.2	0.05350	0.00967	0.00179		
26.1	0.04760	0.01350	0.00159	7.82	
34.9	0.04464	0.01656	0.00198	7.33	
43.0	0.04095	0.02191	0.00109	7.24	
54.8	0.03579	0.02651	0.00072	7.03	
69.0	0.03136	0.03109	0.00019		
80.1	0.02841	0.03416	BDL		
90.0	0.02398	0.03568	BDL	7.02	
98.0	0.02250	0.03951	BDL	6.95	26.0

Reproduced with permission of the copyright owner. Further reproduction prohibited without permission.

Table B-99. Results of Experiment # 103. The Initial Concentration of Reactants and Products are Shown at Time = 0.0 min. UV Light Intensity = 2.30 x 10^{-7} Einstein L^{-1} s^{-1}; λ = 2537Å; $\mu = 5.63 \times 10^{-5}$.

Time (min)	BrO_3^- (mM)	Br^- (mM)	TFB (mM)	pH	Temp (°C)
0.0	0.03225	BDL	BDL	8.38	25.0
2.4	0.03025	0.00030	0.00043	8.33	
5.9	0.02937	0.00180	0.00109		
11.3	0.02782	0.00363	0.00033	8.19	
18.8	0.02494	0.00547	0.00062	8.07	
28.5	0.02250	0.00822	0.00024		
38.8	0.02029	0.01052	0.00033	8.02	
47.4	0.01808	0.01235	0.00019		
54.2	0.01653	0.01488	0.00009	7.59	
63.4	0.01453	0.01488	BDL		
69.0	0.01409	0.01579	BDL	7.64	26.0

Reproduced with permission of the copyright owner. Further reproduction prohibited without permission.

Table B-100. Results of Experiment # 104. The Initial Concentration of Reactants and Products are Shown at Time = 0.0 min. UV Light Intensity = 2.30 x 10^{-7} Einstein L^{-1} s^{-1}; λ = 2537Å; $\mu = 3.13 \times 10^{-4}$.

Time (min)	BrO_3^- (mM)	Br^- (mM)	TFB (mM)	pH	Temp (°C)
0.0	0.00678	BDL	BDL	8.37	25.0
1.8	0.00634	0.00006	0.00014		
4.2	0.00612	0.00019	0.00091		
10.8	0.00590	0.00042	BDL		
17.3	0.00546	0.00088	BDL		
25.3	0.00501	0.00134	BDL		
38.4	0.00457	0.00180	BDL		
48.5	0.00413	0.0225	BDL		
58.3	0.00391	0.00248	BDL		
64.3	0.00346	0.00294	BDL	7.49	26.1

Reproduced with permission of the copyright owner. Further reproduction prohibited without permission.

Table B-101. Results of Experiment # 105. The Initial Concentration of Reactants and Products are Shown at Time = 0.0 min. UV Light Intensity = 2.61 x 10^{-6} Einstein L^{-1} s^{-1}; λ = 2537Å; HCO_3^- = 0.05 mM; μ = 0.050.

Time (min)	BrO_3^- (mM)	Br^- (mM)	TFB (mM)	pH	Temp (°C)
0.0	0.03762	BDL	BDL	7.37	24.6
1.3	0.03620	0.00216	0.00040	7.00	
4.3	0.03074	0.00606	0.00087		
7.1	0.02746	0.00904	0.00010	6.85	
11.2	0.02309	0.01340	0.00083		
15.1	0.01938	0.01685	0.00010	6.64	
21.5	0.01523	0.02167	0.00053		
28.5	0.01130	0.02511	0.00057	6.52	
35.8	0.00890	0.02763	BDL		
42.7	0.00671	0.03039	BDL	6.49	
49.1	0.00540	0.03199	BDL		
60.0	0.00366	0.03383	BDL	6.54	

Reproduced with permission of the copyright owner. Further reproduction prohibited without permission.

Table B-102. Results of Experiment # 106. The Initial Concentration of Reactants and Products are Shown at Time = 0.0 min. UV Light Intensity = 2.61 x 10^{-6} Einstein L^{-1} s^{-1}; $\lambda = 2537$Å; $HCO_3^- = 0.5$ mM; $\mu = 0.500$.

Time (min)	BrO_3^- (mM)	Br^- (mM)	TFB (mM)	pH	Temp (°C)
0.0	0.03620	BDL	BDL	9.04	24.6
1.3	0.03292	0.00193	0.00036	9.03	
4.3	0.03030	0.00583	0.00040		
7.9	0.02528	0.01019	0.00142	9.00	
12.8	0.02025	0.01524	0.00083	8.92	
16.7	0.02763	0.01845	0.00053	9.00	
21.8	0.01414	0.02235	BDL		
27.1	0.01130	0.02534	BDL	9.00	
33.1	0.00868	0.02809	BDL		
38.9	0.00693	0.02993	BDL	8.99	
43.5	0.00562	0.03153	BDL	8.98	
50.0	0.00453	0.03222	BDL	9.00	

Reproduced with permission of the copyright owner. Further reproduction prohibited without permission.

Table B-103. Results of Experiment # 107. The Initial Concentration of Reactants and Products are Shown at Time = 0.0 min. UV Light Intensity = 2.61 x 10^{-6} Einstein L^{-1} s^{-1}; λ = 2537Å; HCO_3^- = 1mM; μ = 1.00.

Time (min)	BrO_3^- (mM)	Br^- (mM)	TFB (mM)	pH	Temp (°C)
0.0	0.03620	BDL	BDL	9.31	24.6
1.4	0.03314	0.00239	0.00074	9.28	
4.5	0.02899	0.00606	0.00083	9.30	
9.2	0.02353	0.01088	0.00193	9.31	
13.2	0.01938	0.01547	0.00074		
19.5	0.01589	0.01960	0.00066	9.28	
24.9	0.01261	0.02304	BDL	9.26	
31.7	0.00955	0.02580	BDL	9.28	
38.5	0.00737	0.02855	BDL		
44.2	0.00628	0.03016	BDL		
48.5	0.00497	0.03153	BDL		
53.3	0.00431	0.03153	BDL		
59.1	0.00366	0.03360	BDL	9.27	

Reproduced with permission of the copyright owner. Further reproduction prohibited without permission.

Table B-104. UV_{254} Absorption of Various Concentrations of Aqueous Bromate.

Concentration (mM)	**Absorbance** (au)
4.17×10^{-4}	0.00401
6.25×10^{-4}	0.01127
8.34×10^{-4}	0.01679
1.04×10^{-3}	0.02242
1.25×10^{-3}	0.02593
2.50×10^{-3}	0.03792

Reproduced with permission of the copyright owner. Further reproduction prohibited without permission.

APPENDIX C

UV-VISIBLE ABSORPION SPECTRA OF BROMATE, BROMIDE, NITRITE, NITRATE & ACETATE

Reproduced with permission of the copyright owner. Further reproduction prohibited without permission.

Spectrum/Peak Report Date 05/14/97 Time 09:17:26 Page 1 of 1

Method file : NEAL.M (modified) Last update: Date 05/14/97 Time 09:04:55
Information : Default Method
Data File : <untitled>

Overlaid Spectra:

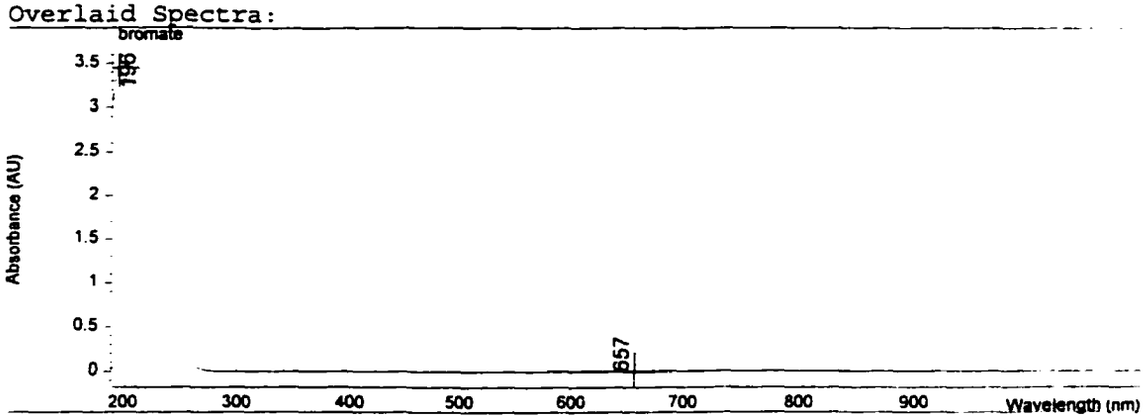

#	Name	Peaks(nm)	Abs(AU)	Valleys(nm)	Abs(AU)
1	bromate	196.0	3.44440	657.0	-4.5395E-4
1		***	***	***	***
1		***	***	***	***

Report generated by : neal Signature:

*** End Spectrum/Peak Report ***

Figure C-1. UV/Visible Absorption Spectrum of Bromate.

Reproduced with permission of the copyright owner. Further reproduction prohibited without permission.

```
==========================================================================
Spectrum/Peak Report        Date 05/14/97  Time 09:10:10 Page 1 of 1
==========================================================================

Method file :          NEAL.M ( modified )      Last update: Date
                       05/14/97  Time 09:04:55
Information :          Default Method
Data File   :          A:\BR4_18.SD     Created : 4/18/97 11:38:51

Overlaid Spectra:
```

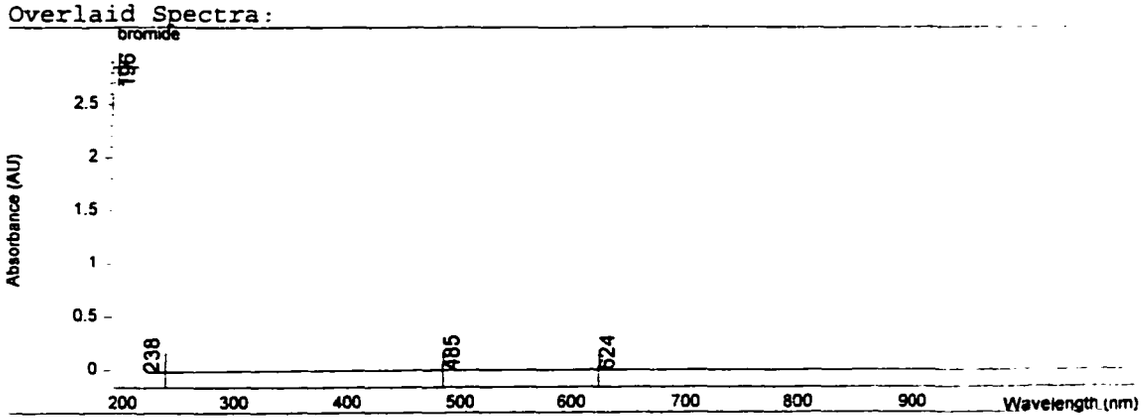

#	Name	Peaks(nm)	Abs(AU)	Valleys(nm)	Abs(AU)
1	bromide	196.0	2.84970	238.0	-2.1172E-2
1		624.0	-5.2042E-3	***	***
1		485.0	-5.6906E-3	***	***

Report generated by : neal Signature: .....

*** End Spectrum/Peak Report ***

Figure C-2. UV/Visible Absorption Spectrum of Bromide.

Reproduced with permission of the copyright owner. Further reproduction prohibited without permission.

Spectrum/Peak Report Date 05/14/97 Time 09:11:03 Page 1 of 1

Method file : NEAL.M (modified) Last update: Date 05/14/97 Time 09:04:55
Information : Default Method
Data File : A:\NO24_18.SD Created : 4/18/97 11:28:28

Overlaid Spectra:

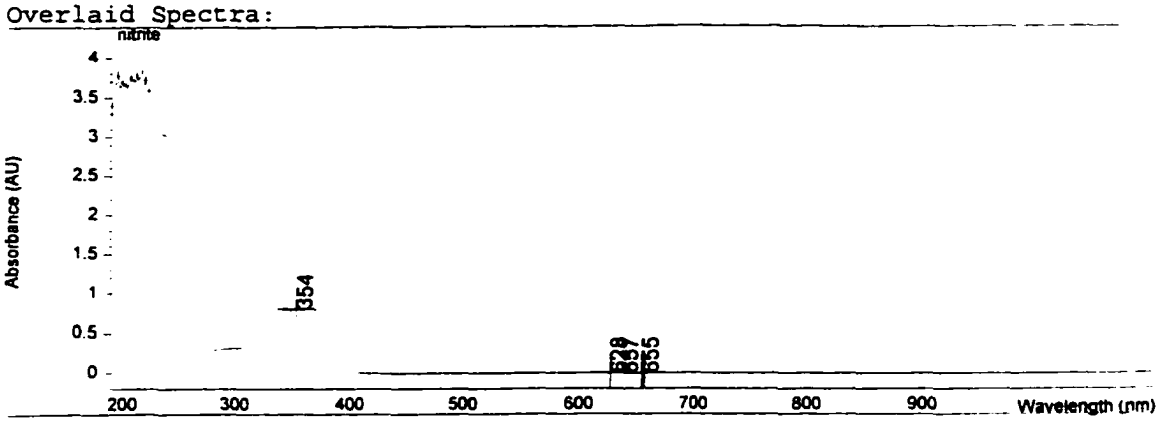

#	Name	Peaks(nm)	Abs(AU)	Valleys(nm)	Abs(AU)
1	nitrite	354.0	0.80159	657.0	-5.3625E-3
1		655.0	-4.3945E-3	***	***
1		628.0	-4.5614E-3	***	***

Report generated by : neal Signature:

*** End Spectrum/Peak Report ***

Figure C-3. UV/Visible Absorption Spectrum of Nitrite.

Reproduced with permission of the copyright owner. Further reproduction prohibited without permission.

Spectrum/Peak Report Date 05/14/97 Time 09:05:05 Page 1 of 1

Method file : NEAL.M (modified) Last update: Date 05/14/97 Time 09:04:55
Information : Default Method
Data File : A:\NO34_18.SD Created : 4/18/97 11:02:21

Overlaid Spectra:

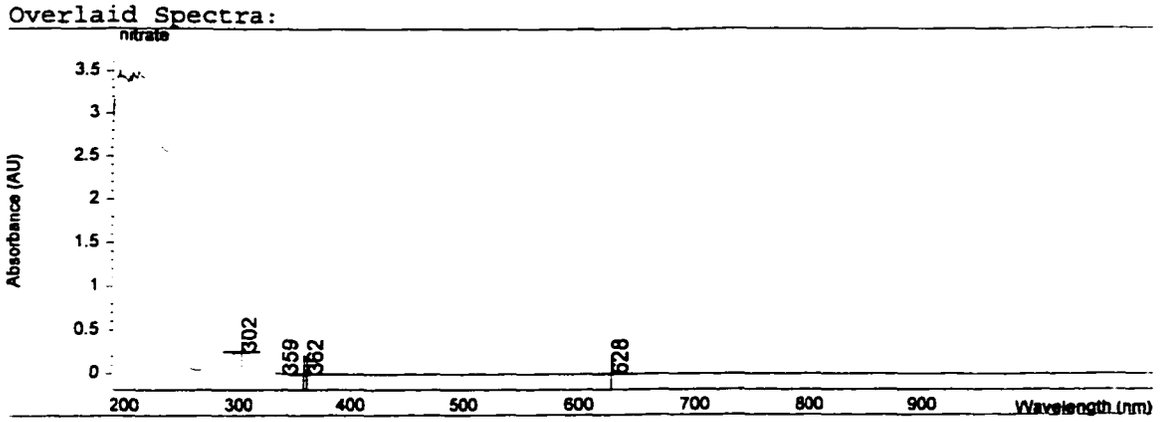

#	Name	Peaks(nm)	Abs(AU)	Valleys(nm)	Abs(AU)
1	nitrate	302.0	0.24924	359.0	-5.7793E-3
1		362.0	-9.7084E-4	***	***
1		628.0	-2.9716E-3	***	***

Report generated by : neal Signature:

*** End Spectrum/Peak Report ***

Figure C-4. UV/Visible Absorption Spectrum of Nitrate.

Reproduced with permission of the copyright owner. Further reproduction prohibited without permission.

Spectrum/Peak Report Date 05/14/97 Time 09:09:54 Page 1 of 1

Method file : NEAL.M (modified) Last update: Date 05/14/97 Time 09:04:55
Information : Default Method
Data File : A:\AC4_18.SD Created : 4/18/97 11:43:36

Overlaid Spectra:

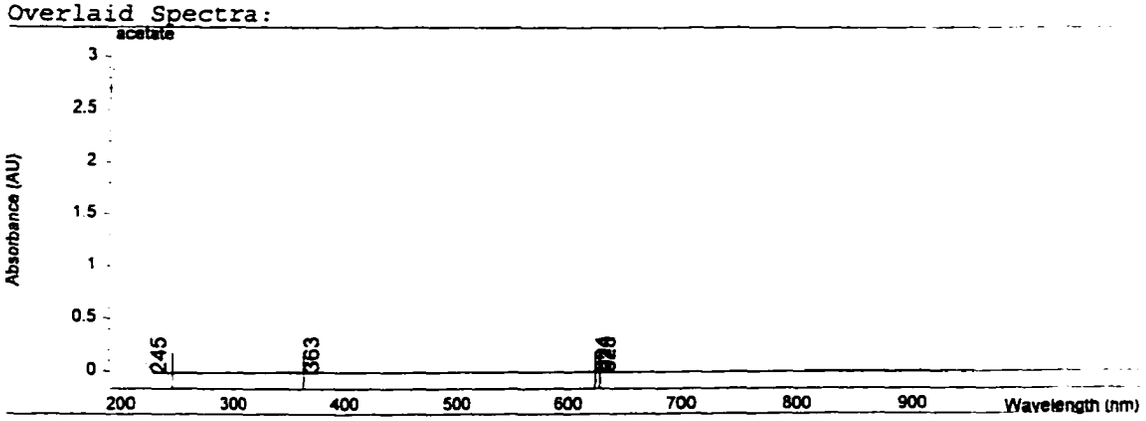

#	Name	Peaks(nm)	Abs(AU)	Valleys(nm)	Abs(AU)
1	acetate	628.0	-4.9601E-3	245.0	-1.5689E-2
1		624.0	-5.1384E-3	***	***
1		363.0	-5.7211E-3	***	***

Report generated by : neal Signature:

*** End Spectrum/Peak Report ***

Figure C-5. UV/Visible Absorption Spectrum of Acetate.

Reproduced with permission of the copyright owner. Further reproduction prohibited without permission.

```
==========================================================================
Kinetics Results Report      Date 05/14/97  Time 14:39:02 Page 1 of 1
==========================================================================


Method file : <untitled>
Information : Default Method of Kinetics Mode

Data File   : C:\HPCHEM\1\DATA\290-350.KD      Created : 4/14/97 12:06:24

Used Wavelengths       : 290 nm, 350 nm
Background correction : none

Run Time     :     120.0 s
Start Time   :       0.0 s
Cycle Time   :       0.5 s

Time Trace:
```

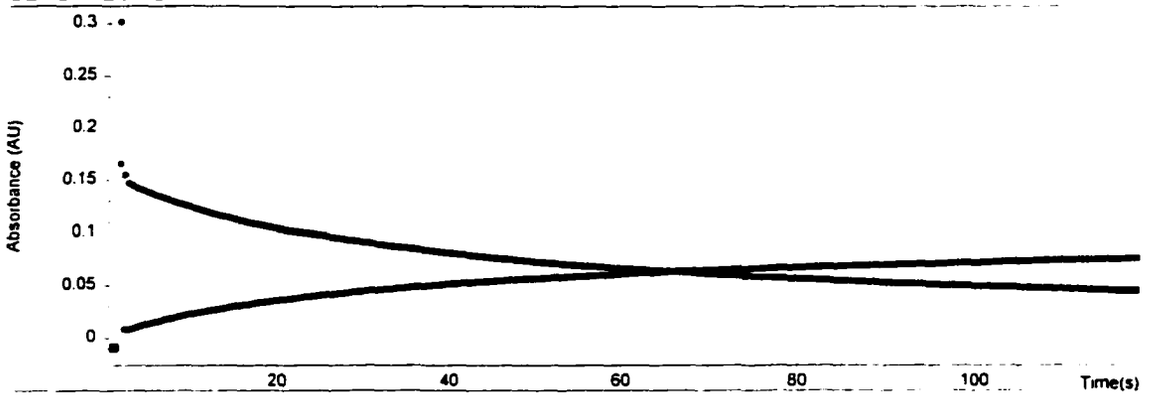


```
Rate Calculation Type    :    First order
Calculation Time Range   :    5 s to 120 s

WL(nm)    Rate(1/s)      Std.Dev      WL(nm)    Rate(1/s)      Std.Dev
--------------------------------    --------------------------------
290         2.7118E-2    6.8832E-4   350         2.6091E-2    1.0266E-3

Report generated by : neal                    Signature:

--------------------------------------------------------------------------
                  *** End Kinetics Results Report ***
--------------------------------------------------------------------------
```

Figure C-6. Monitoring of the Reaction Between Free Chlorine and Bromide with the UV/Visible Photodiode Array Spectrophotometer.

Reproduced with permission of the copyright owner. Further reproduction prohibited without permission.

REFERENCES

Allen, A. O., (1961). *The Radiation Chemistry of Water and Aqueous Solutions*. Van Nostrand, Princeton, New Jersey.

Amichai, O., Czapski, G., and Trinin, A., 1969. *On the Oxybromine Radicals in Aqueous Solution*. Israel J. Chem, 7, pp 351-358.

Amikar, H. J., Patil, S. F., Bodhe, A. A., Pokharkar, R. D., 1975. *Radiolysis of Nitrite in the Presence of Bromate Ion*. Radiochem. Radioanal. Letters, **23** (5-6), pp 307-315.

APHA, AWWA, WEF, 1995. *Standard Methods for the Analysis of Water and Wastewater*.

Atkins, P. W., 1978. *Physical Chemistry* (Third Edition). W. H. Freeman and Company, New York.

Barner, H. E. and Scheuerman, R. V. 1978. *Handbook of Thermochemical Data for Compounds and Aqueous Species*. John Wiley & Sons, N.Y.

Beckwith, R. C., Xiang Wang, T., and Margerum, D. W., 1996. *Equilibrium and Kinetics of Bromine Hydrolysis*. Inorg. Chem., **35**, pp 995-1000.

Bilski, P., Chignell, C. F., Szychlinski, J., Borkowski, A., Oleksy, E., and Reszka, K. 1992. *Photooxidation of Organic and Inorganic Substrates During UV Photolysis of Nitrite Anion in Aqueous Solution*. J. Am. Chem. Soc., **114**, pp 549-556.

Bowen, H. J. M. (1979). *Environmental Chemistry of the Elements*. Academic Press, London.

Bowman, W. D., and Demas, J. N. 1976. *Ferrioxalate Actinomtery. A Warning on its Correct Use*. J. Chem. Phys., **80**, pp 2434-2435.

Boyd, G. E., and Larson, Q. V., 1965. *Production, Identity, and Annealing of the Radiolytic Products Formed in Crystalline Cesium Bromate by Cobalt-60 γ-Rays*. J. Phys. Chem., **69**(4), pp 1413-1419.

Bridge, N. K., and Matheson, M. S., 1960. *The Flash Photolysis of Halate and Other Ions in Solution*. J. Physical Chemistry, **64**, pp 1280-1285.

Reproduced with permission of the copyright owner. Further reproduction prohibited without permission.

British Department of the Environment, 1993. *The Formation of Bromate During Drinking Water Disinfection.* Report No. DW10137.

Cash, J. R., and Karp, A. H., 1990. *ACM Transactions on Mathematical Software*, **16**, pp 201-222.

Chapin, R. M., 1934. *The Effect of Hydrogen Ion Concentration on the Decomposition of Hypohalites*. J. Am. Chem. Soc., **56**, pp 2211-2215.

Collatz, L., 1966. The Numerical Treatment of Differential Equations (Third Edition). Springer, New York.

Demas, J. N. and Bowman, W. D., 1981. *Determination of the Quantum Yield of the Ferrioxalate Actinomter with Electrically Calibrated Radiometers.* J. Chem. Phys., **85**, pp 2766-2771.

Dhar, N. R., 1931. *The Chemical Action of Light*. Blackie and Son Ltd, London.

Ellis, C., and Wells, A. A., 1941. *The Chemical Action of Ultraviolet Rays*. Reinhold Publishing Corporation, New York.

Engel, P., Oplatka, A., Perlmutter-Hayman, B. 1953. *The Decomposition of Hypobromnite and Bromite Solutions*. J. Am. Chem. Soc., **76**, pp 2010-2015.

Farkas, A., and Farkas, L., 1938. *On the Photochemical Primary Process of Ions in Aqueous Solution*. Trans. Faraday Soc., **34**, pp 1113-1120.

Farkas, L., and Klein, F. S., 1948. *On the Photo-Chemistry of Some Ions in Solution*. J. Chem. Phys., **16**, pp 886-893.

Farkas, L., Lewin, M. and Bloch, R. 1949. *The Reaction Between Hypochlorite and Bromides*, J. Am. Chem. Soc., **71**, pp 1988-1991.

Ferraudi, G. J., 1988. *Elements of Inorganic Photochemistry*. John Wiley and Sons, New York.

Flury, M., and Papritz, A. 1993. *Bromide in the Natural Environment: Occurrence and Toxicit.* J. Environ. Qual., **22**, pp 747-758.

Franck, J., and Scheibe, G., 1928. *Quenching of Triplet States by Inorganic Ions. Energy Transfer and Charge Transfer Mechanism*. Z. Physik. Chemie, **A139**, pp 22-28.

Reproduced with permission of the copyright owner. Further reproduction prohibited without permission.

Franck, J., and Haber, F., 1931. *Intramolecular Radiationless Transitions*. Sitz. Preuss Akad. Wiss., pp 250-255.

Gazda, M., and Margerum, D. W. 1994. *Reactions of Monochloramine with Br_2, Br_3^-, HOBr and OBr- : Formation of Bromochloramines*. Inorg. Chem., **33**, pp 118-123.

Gear, C. W., 1971. *Numerical Initial Value Problems in Ordinary Differential Equations*. Prentice Hal, Englewood Cliffs, New Jersey

Gilbert, R.O., 1987. *Statistical Methods for Environmental Pollution Monitoring*. Van Nostrand Rheinhold, New York.

Glaze, W. H., Weinberg, H. S., and Cavanagh, J. E., 1993. *Evaluating the formation of Brominated DBPs During Ozonation*. J. AWWA, **85**(1), pp 96-103.

Haag, W. R., 1981. *Technical Note: On the Disappearance of Chlorine in Sea-Water*: Water Res. **15**, pp 937-940.

Haag, W. R., and Hoigné, J, 1983. *Ozonation of Bromide -Containing Waters: Kinetics of Formation of Hypobromous Acid and Bromate*. Environ. Sci. Technol., **17**, pp 261-267.

Hampel, C. A., and Hawley, G. G., 1973. *The Encylopedia of Chemistry (Third Edition)*. Van Nostrand Reihnold Company, New York.

Harris, D. C., 1987. *Quantitative Chemical Analysis*. W. H. Freeman and Company, New York.

Hatchard, C. G., and Parker, C. A. 1956. *A New Sensitive Chemical Actinometer: Potassium Ferrioxalate as a Standard Chemical Actinometer*. Proc. R. Soc. London, **Ser. A**, **235**, pp 518-536.

Kaplan, A. (Dionex Corporation, Marlton, NJ), 1998. Personal Communication.

Koudjonou, B. K., Muller, M. C., Constentin, E., Racaud, P., Van der Jagt, H., Vilaro, J. S., and Hutchinson, J., 1995. *Bromate Ion Analysis by Ion Chromatography*. Ozone Science & Engineering, **17**, pp 561 - 573.

Krasner, S. W., Glaze, W. H., Weinberg, H. S., Daniel, P. A., Najm, I. N., 1993. *Formation and Control of Bromate During Ozonation of Waters Containing Bromide*.

Reproduced with permission of the copyright owner. Further reproduction prohibited without permission.

J. AWWA, **85** (1), pp 73-81.

Krasner, S. W., Croué, J., Buffle, J., and Perdue, E. M., 1996. *Three Approaches for Characterizing NOM.* J. AWWA, **88**(6), pp 66-79.

Kreyszig, E., 1983. *Advanced Engineering Mathematics*. John Wiley and Sons. New York.

Kruithof, J. C., Meijers, R. T., and Schippers, J. C., 1993. *Formation, Restriction of Formation and Removal of Bromate*. Water Supply, **11**, pp 331-342.

Kurowaka, Y., Takayama, S., Konishi, Y., Hiasa, Y., Asahina, S., Takahshi, M., Maekawa, A., Hayashi, Y., 1986. *Dose Response Studies on the Carcinogenicity of Potassium Bromate in F344 Rats after Long Term Oral Administration*. J. Natl. Cancer Inst., **69**, pp 221-236.

Kurowaka, Y., Maekawa, A., Takahashi, M. and Hayashi, Y. 1990. *Toxicity and Carcinogenicity of Potassium Bromate - A New Renal Carcinogen*. Environmental Health Perspectives, **87**, pp 309-335.

Lefebvre, E., Racaud, P., Parpaillon, Th., and Deguin, A., 1995. *Results of Bromide and Bromate Monitoring at Several Water Treatment Plants*. Ozone. Science & Engineering, **17**, pp 311-327.

Legube, B., 1996. *A Survey of Bromate Ion in European Drinking Water*. Ozone. Science & Engineering, **18**, pp 325-348.

Lengyel, I., Nagy, I., and Bazsa, G., 1989. *Kinetic Study of the Autocatalytic Nitric Acid-Bromide Reaction and its Reverse, the Nitrous Acid-Bromine Reaction*. J. Phys. Chem., **93**, pp 2801-2807.

Lewin, M., and Avrahami, M., 1955. *The Decomposition of Hypochlorite-Hypobromite Mixtures in the pH Range 7-10*. J. Am. Chem. Soc., **77**, pp 4491-4499.

Macalady, D. L., Carpenter, J. H., and Moore, C. A., 1977. *Sunlight-Induced Bromate Formation in Chlorinated Sea-Water*. Science, **195**, pp 1335 - 1337.

Matheson, M. S., Mulac, W. A., and Rabani, J., 1963. *Formation of the Hydrated Electron in the Flash Photolysis of Aqueous Solutions*. J. Phys. Chem., **67**, pp 2613-2617.

Reproduced with permission of the copyright owner. Further reproduction prohibited without permission.

Milazzo, G. and Caroli, S. 1978. *Table of Standard Electrode Potentials*, Wiley, New York.

Mitner, R. J., Shukairy, H. M. and Summers, R. S., 1992. *Disnfection By-product Formation and Control By Ozonation and Biotreatment*. J. AWWA, **84** (17), pp 53-62.

National Toxicology Program, 1990. *NTP Technical Report on the Toxicology and Carcinogenesis Studies of Chlorinated and Chloraminated Water in F344/N Rats and B6C3F1 Mice (Drinking Water Studies)*. NTP Technical Report **392**, National Institute of Health, pp 474.

Neta, P., Huie, R., Ross, A., 1988. *Rate Constants for Reactions of Inorganic Radicals in Aqueous Solutions*. J. Phys. Chem., **17**(3), pp 3-6.

Nussbaum, M. A., Nekimken, H. L., Nieman, T. A. 1987. *Luminol Chemiluminescence for Determination of Iron (II) in Ferrioxalate Chemical Actinomtery*. Anal. Chem., **59**, pp 211- 212.

Ono, Y., Somiya, I., and Mohri, S., 1994. *Evaluation of Genotoxicity of Bromate Ion Produced During Ozonation*. Ozone Science & Engineering, **16**, pp 443- 453.

Palin, A. T., 1967. *Methods for Determination in Water of Free and Combined Available Chlorine, Chlorine Dioxide and Chlorite, Bromine, Iodine, and Ozone using Diethyl-p-Phenylene Diamine (DPD)*. J. Inst. Water Eng., **21**, pp 537-547.

Pourbaix, M. 1966. *Atlas of Electrochemica Equilibria in Aqueous Solutions*. Pergamon Press.

Pourmoghaddas, H., Stevens, A. A., Kinman, R. N., Dressman, R. C., Moore, L. A., and Ireland, J. C., 1993. *Effect of Bromide Ion on Formation of HAAs During Chlorination*. J. AWWA, 85(1), pp 82-87.

Press, W. H., Teukolsky, S. A., Vetterling, W. T., and Flannery, B. P., 1992. *Numerical Recipes in Fortran: The Art of Scientific Computing (2nd Edition)*. Cambridge University Press.

Quick, C. A., Chole, R. A., and Mauer, S. M., 1975. *Deafness and Renal Failure due to Potassium Bromate Poisoning*. Arch. Ontolaryngal, **101**, pp 494 - 495.

Rabinowitch, E., 1942. *Electron Transfer Spectra and Their Photochemical Effects*.

Reproduced with permission of the copyright owner. Further reproduction prohibited without permission.

Reviews of Modern Physics, **14**, pp 112-131.

Richardson, L. B., Burton, D. T., Helz, G. R., and Rhoderick, J. C. 1981. *Residual Oxidant Decay and Bromate Formation in Chlorinated and Ozonated Sea-Water*. Water Research, **15**, pp 1067-1074.

Rollefson, G. K., and Burton, M., 1939. *Photochemistry and the Mechanism of Chemical Reactions*. Prentice Hall, New York.

Shampine, L. F., and Gordon, M. K., 1975. *Computer Solution of Ordinary Differential Equations. The Initial Value Problem*. W.H. Freeman, San Francisco.

Sheffield, G., Hart, E. J., (1964). The Rates of the Reaction of the Hydrated Electron in Aqueous Inorganic Solutions. J. Phys. Chem., **68**(6), pp1524 - 1527.

Shuali, U, Ottolenghi, M., Rabani, J., and Yelin, Z., 1969. *On the Photochemistry of Aqueous Nitrate Solutions Excited in the 195 nm Band*. J. Phys. Chem., **75** (10), pp 3445 - 3451.

Siddiqui, M. S., Amy, G. L., and McCollum, L. J., 1996. *Bromate Destruction By UV Irradiation and Electric Arc Discharge*. Ozone Science & Engineering, **18**, pp 271 - 290.

Siddiqui, M. S., Amy, G. L., Cooper, W. J., Kurucz, C. N., Waite, T. D., Nickelson, M. G., (1996). *Bromate Ion Removal by HEEB Irradiation*. J. AWWA, **88** (10), pp 90 - 101.

Siddiqui, M. S., Amy, G. L., Rice, R. G., 1995. *Bromate Ion Formation: A Critical Review*. J. AWWA, **87**,(11), pp 58-70.

Siddiqui, M. S., Amy, G. L., Ozekin, K., Zhai, W., and Westerhoff, P., 1994. *Alternative Strategies for Removing Bromate*. J. AWWA, **86** (11), pp 81-96.

Sillen, L. G. and Martell, A. E. 1964, 1971. *Stability Constants of Metal Ion Complexes*, The Chemical Society, Special Publications No. 17 and 25.

Song, R., Westerhoff, P., Minear, R., and Amy, G. L., 1997. *Bromate Minimization During Ozonation*. J. AWWA, **89** (6), pp 69-78.

Symons, J. M., and Zheng, M. C. H., 1997. *Technical Note: Does Hydroxyl Radical*

Reproduced with permission of the copyright owner. Further reproduction prohibited without permission.

Oxidize Bromide to Bromate. J. AWWA, **89**(6), pp 106-109.

Treinin, A., and Haynon, E., 1970. *Absorption Spectra and Reaction Kinetics of NO_2, N_2O_3 and N_2O_4 in Aqueous Solution*. J. Am. Chem. Soc., **92**(20), pp 5821-5828.

Turkington, C., 1994. *Poisons and Antidotes*. Facts on File, Inc., New York.

United States Environmental Protection Agency. *National Primary Drinking Water Regulations: Disinfectants and Disinfection Byproducts: Proposed Rule*. Federal Register, **59 (No.** 145) (1994).

Ultra Dynamics Corporation, 1989. *Purification By Ultraviolet Radiation: Technical Bulletin #86*.

United States Environmental Protection Agency, 1993a. *Draft Drinking Water Health Criteria Document for Bromate*. Office of Science and Technology. September 30, 1993.

United States Environmental Protection Agency, 1993b. *Status of DBP Regulatory Negotiation*. Office of Water, August 1993.

United States Environmental Protection Agency, 1994. *National Primary Drinking Water Regulations: Disinfectants and Disinfection Byproducts: Proposed Rule*. Federal Register, **59** (145).

United States Geological Survey, 1993. *Water -Quality Assessment of the South Platte River Basin, Colorado, Nebraska, Wyoming - Analysis of Available Nutrient, Suspended-Sediment, and Pesticide Data, Water Years 1980-92*. Internet Publication.

Velema, M., 1977. *Contaminated Drinking Water as a Potential Cause of Cancer in Humans*. J. Envir. Sci. Health, **5**, pp 1 - 12.

Von Gunten, H., Bruchet, A., and Constentin, E, 1996. *Bromate Fromation in Advanced Oxidation Processes*. J. AWWA, 88(6), pp53-65.

Von Gunten, H., and Elovitz, M., 1997. *Influence of Temperature, pH, and DOM Source on Hydroxyl Radical/Ozone Ratios During Ozonation*. Proceedings of the 7th International Symposium on Chemical Oxidation, Nashville, TN.

Wegman, R. C. C., Greve, P. A., de Heer, H., and Hamaker, P. 1981. *Methyl Bromide and Bromide Ion in Drainage Water after Leaching of Glasshouse Soils*. Water Air

Reproduced with permission of the copyright owner. Further reproduction prohibited without permission.

Soil Pollut., **16**, pp 3 -11.

Wegman, R. C. C., Hamaker, P., and de Heer, H., 1983. *Bromide -ion Balance of a Polder District with Large Scale use of Methylene Bromide for Soil Fumigation*. Food Chem. Toxicol., **21**, pp 361-367.

Weiss, j., 1941. *The Photochemical Primary Process of Ions in Aqueous Solutions*. Trans. Faraday Soc., **37**, pp 463-469.

World Health Organization,1993. *Guidelines for Drinking Water Qualty-Tables of Guideline Values*.

Wong, G. T. F. and Davidson, J. A., 1977. *The Fate of Chlorine in Sea-Water*. Water Res., **11**, pp 971 - 978.

Zafiriou, O. C., and True, M. B., 1979. *Nitrite Photolysis in Seawater by Sunlight*. Geophys. Res. Lett., **6**, pp 81-84.

Zafiriou, O. C., McFarland, M., Bromund, R. H., 1980. *Nitrite Oxide in Seawater*. Science, **207**, pp 637-639.

Zafiriou, O. C., 1983. *Chemical Oceanography*. Academic Press, London.

Reproduced with permission of the copyright owner. Further reproduction prohibited without permission.

IMAGE EVALUATION TEST TARGET (QA-3)

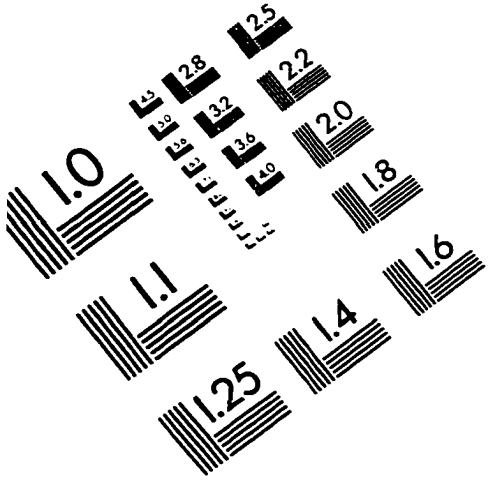

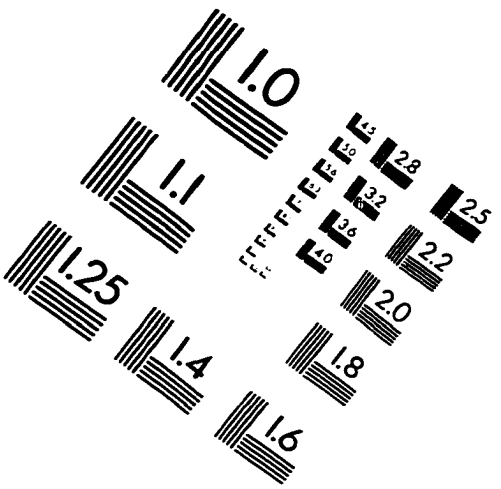

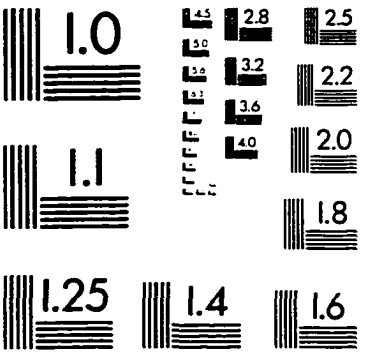

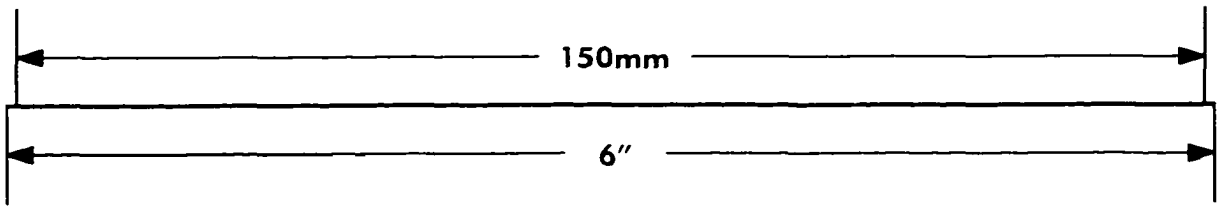

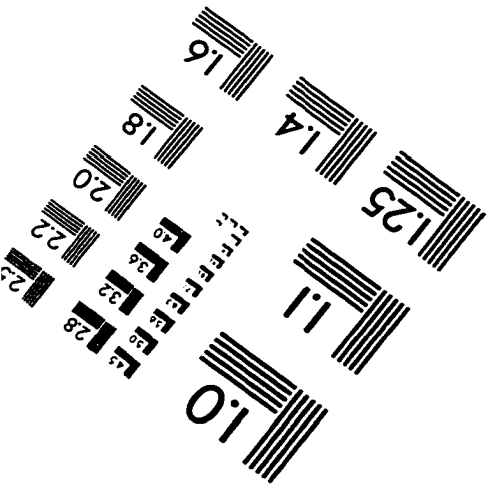

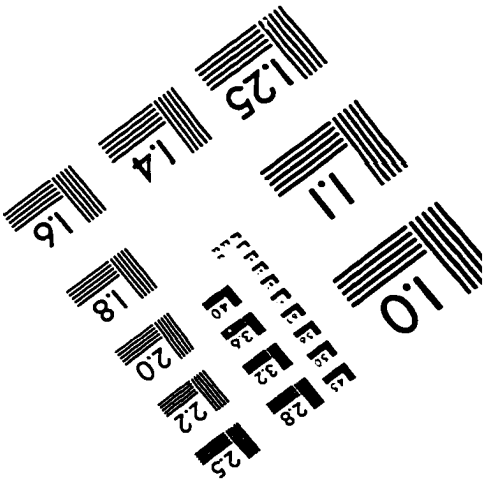

APPLIED IMAGE, Inc
1653 East Main Street
Rochester, NY 14609 USA
Phone: 716/482-0300
Fax: 716/288-5989

© 1993, Applied Image, Inc., All Rights Reserved

Reproduced with permission of the copyright owner. Further reproduction prohibited without permission.